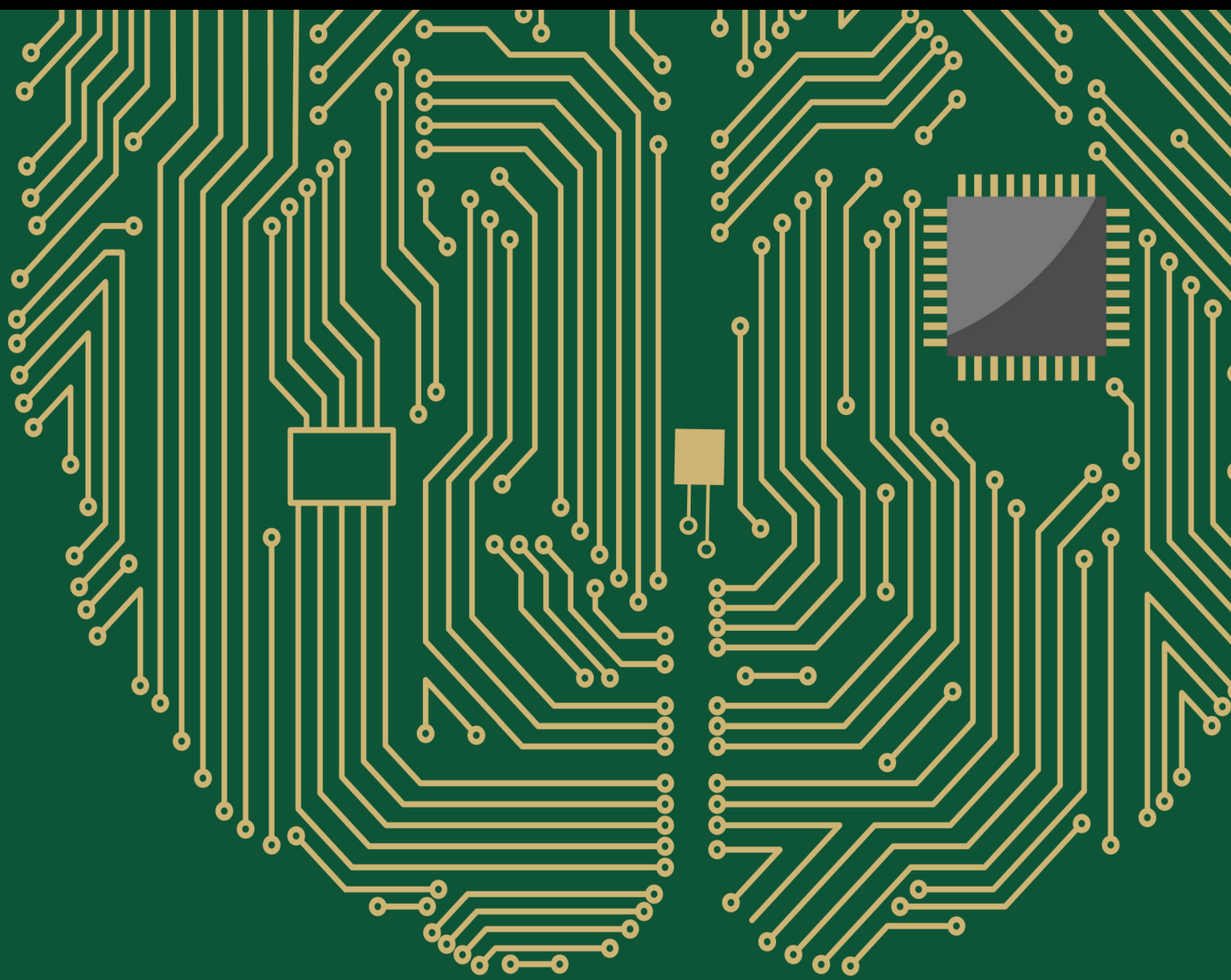# Ubiquitous Artificial Intelligence Enabled Next Generation Wireless Systems

Lead Guest Editor: Rajesh Natarajan
Guest Editors: Bharat Rawal and Francisco R. Castillo-Soria

Ubiquitous Artificial Intelligence Enabled Next Generation Wireless Systems

Ubiquitous Artificial Intelligence Enabled Next Generation Wireless Systems

Lead Guest Editor: Rajesh Natarajan
Guest Editors: Bharat Rawal and Francisco R. Castillo-Soria

Contents

Contents

Hindawi

Research Article

Optimization Strategy of College Students' Education Management Based on Smart Cloud Platform Teaching

Mingjing Zhang ⬚

College of Teacher Education, Pingdingshan University, Pingdingshan, Henan 467000, China

Correspondence should be addressed to Mingjing Zhang; 34100@pdsu.edu.cn

With the passage of time and social changes, the form of education is also changing step by step. In just a few decades, information technology has developed by leaps and bounds, and digital education has not yet been widely promoted. Intelligent education cloud platforms based on big data, Internet of things, cloud computing, and artificial intelligence have begun to emerge. The research on the "smart campus" cloud platform is conducive to improving the utilization rate of existing hardware equipment in colleges and universities and is conducive in improving the level of teaching software deployment. At the same time, this research also provides a new idea for the research in the field of cloud security. While cloud computing brings convenience to teaching work, it also brings new problems to system security. At present, virtualization technology is still in the ascendant stage in the construction of "smart campus" in colleges and universities and is gradually applied to cloud computing service products. At present, there are many cases about the construction of teaching resource platform, but most of them are modified from the early resource management system, which has strong coupling of single system, insufficient functions of collecting, processing, searching, sharing, and reusing resources, and weak application support ability for related business systems. Under this social background, this paper studies the teaching process management system for intelligent classroom.

1. Introduction

In recent years, especially in the last decade or so, with the rapid development and unprecedented prosperity of Internet technology and mobile Internet technology, people's lives have also undergone earth shaking changes [1]. The application of information technology in education and teaching has led to changes in the teaching process, which has attracted the attention of experts, scholars, managers, and front-line teachers. The management of front-line education and instruction, the industrial level, and the nation as a whole have all boosted their information technology efforts. One of the most prominent aspects of the application of information technology in the field of education is the supporting and auxiliary role of teaching resources for daily teaching. Therefore, the construction of teaching resources and the planning of teaching resource service platforms have also become an important part of the educational informatization work [2].

From the multimedia teaching in the late 1990s to today's "smart campus" and "digital campus," education informatization has experienced a long-term development process. "Cloud computing" technology has been widely used in the field of education since its birth. Based on the advantages of "cloud computing," higher vocational colleges in China have begun to build cloud platforms, providing a new platform for student management and teaching. At present, most schools have completed the construction of digital campus. Through the digital campus, students can log on to the campus website and do a series of work, such as inquiring about their grades, applying for courses, and paying fees. The digital transformation of the school provides a lot of convenience for students and teachers [3]. However, with the development of cloud technology and information technology and in order to provide students and teachers with a more efficient and intelligent work and learning environment, the transformation from digital campus to smart campus has become an inevitable trend of

campus information development [4]. Combined with the bus of school management and teaching, the urgent problems to be solved at present are the classification of freshmen at the beginning of the new school year, the arrangement of courses before teaching, the arrangement of examinations before examinations, and the statistics and analysis of scores after examinations [5]. To solve these problems and realize an efficient, scientific, reasonable, intelligent, and fair intelligent education cloud platform, we need not only programming skills but also rigorous data organization structure and clear and efficient algorithms. Therefore, for the difficult problems in the intelligent education cloud platform, we need to summarize, study, and analyze the relevant algorithms and design algorithms suitable for their respective situations [6].

Cloud computing is a new business delivery model, which completely subverts the traditional concept of terminal management; in a sense, it strips the connection between computer terminal software and hardware and is also a new IT infrastructure management method [7]. As a new computing model, a large number of computer file resource pools are used to carry distributed computing and cloud storage tasks, so as to ensure that different application systems can effectively obtain storage, computing capacity and various software services. The development direction of cloud computing is to improve the cloud computing capacity, effectively reduce the burden of user terminals, and ultimately simplify the user terminals into simple input and output devices, while meeting the user's computing processing needs. Through the new service delivery mode, in the cloud computing mode, users only need to access the network through a thin terminal, and the application software and operating system are provided by the cloud in the background through the network in the form of services, which can make the user terminal fundamental. To avoid multilevel problems such as system paralysis, software conflict, and misoperation [8], smart classroom-oriented learning platform is a form of digital campus, and it is a service platform that provides independent learning for school students and student management for teachers [9]. Because the traditional classroom is only based on the single teaching mode of student-teacher, and there is a lack of communication between students and teachers in the teaching process, teachers cannot know the various states and problems of students in real time in the classroom, and teachers cannot put forward targeted opinions on students' existing problems in time [10]. Introducing the cloud platform into education management can bring new opportunities to colleges and universities, improve the penetration of education work with new methods and concepts, expand the management space, and further optimize the management means. Teachers and students can realize online communication through the cloud platform, help teachers understand students' thoughts, grasp their psychological state and ideological trends, improve the effectiveness of education and management, and make school management work run stably.

The purpose of launching the campus virtual desktop platform based on cloud computing in this paper is to use the virtual desktop technology in cloud computing technology to solve the problems such as the shortage of traditional computers on campus, backward teaching management mechanism, rigid teaching methods, and so on. In short, virtual desktop refers to the technology that supports the remote dynamic access of the desktop system and the unified hosting of the data center at the enterprise level. An image analogy is that now we can access our mail system or network disk on the network through any device, at any place, and at any time. In the future, we can access our personal desktop system on the network at any place and at any time through any device. Virtual desktop technology allows users to install simple thin terminals. Virtual desktop technology allows users to avoid hardware failures of traditional computers; virtual desktop technology can make users free from traditional computer viruses and hacker attacks; virtual desktop technology allows users to avoid cumbersome problems such as software and hardware upgrades of traditional computers. At present, the cloud desktop platform has been widely used in the telecommunications industry and has been gradually extended to the general information system application industry. Virtual desktop technology can save users from hardware failures of traditional computers; virtual desktop technology can save users from viruses and hacker attacks on traditional computers; virtual desktop technology can save users from tedious problems such as software and hardware upgrades of traditional computers. At present, the cloud desktop platform has been widely used in the telecommunications industry and has been gradually extended to the general information system application industry. Compared with traditional teaching resources, modern teaching resources generally have the following characteristics: (1) digitization of resource generation technology, (2) multimedia resource processing methods, (3) network communication of resources, (4) resources are personalized, and (5) resource reuse and sharing.

2. Related Work

Since the realization of the strategy for the digitalization of education, China has built the world's largest repository of educational and teaching resources. Over the years, many educational and teaching resources have been developed and constructed.

The construction of teaching resource platform in China is basically synchronized with that in foreign countries. In previous years, due to the great attention paid to the construction of educational resources in China, major resource manufacturers have developed unique teaching resource platforms and sold them to end users as a part of resource services. In recent years, with the introduction of cloud computing technology and the transformation and upgradation of the original resource service platform, domestic resource manufacturers have built a large number of cloud-based resource service platforms to provide users with value-added services.

Reyes and Teaching believed that the distance education system is a manifestation of educational intelligence. In order to improve the design level of this system, virtual reality technology and multiagent system should be fully applied to it. On this basis, scholars constructed the design

framework of VR&MAS-DES and clarified the functions of the system, including learning system and student agent, intelligent teaching system, teacher management system, and teacher agent [11]. Alfoudari et al. believed that the combination of virtualization technology and cloud platform has brought a brand-new resource integration and usage model. On-demand resource allocation and scheduling based on virtualization technology can improve the resource utilization rate of cloud platform, improve the quality of cloud services, and reduce the total cost of ownership of cloud users. "Desktop Cloud" is also developing at a high speed, relying on these two technologies. Here is the development status of desktop virtualization, the core technology of desktop cloud [12]. Aguilar et al. believed that the level of cloud computing data transmission protocol design directly affects the satisfaction of cloud computing user experience. The higher the level of design, the higher the efficiency of cloud computing users, the better the user experience, and the higher the user satisfaction and vice versa [13]. Lampolthammer et al. believed that the role of cloud computing in higher education is mainly manifested in the following five aspects: (1) it can reduce the purchase and maintenance costs of school computers and other hardware equipment, (2) it can provide economic application software for schools, (3) it can save energy, (4) it can ensure the information security of teachers and students and improve network security, and (5) it can make data sharing more convenient. In short, the emergence of cloud computing indicates that the current development of the Internet has reached a new stage, which is also a new opportunity [14]. Hou et al. proposed the S0A design of the overall framework of educational administration management. They believed that the advantage of the information system based on SOA is that it has made a more reasonable design for the system architecture, but the shortcomings of C/S mode design are also very prominent: the system is not easy to transplant, the system is not easy to update, and the interface is lack of humanized design [15]. Wolff et al. pointed out that there is a great contradiction between the limited number of class hours arranged by teachers and the students' demand for class selection, the shortage of classroom resources leads to difficulties in class scheduling, the centralized examination at the end of the term leads to tight classroom arrangements, the problem of checking and saving student status information, and the problem of arranging teaching plans [16]. Cheng et al. summed up the multiobjective optimization problem and laid a theoretical foundation. Up to now, some new mechanisms have been introduced into the multiobjective optimization problem, but there are very few articles on the review of the multiconstraint assignment problem, and most of them are an elaboration of NP-hard problems in multiconstraint assignments [17]. Li et al. put forward the SOA design of the overall framework of educational administration and applied cloud computing in the overall framework. Its advantage is that the system architecture is designed reasonably, but the shortcomings of the C/S mode design are also very prominent: the system is not easy to transplant, the system is not easy to update, and the interface lacks

humanized design [18]. Campo and Cristina proposed an adaptive queuing algorithm for teaching data preprocessing based on cloud computing to solve the queuing mechanism of educational administration management information system [19–21]. Zhang and Wenjun thought that Xen-Desktop has the advantage of designing a digital library information management system of Southeast University which can meet the needs of mobile intelligent digital library. The system can realize the key analysis and design of user authentication and secure login of mobile client, inquiry, and online reading of books on mobile devices, urging the return of books on mobile client and paying overdue fines [22–24].

3. Methodology

3.1. Genetic Algorithm Combined with Cloud Platform Technology Is Used to Analyze Education Management. Since the development of educational informatization, the construction of teaching resources has not been interrupted. At the beginning of the construction of the early campus network, school level resource libraries were equipped for each school, providing some teaching resource content for teachers to use. Cloud computing is a next generation computing model that can provide dynamic resource pooling, virtualization and high availability, and can provide users with "on-demand computing" services. According to the current situation and development trend of education informatization, cloud computing will have extremely important application value in the education industry, such as integrating, developing and utilizing various resources of current education informatization, fully tapping the potential, and improving the utilization rate of resources. Each set of teaching resources is accompanied by a set of resource service platforms, and each set of platforms has its own business logic, data structure, and application system. Jumping and searching between multiple resource platforms to adapt to the operation mode of each platform consume a lot of energy from users, which seriously affect the enthusiasm of users to use, resulting in the phenomenon of not easy to use or unwilling to use. Without a unified construction standard and resource exchange platform, the resource service systems constructed by units at all levels have become isolated islands of resources. However, these resource islands cannot connect well with other business systems, such as lesson preparation system, teaching research system, and self-help learning system, because of their own design problems, and they cannot play a supporting role in basic teaching resources for related business systems. The value of teaching resource service systems built in each stage has shrunk dramatically, and they are gradually forgotten and abandoned, resulting in a large amount of money waste. According to the characteristics of the cloud computing-aided teaching platform, this paper improves the original adaptive genetic algorithm for job scheduling and proposes an improved genetic algorithm to reduce the completion time of tasks and accelerate the response to meet the needs of customers. This algorithm further constrains the selection of genetic genes by adopting the fair mechanism and the data

localization mechanism to shorten the total completion time of tasks and improve the satisfaction of users, so as to improve the performance of the algorithm. So that it can better adapt to the cloud computing environment. Based on our school's urgent demand for cloud applications, using XenApp technology, the virtual desktop platform based on cloud computing puts the application execution environment in the cloud in the teaching system and realizes the SaaS service mode that our school strives to build.

The genetic algorithm was first developed by Professor Holland, who put forward stems from his thinking from natural and artificial adaptive systems. The genetic algorithm is a highly parallel, random, and adaptive search algorithm developed by simulating the mechanism of heredity and mutation in the evolution of the biological world. The search mechanism of the genetic algorithm simulates the reproduction, cross-over, and mutation phenomena that occur in the processes of natural selection and natural inheritance. It keeps a set of candidate solutions in each iteration, chooses the better individuals from the candidate solution set in accordance with a certain index, selects them with genetic operators, combines them by cross-over, and mutation, to generate a new generation of candidate solution sets, a process that is repeated until no more candidates are left. It takes "survival of the fittest" as the principle and gradually finds the optimal solution through heredity, mutation, and selection. This is a global optimization strategy, which can avoid falling into local optimization. A combination is randomly selected as the initialization population, and each individual is evaluated one by one from the perspective of finding the optimal solution, and then the fitness can be formed. This value reflects the contribution of these chromosomes to the last problem. According to the initial population, principle of "survival of the fittest," the genetic evolution is carried out from generation to generation, individuals with low fitness are eliminated, and individuals with high fitness are combined in pairs, so that their excellent genes can be passed on. The genetic algorithm has been widely used in various fields due to its remarkable features such as simplicity, versatility, efficiency, practicability, robustness, and parallelism, and achieved good results, as shown in Figure 1.

If the population size of the genetic algorithm is large, the convergence speed will slow down in the later stage. To solve this problem, the key is to improve the genetic operator and fitness of the genetic algorithm according to the actual situation. The genetic algorithm uses fitness function to calculate and select and evolve the next generation according to the merits and demerits of individuals, so as to find the optimal solution of the problem. Therefore, the selection of fitness function is very important, which will directly affect the convergence speed of the genetic algorithm and the search of optimal solution.

The calculation process of the genetic algorithm is as follows: (1) initialize the population and reasonably set the parameters; (2) through the trained neural network, the excellent value of every individual is judged, and its adaptive value is calculated; and (3) transform the excellent individuals and calculate their fitness values.

3.2. Optimization Design of Teaching Management Based on Cloud Computing Platform.

The biggest advantage and main feature of cloud computing is resource sharing. Therefore, in the application of cloud computing in university teaching management, we should actively and vigorously promote resource sharing. First of all, we must establish a sound and perfect cloud service platform based on cloud computing. Second, with effective integration of existing cloud platform resources on the teaching management platform based on cloud computing technology, all colleges and universities can upload their own high-quality resources to achieve resource sharing, which can provide valuable knowledge wealth for all higher education teaching, scientific research, and management users on the platform. At the same time, to achieve the most correct effect of resource sharing, these resources are not limited to a region or even a country. They can greatly expand the professional vision of users and master more advanced knowledge.

Cloud computing is a next generation computing model that can provide dynamic resource pooling, virtualization, and high availability and can provide users with "on-demand computing" services. According to the current situation and development trend of education informatization, cloud computing will have an extremely important application value in the education industry. First of all, integrate the software and hardware resources of the teaching parks scattered in different regions; improve their reuse rate; eliminate idleness and waste; achieve unified standards, unified management, and unified maintenance of data; gradually interconnect the data of each branch school and each application system in the campus network dynamically and timely; completely eliminate the information island in education informatization; and realize decentralized information collection, centralized security management, and shared application systems. For example, enterprises provide funds or equipment, universities provide technology and site resources, enterprises provide technology and personnel, and universities provide equipment or site resources. Through good cooperation between schools and enterprises, we can improve our brand value, steadily promote the expansion of computer hardware facilities in ordinary universities, and gradually reduce the hardware facilities restrictions in the development of cloud computing mode. We can promote ordinary colleges and universities to give priority to the service of network cloud platform. With the advantages of cloud platform resources and cloud computing, relatively backward colleges and universities can make up for their shortcomings as soon as possible and achieve the rationality of the distribution of various resources.

Through server virtualization technology, various hardware and software resources are virtualized into one or more resource pools, and these virtual resources are managed and allocated intelligently and automatically through the system management platform. Most private cloud-based computing solutions tend to be IaaS (infrastructure as a service). IaaS mainly includes the following parts: (1) the existing enterprise computing environment is usually an x86 platform, and the "smart campus cloud platform" can be
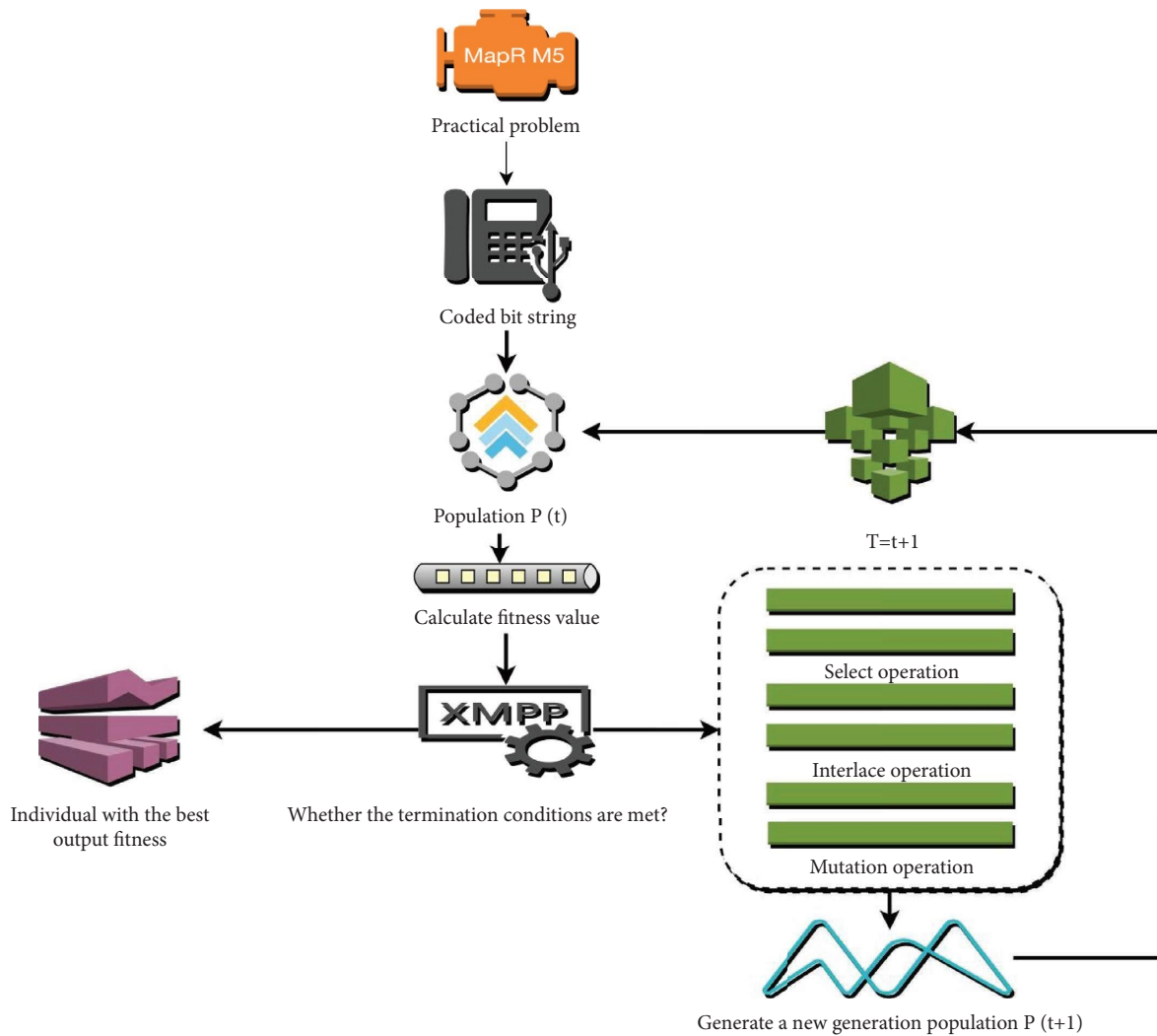
Figure 1: Genetic algorithm process.

accessed through the server. The virtualization is used to integrate and flexibly utilize computing resources and to integrate, dynamically adjust, and migrate server computing resources. (2) An important part of realizing IaaS is cloud storage. A cloud computing infrastructure needs to serve many different business systems or applications, and each business system or application will have different storage requirements. Through storage virtualization management, the "Smart campus cloud platform" enables integration of storage needs and flexible capacity control. (3) With the large-scale deployment of virtualization technology in the cloud computing environment, the traditional network architecture will face many new challenges, including specifications and performance, virtual machine access and control, large layer 2 network deployment, traffic bursts with congestion, and so on.

"Cloud" has a high performance-to-price ratio. Introducing the cloud computing construction mode to integrate and optimize the private hardware resources in the current information can change the traditional "shaft" IT construction mode and improve the operation efficiency and

scalability of the data. At the same time, optimize the way of resource utilization and fundamentally reduce the construction cost of data storage. The cloud computing service architecture is shown in Figure 2.

The infrastructure service layer consists of host, storage, network, and other hardware devices. Virtualization and Cloud management integrates computing resources through virtualization technology and provides basic services such as resources and operating environment to the outside world through pool management. The platform layer mainly provides unified platform system software support services on LAAS, including access control services, data mining, and parallel computing. The application service layer is responsible for external terminal services. Teachers or students can log in to the portal website, cloud application software resources, or virtual desktop according to their needs.

Virtualization technology is the key technology to integrate and utilize various computing resources and storage resources. Among them, server virtualization is to virtualize a physical server into several virtual servers for use. The virtualized entities are all kinds of IT resources,
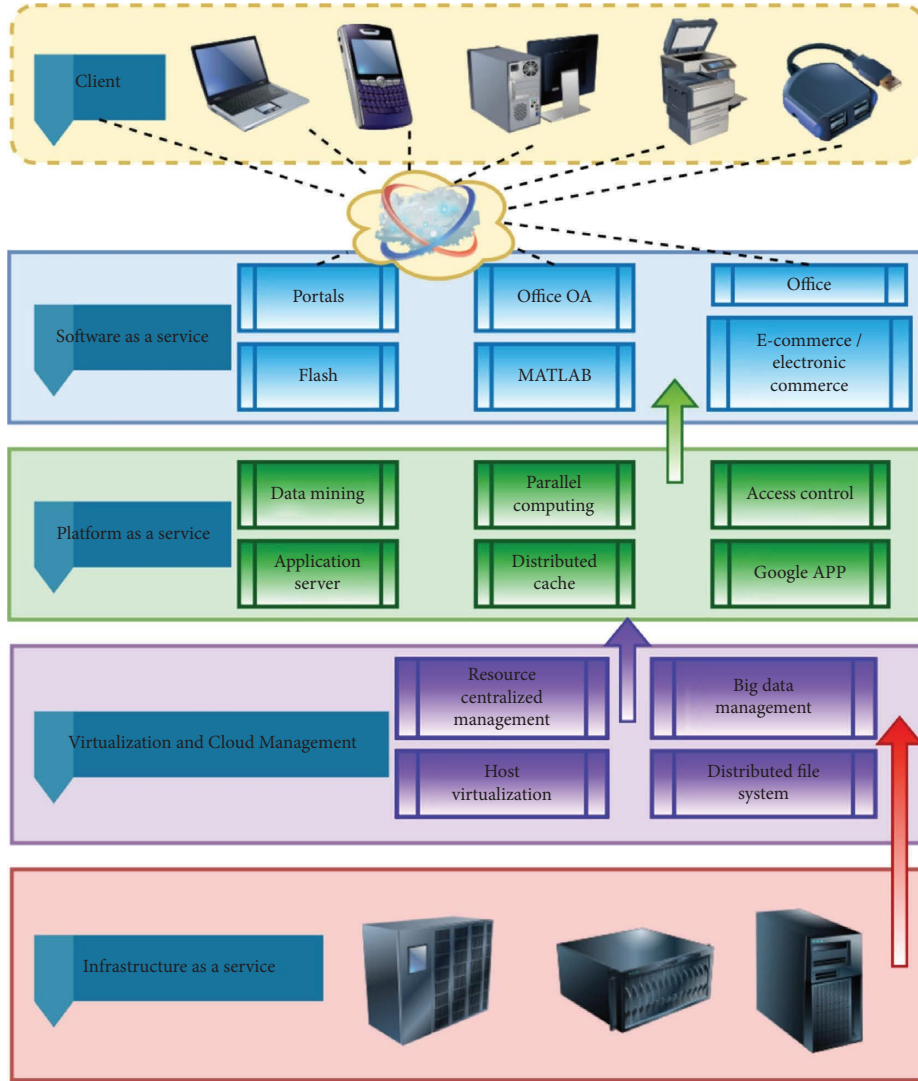
FIGURE 2: Cloud computing architecture.

which can realize the deployment of more virtual servers in the limited hardware server environment, so as to reduce the cost of hardware construction, improve resource utilization, and dynamically schedule resources. Traditional virtualization technology, represented by virtual server, is composed of server hardware, server operating system, virtualization software, and virtual machine. Virtual applications rely on virtual operating system. Data are converted from virtual machine to server hardware through three layers. The interfaces, protocols, and communication standards of each layer are different. Therefore, a lot of performance consumption will be generated, resulting in the running speed of virtual machine far behind the real system.

The prediction residual should be processed by discrete cosine transform, the unit is 4×4 block, the energy can be concentrated on a few coefficient items in the transform

domain, and the spatial redundancy in the video data can be further eliminated. The one-dimensional N-point discrete cosine transform can be expressed as

$$y_k C_k \sum_{n=0}^{N-1} x_n \cos \frac{(2n+1)k\pi}{2N}, \quad (1)$$

where x_n is the nth item in the input time domain sequence, y_k is the kth item in the output frequency domain sequence, and C_k is defined as follows:

$$C_k \begin{cases} \sqrt{\dfrac{1}{N}} k = 0, \\ \\ \sqrt{\dfrac{2}{N}} k = 1, 2, \ldots, N-1 \end{cases}. \quad (2)$$

The corresponding two-dimensional $N \times N$ discrete cosine transform is carried out as follows:

$$Y_{mn} = C_m C_n \sum_{i=0}^{N-1} \sum_{j=0}^{N-1} X_{ij} \cos \frac{(2j+1)n\pi}{2N} \cos \frac{(2i+1)m\pi}{2N},$$

$$X_{mn} = \sum_{i=0}^{N-1} \sum_{j=0}^{N-1} C_m C_n Y_{mn} \cos \frac{(2j+1)n\pi}{2N} \cos \frac{(2i+1)m\pi}{2N}.$$

(3)

At the same time, each 4×4 sub-block should be taken out from the 16×16 luminance block or chrominance block for Hadamard transformation. The encoder will also discard some high-frequency information appropriately, thus reducing the coding length without affecting the video playback effect. The formula for quantizing the conversion coefficient in the matrix y is as follows:

$$Z_{ij} = \text{round}\left(\frac{Y_{ij}}{Q\text{step}}\right),$$

(4)

where Y_{ij} is the conversion coefficient of matrix Y; Z_{ij} is the output quantization coefficient; q step the quantization step size; quantization parameters are from 1 to 52. For each additional 6 steps, the step will be doubled, and each 12% step will reduce the output encoding rate by approximately 12%. After transformation and quantization, the prediction residuals will be reordered by zigzag, and then the redundancy will be further reduced by fan coding.

It is often said that "customers are God." To make a platform well, you must stand from the user's point of view and consider everything for the user. Only when you understand what users really need, you can you design corresponding functions according to their needs. The "Smart Education Cloud Platform" is a platform that integrates school management, teacher teaching, student learning, and parental attention. It is aimed at the entire huge education system, ranging from education authorities to children's parents. Therefore, the platform divides the user groups into six user roles: (1) education authorities, (2) school administrators, (3) ordinary teaching teachers, (4) students, (5) parents, and (6) developmental technical service personnel.

One of the main characteristics of the cloud platform is that it can provide personalized services for users and can continuously expand the content and enrich the platform content and modules according to the user's needs. With the help of the cloud platform system management terminal equipment, users can build personalized content and categories according to their own needs and can also realize the remote upgrade of the platform according to their own needs, so as to promote the continuous expansion and docking of cloud platform functions. Teaching management workers are generally users of college teaching management in the cloud platform. They can manage and use the platform according to the development needs of the school and the development needs of teachers and students, provide more professional and targeted services for teachers and students, and realize the personalized development of college teaching management.

In order to reduce the burden of school users and make the platform more convenient to promote, deploy, maintain, and upgrade, the platform adopts B/S architecture. With the development of information technology, more and more software projects put forward higher requirements for packaging, reuse, and relocation. Adopting the B/S mode three-tier architecture is the best way to solve such problems. The Web side adopts Desktop technology based on Exts, and this interface is just like our commonly used windows operating system and mobile app, which not only change users' operating habits but also can load their required functions according to different users. In order to better develop and maintain the page display layer, this layer is divided into three layers according to MVC pattern: data layer, display layer, and control layer. A good database design can help the system improve service efficiency and meet the needs of various system users. The design of the database and the design of the system are synchronous, the requirements of the system are the basis of the database design, and the design of some data is based on the system requirements document. The design purpose of the database system is to effectively and quickly manage a large number of irregular data, store the data according to the rules formulated by the designer, and establish data query index and other information to facilitate data retrieval. The data in the application system may come from the information in the database; it may also be some equipment systems or services, and the database acts as a supporter.

3.3. Improved Genetic K-Means Clustering Algorithm Model. According to the actual communication between developers and customers, the problem encountered in the teaching system of the virtual desktop platform based on cloud computing is that the continuous growth of existing equipment brings pressure to the computer room space for various departments of the school. The problem encountered in the teaching system of the virtual desktop platform for computing is that the continuous growth of existing equipment brings pressure to the operation and maintenance management of various departments of the school. Schools generally hope to introduce virtual desktop platforms based on heterogeneous cloud computing. The actual requirements of the college's standardized teaching platform based on virtualization and cloud computing technology are as follows: (1) the number of computer room managers in the college is small, generally only one or two people are responsible, so the college requires that the platform must have a good interface. In other words, the management of the platform is required to be simple, which can reduce the workload of managers. (2) The monitoring of the virtual desktop system should be real-time because the number of computer room managers in the college is small (sometimes only one or two people are responsible), so the college data center requires that the standardized teaching platform must be able to monitor all the content of the virtual desktop in real time, and the administrator can extract the computer interface of any operator at any time. (3) In addition to the real-time monitoring module, due to the college's computer

room management, the number of personnel is small, and only one or two people are responsible in special cases. Therefore, the data center of the college requires that in the event of a general system intrusion and other dangerous situations, the system can actively send an alarm to the management personnel. (4) The standardized teaching platform also should have intelligent management capabilities. Under the conditions of virtualization and cloud technology, the system can reflect the use of hard disks in an all-round way. (5) The administrators of the college have limited technical level and limited management energy, so they cannot spend a lot of energy in the process of building a standardized teaching platform. It is necessary for the platform construction procedure to be straightforward and uncomplicated, with clear usage and system construction instructions, and a preplanned handling mechanism for frequently encountered common problems, which can form a detailed standardized teaching based on virtualization and cloud computing technology. The k-means algorithm assumes that there is no change in the adjacent cluster centers, the data object adjustment is completely completed, and the clustering criterion function J converges as the termination condition. A feature of the algorithm is that each data object is checked for correct classification during each iteration, and if not, it is reassigned. After all the data are allocated, modify the cluster center and objective function value and enter the next iteration. The k-means algorithm usually uses Euclidean distance as an index to measure similarity, and the

objective function J for evaluating the quality of division can be defined as

$$J = \sum_{i=1}^{k} \sum_{j=1}^{n} w_{ij} d_{ij}, \tag{5}$$

where k is the number of classes, n is the total number of sample points, $d_{ij} = \|x_i - z_i\|$ is the Euclidean distance, which indicates the distance from the original sample point x_j to the center c_i of class z_i, and z_i is the average of all data objects in class c_i, indicating which class the data objects belong to.

$$w_{ij} = \begin{cases} 1, \\ 0. \end{cases} \tag{6}$$

Formula (5) can also be expressed as

$$J = \sum_{i=1}^{k} \sum_{x_j \in C_i} d_{ij}^{\,2}. \tag{7}$$

d_{ij}^2 in this formula refers to the sum of the squared errors between the data object and the corresponding cluster center, so the objective function is also called the error sum of squares criterion function. Calculate the distance between each remaining data object and the cluster center, if it is satisfied.

$$D(x_i, c_k) = \min\{D(x_i, c_j), i = 1, 2, 3, \cdots i = 1, 2, 3, \cdots n, j = 1, 2, 3, \cdots k\}, \tag{8}$$

where x_i is classified into class C_k. According to the points in the divided sets, a new cluster center $c_1^*, c_2^*, c_3^*, \cdots, c_k^*$ is calculated as follows:

$$c_j^* = \frac{1}{n_j} \sum_{x_m \in C_j} x_m j = 1, 2, 3, \cdots K, \tag{9}$$

where n_j is the number of points in class C_j. Given the data object set $X = \{X1\ (1, 1), X2\ (1.2, 1.2), X3\ (0.8, 1.2), X4\ (0.9, 0.7), X5\ (1.3, 0.9), X6\ (1, 1.4), X7\ (3, 3), X8\ (3.1, 2.8), X9\ (3.2, 3.4), X10\ (2.7, 3), and X11\ (2.6, 2.9)\}$, the number of categories $k = 2$.

THE first iteration: select the third data object (0.8, 1.2) and the eighth data object (3.1, 2.8) as the initial cluster centers of classes $C1$ and $C2$. Calculate the distance from the first data object to the two clustering centers:

$$\|x_1 - x_3\| = \sqrt{(1 - 0.8)^2 + (1 - 1.2)^2} = 0.283,$$
$$\|x_1 - x_3\| = \sqrt{(1 - 3.1)^2 + (1 - 2.8)^2} = 2.766. \tag{10}$$

It can be seen from the abovementioned equations that $\|x_1 - x_3\| < \|x_1 - x_8\|$ divides $x1$ into the class to which $x3$ belongs.

According to the data objects in the divided classes, recalculate the cluster center of each class:

$$z_1 = \frac{((1 + 1.2 + 0.8 + 0.9 + 1.3 + 1), (1 + 1.2 + 1.2 + 0.7 + 0.9 + 1.4))}{6} = (1.033, 1.067). \tag{11}$$

The second iteration: using Z (1.033, 1.067) and Z (2.92, 3.08) as the clustering center of class C, redivide the dataset.

$X_1, X_2, X_3, X_4, X_5, and X_6$ are divided into class C to which x belongs, and $X_1 X_2 X_3 X_4$ are divided into class c to which x belongs.

$$Z_1 = (1.033, 1.067) = z_1,$$
$$Z_2 = (2.92, 3.08) = z_2. \tag{12}$$

During the two iterations, if the data objects in the two classes are changed, the iteration process is stopped. The two clusters obtained are $= \{X_1, X_2, X_3, X_4, X_5,\}$ and $c = \{X_1, X_2, X_3, X_4\}$.

4. Result Analysis and Discussion

Conceptual structure design is the first step of the database design. Conceptual design is a necessary condition for the successful design of logical database, which affects the design of the whole database. The data model includes two convenient contents. On the one hand, it is the static characteristics of data: it mainly includes the basic structure of data, the relationship between data, and the mutual constraints between data; the other is the dynamic characteristics of data: mainly including the methods of data operation. In the conceptual design of data, the commonly used method is to use the entity relation design model. After collecting and processing users' information and analyzing their needs, we provide users with personalized recommendation services. As the last link of the system, the selection and call of the teaching process service play a vital role in the final success or failure of the system. The development of this research system needs two parts: hardware environment and software environment. The hardware needed is router, reader, tag, computer, and network cable; the software environment used is win7 platform, and the program development language used is java programming language. The specific development, operation, and network environment of the system are shown in Table 1.

Selection, also known as heredity, is a natural law that simulates "survival of the fittest" in the biological world. For the initial population, not all individuals are scientifically reasonable, so it is necessary to select excellent individuals to pass on good genes to the next generation, so that the good varieties can be continued, and one generation is better than the other. There are many ways, such as gambling method and sorting method, to choose. This article will use the gambling method to select chromosomes for inheritance. When acquiring the location context information, the outdoor location context information is obtained through the GPS sensor that comes with android. There is a class Location Manager in Android that can locate the location of the mobile phone. For indoor location context information, we use RFID to determine the specific location of the student, and the specific method used is the improved VIRE algorithm mentioned in the previous section. Figures 3 and 4 are the comparison of the positioning error of the improved VIRE algorithm with the original VIRE algorithm and LANDMARC algorithm, as shown in Figures 3 and 4.

The gambling method is equivalent to placing a pointer in the picture below to rotate randomly and selecting chromosomes as parents from which area you go. In order to ensure "survival of the fittest," each area of the gambling table represents a certain range of fitness, and the population with high fitness occupies a large area, while the population with low fitness occupies a small area.

From the actual demand analysis of the virtual desktop teaching platform based on cloud computing, the system involves the following roles, as shown in Table 2.

A good physical classroom environment can effectively promote the teaching activities and directly affect the physical and mental activities of teachers and students. Combined with the characteristics of the Internet of Things technology, real-time comprehensive detection of changes in the classroom environment can be carried out. The experiment selects two factors that have a greater impact on teaching activities, namely, classroom temperature and light conditions, as the experimental monitoring objects, and uses two sets of different sensors to monitor the temperature and light changes in the selected classrooms to test the stability of intelligent nodes. Figure 5 shows the changes in lighting in the smart classroom, and Figure 6 shows the changes in indoor temperature. Figures 5 and 6.

As shown in Figures 5 and 6, the data monitored by different sensors in the same classroom area, the same deployment position, and the same working time have no obvious difference within the allowable error range due to their own energy consumption and the existence of heat generation problems of the equipment.

With the advent of the Internet era, the number of users has increased dramatically, and the performance of the website system has become an important indicator of the quality of the system. The performance indicators of the system mainly include response speed, the maximum number of concurrent users, and the maximum number of online users. After the development of this system, test tools are used to fake user interaction and send requests to the server concurrently. Table 3 shows the test cases of added functions.

This section mainly analyzes the bug introduction stage and defect introduction stage in detail. As shown in Figure 7, the result analysis of the test bug introduction stage is to analyze the proportion of the system requirements' analysis stage, coding stage, guessing stage, and release stage, respectively. It can be seen that most bugs are introduced in the coding part. It is necessary to strengthen the unit test of the system and realize the automation of the unit test. The number of bugs found in the release phase and testing phase is low, as shown in Figure 7.

As shown in Figure 8, the distribution diagram of defect introduction causes is analyzed in three parts: requirement design and related errors, coding errors, data corresponding

TABLE 1: Development environment.

	Client	Server side
Development environment	Myeclipse	MyEclipse + Protege + mysql
Operating environment	Android4.4	Win7 + Tomcat
Network environment	WLAN + GPRS	TYUT_IPv6
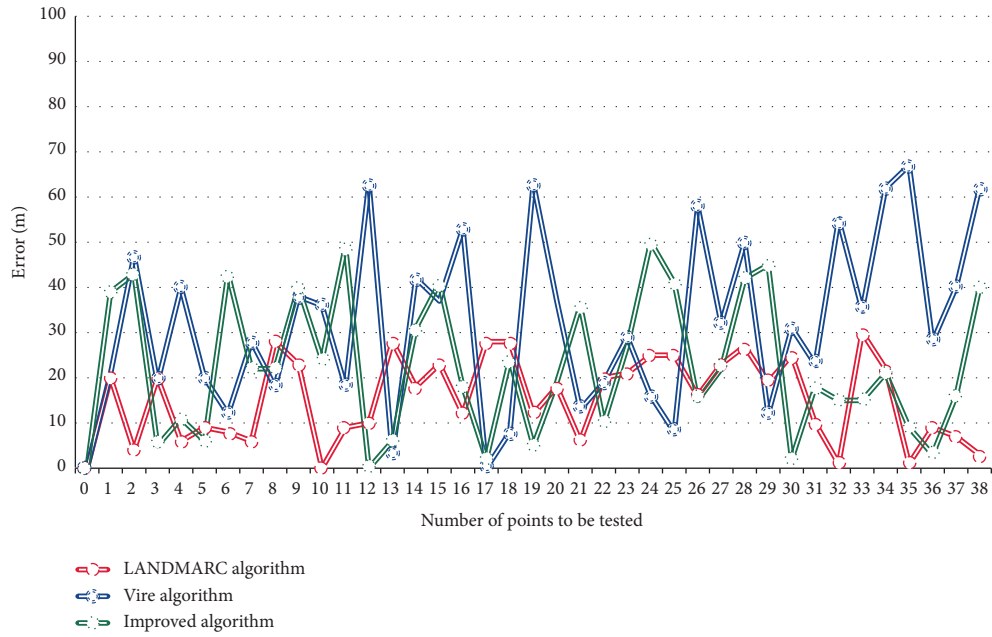
FIGURE 3: Positioning errors of different algorithms.
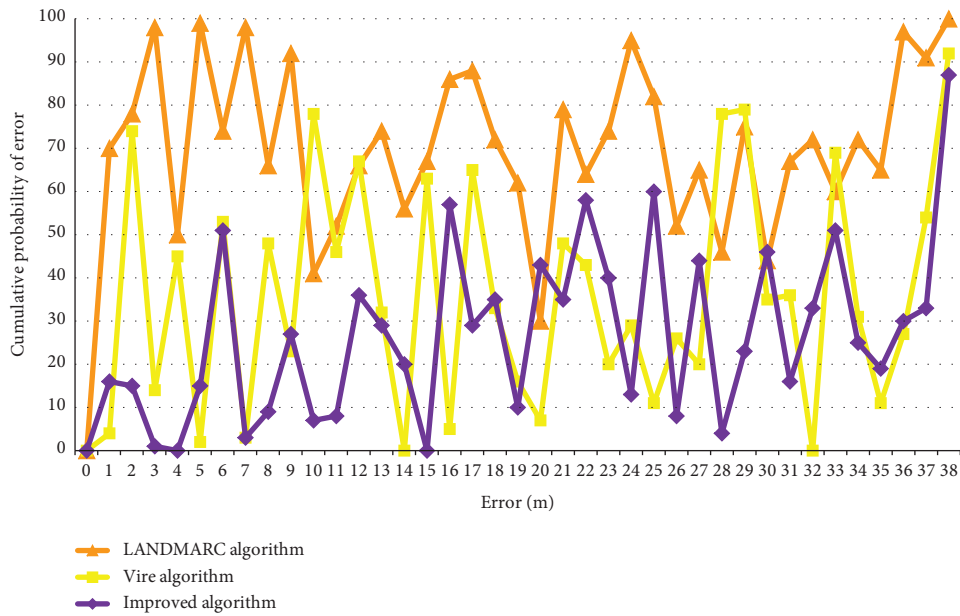
FIGURE 4: Error CDF curves after fitting by different algorithms.

TABLE 2: Role table.

Role	Responsibility or function
Platform management personnel	The main participants of platform management are responsible for the daily hardware maintenance and original update of the platform
Student	Main participants of the platform and users of various tasks of the platform
Teacher	Main participants of the platform and users of various tasks of the platform
Supermanager	The main participants of the platform are responsible for the overall management of the platform
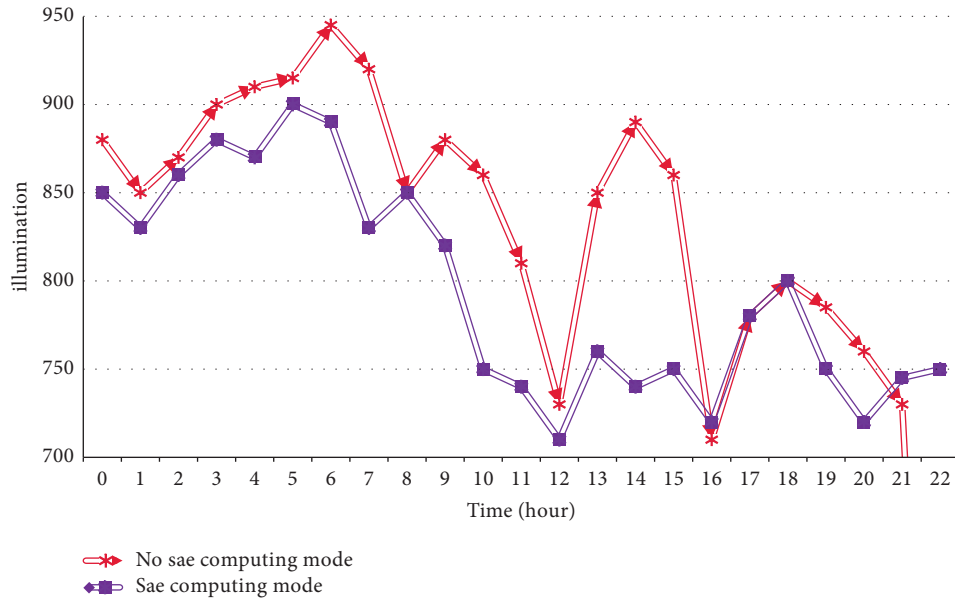
Figure 5: Comparison of teachers' lighting.
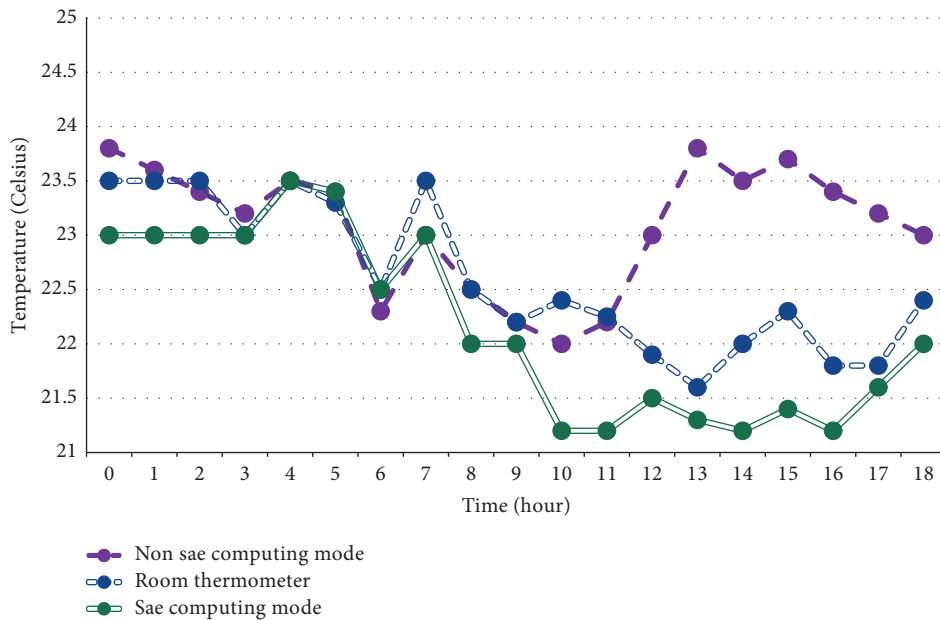
Figure 6: Temperature reading experiment diagram.

Table 3: Added test cases of course information input.

Test item	Added course information
Test content	Enter everything and click the "Submit" button
Preset condition	Turn on the server
Submission time	16 : 2 : 18
Reaction time	16 : 2 : 18
Time spent	<1 second
Print completion time	21 seconds
Time spent	1 second

results and data errors, ease of use, and test understanding errors, as shown in Figure 8.

The whole test results can be summarized as follows: (1) the biggest problem in the test process is the variability of requirements. Due to the deviation of developers and testers' understanding of requirements, everyone works with their own understanding. At this time, some bugs will be generated in the process of work. In addition, the requirements are not accurately defined, and these requirements are related to other functions. The requirements are changed, and the development and testing are also changed. (2) This test is mainly due to manual testing, and it cannot realize a large number of data operation function tests.
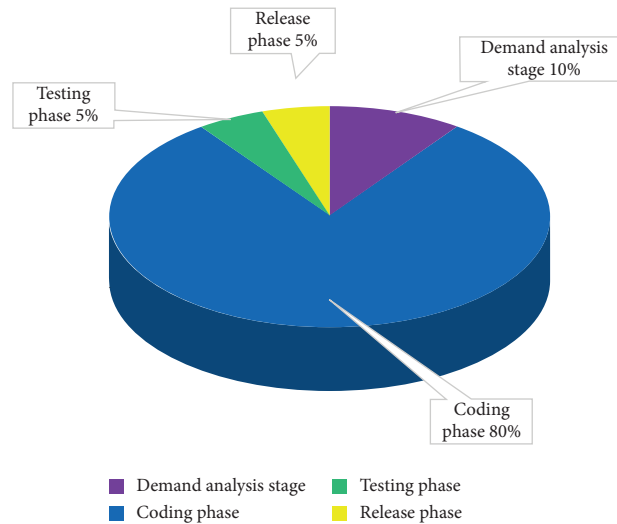
FIGURE 7: Analysis of test bug introduction stage results.
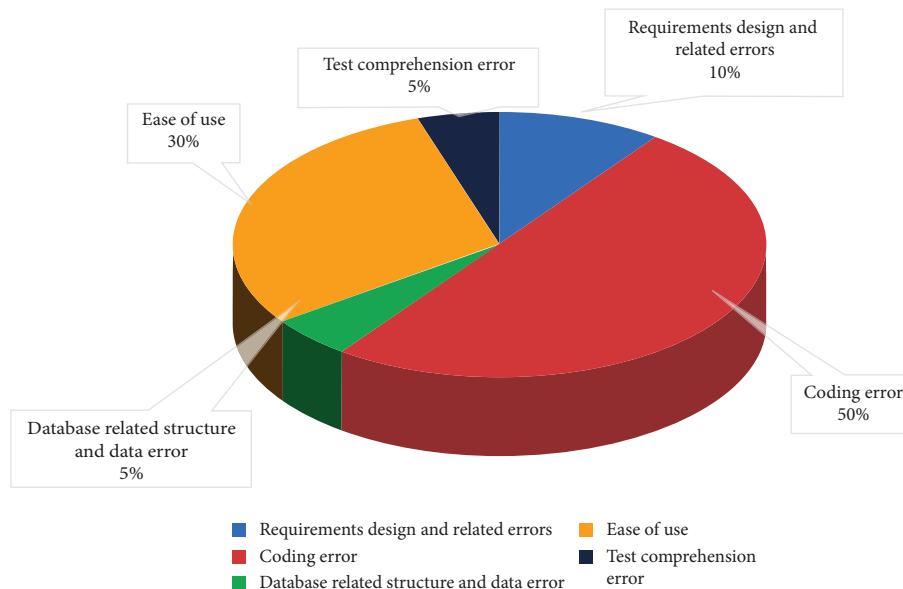
FIGURE 8: Distribution of defect introduction causes.

5. Conclusions

Aiming at the research topic of the teaching process management system for smart classroom, this paper is divided into five parts to analyze and implement. First, it provides convenient resource push and resource support services for the collaborative lesson preparation module, network teaching and research module, and teacher training module and other applications in the regional education cloud platform, which has achieved the original intention of the design. At the same time, because of the cloud computing architecture, it guarantees efficient and powerful computing power and its own stability. Second, the application set of smart campus is studied, and the construction scheme, demand analysis, and system design of the application set are analyzed in detail, so as to complete the construction of

resource sharing platform, teaching platform, and simulation system. This paper provides a test scheme for the application platform of the smart campus, gives the scheme of function test and performance test, and makes a test summary. It provides reference for the construction of similar educational service-sharing platforms. This paper mainly studies the method of building a smart campus cloud service platform and carries out demand analysis, design and implementation, and test summary. The paper is mainly divided into two parts: cloud computing service platform and cloud application platform.

Data Availability

The figures and tables used to support the findings of this study are included within the article.

Conflicts of Interest

The author declares that there are no conflicts of interest.

Acknowledgments

References

[1] N. M. Abrams and C. Management, "Systems for enhanced analysis in teaching laboratories," *Journal of Chemical Education*, vol. 89, no. 4, pp. 482–486, 2012.

[2] W. Li and X. Fan, "Construction of network multimedia teaching platform system of college sports," *Mathematical Problems in Engineering*, vol. 4, no. 7, pp. 36–62, 2021.

[3] J. A. Wickboldt, R. P. Esteves, M. B. de Carvalho, and L. Z. Granville, "Resource management in IaaS cloud platforms made flexible through programmability," *Computer Networks*, vol. 68, pp. 54–70, 2014.

[4] B. Wei, "Research on the application of distributed energy storage system based on energy cloud management platform," *Electrical Engineering*, vol. 4, no. 884, pp. 64–864, 2018.

[5] J. Song, "Huang. A scientific workflow management system architecture and its scheduling based on cloud service platform for manufacturing big data analytics," *International Journal of Advanced Manufacturing Technology*, vol. 367, no. 7, pp. 362–787, 2016.

[6] P. Y. Thomas, "Cloud computing: a potential paradigm for practising the scholarship of teaching and learning," *The Electronic Library*, vol. 29, no. 2, pp. 214–224, 2011.

[7] J. Macleod, H. H. Yang, S. Zhu, and Y. Li, "Understanding students' preferences toward the smart classroom learning environment: development and validation of an instrument," *Computers and Education*, vol. 122, no. 8, pp. 80–91, 2018.

[8] J. Hochweber, I. Hosenfeld, and E. Klieme, "Classroom composition, classroom management, and the relationship between student attributes and grades," *Journal of Educational Psychology*, vol. 106, no. 1, pp. 289–300, 2014.

[9] V. Taras, V. C. Dan, and D. Rottig, "A global classroom? Evaluating the effectiveness of global virtual collaboration as a teaching tool in management education," *The Academy of Management Learning and Education*, vol. 436, no. 7, pp. 36–675, 2013.

[10] A. Reeves, "Classroom collaborations: enabling sustainability education via student-community co-learning," *International Journal of Sustainability in Higher Education*, vol. 43, no. 32, pp. 534–9852, 2019.

[11] S. Reyes and D. Teaching, "Competence in higher education," *Sustainability*, vol. 13, no. 457, pp. 32–692, 2021.

[12] A. M. Alfoudari, C. M. Durugbo, and F. M. Aldhmour, "Understanding socio-technological challenges of smart classrooms using a systematic review," *Computers and Education*, vol. 173, no. 85, pp. 104282–104367, 2021.

[13] J. Aguilar, M. Sánchez, and J. Cordero, "Learning analytics tasks as services in smart classrooms," *Universal Access in the Information Society*, no. 47, pp. 4562–5386, 2017.

[14] T. J. Lampoltshammer, V. Albrecht, and C. Raith, "Teaching digital sustainability in higher education from a transdisciplinary perspective," *Sustainability*, vol. 13, no. 42, pp. 473–587, 2021.

[15] Z. K. Hou, H. L. Cheng, S. W. Sun, J. Chen, D. Q. Qi, and Z. B. Liu, "Crack propagation and hydraulic fracturing in different lithologies," *Applied Geophysics*, vol. 16, no. 2, pp. 243–251, 2019.

[16] C. E. Wolff, H. Jarodzka, and H. Boshuizen, "Classroom management scripts: a theoretical model contrasting expert and novice teachers' knowledge and awareness of classroom events," *Educational Psychology Review*, vol. 2020, no. 5, pp. 473–327, 2020.

[17] H. Cheng, J. Wei, and Z. Cheng, "Study on sedimentary facies and reservoir characteristics of Paleogene sandstone in Yingmaili block," *Tarim basin Geofluids*, vol. 2022, p. 2321, 2022.

[18] X. Li, J. Song, and B. Huang, "A scientific workflow management system architecture and its scheduling based on cloud service platform for manufacturing big data analytics," *International Journal of Advanced Manufacturing Technology*, vol. 84, no. 1-4, pp. 119–131, 2016.

[19] D. Campo and C.-M. Cristina, "Useful interactive teaching tool for learning: clickers in higher education," *Interactive Learning Environments*, vol. 234, no. 4, pp. 346–434, 2016.

[20] M. H. Baturay and O. F. Bay, "The effects of problem-based learning on the classroom community perceptions and achievement of web-based education students," *Computers and Education*, vol. 55, no. 1, pp. 43–52, 2010.

[21] J. Han, H. Cheng, Y. Shi, L. Wang, Y. Song, and W. Zhnag, "Connectivity analysis and application of fracture cave carbonate reservoir in Tazhong," *Science Technology and Engineering*, vol. 16, no. 5, pp. 147–152, 2016.

[22] J. Zhang and L. I. Wenjun, "Cloud media platform applied to explore the advantages of broad-spectrum innovation and entrepreneurship education," *Journal of Higher Education*, vol. 42, no. 00, pp. 43–682, 2018.

[23] H. Cheng, P. Ma, G. Dong, S. Zhang, J. Wei, and Q. Qin, "Characteristics of carboniferous volcanic reservoirs in beisantai oilfield, junggar basin," *Mathematical Problems in Engineering*, vol. 2022, pp. 1–10, 2022.

[24] M. Goos and A. Salomons, "Measuring teaching quality in higher education: assessing selection bias in course evaluations," *Research in Higher Education*, vol. 37, no. 837, pp. 724–547, 2017.

Retraction

Retracted: Effects of Gemcitabine and Oxaliplatin Combined with Apatinib on Immune Function and Levels of SIL-2R and sicAM-1 in Patients with Gallbladder Cancer

Computational Intelligence and Neuroscience

This article has been retracted by Hindawi following an investigation undertaken by the publisher [1]. This investigation has uncovered evidence of one or more of the following indicators of systematic manipulation of the publication process:

(1) Discrepancies in scope

(2) Discrepancies in the description of the research reported

(3) Discrepancies between the availability of data and the research described

(4) Inappropriate citations

(5) Incoherent, meaningless and/or irrelevant content included in the article

(6) Peer-review manipulation

The presence of these indicators undermines our confidence in the integrity of the article's content and we cannot, therefore, vouch for its reliability. Please note that this notice is intended solely to alert readers that the content of this article is unreliable. We have not investigated whether authors were aware of or involved in the systematic manipulation of the publication process.

Wiley and Hindawi regrets that the usual quality checks did not identify these issues before publication and have since put additional measures in place to safeguard research integrity.

We wish to credit our own Research Integrity and Research Publishing teams and anonymous and named external researchers and research integrity experts for contributing to this investigation.

The corresponding author, as the representative of all authors, has been given the opportunity to register their agreement or disagreement to this retraction. We have kept a record of any response received.

References

[1] L. Qu, K. Li, K. Liu, and W. Hu, "Effects of Gemcitabine and Oxaliplatin Combined with Apatinib on Immune Function and Levels of SIL-2R and SicAM-1 in Patients with Gallbladder Cancer," *Computational Intelligence and Neuroscience*, vol. 2022, Article ID 4959840, 8 pages, 2022.

Retraction

Retracted: Study on the Relationship between Unexplained Recurrent Abortion and HLA-DQ Gene Polymorphism

Computational Intelligence and Neuroscience

This article has been retracted by Hindawi following an investigation undertaken by the publisher [1]. This investigation has uncovered evidence of one or more of the following indicators of systematic manipulation of the publication process:

(1) Discrepancies in scope

(2) Discrepancies in the description of the research reported

(3) Discrepancies between the availability of data and the research described

(4) Inappropriate citations

(5) Incoherent, meaningless and/or irrelevant content included in the article

(6) Peer-review manipulation

The presence of these indicators undermines our confidence in the integrity of the article's content and we cannot, therefore, vouch for its reliability. Please note that this notice is intended solely to alert readers that the content of this article is unreliable. We have not investigated whether authors were aware of or involved in the systematic manipulation of the publication process.

In addition, our investigation has also shown that one or more of the following human-subject reporting requirements has not been met in this article: ethical approval by an Institutional Review Board (IRB) committee or equivalent, patient/participant consent to participate, and/or agreement to publish patient/participant details (where relevant).

Wiley and Hindawi regrets that the usual quality checks did not identify these issues before publication and have since put additional measures in place to safeguard research integrity.

We wish to credit our own Research Integrity and Research Publishing teams and anonymous and named external researchers and research integrity experts for contributing to this investigation.

The corresponding author, as the representative of all authors, has been given the opportunity to register their agreement or disagreement to this retraction. We have kept a record of any response received.

References

[1] J. Tang, J. Zhu, L. Shu, X. Huang, and S. Ma, "Study on the Relationship between Unexplained Recurrent Abortion and HLA-DQ Gene Polymorphism," *Computational Intelligence and Neuroscience*, vol. 2022, Article ID 8005538, 5 pages, 2022.

Retraction

Retracted: Analysis of Therapeutic Effect of Elderly Patients with Severe Heart Failure Based on LSTM Neural Model

Computational Intelligence and Neuroscience

This article has been retracted by Hindawi following an investigation undertaken by the publisher [1]. This investigation has uncovered evidence of one or more of the following indicators of systematic manipulation of the publication process:

(1) Discrepancies in scope

(2) Discrepancies in the description of the research reported

(3) Discrepancies between the availability of data and the research described

(4) Inappropriate citations

(5) Incoherent, meaningless and/or irrelevant content included in the article

(6) Peer-review manipulation

The presence of these indicators undermines our confidence in the integrity of the article's content and we cannot, therefore, vouch for its reliability. Please note that this notice is intended solely to alert readers that the content of this article is unreliable. We have not investigated whether authors were aware of or involved in the systematic manipulation of the publication process.

In addition, our investigation has also shown that one or more of the following human-subject reporting requirements has not been met in this article: ethical approval by an Institutional Review Board (IRB) committee or equivalent, patient/participant consent to participate, and/or agreement to publish patient/participant details (where relevant).

Wiley and Hindawi regrets that the usual quality checks did not identify these issues before publication and have since put additional measures in place to safeguard research integrity.

We wish to credit our own Research Integrity and Research Publishing teams and anonymous and named external researchers and research integrity experts for contributing to this investigation.

The corresponding author, as the representative of all authors, has been given the opportunity to register their agreement or disagreement to this retraction. We have kept a record of any response received.

References

[1] S. Chen and S. He, "Analysis of Therapeutic Effect of Elderly Patients with Severe Heart Failure Based on LSTM Neural Model," *Computational Intelligence and Neuroscience*, vol. 2022, Article ID 7250791, 10 pages, 2022.

Retraction

Retracted: Analytical Study of Financial Accounting and Management Trends Based on the Internet Era

Computational Intelligence and Neuroscience

This article has been retracted by Hindawi following an investigation undertaken by the publisher [1]. This investigation has uncovered evidence of one or more of the following indicators of systematic manipulation of the publication process:

(1) Discrepancies in scope

(2) Discrepancies in the description of the research reported

(3) Discrepancies between the availability of data and the research described

(4) Inappropriate citations

(5) Incoherent, meaningless and/or irrelevant content included in the article

(6) Peer-review manipulation

The presence of these indicators undermines our confidence in the integrity of the article's content and we cannot, therefore, vouch for its reliability. Please note that this notice is intended solely to alert readers that the content of this article is unreliable. We have not investigated whether authors were aware of or involved in the systematic manipulation of the publication process.

Wiley and Hindawi regrets that the usual quality checks did not identify these issues before publication and have since put additional measures in place to safeguard research integrity.

We wish to credit our own Research Integrity and Research Publishing teams and anonymous and named external researchers and research integrity experts for contributing to this investigation.

The corresponding author, as the representative of all authors, has been given the opportunity to register their agreement or disagreement to this retraction. We have kept a record of any response received.

References

[1] Q. Li, "Analytical Study of Financial Accounting and Management Trends Based on the Internet Era," *Computational Intelligence and Neuroscience*, vol. 2022, Article ID 5922614, 11 pages, 2022.

Retraction

Retracted: Urban Landscaping Landscape Design and Maintenance Management Method Based on Multisource Big Data Fusion

Computational Intelligence and Neuroscience

This article has been retracted by Hindawi following an investigation undertaken by the publisher [1]. This investigation has uncovered evidence of one or more of the following indicators of systematic manipulation of the publication process:

(1) Discrepancies in scope

(2) Discrepancies in the description of the research reported

(3) Discrepancies between the availability of data and the research described

(4) Inappropriate citations

(5) Incoherent, meaningless and/or irrelevant content included in the article

(6) Peer-review manipulation

The presence of these indicators undermines our confidence in the integrity of the article's content and we cannot, therefore, vouch for its reliability. Please note that this notice is intended solely to alert readers that the content of this article is unreliable. We have not investigated whether authors were aware of or involved in the systematic manipulation of the publication process.

Wiley and Hindawi regrets that the usual quality checks did not identify these issues before publication and have since put additional measures in place to safeguard research integrity.

We wish to credit our own Research Integrity and Research Publishing teams and anonymous and named external researchers and research integrity experts for contributing to this investigation.

The corresponding author, as the representative of all authors, has been given the opportunity to register their agreement or disagreement to this retraction. We have kept a record of any response received.

References

[1] L. Zhu, "Urban Landscaping Landscape Design and Maintenance Management Method Based on Multisource Big Data Fusion," *Computational Intelligence and Neuroscience*, vol. 2022, Article ID 1353668, 8 pages, 2022.

Retraction

Retracted: Cloud Statistics of Accounting Informatization Based on Statistics Mining

Computational Intelligence and Neuroscience

This article has been retracted by Hindawi following an investigation undertaken by the publisher [1]. This investigation has uncovered evidence of one or more of the following indicators of systematic manipulation of the publication process:

(1) Discrepancies in scope

(2) Discrepancies in the description of the research reported

(3) Discrepancies between the availability of data and the research described

(4) Inappropriate citations

(5) Incoherent, meaningless and/or irrelevant content included in the article

(6) Peer-review manipulation

The presence of these indicators undermines our confidence in the integrity of the article's content and we cannot, therefore, vouch for its reliability. Please note that this notice is intended solely to alert readers that the content of this article is unreliable. We have not investigated whether authors were aware of or involved in the systematic manipulation of the publication process.

Wiley and Hindawi regrets that the usual quality checks did not identify these issues before publication and have since put additional measures in place to safeguard research integrity.

We wish to credit our own Research Integrity and Research Publishing teams and anonymous and named external researchers and research integrity experts for contributing to this investigation.

The corresponding author, as the representative of all authors, has been given the opportunity to register their agreement or disagreement to this retraction. We have kept a record of any response received.

References

[1] T. Jin, B. Zhang, and Z. Yang, "Cloud Statistics of Accounting Informatization Based on Statistics Mining," *Computational Intelligence and Neuroscience*, vol. 2022, Article ID 3493678, 10 pages, 2022.

Hindawi

Retraction

Retracted: Dynamic Evaluation of Intensive Land Use Based on Objective Empowerment by Entropy Method and Neural Network Algorithm

Computational Intelligence and Neuroscience

This article has been retracted by Hindawi following an investigation undertaken by the publisher [1]. This investigation has uncovered evidence of one or more of the following indicators of systematic manipulation of the publication process:

(1) Discrepancies in scope

(2) Discrepancies in the description of the research reported

(3) Discrepancies between the availability of data and the research described

(4) Inappropriate citations

(5) Incoherent, meaningless and/or irrelevant content included in the article

(6) Peer-review manipulation

The presence of these indicators undermines our confidence in the integrity of the article's content and we cannot, therefore, vouch for its reliability. Please note that this notice is intended solely to alert readers that the content of this article is unreliable. We have not investigated whether authors were aware of or involved in the systematic manipulation of the publication process.

Wiley and Hindawi regrets that the usual quality checks did not identify these issues before publication and have since put additional measures in place to safeguard research integrity.

We wish to credit our own Research Integrity and Research Publishing teams and anonymous and named external researchers and research integrity experts for contributing to this investigation.

The corresponding author, as the representative of all authors, has been given the opportunity to register their agreement or disagreement to this retraction. We have kept a record of any response received.

References

[1] T. Yang, H. Cheng, H. Zhao, and D. Cadasse, "Dynamic Evaluation of Intensive Land Use Based on Objective Empowerment by Entropy Method and Neural Network Algorithm," *Computational Intelligence and Neuroscience*, vol. 2022, Article ID 2429826, 7 pages, 2022.

Retraction

Retracted: Mutual Trust Influence on the Correlation between the Quality of Corporate Internal Control and the Accounting Information Quality Using Deep Learning Assessment

Computational Intelligence and Neuroscience

This article has been retracted by Hindawi following an investigation undertaken by the publisher [1]. This investigation has uncovered evidence of one or more of the following indicators of systematic manipulation of the publication process:

(1) Discrepancies in scope

(2) Discrepancies in the description of the research reported

(3) Discrepancies between the availability of data and the research described

(4) Inappropriate citations

(5) Incoherent, meaningless and/or irrelevant content included in the article

(6) Peer-review manipulation

The presence of these indicators undermines our confidence in the integrity of the article's content and we cannot, therefore, vouch for its reliability. Please note that this notice is intended solely to alert readers that the content of this article is unreliable. We have not investigated whether authors were aware of or involved in the systematic manipulation of the publication process.

Wiley and Hindawi regrets that the usual quality checks did not identify these issues before publication and have since put additional measures in place to safeguard research integrity.

We wish to credit our own Research Integrity and Research Publishing teams and anonymous and named external researchers and research integrity experts for contributing to this investigation.

The corresponding author, as the representative of all authors, has been given the opportunity to register their agreement or disagreement to this retraction. We have kept a record of any response received.

References

[1] Y. Zhao, "Mutual Trust Influence on the Correlation between the Quality of Corporate Internal Control and the Accounting Information Quality Using Deep Learning Assessment," *Computational Intelligence and Neuroscience*, vol. 2022, Article ID 8257880, 10 pages, 2022.

Retraction

Retracted: Hypoxia-Induced Nestin Regulates Viability and Metabolism of Lung Cancer by Targeting Transcriptional Factor Nrf2, STAT3, and SOX2

Computational Intelligence and Neuroscience

This article has been retracted by Hindawi following an investigation undertaken by the publisher [1]. This investigation has uncovered evidence of one or more of the following indicators of systematic manipulation of the publication process:

(1) Discrepancies in scope

(2) Discrepancies in the description of the research reported

(3) Discrepancies between the availability of data and the research described

(4) Inappropriate citations

(5) Incoherent, meaningless and/or irrelevant content included in the article

(6) Peer-review manipulation

The presence of these indicators undermines our confidence in the integrity of the article's content and we cannot, therefore, vouch for its reliability. Please note that this notice is intended solely to alert readers that the content of this article is unreliable. We have not investigated whether authors were aware of or involved in the systematic manipulation of the publication process.

Wiley and Hindawi regrets that the usual quality checks did not identify these issues before publication and have since put additional measures in place to safeguard research integrity.

We wish to credit our own Research Integrity and Research Publishing teams and anonymous and named external researchers and research integrity experts for contributing to this investigation.

The corresponding author, as the representative of all authors, has been given the opportunity to register their agreement or disagreement to this retraction. We have kept a record of any response received.

References

[1] Y. Liu, X. Zhang, T. Jiang, and N. Du, "Hypoxia-Induced Nestin Regulates Viability and Metabolism of Lung Cancer by Targeting Transcriptional Factor Nrf2, STAT3, and SOX2," *Computational Intelligence and Neuroscience*, vol. 2022, Article ID 9811905, 7 pages, 2022.

Retraction

Retracted: Impact of Diabetic Nephropathy on Pulmonary Function and Clinical Outcomes

Computational Intelligence and Neuroscience

This article has been retracted by Hindawi following an investigation undertaken by the publisher [1]. This investigation has uncovered evidence of one or more of the following indicators of systematic manipulation of the publication process:

(1) Discrepancies in scope

(2) Discrepancies in the description of the research reported

(3) Discrepancies between the availability of data and the research described

(4) Inappropriate citations

(5) Incoherent, meaningless and/or irrelevant content included in the article

(6) Peer-review manipulation

The presence of these indicators undermines our confidence in the integrity of the article's content and we cannot, therefore, vouch for its reliability. Please note that this notice is intended solely to alert readers that the content of this article is unreliable. We have not investigated whether authors were aware of or involved in the systematic manipulation of the publication process.

Wiley and Hindawi regrets that the usual quality checks did not identify these issues before publication and have since put additional measures in place to safeguard research integrity.

We wish to credit our own Research Integrity and Research Publishing teams and anonymous and named external researchers and research integrity experts for contributing to this investigation.

The corresponding author, as the representative of all authors, has been given the opportunity to register their agreement or disagreement to this retraction. We have kept a record of any response received.

References

[1] C. Niu, L. Liu, Y. Li, and X. Li, "Impact of Diabetic Nephropathy on Pulmonary Function and Clinical Outcomes," *Computational Intelligence and Neuroscience*, vol. 2022, Article ID 8164034, 11 pages, 2022.

Research Article

Biometric Authentication and Correlation Analysis Based on CNN-SRU Hybrid Neural Network Model

Houding Zhang [iD] [1] **and Zexian Yang** [2]

[1]*University of Wollongong, Wollongong, Australia*
[2]*China Foreign Affairs University, Beijing, China*

Correspondence should be addressed to Houding Zhang; hz138@uowmail.edu.au

With the continuous development of computer technology, many institutions in society have higher requirements for the efficiency and reliability of identification systems. In sectors with a high-security level, the use of traditional key and smart card system has been replaced by the identification system of biometric technology. The use of fingerprint and face recognition in biometric technology is a biometric technology that does not constitute an infringement on the human body and is convenient and reliable. The biometric technology has been continuously improved, and the existing biometric technologies are based on unimodal biometric features. The unimodal biometric technology has its own limitations such as proposing single information and checking data affected by the environment, which makes it difficult for the technology to play its advantages in practical applications. In this paper, we use CNN-SRU deep learning to preprocess a large amount of complex data in the perceptual layer. The data collected in the perceptual layer are first transmitted to CNN convolutional neural network for simple classification and analysis and then arrives at the LSTM session to update again and optimize the screening to improve the biometric performance. The results show that the CNN-LSTM, CNN-GRU, and CNN algorithms show a decreasing trend in accuracy under the three error evaluation criteria of RMSE, MAE, and ME, from 0.35 to 0.07, 0.58 to 0.19, and 0.38 to 0.15, respectively. The recognition rate of multifeature fusion can reach 95.2%; the recognition efficiency of the multibiometric authentication system and accuracy rate has been significantly improved. It provides a strong guarantee for the regional standardization, high integration, generalization, and modularization of multibiometric identification system application products.

1. Introduction

The rapid development of computer information technology has put forward higher requirements for the update and processing of information technology [1, 2]. In the field of system security protection, relying solely on hardware devices has been difficult to meet customer needs. The traditional key-based authentication method becomes more and more unreliable and stable due to the large amount of data, the rapid spread, and the simple replication. Therefore, according to customer needs, we provide an overall solution and provide a multibiometric authentication platform to meet their actual needs. Biometric technology is a technology for automatic identification by collecting the

physiological characteristics and biological characteristics of the human body [3]. Human biometrics are relatively stable, and there are no problems such as loss and forgetting. Compared with the traditional cryptographic key authentication method [4–7], it has more effective system security. The biometric identification method uses the human body marking method, which is easy to carry with you and can realize real-time collection, identification, and judgment of biometric information. Generally speaking, human biometrics have seven characteristics, including universality, uniqueness, permanence, collectability, acceptability, safety, and performance requirements [8–10]; biometrics do not change with time and the environment. Large changes can be quantitatively collected and analyzed, the collected

feature information can meet the needs of users, and the features are not easy to be imitated or forged [11, 12]. The bottom line is that everyone is biometric and different.

Biometric technology has the characteristics of good anticounterfeiting performance, high security, and reliability and has become the most widely used security and identity authentication technology [13, 14]. Biometric technology relies heavily on physiological or behavioral features, and common face recognition [15, 16], language control [17], and fingerprint recognition [16, 18] can be used as biometrics. At present, the application of the above-mentioned biometric technology has made great progress, and the related scientific research at home and abroad has become more and more extensive. We are conducting a visual analysis of biometrics related to Chinese and English documents in the CNKI database, as shown in Figure 1. We found that the number of studies on biometrics gradually increased from 2000, and after 2005, the number of articles published each year was more than 1000, and in recent years, it reached more than 2000; meanwhile, in the study of the distribution of keywords and topics co-occurring in the articles, we could find that the keywords with the highest frequency were mainly biological characteristics, as shown in Figure 1. Face recognition, fingerprint recognition, algorithm research, recognition technology, etc., show that the algorithm research has gradually deepened and achieved extraordinary results in the research of biometrics. The study [19] focused their work on the application of machine learning to biometric speech, and they focused on the same concept of examining the recognition accuracy of the machine learning algorithm REPTree on a selected speech biometric dataset that was deployed and evaluated with the mining tool WEKA. The goal was to achieve a percentage greater than or equal to 95 in order to accurately classify the given sample data. In terms of processing other biometric information, a systematic study and comparison in ear biometrics has been conducted by [20]. They proposed another idea to perceive the ear in an online irregular orientation. This work can touch on the fitting of inwardly curved ears and the extraction of highlights from the internal drills of the ear edges. Here, the watchful edge recognition computation is used to locate the edges of the ear. The ear images are processed by the shape follower computation and then the rough images with edges are found as the yield of the frame. Finally, each of the three component vectors is decontrasted and compared with an alternate library of ear pictures and tracked for a specific match. In [21], they mainly used algorithms to enhance the security of face recognition techniques. In their paper, they proposed a fast and robust fuzzy C-mean clustering (FRFCM) algorithm and face recognition optically selective encryption scheme for biometric medical images. In the proposed scheme, a new selection method for obtaining regions of interest (ROI) based on the FRFCM algorithm is proposed. The security and robustness of the proposed cryptosystem is also verified by numerical simulations. The study [22] systematically analyzes the key points and difficulties of biometric techniques in spectral imaging. The reliability of conventional face recognition systems working in the visible range will be
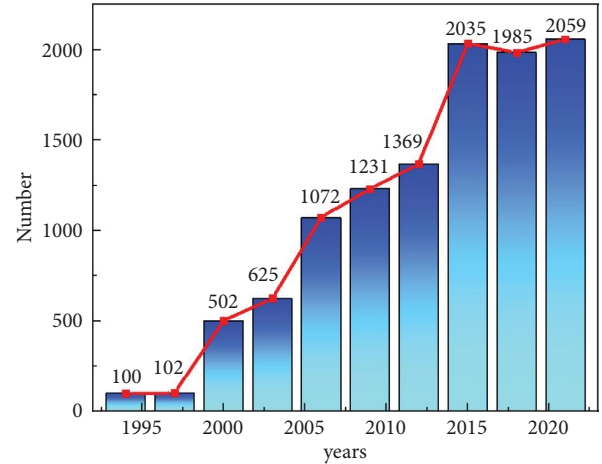
FIGURE 1: Trends in biometrics research.

affected by light variations, pose variations, and spoofing attacks. There are no large databases available for benchmark evaluation. Existing databases do not capture the same test subjects on all possible frequency bands for which experimental evaluations have been carried out. Also, this has been limited so far due to the small number of test objects and their images in the existing database. Deep learning based methods require a large number of parameters for training. This leads to overfitting due to the small number of such samples in the existing databases. The study [12] was conducted to remotely determine current human biological parameters by algorithmically processing infrared images of human faces. The problems that hinder the widespread use of remote biometric algorithms in practice are highlighted. The urgency of creating a metrological database containing video recordings of face images in the infrared range to assess the efficiency of biometric algorithms, time-synchronized records of human biometric parameters, and information on the complexity of the test tasks performed was confirmed. The structure of the laboratory system used to acquire complex data of the tested person is considered. A typical data structure for a single test cycle is given as shown in Figures 1 and 2.

Through the analysis and summary of the above-given literature research work, it can be seen that the development and application optimization of deep learning in biometrics has carried out systematic excellence. However, the research work on multibiometrics technology is still at an immature stage, and the evaluation standards are not uniform. Secondly, multibiometrics authentication also increases the burden on users. Not perfect in multibiometric fusion. Therefore, this paper studies the multibiometric recognition system through the fusion of facial features, speech recognition, and fingerprint recognition. In addition, we introduce three algorithms of CNN, LSTM, and GRU to extract and fuse biometric parameters. Optimization studies are conducted. In view of the problems such as the continuous increase of biometric data, the untimely update of features, and the resulting system lag, we optimize the algorithm to improve the system update rate and improve the
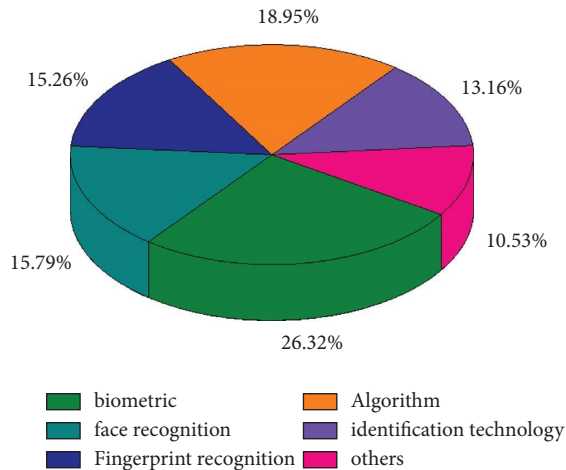
FIGURE 2: Proportion of research on keywords and topics.

security and stability of the biometric identification system. In addition, we analyze and study the collected 2000 data, and verify the robustness and accuracy of the algorithm through simulation.

Biometric identification technology, referred to as biometrics, is the identification and authentication of personal identity by acquiring biometric characteristics unique to human beings. We classify these inherent biometric characteristics into two major categories, namely, physiological characteristics and behavioral characteristics. Physiological characteristics are those that are innate and would not have led to changes in the absence of special factors. Typical examples are fingerprints, iris, DNA, etc. The other behavioral traits are mainly acquired habits. Typically, they are the voice of the person speaking, the font of the signature, etc., [23, 24].

All biometrics include the following processes: acquisition, decoding, comparison, and matching. The basic process is shown in Figure 3.

Biometric identification technology is mainly through the detection of the physical characteristics that the human body has always had so as to carry out identity confirmation, not all the characteristics of the human body can be used as the collection point for identification, and the characteristics that need to meet the following conditions can be used as the identification target:

(1) Uniqueness

Most of the human body's biological information has the characteristic of uniqueness, uniqueness mainly for the comparison between individual people, absolutely unique. In the case of fingerprints, the texture details are not the same between each individual.

(2) Stability

The biological information of a human individual always remains the same from birth to death, but of course, if the feature is changed or damaged by human or external factors, it will change. For this reason, it can be used to identify individuals.

(3) Identifiability

The biometric characteristics of human beings are very different from each other, and by using certain computer algorithms, it is possible to distinguish this information and identify the key elements of the characteristics, making it possible to use the identification technology in a wide area.

(4) Capturability

With the development of computer technology and related hardware technology, the image quality and pixels of the feature image information collected by the instrument are also improved, making the image a convenient carrier for recognition.

2. The Feasibility of CNN Network in Biometric Authentication

With the rapid development of science and technology, more and more information is obtained and authorized remotely through online, and the required resources can be legally accessed and the right of application is a necessary condition for the security of the internal data of the communication system. In addition, in the network environment, how to identify and verify the reliability of biometric information, safely realize remote authentication, and ensure the privacy of biometrics from illegal use has become the main problem to be solved in this paper. Therefore, this paper proposes a 2D CNN network to track the lines in electronic data and implement vectorization to realize the recognition processing. 2D CNN can not only extract features from a large number of graphs, data reconstruction, and other preprocessing methods. At the same time, each computing layer itself has the same weight for sharing links, which greatly reduces the computing cost and computing time and avoids too many parameters affecting the clarity of text/graphics. In addition, LSTM can easily and accurately capture the main information of the sequence from pictures to speech because of its linear structure. Strive to propose a CNN-LSTM network based on deep learning biometric authentication to provide an effective solution quickly, conveniently, and safely.

2.1. Structure of CNN Network. Figure 4 presents a generalized framework for digital image source forensics under the CNN model theory. In the image preprocessing, the image to be detected is first cut into image blocks (P_k in Figure 4(a) indicates the k th image block), and then the image fingerprint characterizing the source of the shot is extracted using CNN (image feature extraction in Figure 4(b)), and the detection result Y_k of each image block is output (Y_k in Figure 4(c) indicates the feature extractor predicts the label for the k th image block), and the majority voting algorithm is used to fuse the detection results of the k th image block and output the image level prediction results, i.e., device model multiclassification identification.
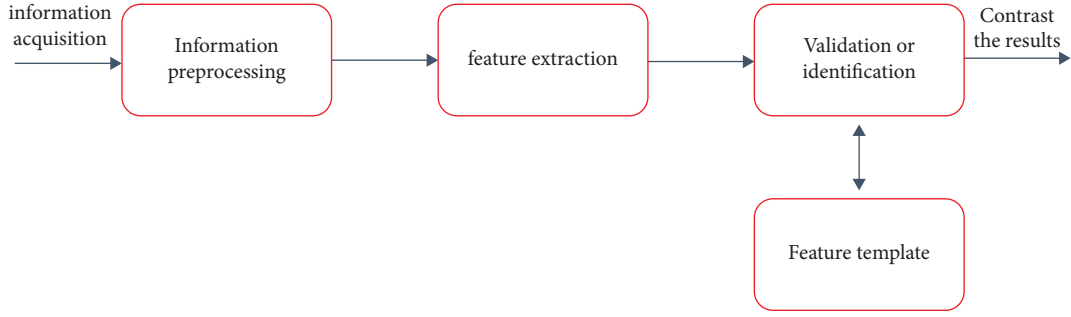
FIGURE 3: Biometric basic processing flow.

(a)   (b)   (c)
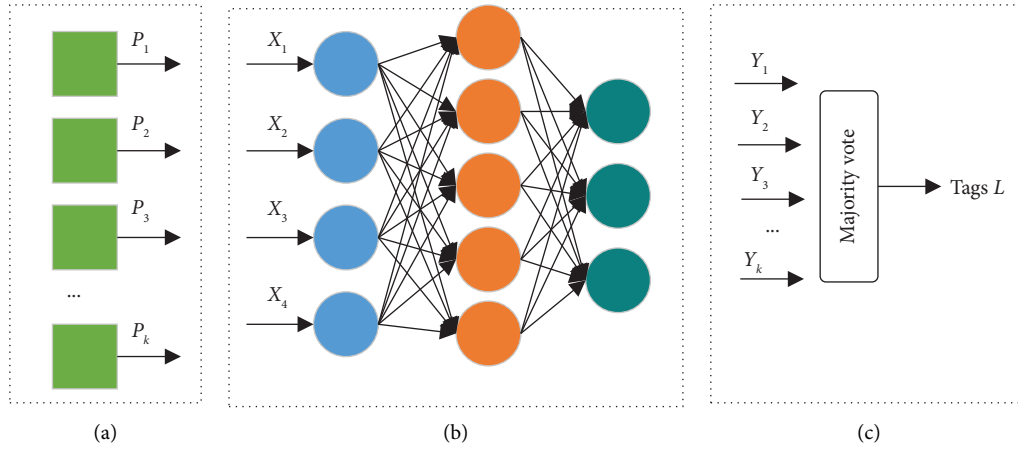
FIGURE 4: Digital image source framework based on CNN. (a) Image preprocessing. (b) Image feature extraction. (c) Classification result voting.

2.2. Learning Algorithm of CNN Network. The training process of the CNN network is mainly divided into forward propagation and back propagation [25]. First, by inputting data to the convolution layer, the feature extraction is performed on the convolution operation based on the filter and the convolution kernel (Kernel), the feature map is obtained, and the bias term is added to it, and then the activation function (ReLu, Tanh, sigmoid, and softmax) to calculate the output of the convolutional layer; the pooling layer samples the data processed by the receiving convolutional layer, and then converts the feature map into a vector by stretching and sums the weighted biases. Finally, the class probability output is obtained through the activation function, and the calculation is repeated until the loss function is the minimum value [26].

(1) Calculation of the convolutional layer. The convolution formula is shown in equation (1), the input x is weighted w, and the bias b is added, and finally the total sum obtained is output through the nonlinear activation function f.

$$a_{d,i,j} = f\left(\sum_{d=0}^{D-1}\sum_{m=0}^{F-1}\sum_{n=0}^{F-1} w_{d,m,n} x_{d,j+m,j+n} + b\right). \quad (1)$$

Among them, D and F are the number of filters and the size of the convolution kernel, respectively.

(2) Calculation of pooling layer and full connection. The pooling layer retains the main effective information by locally sampling the feature map and reduces the influence of unnecessary data on the calculation result. In addition, as long as there is a relative relationship with the main information of the feature map, no matter whether the image is scaled, distorted, translated, etc., the accuracy of the result cannot be affected. After the data is passed through the pooling layer, a large number of parameters can be filtered out, which can improve the training accuracy and reduce the error. The average sampling method sampled in this paper samples the feature map, and in the traversed region, the average value is selected as the new feature of the region. Due to the characteristics of CNN itself, under the action of the fully connected layer, the output of the convolutional layer is weighted w offset summation, and then output through the activation function f, as shown in the following equation:

$$y = f(w \cdot x + b). \quad (2)$$

(3) Calculation of softmax output layer. The activation function nonlinearizes the total number of weighted bias sums to solve the multiclass problem, and its calculation formula is as follows:

$$y_k = \frac{e^{a_j}}{\sum_{i=1}^{n} e^{a_i}}. \tag{3}$$

In the formula, n is the number of inputs.

(4) Back propagation

(1)–(3) are forward propagation, and the error is calculated by the loss function for reverse propagation. The process is divided into three main parts:

(a) Calculate the network error from the predicted and actual results:

$$\delta^{i,l} = -\left(y_{\text{real}}(i) - y_{\text{predict}}(i)\right) * \sigma\left(a^{i,l}\right). \tag{4}$$

Among them, y_{predict} is the prediction data, y_{real} is the experimental data.

(b) The calculation error is passed in the reverse direction. The specific propagation formula of CNN is as follows:
Fully connected layer.

$$\delta^{i,l} = \left(w^{l+1}\right)^T \delta^{i,l+1} \odot \sigma\left(a^{i,l}\right). \tag{5}$$

Convolutional layer.

$$\delta^{i,l} = \delta^{i,l+1} * \text{rot}180\left(w^{l+1}\right) \odot \sigma\left(a^{i,l}\right). \tag{6}$$

Pooling layer.

$$\delta^{i,l} = \text{upsample}\left(\delta^{i,l+1}\right) \odot \sigma\left(a^{i,l}\right). \tag{7}$$

Among them, l is the current layer and $\sigma\left(a^{i,l}\right)$ is the activation function.

(c) The final goal of reverse transfer is to update the weight w and bias b, and the specific calculation is as follows.
Weight update in the fully connected layer:

$$w^l = w^l - \alpha \sum_{i=1}^{m} \delta^{i,l}\left(\alpha^{i,l-1}\right)^T. \tag{8}$$

Fully connected layer bias update.

$$b^l = b^l - \alpha \sum_{i=1}^{m} \delta^{i,l}. \tag{9}$$

Weight update in the fully connected layer.

$$w^l = w^l - \alpha \sum_{i=1}^{m} \alpha^{i,l-1} * \delta^{i,l}. \tag{10}$$

Bias update in fully connected layer:

$$b^l = b^l - \alpha \sum_{i=1}^{m} \sum_{u,v} \left(\delta^{i,l}\right)_{u,v}. \tag{11}$$

Among them, $\alpha^{i,l-1}$ is the output of the ith neuron in the l-1th layer.

In addition, this paper chooses the cross entropy loss function as the loss function, and the formula is as follows:

$$J_c = -\frac{1}{N} \sum_{1}^{N} \sum_{i=1}^{k} y(i)\log\left(y_c(i)\right). \tag{12}$$

Among them, $y_c(i)$ is the predicted value, $y(i)$ is the real value, and N is the number of samples.

2.3. LSTM Network. A single-channel LSTM-based method for analyzing factors related to youth physical activity behavior mainly includes: LSTM neural networks that use memory units to avoid gradient disappearance and gradient explosion during backpropagation and can learn long-term dependencies and make full use of historical information. The LSTM was improved and extended in 2013 by [27, 28], making it widely used in natural language processing, speech recognition, and other fields.

As shown in Figure 5, the LSTM unit has a memory unit c for saving historical information. The updating and utilization of the history information is controlled by three gates: input gate i, forget gate f, and output gate o. The updating process of the LSTM unit at time t is as follows:

$$\begin{aligned}
i_t &= \sigma W_i x_t + U_i h_{t-1} + V_i c_{t-1}), \\
c_t &= \tan h\left(W_c x_t + U_c h_{t-1}\right), \\
f_t &= \sigma W_f x_t + U_f h_{t-1} + V_f c_{t-1}), \\
c_t &= f_t \odot c_{t-1} + i_t \odot c_t, \\
o_t &= \sigma W_o x_t + U_o h_{t-1} + V_o c_t), \\
h_t &= o_t \odot \tanh\left(c_t\right),
\end{aligned} \tag{13}$$

where x_i is the input data of the memory unit, σ is the logistic sigmoid function, the symbol $\odot$ is the dot product operation between vectors, and $W_i, W_f, W_c, W_o, U_i, U_f, U_c, U_o, V_o$ is the weight matrix. i_t, o_t, f_t, c_t are the values of the input gate, output gate, forgetting gate, and memory cell at time t, respectively, c_t are the values of the candidate memory states of the memory cell, and h_t are the outputs of the LSTM cell at time t.

For the analysis of the factors associated with youth physical activity behavior, we first used the random undersampling method to obtain a balanced sample of the factors associated with each youth physical activity behavior and then used a single-channel LSTM neural network as the classification method. Figure 6 shows the framework of the single-channel LSTM neural network classifier, which has only one LSTM layer. The first dashed box shows the internal structure of the single-channel LSTM model, and the second dashed box shows the process of unbalanced samples. The input to the LSTM model is a word vector representation of the training samples, which has good semantic features and is a common way to represent word features. The input feature vectors are passed through the LSTM layer to obtain high-dimensional vectors, which can learn deeper features that can better describe the samples. The fully-connected
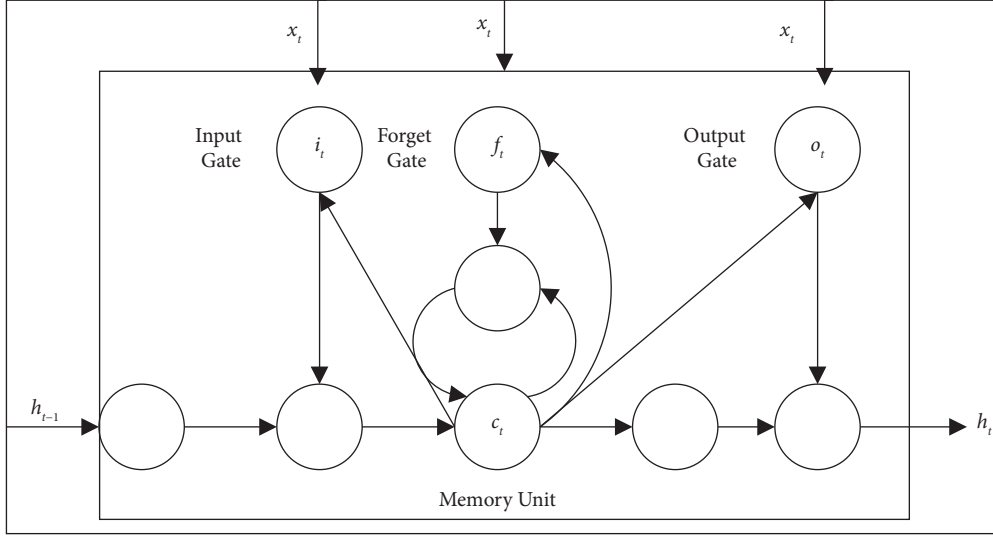
FIGURE 5: LSTM unit.
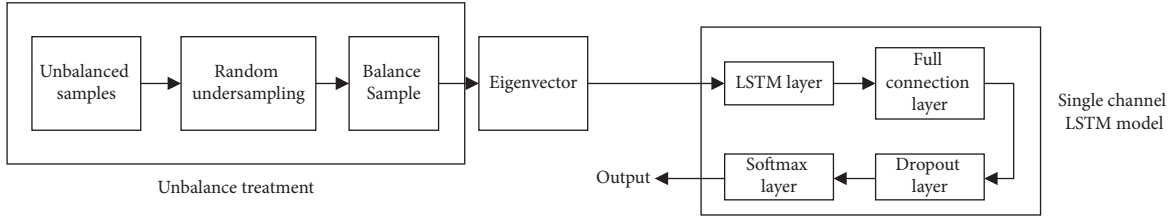
FIGURE 6: Single-channel LSTM neural network classifier framework.

layer is similar to the hidden layer of a traditional multilayer perceptron, receiving all the outputs from the previous layer, weighting and summing these output vectors, and propagating the weighted outputs through the excitation function to the dropout layer. In this experiment, the layer uses ReLu as the excitation function, which reduces the interdependence between parameters and is closer to the biological activation model, and the excitation function is shown in (14).

$$g(x) = \max(0, x), \tag{14}$$

where x is the output vector and the ReLu function sets all values less than 0 to 0, with the ability to bootstrap moderate sparsity. The dropout layer randomly leaves some hidden layer nodes in the network inactive during training and prediction, reducing the number of features and effectively preventing the network from overfitting. The dropout layer appears as a hidden layer in the LST M neural network model, as shown in the following equation:

$$g = h^* \bullet D(p), \tag{15}$$

where D denotes the dropout operator and p is an adjustable superparameter (the ratio of retained hidden layer cells).

Finally, the output of the single-channel LST M model is used to classify the samples by the Softmax output layer. We choose the category with the highest posterior probability as the prediction label, as shown in the following equation:

$$\text{label}_{\text{pred}} = \text{argmax}_i P(Y = i | x, W, U, V), \tag{16}$$

where x is the upper layer output vector, i is the label prediction, W, U, V are the coefficient matrices in the LSTM update method, and $\text{label}_{\text{pred}}$ is the predicted label with the highest posterior probability.

2.4. Data Preprocessing and Model Parameter Determination

2.4.1. Normalization Processing. Since the magnitude of data input by different channels is very different, it will affect the increase of training error. Therefore, we first need to normalize the data to normalize all inputs to the same interval. In this paper, we choose max-min normalization for normalization, and the calculation method is as follows:

$$X = \frac{x - x_{\min}}{x_{\max} - x_{\min}}. \tag{17}$$

Among them, $x_{\max}$ is the maximum value in the data set, $x_{\min}$ is the minimum value in the data set. After normalization, the training error will not increase due to the order of magnitude between the data.

2.4.2. Determination of Model Parameters. The main influencing factors of biometric vectorization are physiological characteristics and behavioral characteristics. Physiological features include fingerprints, facial images, and

irises which are identified according to each individual's unique biological features; behavioral features are gait, voice, handwriting, etc., which are also a method of identifying the appraiser. For example, when identifying a person's handwriting, the outline of the font is clear and distinct, and the effect of the network calculation on displaying the vector diagram is more obvious; the more the number of words, the more data the network can obtain, which makes the network output results have a certain robustness. Specific steps are as follows:

(1) The two categories of parameters, physiological characteristics, and behavioral characteristics, are used as the input nodes of the prediction model, and predictions are used as the output nodes of the prediction model.

(2) The hidden layer plays a key role in the network architecture. The number of filters in the convolutional layer in this model 2D CNN is 2, the size of the convolution kernel is 16, the stride is 1, and the padding is 2. The LSTM layer nodes are 4, and the fully connected layer nodes are 3.

(3) In order to adjust the appropriate learning rate parameters and avoid overfitting or underfitting, it is necessary to continuously test and adjust. The Adam algorithm model is used, and the learning rate parameter is finally selected as 0.0014 and the decay rate is 0.08 [29].

(4) After data preprocessing, the data can be used as an input layer node to output the results.

2.4.3. Several Multibiometric Systems. We can use different feature points, sensors, and feature extraction quantities and methods, multibiometric systems can have the following combinations:

(1) Unimodal biometric, a combination of multiple sensors, where the biometric features of the same target are acquired by multiple sensors, so that the sample data can be acquired twice. By acquiring face feature data in this way, this data is combined in the data layer and the matching layer, which can effectively improve the recognition rate of the face recognition system.

(2) The combination of unimodal biometric features, multiple classifiers, and one sensor is different from unimodal biometric features in that biometric data is acquired by one sensor and these sample data are processed by multiple classifiers. The respective defined features are generated. Matching at the logical layer can improve the recognition rate.

(3) Unimodal biometric features, a combination of multiple categories, in the case of iris and fingerprint features, extracts two or more biometric information from the target person. This combination does not require multiple sensors to acquire information and is not particularly demanding for multiple feature extraction and matching models.

(4) Combination of multiple biometric features, the combination is to use multiple biometric features for recognition and obtain different feature data by different sensors. Due to the relative independence of the biometric features and thus the accuracy of the recognition system is greatly improved.

3. Experimental Verification and Comparative Analysis

3.1. Comparative Analysis of Recognition Accuracy of Biometric Results. In order to verify that the CNN-LSTM network has better performance, this paper compares and analyzes CNN, CNN-GRU, and CNN-LSTM. In order to further analyze the performance of these three networks, we choose root mean square error as the evaluation index: root mean square error (RMSE): measure the error between the observed value and the actual value which is calculated as follows:

$$\text{RMSE}(X, h) = \sqrt{\frac{1}{N} \sum_{i=1}^{N} \left(h(x_i) - y_i \right)^2}. \tag{18}$$

Specifically, compared with the actual results, the RMSE of the CNN-LSTM algorithm is smaller than that of the CNN-GRU algorithm and CNN algorithm, which are 0.07, 0.17, and 0.35, respectively, and the CNN-LSTM algorithm is improved by 59% and 80%, as shown in Figure 7. Using the CNN-LSTM recognition technology with fast acquisition speed and high efficiency of feature comparison for effective recognition has great potential value for future biometric optimization, as shown in Figure 7.

In addition, the error of the CNN-LSTM algorithm is smaller than that of the CNN-GRU algorithm and CNN algorithm, which are 0.19, 0.31, and 0.58, respectively, and the CNN-LSTM algorithm improves 38% and 57% compared with the actual results of physiological features, as shown in Figure 8.

Finally, compared with the actual results, the CNN-LSTM algorithm has smaller errors than the CNN-GRU algorithm and CNN algorithm in terms of physiological and behavioral features of speech, which are 0.15, 0.22, and 0.38, respectively, and the improvement of the CNN-LSTM algorithm is 32% and 60%, respectively,
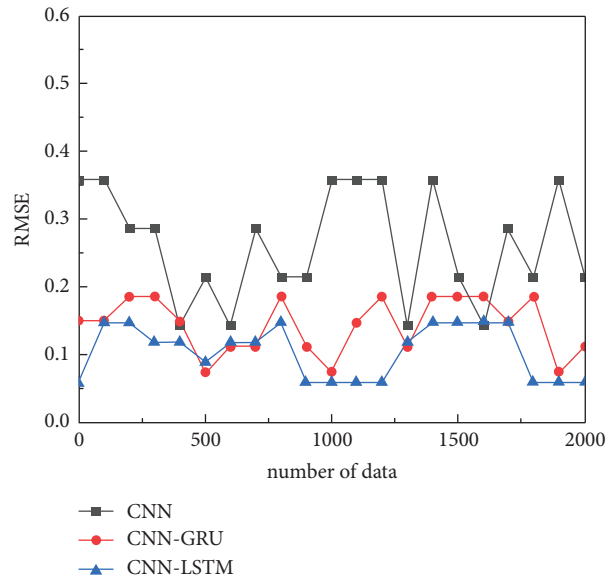
Figure 7: RMSE error plot of fingerprint biometrics in physiological features.
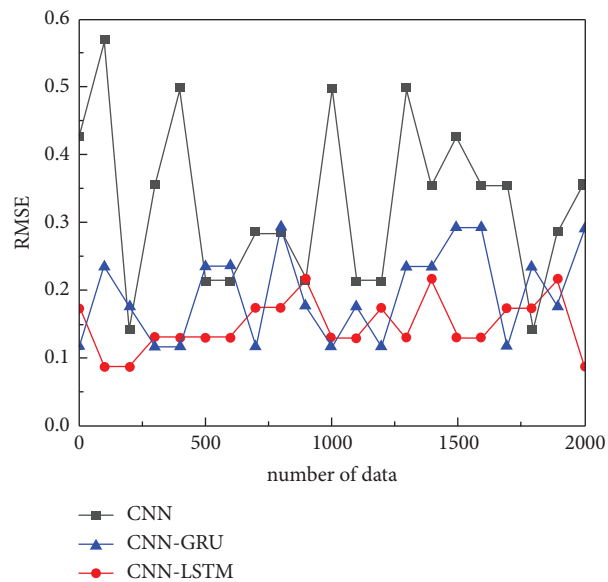
Figure 8: RMSE error plot of face biometric recognition in physiological features.

illustrating the excellent performance of CNN-LSTM deep learning in biometric recognition as shown in Figure 9.

In the biometric system, only the sound feature is used in long-term applications, and the biometric recognition accuracy can reach up to 67.7%, the fingerprint recognition accuracy can reach up to 82.1%, and the face recognition accuracy can reach up to 84.5%. The multifeature fusion recognition can reach up to 95.2%. This shows that the algorithm can better match the actual needs of biometric identification. It can greatly improve the recognition accuracy and improve the recognition efficiency as shown in Figure 10 and Table 1.
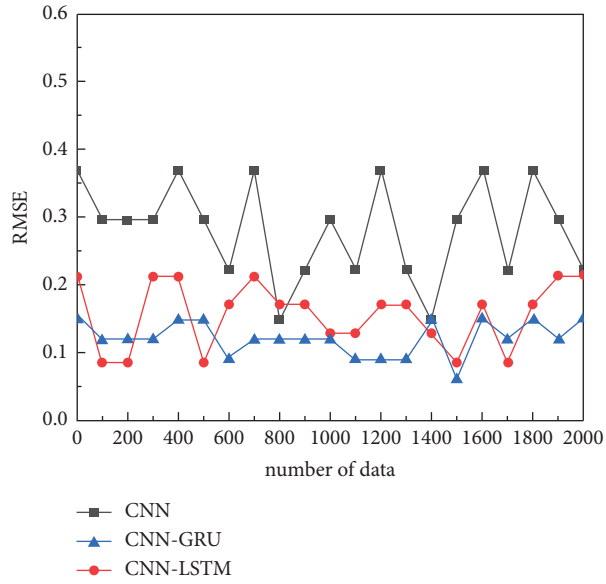
FIGURE 9: RMSE error plot for biometric recognition of voices in behavioral traits.
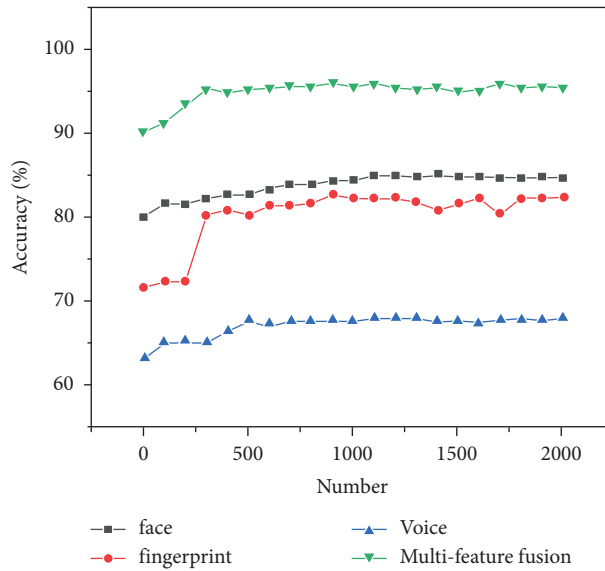
FIGURE 10: Overall recognition result of biometric identification of fingerprints, faces in physiological features, and voices in behavioral features.

TABLE 1: Comparison of RMSE of three algorithms in different application scenarios.

	Fingerprint identification	Image recognition	Voice recognition
CNN	0.35	0.58	0.38
CNN-GRU	0.17	0.31	0.22
CNN-LSTM	0.07	0.19	0.15

4. Conclusion

In this paper, we give a basic description of the concept of multicommunication framework and neural network algorithm and introduce the structure and calculation process of SRU algorithm for wireless communication receiving module. And, we compared the three algorithms of SRU, GRU, and LSTM, and the hidden layer, number of nodes, number of iterations, learning rate, and activation function in the network structure are all the same. the result shows the following theories:

(1) In the fingerprint biometric identification of physiological characteristics, the accuracy of CNN-LSTM, CNN-GRU, and CNN algorithm shows a downward trend under the RMSE error evaluation standard, from a maximum of 0.35 to 0.07, a maximum increase of 80%;

(2) The accuracy of CNN-LSTM, CNN-GRU, and CNN algorithms in facial biometric recognition in physiological features shows a downward trend under the RMSE error evaluation standard, from a maximum of 0.58 to 0.19, a maximum increase of 57%;

(3) In the biometric recognition of sounds in behavioral features, the accuracy of CNN-LSTM, CNN-GRU, and CNN algorithms shows a downward trend under the RMSE error evaluation standard, from a maximum of 0.38 to 0.15, a maximum increase of 60%; It illustrates the excellent performance of CNN-LSTM deep learning in biometric identification.

(4) Multifeature fusion recognition can reach up to 95.2%, compared with 84.5%, 82.1%, and 67.7% of single face recognition, fingerprint recognition, voice recognition, etc., which have a great improvement, which shows that the algorithm can better match the actual needs of biometrics. It provides a strong guarantee for the regional standardization, high integration, generalization, and modularization of multibiometrics system application products.

At present, the system has been applied in a large number of customers, but after the actual use, the system still reveals some problems, and recognition technology still needs to be improved; these will be the focus of later work. With the biometric identification technology application in the field is deepening and the scope is expanding, many enterprises are investing more and more in this technology. The updated speed of biometric identification technology will also be accelerated. For the application software of biometrics technology, if it needs to have a lasting vitality, it needs to keep up with the advanced technology. Due to the development period and resources, this system still has many unsatisfactory points and needs to be improved later.

Data Availability

The experimental data used to support the findings of this study are available from the corresponding author upon request.

Conflicts of Interest

The authors declared that there are no conflicts of interest regarding this work.

References

[1] M. S. Alkatheiri, "Artificial intelligence assisted improved human-computer interactions for computer systems," *Computers & Electrical Engineering*, vol. 101, Article ID 107950, 2022.

[2] C. Gonzalez Viejo, S. Fuentes, K. Howell, D. Torrico, and F. R. Dunshea, "Robotics and computer vision techniques combined with non-invasive consumer biometrics to assess quality traits from beer foamability using machine learning: a potential for artificial intelligence applications," *Food Control*, vol. 92, pp. 72–79, 2018.

[3] Y. Yu, H. Wang, H. Sun, Y. Zhang, P. Chen, and R. Liang, "Optical coherence tomography in fingertip biometrics," *Optics and Lasers in Engineering*, vol. 151, Article ID 106868, 2022.

[4] M. R. Abuturab and A. Alfalou, "Multiple color image fusion, compression, and encryption using compressive sensing, chaotic-biometric keys, and optical fractional Fourier transform," *Optics & Laser Technology*, vol. 151, Article ID 108071, 2022.

[5] S. Padmanabhan and R. Kr, "Optimal feature selection-based biometric key management for identity management system: emotion oriented facial biometric system," *Journal of Visual Communication and Image Representation*, vol. 74, Article ID 103002, 2021.

[6] E. S. A. El-Dahshan, M. M. Bassiouni, S. Sharvia, and A. B. M. Salem, "PCG signals for biometric authentication systems: an in-depth review," *Computer Science Review*, vol. 41, Article ID 100420, 2021.

[7] Z. Müftüoğlu and T. Yildirim, "Comparative analysis of crypto systems using biometric key," *Procedia Computer Science*, vol. 154, pp. 327–331, 2019.

[8] M. M. Anwar, "Brain-printing biometrics underlying mechanism as an early diagnostic technique for Alzheimer's disease neurodegenerative type," *Current Research in Physiology*, vol. 4, pp. 216–222, 2021.

[9] A. I. Awad, "From classical methods to animal biometrics: a review on cattle identification and tracking," *Computers and Electronics in Agriculture*, vol. 123, pp. 423–435, 2016.

[10] N. Ambiga and A. Nagarajan, "Possibilities of using nano particles in human urine for transient biometrics," *Materials Today Proceedings*, 2021.

[11] R. Srivastava, A. Singh, and Y. N. Singh, "PlexNet: a fast and robust ECG biometric system for human recognition," *Information Sciences*, vol. 558, pp. 208–228, 2021.

[12] M. V. Alyushin and L. V. Kolobashkina, "Development of a metrological database with images of a human face in the infrared range to evaluate the effectiveness of biometric algorithms," *Procedia Computer Science*, vol. 123, pp. 7–11, 2018.

[13] G. Gautam and S. Mukhopadhyay, "Challenges, taxonomy and techniques of iris localization: a survey," *Digital Signal Processing*, vol. 107, Article ID 102852, 2020.

[14] P. Kumari and K. R. Seeja, "Periocular biometrics: a survey," *Journal of King Saud University - Computer and Information Sciences*, vol. 34, no. 4, pp. 1086–1097, 2022.

[15] S. Chakraborty, V. Balasubramanian, and S. Panchanathan, "Generalized batch mode active learning for face-based biometric recognition," *Pattern Recognition*, vol. 46, no. 2, pp. 497–508, 2013.

[16] Z. Wang, Y. S Ong, and H. Ishibuchi, "On scalable multi-objective test problems with hardly-dominated boundaries," *IEEE Transactions on Evolutionary Computation*, vol. 23, no. 2, pp. 217–231, 2019.

[17] G. Guven, U. Guz, and H. Gürkan, "A novel biometric identification system based on fingertip electrocardiogram and speech signals," *Digital Signal Processing*, vol. 121, Article ID 103306, 2022.

[18] M. M. Rahman, T. I. Mishu, and M. A. A. Bhuiyan, "Performance analysis of a parameterized minutiae-based approach for securing fingerprint templates in biometric authentication systems," *Journal of Information Security and Applications*, vol. 67, Article ID 103209, 2022.

[19] S. Shakil, D. Arora, and T. Zaidi, "Feature based classification of voice based biometric data through Machine learning algorithm," *Materials Today Proceedings*, vol. 51, pp. 240–247, 2022.

[20] P. Kavipriya, M. Ebenezar Jebarani, T. Vino, and G. Jegan, "WITHDRAWN: ear biometric for personal identification using canny edge detection algorithm and contour tracking method," *Materials Today Proceedings*, 2021.

[21] Y. Shen, C. Tang, M. Xu, and Z. Lei, "Optical selective encryption based on the FRFCM algorithm and face biometric for the medical image," *Optics & Laser Technology*, vol. 138, Article ID 106911, 2021.

[22] R. Munir and R. A. Khan, "An extensive review on spectral imaging in biometric systems: challenges & advancements," *Journal of Visual Communication and Image Representation*, vol. 65, Article ID 102660, 2019.

[23] D. Chang, S. Garg, M. Ghosh, and M. Hasan, "BIOFUSE: a framework for multi-biometric fusion on biocryptosystem level," *Information Sciences*, vol. 546, pp. 481–511, 2021.

[24] L. C. O. Tiong, S. T. Kim, and Y. M. Ro, "Multimodal facial biometrics recognition: dual-stream convolutional neural networks with multi-feature fusion layers," *Image and Vision Computing*, vol. 102, Article ID 103977, 2020.

[25] Y. Ji, H. Zhang, Z. Zhang, and M. Liu, "CNN-basedencoder-decoder networks for salient object detection: a comprehensive review and recent advances," *Information Sciences*, vol. 546, pp. 835–857, 2021.

[26] Y. Kortli, S. Gabsi, L. F. L. Y. Voon, M. Jridi, M. Merzougui, and M. Atri, "Deep embedded hybrid CNN–LSTM network for lane detection on NVIDIA Jetson Xavier NX," *Knowledge-Based Systems*, vol. 240, Article ID 107941, 2022.

[27] B. Lindemann, B. Maschler, N. Sahlab, and M. Weyrich, "A survey on anomaly detection for technical systems using LSTM networks," *Computers in Industry*, vol. 131, Article ID 103498, 2021.

[28] X. Guo, Y. Wang, S. Mei et al., "Monitoring and modelling of PM2.5 concentration at subway station construction based on IoT and LSTM algorithm optimization," *Journal of Cleaner Production*, vol. 360, Article ID 132179, 2022.

[29] J. Zhou, D. Zhang, W. Ren, and W. Zhang, "Auto color correction of underwater images utilizing depth information," *IEEE Geoscience and Remote Sensing Letters*, vol. 19, pp. 1–5, 2022.

Hindawi

Research Article

Load-Balancing Strategy: Employing a Capsule Algorithm for Cutting Down Energy Consumption in Cloud Data Centers for Next Generation Wireless Systems

Jyoti Singh,[1] Jingchao Chen,[1] Santar Pal Singh,[2] Mukund Pratap Singh [ID],[3] Montaser M. Hassan,[4] Mohamed M. Hassan [ID],[4] and Halifa Awal [ID][5]

[1]*College of Information Science & Technology, Donghua University, Shanghai, China*
[2]*Department of Computer Science & Engineering, Rashtrakavi Ramdhari Singh Dinkar College of Engineering, Begusarai, India*
[3]*School of Computer Science Engineering & Technology, Bennett University, Greater Noida, India*
[4]*Department of Biology, College of Science, Taif University, P.O. Box 11099, Taif 21944, Saudi Arabia*
[5]*Tamale Technical University, Tamale, Ghana*

Correspondence should be addressed to Halifa Awal; ahalifa@tatu.edu.gh

Per-user pricing is possible with cloud computing, a relatively new technology. It provides remote testing and commissioning services through the web, and it utilizes virtualization to make available computing resources. In order to host and store firm data, cloud computing relies on data centers. Data centers are made up of networked computers, cables, power supplies, and other components. Cloud data centers have always had to prioritise high performance over energy efficiency. The biggest obstacle is finding a happy medium between system performance and energy consumption, namely, lowering energy use without compromising system performance or service quality. These results were obtained using the PlanetLab dataset. In order to implement the strategy we recommend, it is crucial to get a complete picture of how energy is being consumed in the cloud. Using proper optimization criteria and guided by energy consumption models, this article offers the Capsule Significance Level of Energy Consumption (CSLEC) pattern, which demonstrates how to conserve more energy in cloud data centers. Capsule optimization's prediction phase F1-score of 96.7 percent and 97 percent data accuracy allow for more precise projections of future value.

1. Introduction

Cloud computing is an extension of grid, parallel, and distributed computing techniques [1]. To achieve cloud computing, it conveys an assortment of equipment administrations, framework administrations, stage administrations, program administrations, and capacity administrations over the Web. Clients of cloud computing can utilize it on-demand, pay for it on-demand, and scale it up and down easily. Data centers have grown in size as cloud services have grown in popularity, necessitating a considerable amount of energy consumption. The authors pointed out in [2] that data centers consume 1.5% of the yearly control created within the assembled states, agreeing with

insights from the US Division of Energy. China's data centers are projected to consume about the same amount of energy as the United States and have surpassed the Gorges' yearly power generation. The estimation of energy consumption has become the most difficult challenge in today's data center, so reducing energy consumption is a pressing issue that needs to be addressed in cloud computing research. One of the most predominant ways of bringing down vitality utilization is virtual machine solidification. The overload/underload location, virtual machine determination, virtual machine arrangement [3–5], and virtual machine relocation [6, 7] are all cases of positive virtual machine combination. Virtual machine movement can take a long time, squander a part of assets, and meddle with the
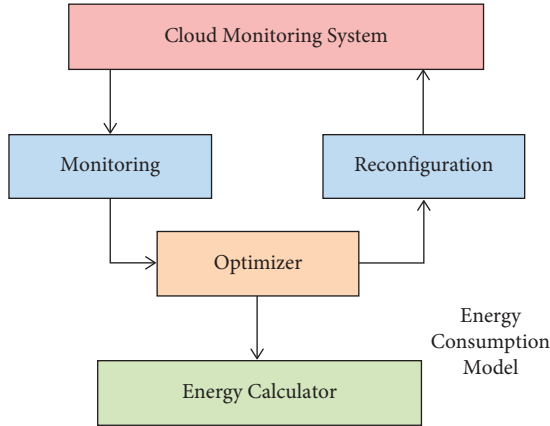
Figure 1: Energy consumption architecture.

working of other virtual machines on the server, resulting in a decrease in framework execution. Virtual machine relocation too requires the utilization of additional organized capacity [8]. The detailed descriptions of energy consumption architecture and data flow are given below in Figure 1.

Virtualization is an important method in data centers because it allows customers to share resources by using virtual machines (VMs). Each virtual machine is separated and utilized to run customer applications, with storage capacity, primary memory, CPU, I/O capabilities, and network bandwidth requirements [9]. Some of the important characteristics that promote cloud computing performance are physical machine consolidation, fault tolerance, and load balancing. Physical Machine (PM) consolidation occurs through Virtual Machine (VM) migration, which occurs when a virtual machine's requested resources are unavailable on the physical machine, causing the virtual machine to be relocated. The VM is moved to another physical computer to meet the VM requirement [10]. The suggested method forecasts the power of each VM before VM migration, and then VMs are migrated to certain PMs based on this prediction and resource availability. The VM power prediction improves system availability, reduces infrastructure complexity, and lowers cloud providers' operational costs, allowing customers to pay less [11]. To manage operations faster and deliver more reliable services to clients, it is necessary to forecast the VM's power in advance. Power conservation can be achieved by using various machine-learning approaches to forecast power use. This machine-learning-based technique is used in this study to forecast virtual machine power consumption, enrich cloud computing infrastructure, and improve service for IT industries. Furthermore, the power consumption of virtual computers is forecasted before they are assigned to physical machines [12].

The proposed technique is exceptionally good at finding acceptable computer resources in unknown networks since it incorporates a great positive input instrument and a dispersed look strategy. This article has provided a user-experience-based procedure for finding energy-saving virtual machines. The strides roulette likelihood choice component

guides and maintains a strategic distance from the calculation entering the basic information to untimely joining, viably decreasing vitality utilization, and accomplishing an adjustment between vitality utilization and client encounter by altering the pheromone and heuristic calculate upgrade strategies and characterizing the parameter administrative calculate. Cloud information centers offer various benefits, including on-demand assets, elasticity, flexibility, portability, and calamity recuperation [13]. One of the most important aspects of the cloud worldview is adaptability, which enables an application to grow its asset requests at any time [14]. Instead of purchasing and controlling computing resources, it has become more common to rent hardware, software, and network resources. With an Internet connection, users can take advantage of the entire processing infrastructure. It can be used in a wide variety of contexts, including commercial management, academic research, hospital administration, manufacturing, marketing, and many more [15].

The following is our contribution:

(i) Using historical data, we investigate and analyze the energy use of the data center. The results of this article are utilized to create a statistical model that links meteorological variables to energy use.

(ii) To use the statistical model to create a forecast model that can predict the data center's energy usage based on the weather forecast. The model is validated by comparing it to real-world resource usage data obtained using the capsule optimization technique.

(iii) To provide data center operators with an energy consumption forecast technique that allows them to optimize their power distribution and energy consumption by providing estimations of their resource utilization.

The structure of the paper is laid out underneath. Section 2 has literature from past inquiries about workload estimation and vitality utilization in a cloud information center. The proposed framework for controlling utilization based on ML-based approaches is examined in Section 3. Section 4 depicts the proposed approach's performance evaluation and serves as a conclusion in Section 5.

2. Literature Review

In the context of cloud server energy consumption management, the background of research, such as CPU utilization forecasting and resource usage forecasting and management, is one of the most successful techniques for anticipating the future. The amount of power required to run and cool down the devices in the cloud data center increases day by day, increasing cloud service providers' operational costs. For better performance of a complex function, power consumption prediction is utilized to estimate the nonlinear future value. In [16], the author discussed an adaptive threshold method, local regression, and robust local regression to evaluate overloaded servers in IaaS infrastructure based on CPU use. The threshold is automatically changed

TABLE 1: Study of energy efficiency methods and algorithms.

Energy efficiency algorithm	Approaches	Weakness	Tools used
Novel resource allocation algorithm for energy efficiency [24]	Autoregressive linear prediction	Energy consumption is not efficient	Power edge
Energy-based scheduling and accounting of VM [25]	Supervised learning methods	High in energy consumption	Simulator (self-designed)
Energy-efficient VM allocation technique using interior search algorithm [26]	Self-adaptive differential evolution algorithm	Maximum the power consumed by data centers	Open-source cloud middleware *Eucalyptus*
Exact allocation and migration algorithm [27]	Adaptive selector neural network	Power consumed by data centers has not reduced and low reduction in the rate of task rejection	Cloud hypervisor xen
Energy-saving VM migration [28]	Linear regression	No support to the heterogeneous environment and unstable QoS	Scheduler is implemented
Energy-aware resource allocation algorithm [29]	Neural network	SLA nonviolation, no control wastage, and given no scalability	Cloud sim
Energy-efficient dynamic resource management [30]	Gradient boosting tree	Reduction in control utilization with the nonviolation of SLA	Cloud sim

based on previous data analysis and manipulation with estimators such as mean absolute deviation and interquartile range. The author [17] focused on applying autoregressive linear prediction to anticipate network demand. In this strategy, the data samples utilized for training to discover the link between attributes were smaller using cross-validation and the black box method. The author in [18] introduced a tree regression (TR)-based model to compute VM power usage. The black box method is used to collect information on the VM and server features. For their prediction model, they used data as linear values. The author discussed the linear regression approach for forecasting cloud service workload [19]. They also used the auto-scaling technique to lower the operational costs of virtual resources by scaling them both vertically and horizontally. Using NASA trace and Saskatchewan trace, we devised a self-adaptive differential evolution algorithm to estimate the workload used by the cloud data center in [18]. The author discussed fitness function, mutation, and crossover in this method, which they found to be superior to other approaches such as particle swarm optimization (PSO), genetic algorithm (GA), and others.

In [20], the author discussed three versatile models for high vitality utilization and infringement of service-level understandings. When selecting virtual machines from overburden to decrease vitality utilization, SLA infringement was taken into consideration. At the same time, the execution of cloud information centers can be ensured. In [21], the author discussed the models for diminishing the vitality utilization of portable cloud information centers amid periods when virtual machines are inadequate or overburdened. For virtual machine determination and energetic blending, the recommended versatile heuristic energy-aware calculation perceives the history of CPU usage, which diminishes add up to vitality utilization and improves benefit quality. Compared to the most existing research, in [22], the author explored two extra key variables while handling the challenges of cloud data center energy usage and SLA violations: (1) Examining the stability of the CPU consumption upper limit. (2) When picking the virtual machine of the overburden based on the CPU utilization expectation, the execution debasement time and SLA infringement are diminished. To decrease vitality utilization with negligible SLA taking a toll, a heuristic method is displayed to identify the least-squares relapse of the overburden and select the virtual machine from the overburden with the lowest utilization estimate. In [23], the author discussed an energy-aware energetic virtual machine choice calculation proposed in [23] for the issue of virtual machine integration to coordinate virtual machines from overburdened or underloaded to upgrade vitality utilization and expand benefit quality. There are a few pieces of literature listed below in Table 1.

In [31], the author discussed the problems of reducing VM power usage and cloud vendor operational costs in a cloud setting. They used an ad-hoc framework for VM consolidation, but this method ignored VM requirements such as disc space, network bandwidth, and the time it took a VM to execute a task. The author has suggested [32] the

use of a radial basis function (RBF) neural network to examine the power of VM with normalized parameters that satisfy the correlation coefficient of VM's power. This method used a tiny amount of samples for training and testing data, resulting in a neural network that could not make an accurate prediction. In [33], the author used machine learning methods to estimate VM resource management in the cloud platform based on Azure workload parameters such as first-party IaaS and third-party PaaS services. The authors used the fast Fourier transform to determine the type of VM workload and the cumulative distribution function to produce the graphs for CPU, memory, CPU core utilization per VM, and VM lifetime. After each prediction, accumulate the results in the Dynamically Linked Library (DLL) and determine whether the forecast was worthwhile. In [34], the author used supervised learning algorithms to analyze the workload of VM to reduce its power consumption. They compiled a list of different scheduling strategies for reducing carbon dioxide emissions from a data center. The prediction error was calculated using statistical metrics such as RMSE, R squared, and accuracy, which were calculated using an algorithm. The recurrent neural network was used to forecast and manage resource allocation to a cloud server. They used time-delay neural network (TDNN) and regression approaches to compare the outcomes of the server workload prediction. In [35], an adaptive selector neural network was developed for selecting the strategy for active VM reduction, and the results were compared to those of linear regression. The customer's Service Level Agreement (SLA) with the cloud service provider was also crucial to this strategy; however, SLAs are still not met when customer requirements change. The contribution of this study is also found in the description of a load-balancing algorithm inspired by energy consumption patterns that shows how we may save more energy in cloud data centers by using appropriate optimization rules informed by our energy consumption models in the literature.

3. Proposed Methodology

The points of interest of the proposed demonstration counting preprocessing step and demonstration portrayal are given in the following segment. The proposed model and data flow are given in Figure 2. This work has been gathered from input requests from a user and includes data cleaning, data balancing, transformation, aggregation, and data normalisation in the data preprocessing steps of the proposed model.

The estimation of energy consumption uses a machine learning data model, which has been included in a Capsule algorithm that drops out fully connected layers. The cross-entropy has been calculated using the Softmax layer. The evaluation metrics are calculated using the proposed model and compare the accuracy of the model with the state-of-the-art models (ant colony and random forest). Figure 3 depicts a visual representation of the data center.

The request of a user has to supply in two ways request such as power path to IT and power to secondary support.
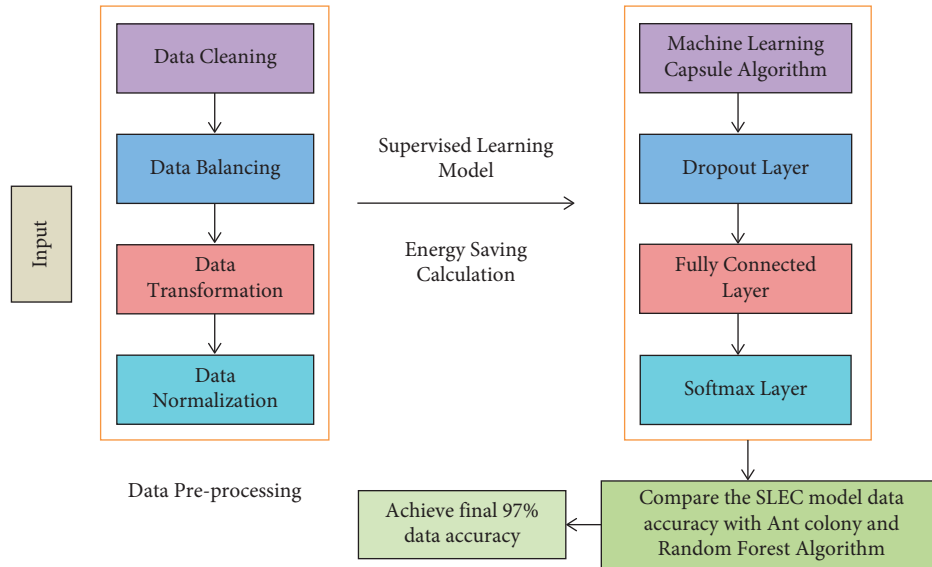
FIGURE 2: The proposed model.
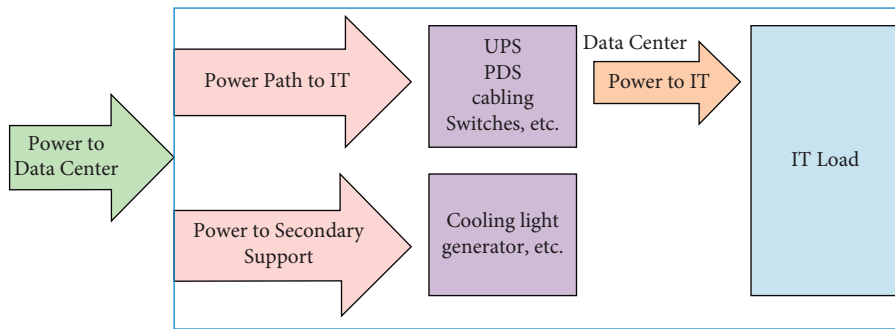
FIGURE 3: Pictorial representation of data center.

The data center consisted of an uninterruptible power supply (UPS) and a Paragon Development System (PDS), as well as cabling and cooling light conditions. Furthermore, the data request was transferred to the IT load. There are a few abbreviations given in Table 2.

The data flow of the proposed capsule significance level of energy consumption (CSLEC) is given in the form of a few steps, which are described in Algorithm 1 and Figure 4.

Step 1: the operational module gets the machine's current working status within the cloud data middle and then performs state control on each host

Step 2: we exchange the host's running status and virtual machine line state to the client encounter module and obtain the accessible assets based on the CPU use edge you set

Step 3: within the virtual machine planning module, initialize the pheromone for accessible resources

Step 4: we put all of the capsules on the accessible at random

Step 5: the capsule chooses another by calculating the likelihood determination instrument based on the

TABLE 2: The abbreviation used in the proposed algorithm.

Name	Abbreviation
F_{ev}	Feature value
S_l	Significance level
Cm	Capsule model

pheromone concentration, the heuristic figure, and the alteration factor

Step 6: in case the CSLEC algorithm completes the look, upgrade the neighborhood and worldwide pheromones; on the off chance that it does not, return to Step 5

Step 7: the framework produces the ideal assignment scenario when the number of initialization emphases is met; otherwise, it returns to Step 4

Step 8: we check to see if there are any virtual machines

The complete steps have been described in Algorithm 1. The flowchart of the proposed CSLEC model is shown in Figure 4. The data are entered into the host voltage system, where the information is controlled and the profit matrix is
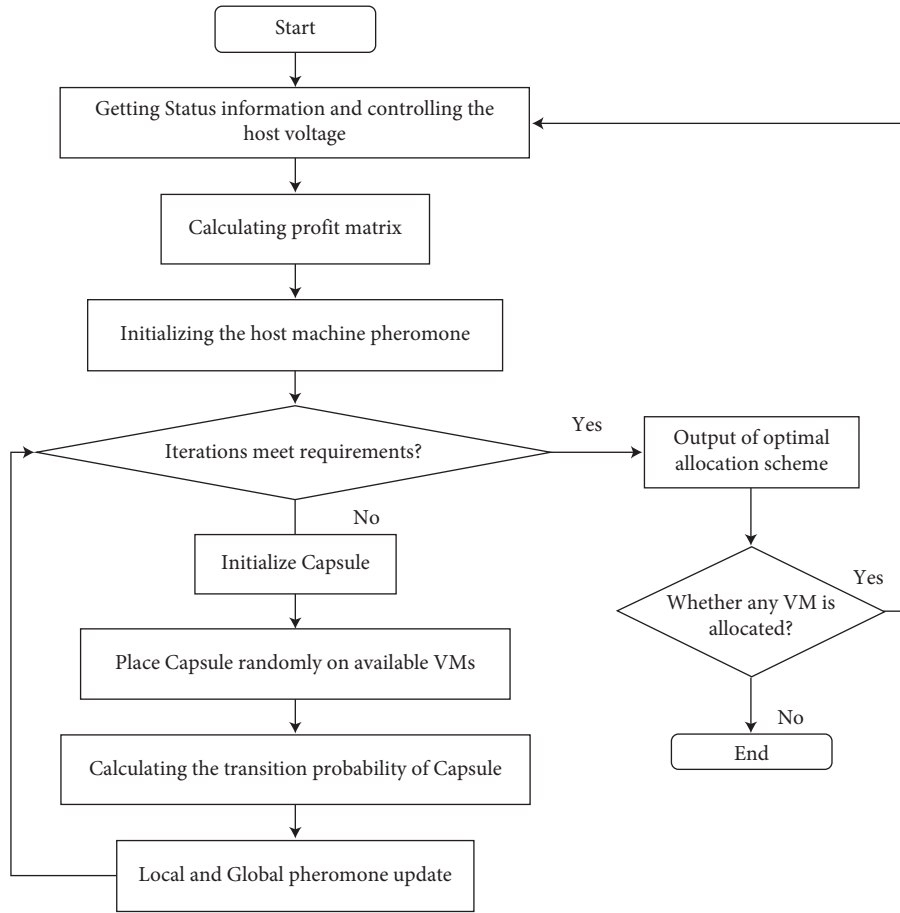
FIGURE 4: Flowchart of energy saving with the CSLEC algorithm.

Input: Significance Level (Sl)
Output: F_{ev} Feature Value
(1) Calculate all the values of F_{ev}.
(2) The Sl significant level is selected for staying in the model.
(3) For all F_{ev} fit Cm.
(4) Do
(5) Remove the Fev of highest values from the $F = ((F_{ev}))$ Feature set.
(6) Fit capsule model with an updated feature set.
(7) Recalculate all the feature values.
(8) While $(F_{ev} \geq Sl)$
(9) The set of independent variables for the forecast model is ready.

ALGORITHM 1: Capsule significance level of energy consumption (CSLEC).

calculated. The performance of the host machine is initialized, and if it meets the iterations of the system, then the output is calculated. If it does not meet the requirements, then the capsule model is placed and put in VM after calculating the transition probability with local and global updates.

3.1. Fitness Function Design. The suggested technique's main purpose is to provide tighter cloud load balancing. Cloud computing has a certain number of PMs, each of which has a certain number of VMs. The first item in equation (1) stands for control utilization (P), the moment term stands for movement taken a toll (MC), and the third term is for memory

utilizes (MU). The outright Euclidean separate (ED) of all the energetic PM at the same time determines the framework's power usage. The load-balanced system with the reduced ED is thought to be better. When no assignment is run in the relevant PM, the PM is turned off. The power efficient factor (EF) of each active node is calculated based on equation (2).

$$\text{Fitness\_function} = \text{Min}\left(\beta_1(q) + \beta_2(MC) + \beta_3(MU)\right). \tag{1}$$

The first component in equation (1) stands for control utilization (q), the moment term stands for movement taking a toll (MC), and the third term stands for memory utilization (MU). The outright Euclidean separate (ED) of all the energetic PM at the same time decides the framework's control utilization. The load-balanced framework with the diminished ED is thought to be way better. When no task is run within the significant PM, the PM is turned off. Condition is utilized to decide the control proficiency figure (EF) of each dynamic hub equation (3).

$$E_F = \sqrt{\sum_{k=1}^{d}(V - V\text{Best}_i)^2}, \tag{2}$$

where $i \longrightarrow$ Memory resources. $Vi \longrightarrow$ Given resource utilization. $V\text{Best}_i \longrightarrow$ Best utilization of resource i for power efficiency in each physical node.

Power efficiency at time t is calculated as follows in equation (4):

$$PT = \sum EF. \tag{3}$$

System total power efficiency is represented as

$$P = \sum_{t=0}^{T} E^t. \tag{4}$$

Another consideration for the objective function is the cost of migration. When the number of motions increases, the MC of the VM expands. The best load-balancing system should have the least amount of movement. The MC of the entire cloud arrangement is calculated using the conditions provided in

$$MC = \frac{1}{V}\sum_{i=1}^{v}\left(\frac{\text{No\_of\_migration\_in\_}VM_s}{\text{Total\_no\_of\_}VM_s}\right). \tag{5}$$

Another aspect of the load-balancing target function is memory use. Memory is nothing more than a jumble. The heap structure is honestly based on the VM's benefits for setting up the assignments from various customers. CPUs and memory storage are among the resources used by the VM. The storage utilization of the entire cloud setup is calculated using conditional logic equation:

$$MU = \frac{1}{PM \times VM}\left[\sum_{i=1}^{PM}\sum_{j=1}^{VM}\frac{1}{2}\left(\frac{\text{CPU\_Utilization}_{ij}}{PU_{ij}} + \frac{\text{Memory\_Utilization}_{ij}}{\text{Memory}_{ij}}\right)\right]. \tag{6}$$

In condition (1), the objective work of our investigation is indicated. In this paper, the overobjective work is getting to be minimized by utilizing the ACSO calculation.

3.1.1. Data Balancing. The class imbalance problem happens when the quantity of samples in distinct classes of a dataset is unequally distributed. Minority classes receive fewer samples than other target groups, whereas majority classes receive more samples [36]. Minority classes must be properly supplemented since they are crucial for extracting information from unbalanced datasets. A method for boosting the sample size of minority groups is the Synthetic Minority Oversampling Technique (SMOTE). Using this technique, new artificial samples are produced next to existing samples and then arranged in a line. After that, samples from nearby minority groups are matched with them. Notably, the sample features in adjacent classes are unaffected, permitting SMOTE to create tests that drop interior with the most dispersion. The recently made counterfeit information, which is calculated and utilized, is

$$D_{\text{new}} = D_i\left(D_l^* - D_i\right) \times \delta. \tag{7}$$

It is a number between 0 and 1, where D_i represents the number related to minority samples and is the closest neighbour. The capacity to generate new samples close to minority class data is one of the SMOTE technique's most noticeable advantages over other resampling techniques. This strategy is less complex and simpler than other databalancing methods like cost-sensitive ones.

3.2. Feature Transformation. In our suggested model, label encoding is employed to convert nominal properties into numeric ones that may be interpreted by neural networks. Label embedding takes into account a number between zero and $n-1$ for each sample with nominal properties [18]. The reason for using this strategy is that it does not alter the data's dimensionality.

3.2.1. Data Aggregation. It envelops methods that result in the creation of modern highlights by combining two or more existing features. In comparison to the first highlights, the modern highlights must be able to specify the dataset's data more successfully and totally. The proposed work employments information accumulation to decrease dimensional

whereas moreover expanding the value of highlights and information soundness [20].

3.2.2. Normalization. The suggested model normalises the input data using the Max-Min normalisation method. This method applies a linear change to the original data while preserving the correlation between them [13]. The normalisation approach is employed because the relationship between independent variables and the correlation between data are important in the prediction stated in

$$X(n) = \frac{x - \text{Min}(A)}{\text{Max}(A) - \text{Min}(A)}, \qquad (8)$$

where $\text{Min}(A)$ and $\text{Max}(A)$ denote the feature's minimal and maximum values, respectively, and x denotes the feature's current value.

3.3. Proposed Model. A capsule may be a collection of neurons whose movement vector speaks to the instantiation parameters of a specific sort of substance, such as a protest or a question parcel [14]. To put it another way, capsules encapsulate in vector form all relevant information about the status of the feature they are detecting [18]. Since the capsule is a vector, the length of it is a probability of detection of a feature, which means that even if the detected object has rotated, the length of the vector will be the same (the probability still stays the same), but the vector direction will change in the direction of the change. For example, let's assume that the current capsule has detected a face within an input image with a probability of 0.9. When the face starts to change location across the image, the capsule's vector will change direction, which means that it still detects; however, the length will be the same. This is exactly the form of invariance, which is not the max-pool offer in CNN.

3.3.1. Fully Connected (FC) Layer. Fully linked layers in neural networks are ones where all of the inputs from one layer are connected to each enactment unit of the following layer. Most common machine learning models' final few layers are complete related layers that combine the data retrieved by earlier levels to produce the final result [15]. A "Fully Connected (FC)" layer is planned to proficiently handle vector information. The model's depth should be properly calculated. We used one layer of fully linked layers in this example, but a service provider can alter it to establish a balance between the target model's complexity and the complexity of the target model (better detection accuracy).

3.3.2. Dropout Layer. To avoid overfitting, the dropout layer is used. Dropout is a neural network regularization strategy that reduces recurrent learning between neurons. As a result, certain neurons are disregarded at random during the training process [18].

3.3.3. Classification Layer (Softmax). In the last layer, Softmax is utilized to categorise the data. The last

TABLE 3: Accuracy (%) comparison.

Sr. no	Algorithm	Accuracy (%)
1	LR	70
2	PSO	76
3	Capsule network	85
4	CNN	94
5	Proposed CSLEC model	97

classification layer of a neural network uses a nonlinear activation function called Softmax [5]. Softmax is calculated using equation (9), and the output values are normalized so that the sum of the values is one.

$$P(Y = K, X = x_i) = \frac{e^{sk}}{\sum_{j=1}^{m} e^{sj}}, \qquad (9)$$

where k is the conventional exponential function applied to each element of the input vector and is the k-dimensional input vector. The fraction's denominator guarantees that all output values are between 0 and 1. The relevant class's score must be maximized in the next section.

4. Result and Discussion

This work has provided a comprehensive analysis of energy-saving calculations based on the arrival, processing, and response time of the virtual server. There are two different factors: processor utilization and energy consumption. The experimental evaluation is carried out using the Clouds toolkit. It is a common framework for simulating cloud computing systems on local devices [37]. Cloud components such as data centers, virtual machines, and resource provisioning limits can be simulated using the CloudSim toolkit. Also, for the experiment, choose a sample size of 100 tasks, which were initially distributed over five virtual machines [38].

4.1. Evaluation Metrics. The proposed model is evaluated using the accuracy, precision, and recall metrics as given in equations (10)–(12), respectively, where "TP" and "TN" refer to correctly categorized true positive and true negative samples [39]. Positive and negative instances that have been erroneously categorized are also referred to as FP and FN:

$$\text{Accuracy} = \frac{\text{TP} + \text{TN}}{\text{TP} + \text{FP} + \text{TN} + \text{FN}}, \qquad (10)$$

$$\text{Precision} = \frac{\text{TP}}{\text{TP} + \text{FP}}, \qquad (11)$$

$$\text{Recall} = \frac{\text{TP}}{\text{TP} + \text{FN}}. \qquad (12)$$

Table 3 compares the proposed model's accuracy to that of other current models.

The accuracy in Table 3 shows the comparison of different models; the proposed capsule model shows better accuracy in comparison with other pretrained models. This work compares the four different models, such as LR, PSO,

TABLE 4: Comparison of the number of trainable parameters and training time for the proposed model and other models.

Sr. no	Algorithm	Trainable parameters	Training time (ms)
1	LR	16896	588.31
2	PSO	17154	946.52
3	Capsule network	20960	967.14
4	CNN	33410	1702.43
5	Proposed CSLEC model	25346	1577.87

TABLE 5: The electric energy consumed by the considered servers at different levels of workload in watts (W).

Server capacity	0 (%)	10 (%)	20 (%)	30 (%)	40 (%)	50 (%)	60 (%)	70 (%)	80 (%)	90 (%)	100 (%)
Fujitsu M1	14.4	19.4	22.2	24.5	27.6	30.7	35.8	41.8	47.9	58.5	61
Fujitsu M3	13.5	17.8	20.5	22.5	24.5	27.2	30.8	35.9	42	48.2	52.3
Hitachi TS10	41	42.9	44.3	46.6	49.9	53.9	58.9	66.2	74.9	81.9	86.2
Hitachi SS10	37	39.9	42.3	44.8	47.4	50.5	54.2	59.9	65.3	68	70.8

Capsule, and CNN, that achieved 70%, 76%, 85%, and 95% data accuracy, respectively [40]. The proposed CSLEC data model has achieved 97% data accuracy, which is better than another model's accuracy. Also, depending on the number of parameters in the trainable stage, the time taken for the training of the proposed model shows a better time in comparison with the pretrained CNN model shown in Table 4.

The accuracy Table 3 shows the comparison of different models; the proposed capsule model shows better accuracy in comparison with other pretrained models. Also, depending on the number of parameters in the trainable stage, the time taken for the training of the proposed model shows better time in comparison with the pretrained CNN model shown in Table 4. The proposed model has been using 25346 trainable parameters, and it has consumed 1577.87 ms of time. This work has compared the four different algorithms: LR, PSO, Capsule network [41], and CNN. The LR algorithm has used 16896 trainable parameters and consumed 588.31 training time. In comparison with the LR model, the PSO model has been used with 17154 parameters and a training time consumption of 946.52 ms. The other training networks, Capsule and CNN, used 20960 and 33410 trainable parameters, respectively, consuming 967.14 and 1702.43 seconds. Out of this basic model, our proposed model has been trained with a large number of data and a 1577.87 consumption rate. Table 5 shows the difference in energy consumption with the use of different servers in Watts (W). As the level of workload increases, the percentage value of the Hitachi TS10 increases and reaches a maximum of 86.2 watts.

The electric energy consumption has been considered by Fujitsu M1, Fujitsu M3, Hitachi TS10, and Hitachi SS10 server capacities, which has been considered in the range of 0% to 100% workload, and maximum server capacity has been estimated by Hitachi TS10 server as 41 42.9%, 44.3%, 46.6%, 49.9%, 53.9%, 58.9%, 66.2%, 74.9%, 81.9%, and 86.2%. The maximum server capacity and accuracy in Table 5 show the comparison of different server capacities; the proposed capsule model shows better accuracy in comparison with other pretrained models [42]. Also,
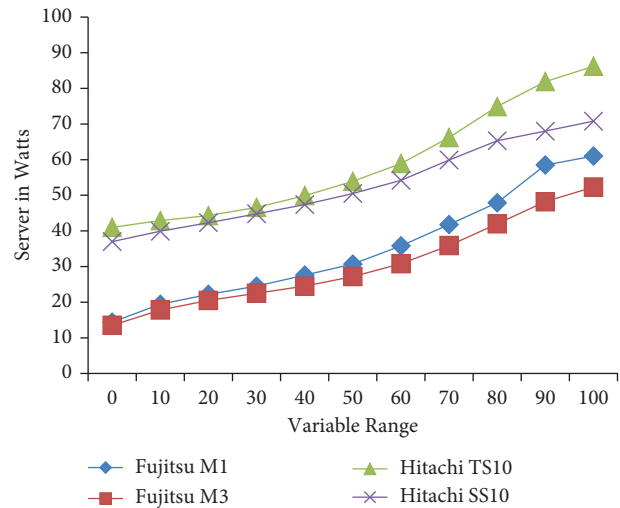
FIGURE 5: Electric energy consumed by the considered servers.

depending upon the number of parameters in the trainable stage, the time taken for the training of the proposed model shows a better time in comparison with the pretrained CNN model shown in Table 4. Table 5 shows the difference in energy consumption with the use of different servers in watts (W). As the level of workload increases, the percentage value of the Hitachi TS10 increases and reaches a maximum of 86.2 watts.

The server capacity of this work is shown in Figure 5. The Hitachi TS10 has shown maximum electric consumption. This work has been estimating the electric energy consumption using different four types of servers, such as the "Fujitsu M1," "Fujitsu M3," "Hitachi TS10," and "Hitachi SS10." Hitachi TS10 [30] has achieved the best energy consumption accuracy of 86.2%. This work has also observed that the Fujitsu M1, Fujitsu M3, and Hitachi TS10 do not provide better energy consumption in terms of watts. The result of the capsule algorithm in the form of different tasks is shown in Table 6.

TABLE 6: Computed results for Capsule algorithm.

Task	Arrival time	Processing time	Response time	Processor utilization	Energy consumption
T0	0	9	9	27	29.5
T1	1	3	2	13	14.1
T2	8	5	2	42	43.5
T3	16	2	15	53	54.7
T4	22	5	16	82	84.1
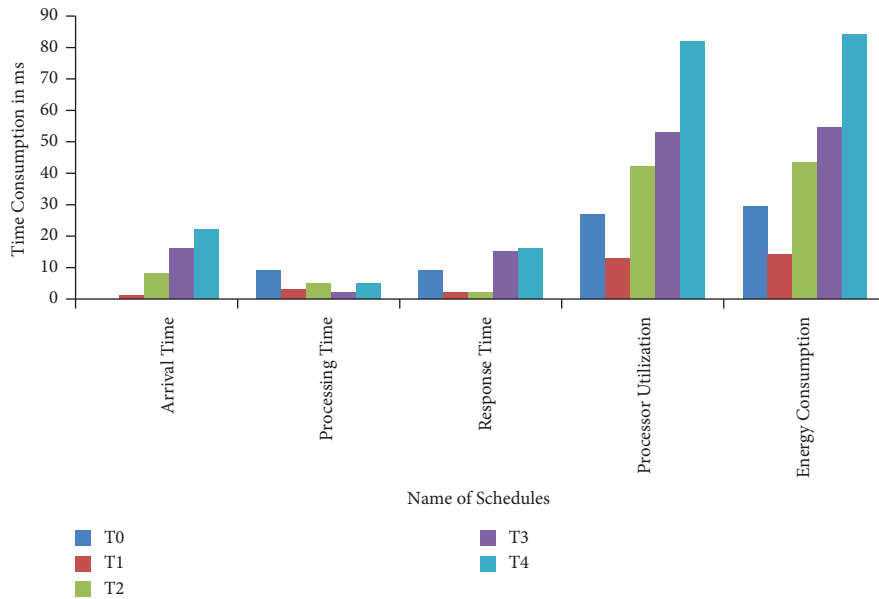
FIGURE 6: Energy consumed by the considered servers.
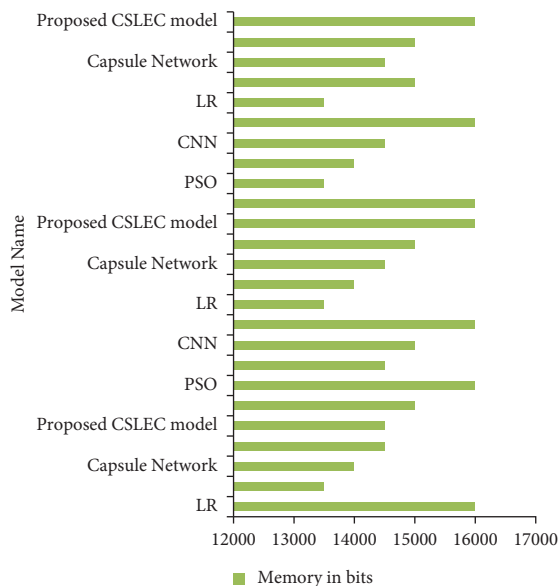
FIGURE 7: Memory utilization in the model.

This work used the task, arrival time, response time, processing time, and energy consumption estimated in the unit of ms. The task has been divided into five different terms, such as T0, T1, T2, T3, and T4. The user request was sent, and the server scheduled it based on the arrival time. The maximum arrival time for task T4 is 22 ms, which is better than other tasks in comparison with processing time. But task T3 takes less processing time in comparison with others and also utilizes the minimum processor with an energy consumption of 54.7. The energy consumed by the considered servers is shown in the form of a graph in Figure 6.

The experiment was double-checked using a larger number of tasks and virtual machines in this paper. The recorded results are also compared in order to assess the research project [43]. The PSO load balancer algorithm is used to parse the simulations, and the results are then logged. The Firefly load balancer is then used to run the same simulations. The findings are analyzed using fixed characteristics such as CPU utilization, reaction time, and throughput [44]. The usage times of both approaches are now calculated using the above-mentioned energy formula.
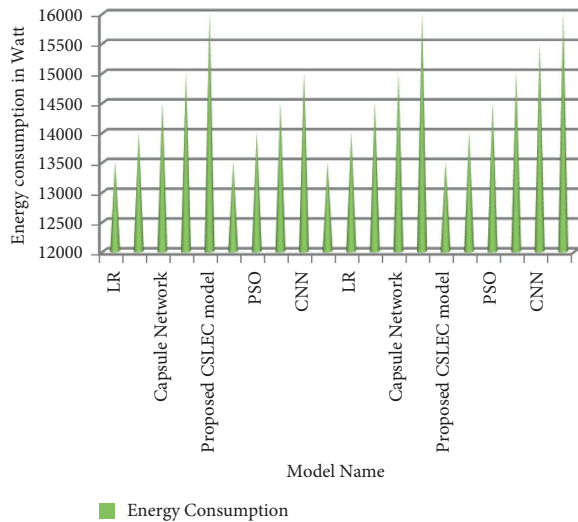
Figure 8: Comparative study of energy consumption.

For both the PSO and Capsule algorithms, this yields the energy consumption parameter. The information gathered is analyzed and compared with the algorithms of PSO and Capsule [45]. The information gathered is analyzed and compared [46].

Figure 7 compares the LR, CNN, and PSO models with the proposed model in terms of memory utilization. The proposed model has efficiently provided the accuracy of memory utilization of 170000 nm. The comparative study of the energy consumption is shown in Figure 8.

This project explored a few versions before settling on a few to graphically depict the status. The processing usage of the Capsule load balancer is higher than that of the PSO load balancer [47]. The final parameter for comparing the two algorithms is energy consumption, which is calculated using this utilization [48]. A Firefly load balancer's average response time is faster than a PSO load balancer's. As previously stated, the response time has a wide-ranging impact on energy use. As a result of the faster response time, less energy is consumed [49]. The amount of energy consumed is calculated by employing an equation that utilizes a settled value for the greatest control that can be devoured when the machine is completely stacked and a foreordained value for the least control that will be devoured when the machine is nearly still [50].

5. Conclusion

In a cloud data center, energy consumption is a major concern. With the rise in requests and a broad selection of cloud computing, it is presently fundamental to preserve successful and efficient data center methodologies to meet the approaching demands with the slightest amount of assets. In this work, we compared the training parameters and training time of different models, such as CNN, PSO, and Capsule, with the proposed model of CSLEC. The CSLEC model has been used with 25346 training parameters and 1.57 training minutes (ms). The proposed model has achieved an accuracy of 97%. The proposed CSLEC algorithm's mathematical explanation has been thoroughly explained. The experimental

outcomes are represented using a variety of measures. In comparison to the existing method, the proposed strategy has the briefest make span and employs the least amount of vitality. In the future, we will actualize our strategy in real time and place a greater emphasis on it. In addition, this work calculated the energy consumed to assess the performance of the Capsule Significance Level of Energy Consumption (CSLEC). Comparative evaluations uncover that the proposed strategy is more successful at optimizing the vitality utilization parameter than the Molecule Swarm optimization calculation. When compared to PSO, the energy consumption of CSLEC is 10–14% lower.

Data Availability

The data used in this work are available at https://planetlab. cs.princeton.edu/datasets.html.

Conflicts of Interest

The authors declare that they have no conflicts of interest regarding the publication of this manuscript.

Acknowledgments

References

[1] S. Ismaeel, R. Karim, and A. Miri, "Proactive dynamic virtual-machine consolidation for energy conservation in cloud data centres," *Journal of Cloud Computing*, vol. 7, no. 1, p. 10, 2018.

[2] K. Mason, M. Duggan, E. Barrett, J. Duggan, and E. Howley, "Predicting host CPU utilization in the cloud using evolutionary neural networks," *Future Generation Computer Systems*, vol. 86, pp. 162–173, 2018.

[3] K. Kumar, "P2BED-C: a novel peer to peer load balancing and energy efficient technique for data-centers over cloud," *Wireless Personal Communications*, vol. 123, no. 1, pp. 311–324, 2022.

[4] F. Zhang, G. Liu, X. Fu, and R. Yahyapour, "A survey on virtual machine migration: challenges, techniques, and open issues," *IEEE Communications Surveys & Tutorials*, vol. 20, no. 2, pp. 1206–1243, 2018.

[5] K. Amit and D. Rai, "Machine learning approach for load balancing of vm placement cloud computing," *Journal of Positive School Psychology*, vol. 6, no. 3, pp. 7279–7283, 2022.

[6] Z. Usmani and S. Singh, "A survey of virtual machine placement techniques in a cloud data center," *Procedia Computer Science*, vol. 78, pp. 491–498, 2016.

[7] R. Kumar, S. K. Khatri, and M. J. Diván, "Optimization of power consumption in data centers using machine learning based approaches: a review," *International Journal of Electrical and Computer Engineering*, vol. 12, no. 3, p. 3192, 2022.

[8] A. Beloglazov and R. Buyya, "Optimal online deterministic algorithms and adaptive heuristics for energy and performance efficient dynamic consolidation of virtual machines in cloud data centers," *Concurrency and Computation: Practice and Experience*, vol. 24, no. 13, pp. 1397–1420, 2012.

[9] Y. A. G. Alyouzbaki and M. F. Al-Rawi, "Novel load balancing approach based on ant colony optimization technique in cloud computing," *Bulletin of Electrical Engineering and Informatics*, vol. 10, no. 4, pp. 2320–2326, 2021.

[10] C. Gu, P. Shi, S. Shi, H. Huang, and X. Jia, "A tree regression-based approach for VM power metering," *IEEE Access*, vol. 3, pp. 610–621, 2015.

[11] A. D. Gaikwad, K. R. Singh, S. D. Kamble, and M. M. Raghuwanshi, "A comparative study of energy and task efficient load balancing algorithms in cloud computing," *Journal of Physics: Conference Series*, vol. 1913, Article ID 012105, 2021.

[12] J. Kumar and A. K. Singh, "Workload prediction in cloud using artificial neural network and adaptive differential evolution," *Future Generation Computer Systems*, vol. 81, pp. 41–52, 2018.

[13] A. Yousefipour, A. M. Rahmani, and M. Jahanshahi, "Improving the load balancing and dynamic placement of virtual machines in cloud computing using particle swarm optimization algorithm," *International Journal of Engineering*, vol. 34, no. 6, pp. 1419–1429, 2021.

[14] H. Xu, X. Zuo, C. Liu, and X. Zhao, "Predicting virtual machine's power via an RBF neural network," in *Proceedings of the International Conference on Swarm Intelligence*, pp. 370–381, Brussels, Belgium, June 2016.

[15] S. Jeyalaksshmi, J. Anita Smiles, D. Akila, D. Mukherjee, and A. J. Obaid, "Energy-efficient load balancing technique to optimize average response time and data center processing time in cloud computing environment," *Journal of Physics: Conference Series*, vol. 1963, Article ID 012145, 2021.

[16] E. Cortez, A. Bonde, A. Muzio, M. Russinovich, M. Fontoura, and R. Bianchini, "Resource central: understanding and predicting workloads for improved resource management in large cloud platforms," in *Proceedings of the 26th Symposium on Operating Systems Principles*, pp. 153–167, Shanghai, China, October 2017.

[17] D. Saxena and A. K. Singh, "Communication cost aware resource efficient load balancing (carelb) framework for cloud datacenter," *Recent Advances in Computer Science and Communications (Formerly: Recent Patents on Computer Sciences)*, vol. 14, pp. 2920–2933, 2021.

[18] L. Shen, J. Li, Y. Wu, Z. Tang, and Yi Wang, "Optimization of artificial bee colony algorithm based load balancing in smart grid cloud," in *Proceedings of the 2019 IEEE Innovative Smart Grid Technologies-Asia (ISGT Asia)*, pp. 1131–1134, Chengdu, China, May 2019.

[19] J. N. Witanto, H. Lim, and M. Atiquzzaman, "Adaptive selection of dynamic VM consolidation algorithm using neural network for cloud resource management," *Future Generation Computer Systems*, vol. 87, pp. 35–42, 2018.

[20] R. Chandran, S. Rakesh Kumar, and N. Gayathri, "Genetic algorithm-based tabu search for optimal energy-aware allocation of data center resources," *Soft Computing*, vol. 24, no. 21, pp. 16705–16718, 2020.

[21] G. James, D. Witten, T. Hastie, and R. Tibshirani, "Linear model selection and regularization," in *An Introduction to Statistical Learning*, pp. 203–264, Springer, Berlin, Germany, 2013.

[22] J. Chen, K. Li, Z. Tang et al., "A parallel random forest algorithm for big data in a spark cloud computing environment," *IEEE Transactions on Parallel and Distributed Systems*, vol. 28, no. 4, pp. 919–933, 2017.

[23] U. K. Jena, P. K. Das, and M. R. Kabat, "Hybridization of meta-heuristic algorithm for load balancing in cloud computing environment," *Journal of King Saud University-Computer and Information Sciences*, vol. 34, no. 6, pp. 2332–2342, 2022.

[24] P. S. Junior, D. Miorandi, and G. Pierre, "Stateful container migration in geo-distributed environments," in *Proceedings of the Cloud Com2020-12th IEEE International Conferenceon Cloud Computing Technology and Science*, Bangkok, Thailand, December 2020.

[25] S. Tuli, S. Ilager, K. Ramamohanarao, and R. Buyya, "Dynamic scheduling for stochastic edge-cloud computing environments using a3c learning and residual recurrent neural networks," *IEEE Transactions on Mobile Computing*, vol. 21, 2020.

[26] N. Gholipour, E. Arianyan, and R. Buyya, "A novel energy-aware resource management technique using joint VM and container consolidation approach for green computing in cloud data centers," *Simulation Modelling Practice and Theory*, vol. 104, pp. 102127–127, 2020.

[27] Z. Miao, P. Yong, Y. Mei, Y. Quanjun, and X. Xu, "A discrete PSO-based static load balancing algorithm for distributed simulations in a cloud environment," *Future Generation Computer Systems*, vol. 115, pp. 497–516, 2021.

[28] A. Javadpour, G. Wang, S. Rezaei, and S. Chend, "Power curtailment in cloud environment utilising load balancing machine allocation," in *Proceedings of the 2018 IEEE SmartWorld, ubiquitous intelligence & computing, advanced & trusted computing, scalable computing & communications, cloud & big data computing, Internet of People and Smart City Innovation (SmartWorld/SCALCOM/UIC/ATC/CBDCom/IOP/SCI)*, pp. 1364–1370, Guangzhou, China, 2018 October.

[29] S. Azizi, M. Shojafar, J. Abawajy, and R. Buyya, "Grvmp: a greedy randomized algorithm for virtual machine placement in cloud data centers," *IEEE Systems Journal*, vol. 15, no. 2, pp. 2571–2582, 2021.

[30] V. N. Volkova, L. V. Chemenkaya, E. N. Desyatirikova, M. Hajali, A. Khodar, and A. Osama, "Load balancing in cloud computing," in *Proceedings of the 2018 IEEE Conference of Russian Young Researchers in Electrical and Electronic Engineering (EIConRus)*, pp. 387–390, St. Petersburg, Russia, 2018 January.

[31] Z. Mohamad, A. A. Mahmoud, W. N. S. W. Nik, M. A. Mohamed, and M. M. Deris, "A genetic algorithm for optimal job scheduling and load balancing in cloud computing," *International Journal of Engineering & Technology*, vol. 7, no. 3, pp. 290–294, 2018.

[32] F. F. Moges and S. L. Abebe, "Energy-aware VM placement algorithms for the OpenStack Neat consolidation framework," *Journal of Cloud Computing*, vol. 8, no. 1, pp. 2–12, 2019.

[33] P. K. Shukla, L. Sharma, K. R. Bhatele, P. Sharma, and P. Shukla, "Design, architecture, and security issues in wireless sensor networks," in *Next Generation Wireless Network Security and Privacy*, pp. 211–237, IGI Global, Hershey, Pennsylvania, 2015.

[34] M. Lawanya Shri, E. Ganga Devi, B. Balusamy, S. Kadry, S. Misra, and M. Odusami, "A fuzzy based hybrid firefly optimization technique for load balancing in cloud datacenters," in *Proceedings of the International Conference on Innovations in Bio-Inspired Computing and Applications*, pp. 463–473, New York, NY, USA, 2018 December.

[35] H. Nashaat, N. Ashry, and R. Rizk, "Smart elastic scheduling algorithm for virtual machine migration in cloud computing," *The Journal of Supercomputing*, vol. 75, no. 7, pp. 3842–3865, 2019.

[36] D. Ahirwar, P. K. Shukla, K. R. Bhatele, P. Shukla, and S. Goyal, "Intrusion detection and tolerance in next generation wireless network," in *Next Generation Wireless Network Security and Privacy*, pp. 313–335, IGI Global, Hershey, Pennsylvania, 2015.

[37] S. K. Mishra, M. A. Khan, B. Sahoo, D. Puthal, M. S. Obaidat, and K. F. Hsiao, "Time efficient dynamic threshold-based load balancing technique for Cloud Computing," in *Proceedings of the 2017 International Conference on Computer, Information and Telecommunication Systems (CITS)*, pp. 161–165, Dalian, China, 2017 July.

[38] S. Subalakshmi and N. Malarvizhi, "Enhanced hybrid approach for load balancing algorithms in cloud computing," *International Journal of Scientific Research in Computer Science, Engineering and Information Technology*, vol. 2, no. 2, pp. 136–142, 2017.

[39] N. K. Das, M. S. George, and P. Jaya, "Incorporating weighted round robin in honeybee algorithm for enhanced load balancing in cloud environment," in *Proceedings of the 2017 International Conference on Communication and Signal Processing (ICCSP)*, pp. 0384–0389, IEEE, Melmaruvathur, India, April 2017.

[40] N. Thilagavathi, D. D. Dharani, R. Sasilekha, V. Suruliandi, and V. R. Uthariaraj, "Energy efficient load balancing in cloud data center using clustering technique," *International Journal of Intelligent Information Technologies*, vol. 15, no. 1, pp. 84–100, 2019.

[41] T. Sasidhar, V. Havisha, S. Koushik, M. Deep, and V. Krishna Reddy, "Load balancing techniques for efficient traffic management in cloud environment," *International Journal of Electrical and Computer Engineering*, vol. 6.

[42] M. Sathya, M. Jeyaselvi, L. Krishnasamy et al., "A novel, efficient, and secure anomaly detection technique using DWU-ODBN for IoT-enabled multimedia communication systems," *Wireless Communications and Mobile Computing*, vol. 2021, Article ID 4989410, 12 pages, 2021.

[43] J. Wu, W. Xu, and J. Xia, "Load balancing cloud storage data distribution strategy of internet of things terminal nodes considering access cost," *Computational Intelligence and Neuroscience*, vol. 2022, Article ID 7849726, 11 pages, 2022.

[44] R. Kanniga Devi, G. Murugaboopathi, and M. Muthukannan, "Load monitoring and system-traffic-aware live VM migration-based load balancing in cloud data center using graph theoretic solutions," *Cluster Computing*, vol. 21, no. 3, pp. 1623–1638, 2018.

[45] K. Kaur, S. Garg, G. Kaddoum, F. Gagnon, and D. N. K. Jayakody, "Enlob: energy and load balancing-driven container placement strategy for data centers," in *Proceedings of the 2019 IEEE Globecom Workshops (GC Wkshps)*, pp. 1–6, IEEE, Waikoloa, HI, USA, December 2019.

[46] W. A. Banu and R. Narayani, "Fairness-based heuristic workflow scheduling and placement in cloud computing," *International Journal of Vehicle Information and Communication Systems*, vol. 4, no. 4, pp. 355–374, 2019.

[47] Y. Fahim, H. Rahhali, M. Hanine et al., "Load balancing in cloud computing using meta-heuristic algorithm," *Journal of Information Processing Systems*, vol. 14, no. 3, pp. 569–589, 2018.

[48] J. K. Jeevitha and G. Athisha, "Energy-efficient virtualized scheduling and load balancing algorithm in cloud data centers," *International Journal of Information Retrieval Research*, vol. 11, no. 3, pp. 34–48, 2021.

[49] S. K. Mishra, B. Sahoo, and P. P. Parida, "Load balancing in cloud computing: a big picture," *Journal of King Saud University-Computer and Information Sciences*, vol. 32, no. 2, pp. 149–158, 2020.

[50] T. Deepika and P. Prakash, "Power consumption prediction in cloud data center using machine learning," *International Journal of Electrical and Computer Engineering*, vol. 10, no. 2, pp. 1524–1532, 2020.

Hindawi

Research Article

Study on Volleyball-Movement Pose Recognition Based on Joint Point Sequence

Xi Li (ID)

Physical Education Department, Taihu University of Wuxi, Wuxi 214000, Jiangsu, China

Correspondence should be addressed to Xi Li; 000058@wxu.edu.cn

With the high-speed operation of society and the increasing development of modern science, people's quality of life continues to improve. Contemporary people are increasingly concerned about their quality of life, pay attention to body management, and strengthen physical exercise. Volleyball is a sport that is loved by many people. Studying volleyball postures and recognizing and detecting them can provide theoretical guidance and suggestions for people. Besides, when it is applied to competitions, it can also help the judges to make fair and reasonable decisions. At present, pose recognition in ball sports is challenging in action complexity and research data. Meanwhile, the research also has an important application value. Therefore, this article studies human volleyball pose recognition by combining the analysis and summary of the existing human pose recognition studies based on joint point sequences and long short-term memory (LSTM). This article proposes a data preprocessing method based on the angle and relative distance feature enhancement and a ball-motion pose recognition model based on LSTM-Attention. The experimental results show that the data preprocessing method proposed here can further improve the accuracy of gesture recognition. For example, the joint point coordinate information of the coordinate system transformation significantly improves the recognition accuracy of the five ball-motion poses by at least 0.01. In addition, it is concluded that the LSTM-attention recognition model is not only scientific in structure design but also has considerable competitiveness in gesture recognition performance.

1. Introduction

The posture of the human body is one of the important biological characteristics of the human body. It has many application scenarios, such as gait analysis, video surveillance, augmented reality, human-computer interaction, finance, mobile payment, entertainment and games, and sports science. Gesture recognition allows computers to know what a person is doing and who they are. Especially in the field of monitoring, it is a good solution when the resolution of the face image obtained by the camera is too small. It can also be used as an important auxiliary verification method in the target identification system to reduce the effect of misidentification. Human gesture recognition includes action recognition and identity recognition, and the key lies in human feature extraction. The human body feature extraction mainly completes action feature extraction and identity feature extraction. In volleyball, detecting and identifying relevant poses in motion sequences can not only provide coaches and players with data-based guidance and advice but also help referees make fair and reasonable decisions in various games. However, most of the existing human gesture recognition methods are aimed at the recognition of daily simple actions [1]. Data collection is simple and further research is needed.

Most of the traditional human pose recognition research is done on sequences of video frames [2]. Although some research results have been achieved, it is difficult to break through the bottleneck of human pose recognition research using video due to changes in light intensity, interference from complex backgrounds, and the self-occlusion of target users. In the recent years, with the rapid development of video capture technology, such as Kinect, researchers can easily obtain coordinated information on the image, depth

image, and skeletal joint points [3, 4]. The information provided by depth images [5] can reflect the three-dimensional structural information and the geometry of target objects well compared with the images. Moreover, it has strong robustness to the influence of factors such as light intensity and scale changes. The posture of ball sports is more complex compared with the simple daily posture of the human body, and it also has requirements for research data. Besides, the existing recognition methods cannot effectively judge the ball movement gestures due to the change in the difficulty of gesture recognition. Therefore, further research on pose data and recognition methods is needed to improve the accuracy of ball-motion pose prediction classes.

In this article, volleyball is represented. The problem of volleyball-gesture recognition is studied combined with the analysis and summary of the existing research on human gesture recognition based on the joint point sequence and the long short-term memory (LSTM) network [6]. In addition, this article proposes a data preprocessing method based on the angle and relative distance feature enhancement and a volleyball-motion pose recognition model based on LSTM-attention. Experimental results show that the data preprocessing method reported here can further improve the accuracy of gesture recognition. Besides, the LSTM-attention recognition model is not only scientific in structure design but also has considerable competitiveness in gesture recognition performance, which can provide a basis for the research on gesture recognition in volleyball. Although the LSTM-attention recognition model is not only scientifically designed in structure but also quite competitive in gesture recognition performance, this approach is not yet universal and should be refined in future studies.

2. Materials and Methods

2.1. Recurrent Neural Network (RNN). The RNN is obtained by simulating the human neural transmission system [7]. When humans are thinking, such as reading an article, they may not be able to understand the meaning of the article only by relying on the information currently read. It is often necessary to combine the previous content to understand the essence of the article. This shows that humans are not in a blank brain when they think about problems. The brain will not discard the content of the articles that have been read before but will understand and analyse based on the previous readings. This reveals that human thinking is a continuous process [8]. However, traditional neural networks cannot achieve this, so there is an RNN. The RNN is a neural network with a short-term memory and continuously transmits information by adding loops to the network. It is suitable for processing sequential data. Figure 1 shows the general structure of an RNN. In Figure 1, h_t is the value of the hidden layer at time t, x_t is the input of the network at time t, and h_t is its output.

Each block of the neural network in Figure 1 is represented by A. Figure 2 shows the extended structure of the RNN, which is also the internal structure of the RNN transformed according to the time dimension [9]. In the RNN, there is a signal transfer between all the hidden layer
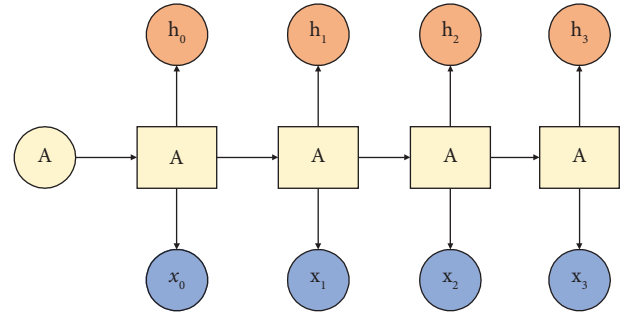
Figure 1: RNN structure diagram.
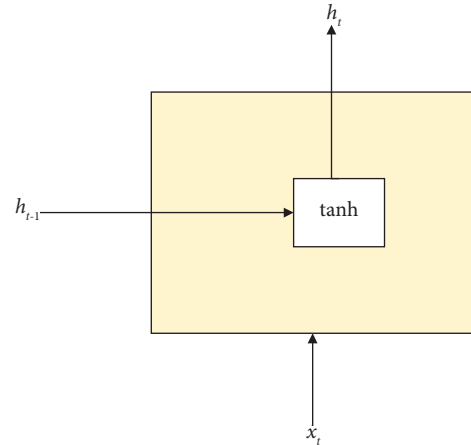
Figure 2: RNN internal structure diagram.

nodes [10]. The output of the hidden layer of the RNN at time t is fed back to the RNN at time $t + 1$. Then, the input of the RNN at time $t + 1$ and the output of the RNN at time t will act on the output of the RNN at time $t + 1$. The chain structure of the RNN essentially determines its strong processing capability for the sequence data. In the recent years, the RNN has performed very well in language modeling, speech recognition, image captioning, and machine translation.

The number of units in the input layer of a neural network is fixed, so inputs of variable length must be processed in a loop or recursion. RNN implements the former. It works by dividing an input of variable length into small chunks of equal length. Then, they are sequentially input into the network, realizing the processing of the variable length input by the neural network. The RNN can encode a tree/graph structure information as a vector, mapping the information into a semantic vector space. This semantic vector space satisfies a class of properties. For example, semantically similar vectors are close together. However, a big limitation of the RNN is the vanishing gradient problem [11]. The RNN is a short-term memory neural network that can only memorize short-distance information sequences. When the time interval becomes large, the RNN will gradually lose its ability to learn the information of the previous time nodes, which will make the learning of the RNN very difficult. This problem is also known as the "long sentence dependency problem."

2.2. LSTM. The researchers make related improvements to its basic structure to solve the "long sentence dependency problem" of the RNN. The researchers design the cell state internally to record the historical state information [12] and introduce the gating unit to control the node information of the hidden layer. This variant of the RNN can solve the above problems very well. It can memorize long-term information related to the current recognition task. This variant is called the LSTM network.

LSTM can be regarded as a special type of the RNN [13], which can greatly enhance the network's ability to store information within long time intervals. For LSTM and the RNN, the same is that they are both chain structures, and the difference is the structure inside their network. LSTM is the most effective sequence model in deep learning (DL) [14], which mainly consists of the forget gate, input gate, and output gate. The RNN model has the problem of missing gradients. LSTM effectively avoids this drawback and proposes a new cell structure, which can judge the retention or forgetting of data. Real-time data are processed from the far left to the far right [15]. Also, the data are processed from the input. Therefore, it is necessary to judge which information continues to run and which is abandoned in the endless input information. This process follows a switch control, which is $f((t))$.

The control function is as follows:

$$f^{(t)} = \sigma\left(w_f\left[h^{(t-1)}, x^t\right] + b_f\right). \tag{1}$$

In equation (1), w_f and b_f are the weight and bias of the forget gate, respectively. The previous information is input into the input gate. The task at this layer is to decide which information needs to be updated and how much to update. σ represents the activation function, b_f represents the bias value, $h^{(t-1)}$ represents the short-term memory, and x^t represents the current input.

$$i^t = \sigma\left(w_i\left[h^{(t-1)}, x^t\right] + b_i\right), \tag{2}$$

$$c^t = \sigma\left(w_c\left[h^{(t-1)}, x^t\right] + b_c\right), \tag{3}$$

$$C^t = i^t * c^t + f^{(t)} * C^{t-1}. \tag{4}$$

In equations (2)–(4), w_i and w_c represent the corresponding weights, b_i and b_c represent the corresponding biases, and C^t represents the current cell state value. After the screening of the first two gates is completed, the output gate determines which information needs to be output. There is a switch to control the output in the output gate.

$$\sigma^t = \sigma\left(w_o\left[h^{(t-1)}, x^t\right] + b_o\right), \tag{5}$$

$$h^t = o^{t*} \tanh^{-1}\left(c^t\right). \tag{6}$$

In equations (5) and (6), w_o and b_o represent the weight and bias of the output gate. o^t represents the output gating unit, h^t is the output value of the current unit, and σ represents the activation function.

2.3. Volleyball-Movement Pose Recognition Method Based on LSTM-Attention. This section constructs a volleyball-movement posture recognition method based on LSTM-Attention to help LSTM effectively extract the feature information before and after the action [16]. This section first gives a brief overview of the model and analyses the various modules involved. The experimental results demonstrate the effectiveness of the LSTM-Attention method proposed here in ball-motion pose recognition. In the recent years, the research on human gesture recognition has gradually replaced the status of traditional methods with the continuous development of DL-related technologies. In human gesture recognition, although the RNN-based gesture recognition method has obvious advantages in short-term memory, it has great difficulties in dealing with some recognition scenarios that require long-term memory. As a special type of the RNN, LSTM can not only solve the problem of the disappearance of the RNN gradient but also enhance the network's ability to memorize information for long time intervals. The latter is favored by many researchers compared with the former because it is good at obtaining feature information between long-term sequences. Many networks optimized based on this have been produced with the in-depth study of the LSTM neural network. They are widely used in text, speech, and image recognition. In the research on human posture recognition, different human skeletal structures will produce great differences when they are playing volleyball. This can lead to indistinguishable target users in the same ball game pose. For this problem, this article proposes a feature enhancement preprocessing method based on the angle and the relative distance. Besides, contextual information between action sequences plays a crucial role in gesture recognition. This section constructs a ball-motion pose recognition method based on the LSTM-Attention model to effectively extract the long-sequence feature information of ball motion poses. The overall process of ball sports gesture recognition is shown in Figure 3.

First, Kinect is used to acquire the joint point coordinate data of the human skeleton performing ball motion [17]. Then, the scale-invariant angle and relative distance features are extracted from the joint point information. Finally, the LSTM-attention network is used to mine the deep timing information in the skeleton sequence of the human body when ball sports are performed. Furthermore, this information is combined with spatial features to recognize the ball motion pose of the human body [18]. The model learns the correlation between the time series data of ball motion poses autonomously and effectively by combining LSTM with the attention mechanism to improve the accuracy of the model pose recognition.

2.4. Angle Feature Extraction. In the process of the human body performing ball sports, the features selected based on joint point information should have general behavior [19]. Features do not vary greatly due to differences in the human skeletal structure, and they do not shift because the target user and the Kinect depth sensor are in different
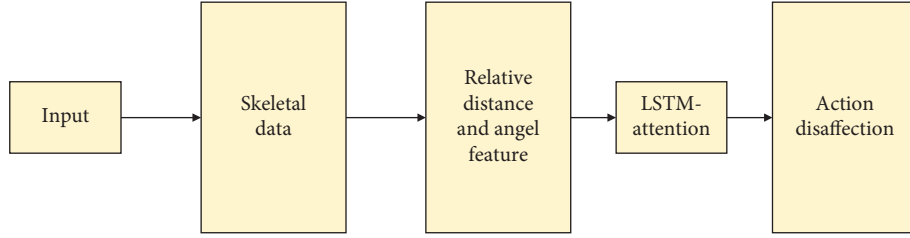
FIGURE 3: Flowchart of volleyball gesture recognition.

positions. Therefore, the angle features extracted based on the joint point information are used to predict the pose category of the human body during ball sports [20]. When the human body performs different ball sports, there will be different angular relationships between the joint points of the human bones in space. Especially for the joint points on the arm, the included angle between the joint points involved in the corresponding action of the ball sports will have a relatively fixed range of variation. This can intuitively describe the ball game posture. Therefore, the coordinate information of the eight joint points is decomposed into five parts according to the human body structure, including the trunk and the limbs. Then, the angle feature extraction is performed on the joint-point coordinate information of these five parts.

When the angle of the joint point information of the human skeleton is calculated, the limbs of each part in the human skeleton model need to be regarded as a vector. The correspondence between the angles between the joint points and each component vector is shown in Table 1. r_{ij} represents the vector that forms the angle of a joint point.

In Figure 4, the right arm model of the human body is taken as an example [21], and the joint angle r_5 consists of two vectors, $r_{4,5}$ and $r_{5,6}$, respectively.

2.5. Relative Distance Feature Extraction.

The relative distance feature between the human skeleton joint points is a kind of information that can express different ball-motion pose data in the spatial dimension [22]. When the human body performs a ball action, the spatial position information of the joint points of each part of the human skeleton will also change. Moreover, the relative distance between some joint points that change with the movement will also form a change rule for an action posture [23]. For example, when people perform a badminton swing, the relative distance between the user's hand and the base of the spine is a very expressive information. Therefore, the relative distance feature extracted based on joint point information is used here to analyse the pose category of the human body when they perform ball sports.

It is found that the joint points at the base of the spine have stability in the process of the human body movement in expressing the human body ball sports posture through analysis of the joint point data when the human body performs ball sports posture. Therefore, this article regards the joint point at the base of the spine as the center point and

TABLE 1: Correspondence between the angle between the joint points and each component vector.

Joint angle number	Composition vector
1	$r_{1,2}$, $r_{1,3}$
2	$r_{2,1}$, $r_{2,3}$
3	$r_{3,1}$, $r_{3,2}$
4	$r_{4,5}$, $r_{4,6}$
5	$r_{5,4}$, $r_{5,6}$
6	$r_{6,4}$, $r_{6,5}$
7	$r_{7,8}$, $r_{7,9}$
8	$r_{8,7}$, $r_{8,9}$
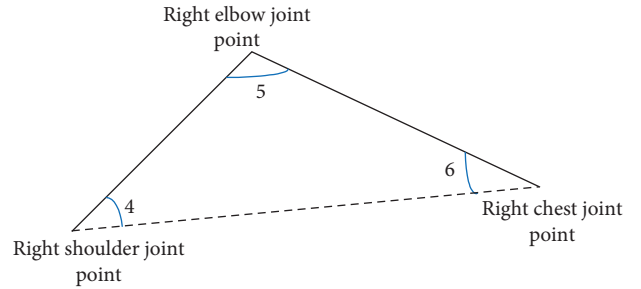
FIGURE 4: Schematic diagram of the characteristics of the right arm.

analyses the ball sports posture based on the relative distance between the center point and other joint points.

2.6. Ball-Movement Pose Recognition Method Based on LSTM-Attention.

Here, Kinect is used to collect the joint point data of the human body during ball sports [24]. Based on this, two kinds of geometric features are artificially designed to describe the pose of the ball. The appropriate relevant parameters in the model are obtained after the LSTM-attention network model constructed here is trained on the ball sports training set. Besides, the recognition and classification of ball sports poses are carried out on the test set. Its network structure is demonstrated in Figure 5.

In this model, a multilevel LSTM structure is designed to improve the learning ability of the recognition network [25] to handle complex feature representations in ball sports poses. The number of network layers of LTSM is designed to be three layers. An attention mechanism is added to the model. This design enables the feature vector to spontaneously perceive the network weights that significantly impact the recognition results of ball motion gestures. Some important feature information gets attention. This can also

perform further feature enhancement on the feature data extracted from the previous network layers. In addition, a dropout layer is added between the LSTM structures. This can reduce the occurrence of overfitting of the gesture recognition model when the number of experimental samples is limited. To sum up, feature learning through the multilevel LSTM network is combined with feature enhancement of the attention mechanism. This enables the network model to fully and effectively learn the correlation between the time series data in the ball motion poses, thereby improving the pose recognition ability of the entire network model.

Figure 5 displays a diagram of the LSTM-attention network model that is expanded according to time. The model can form an action sequence according to the time sequence of the features of the human body during ball sports, and it is used as the input of the ball-sports pose recognition network. The input includes an angle feature and a relative distance feature. The ball motion features of each human body have become a 38-dimensional data through the previously mentioned joint evaluation, repair, and feature extraction. Also, the length of each action sequence will be affected by the different frame numbers of different actions. It is indispensable to perform isometric operations on the data in the dataset before the feature data are input into the gesture recognition network model. According to the longest frame value in each ball motion sequence, the other motion sequences are zeroed.

The multidimensional feature sequence is input into the LSTM-attention network, which is processed by LSTM, dropout, and the attention mechanism. The intermediate value is sent to the output layer. The function used in this layer is the softmax function. The function can judge the corresponding ball sports posture and output the probability value of five different ball-sports posture labels. Finally, the maximum value of the probability evaluation values is selected as the output category of the final ball-motion pose.

When the human body performs different ball motion poses, all the joint motion data contained in the human skeleton are not equally important. For example, the changes in the joint point data of the human bones are mainly concentrated in the right arm part in the process of the human body completing the badminton swing. The joint point data of other parts of the body have little effect on the final gesture recognition effect. Therefore, the attention mechanism is introduced into the improved human ball-motion pose recognition model. In the process of movement, the important data of human limbs and joints can be marked and much attention can be given to them. In the research data here, the coordinate data of fifteen joint points of the human body during ball sports are collected, and the human skeleton model is established based on this. In most cases, the joint point information that a ball motion pose can be associated with is fixed. These fixed-joint point information will be converted into feature vectors through LSTM. The essence of the attention mechanism is to perform a weighted summation of these feature vectors to find out the
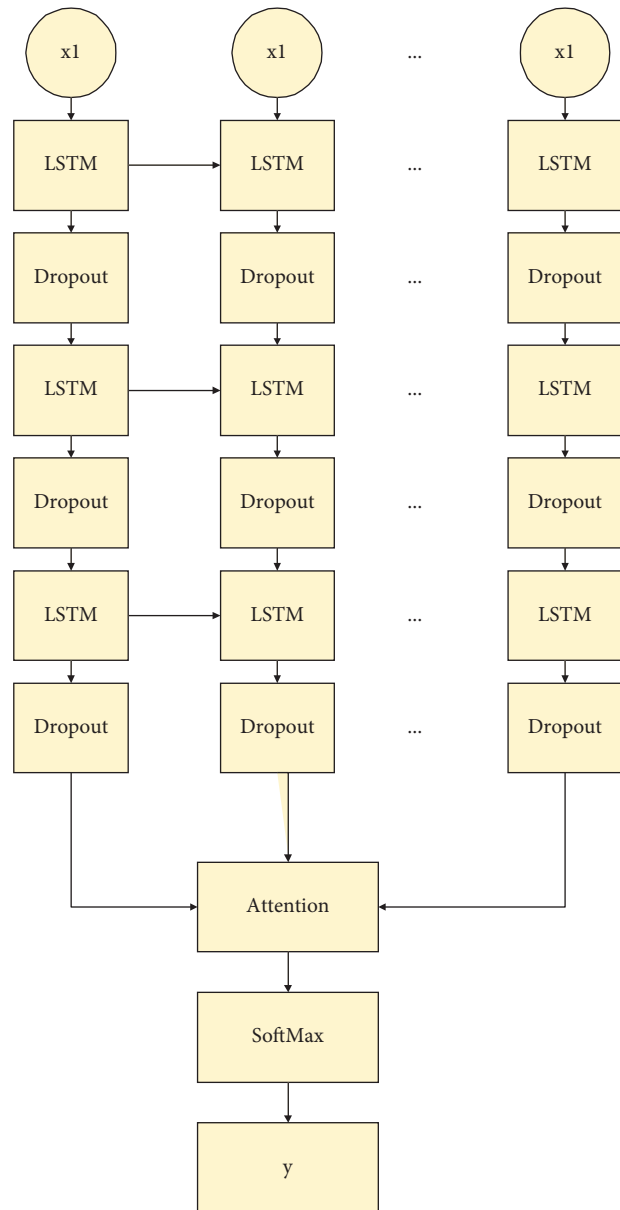
Figure 5: Network structure of volleyball pose recognition.

joint point information that importantly impacts the recognition of ball motion poses.

3. Results and Discussion

The comparative experiments before and after the coordinate system transformation of joint point information verify the improvement effect of the joint-point preprocessing method based on the coordinate system transformation on the accuracy of gesture recognition. This section conducts experiments. First, this article conducts experiments on the joint point data before and after the coordinate system transformation through the traditional LSTM-pose recognition network model. MATLAB software is used to simulate and simulate the gesture recognition process of the network model. The results are shown in Figure 6.
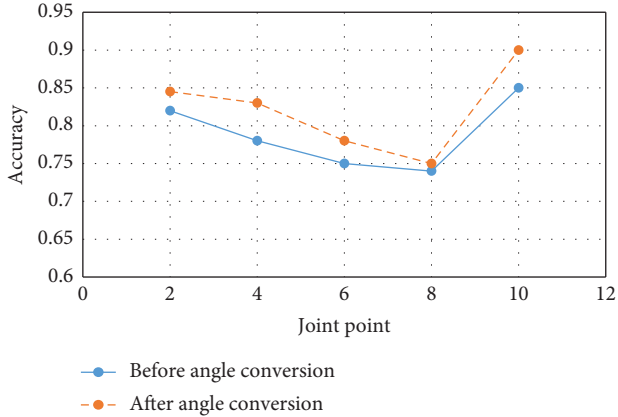
Figure 6: LSTM prediction results before and after angle conversion.

Figure 7: Overall prediction results before and after angle conversion.

Figure 6 shows the comparative experimental results before and after the coordinate information conversion preprocessing of the joint point data through the LSTM neural network. The experimental results indicate that the joint-point coordinate information of the coordinate system transformation significantly improves the recognition accuracy of the five ball motion poses by at least 0.01. However, the improvement in gesture recognition accuracy for smash actions is lower compared to the improvements in gesture recognition accuracy for serve, lift, high clear, and backhand. This also means that gesture recognition accuracy for actions like smash is less affected by angular changes during data collection than other actions.

In addition to LSTM, this section also conducts comparative experiments on gesture recognition methods such as BiLSTM, linear SVM, and multilayer LSTM. The experimental data and settings remain the same as in the above LSTM experiments. BiLSTM is the abbreviation of bidirectional long short-term memory, which means a bidirectional long and short-term neural network. It is composed of forward LSTM and backward LSTM. Both are often used to model contextual information in natural language processing tasks. Figure 7 shows the overall prediction results of each gesture recognition method for the joint-point coordinate information before and after the coordinate system conversion.

The experimental results show that the joint-point coordinate information after the coordinate system transformation can effectively improve the overall accuracy of the ball-motion gesture recognition network model. After converting the coordinate system, the accuracy is improved by at least 0.01, and the accuracy of the method proposed here is higher than the other methods. The optimal hierarchical experiment of the LSTM multilayer structure is expected to integrate the feature information of the long-term sequence on a global scale and realize the high-level abstraction of the input human skeleton joint point data. Therefore, this article constructs a multilevel LSTM structure based on a classification model. However, if the number of layers in the LSTM multilayer structure is large, the model will take a lot of time to converge, which will complicate the
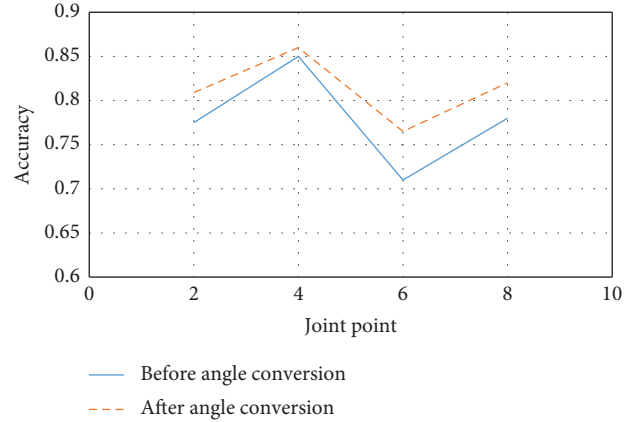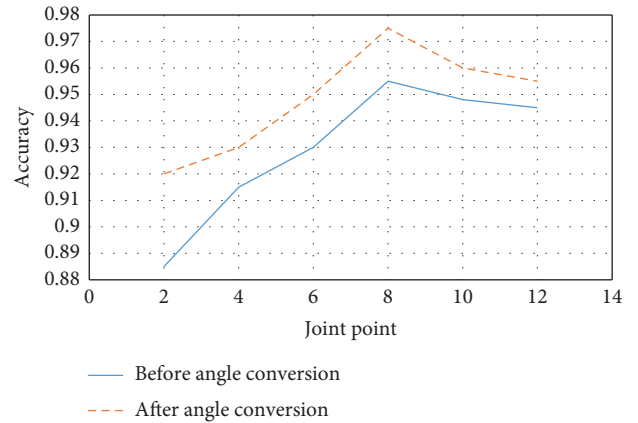
Figure 8: Comparative experiments of different LSTM layer structures in action recognition.

model. Therefore, this article conducts comparative experiments on different layers of LSTM structures on the BadmintonData and MSRAction3D datasets to verify the scientificity and effectiveness of the ball-motion gesture recognition model based on the three-layer LSTM structure designed here. The BadmintonData dataset contains various volleyball poses. The MSRAction3D dataset records 20 actions and ten subjects. Each subject performs each action two to three times. There are a total of 567 depth map sequences with a resolution of $640 * 240$. Data are recorded with a depth sensor similar to the Kinect unit.

The number of layers of the LSTM multilayer structure is set as one, two, three, four, and five, respectively. LSTM-Attention_n is a model that fuses the n-layer LSTM structure and the attention mechanism, respectively. Besides, LSTM is a model that only contains a single-layer LSTM structure without an attention mechanism. The results are revealed in Figure 8.

The purpose of the comparative experiment before and after the restoration of joint point information is to verify the improvement effect of the joint-point processing method based on the bone length and motion continuity on the performance of the pose recognition method. Its essence is

TABLE 2: Comparative experiments before and after the data recovery of joint points.

Experimental data	LSTM _	B I-LSTM	Linear SVM	Multilayer LSTM
Badminton data	0.81	0.87	0.76	0.82
BadmintonData_Repairing	0.83	0.88	0.83	0.85
MSRAction3D_	0.90	0.95	0.92	0.95
MSRAction3D_Repairing	0.92	0.96	0.93	0.95

to evaluate the influence of the joint point data with errors on the accuracy of human pose recognition.

This section uses the abovementioned gesture recognition methods to conduct comparative experiments on the BadmintonData and MSRAction3D datasets. In the experiment, other experimental configurations are the same except for the preprocessing process of joint-point data repair. The two datasets after joint data repair processing are recorded as BadmintonData_Repairing and MSRAction3D_Repairing, respectively. Then, model generation and prediction are performed on the BadmintonData, MSRAction3D, BadmintonData_Repairing, and MSRAction3D_Repairing datasets using the above four pose recognition methods, respectively. The predicted results are shown in Table 2.

From the experiment, the same action poses in the BadmintonData_Repairing and MSRAction3D_Repairing datasets are recognized, and the pose recognition results after the joint repair operation will be much higher than the data without joint repair. It is proved that the processing method based on the bone length and motion continuity proposed in this article can improve the final accuracy of the gesture recognition network. Therefore, it is crucial to evaluate the reliability of the joint-point coordinate information obtained by Kinect and restore the joint point information with errors before the joint-point coordinate information is used for action and pose recognition.

4. Conclusion

Studying, recognizing, and detecting volleyball postures can provide theoretical guidance and suggestions for people, which can be applied in competitions. It also helps event judges make sound decisions. At present, the pose recognition of ball sports is very challenging in action complexity and research data, and this research also has an important application value. This article takes volleyball as the representative to study the problem of volleyball movement pose recognition combined with the analysis and summary of the existing human pose recognition research based on the joint point sequence and the LSTM network. This article proposes a data preprocessing method based on the angle and relative distance feature enhancement and a volleyball motion pose recognition model based on LSTM-attention. The experimental results imply that the data preprocessing method reported here can further improve the accuracy of gesture recognition. The joint-point coordinate information of the coordinate system transformation significantly improves the recognition accuracy of the five ball motion poses by at least 0.01. Moreover, it is concluded

that the LSTM-attention recognition model is not only scientific in structure design but also has considerable competitiveness in gesture recognition performance. However, this method is not yet universal and should be refined in future research.

Data Availability

The experimental data used to support the findings of this study are available from the corresponding author upon request.

Conflicts of Interest

The authors declare that they have no conflicts of interest.

References

[1] Q. Dang, J. Yin, B. Wang, and W. Zheng, "Deep learning based 2d human pose estimation: a survey," *Tsinghua Science and Technology*, vol. 24, no. 6, pp. 663–676, 2019.

[2] Y. Yu, X. Si, C. Hu, and J. Zhang, "A review of recurrent neural networks: LSTM cells and network architectures," *Neural Computation*, vol. 31, no. 7, pp. 1235–1270, 2019.

[3] J. Huang, C. Chi, W. Wang, and H. Huang, "A sequence-scheduled and query-based mac protocol for underwater acoustic networks with a mobile node," *Journal of Communications and Information Networks*, vol. 5, no. 2, pp. 150–159, 2020.

[4] D. Bodur and M. Demiralp, "Influence of a simple pole on the convergence of separate node ascending derivatives expansion (SNADE) on a sequence of nodes alternating between 2 values," *Mathematical Methods in the Applied Sciences*, vol. 41, no. 17, pp. 7333–7350, 2018.

[5] K. Smagulova and A. P. James, "A survey on LSTM memristive neural network architectures and applications," *The European Physical Journal - Special Topics*, vol. 228, no. 10, pp. 2313–2324, 2019.

[6] Y. Huang, M. Kaufmann, E. Aksan, M. J. Black, O. Hilliges, and G. Pons-Moll, "Deep inertial poser: learning to reconstruct human pose from sparse inertial measurements in real time," *ACM Transactions on Graphics*, vol. 37, no. 6, pp. 1–15, 2018.

[7] Y. Xiao and J. Wu, "Data transmission and management based on node communication in opportunistic social networks," *Symmetry*, vol. 12, no. 8, p. 1288, 2020.

[8] T. Jamal and S. A. Butt, "Malicious node analysis in MANETS," *International Journal of Information Technology*, vol. 11, no. 4, pp. 859–867, 2019.

[9] J. U. Seong, B. H. Lee, and D. Yang, "A multi-node channel rendezvous algorithm in cognitive radio ad-hoc networks," *Journal of the Korea Institute of Information and Communication Engineering*, vol. 23, no. 4, pp. 453–461, 2019.

[10] R. Wang, Y. Liu, and J. Chen, "Network representation learning algorithm combined with node text information," *Journal of Physics: Conference Series*, vol. 1769, no. 1, Article ID 012054, 2021.

[11] D. Cai and W. Lam, "Graph transformer for graph-to-sequence learning," *Proceedings of the AAAI Conference on Artificial Intelligence*, vol. 34, no. 5, pp. 7464–7471, 2020.

[12] R. Ma, X. Zheng, P. Wang, H. Liu, and C. Zhang, "The prediction and analysis of COVID-19 epidemic trend by combining LSTM and Markov method," *Scientific Reports*, vol. 11, no. 1, Article ID 17421, 2021.

[13] C. Liu, Y. Zhang, J. Sun, Z. Cui, and K. Wang, "Stacked bidirectional LSTM RNN to evaluate the remaining useful life of supercapacitor," *International Journal of Energy Research*, vol. 46, no. 3, pp. 3034–3043, 2022.

[14] H. Lu, L. Jin, X. Luo, B. Liao, D. Guo, and L. Xiao, "RNN for solving perturbed time-varying underdetermined linear system with double bound limits on residual errors and state variables," *IEEE Transactions on Industrial Informatics*, vol. 15, no. 11, pp. 5931–5942, 2019.

[15] J. A. Nasir, O. S. Khan, and I. Varlamis, "Fake news detection: a hybrid CNN-RNN based deep learning approach," *International Journal of Information Management Data Insights*, vol. 1, no. 1, Article ID 100007, 2021.

[16] A. Shewalkar, D. Nyavanandi, and S. A. Ludwig, "Performance evaluation of deep neural networks applied to speech recognition: RNN, LSTM and GRU," *Journal of Artificial Intelligence and Soft Computing Research*, vol. 9, no. 4, pp. 235–245, 2019.

[17] N. Majumder, S. Poria, D. Hazarika, R. Mihalcea, A. Gelbukh, and E. Cambria, "Dialoguernn: an attentive rnn for emotion detection in conversations," *Proceedings of the AAAI Conference on Artificial Intelligence*, vol. 33, no. 01, pp. 6818–6825, 2019.

[18] A. H. Khan, S. Li, and X. Luo, "Obstacle avoidance and tracking control of redundant robotic manipulator: an RNN-based metaheuristic approach," *IEEE Transactions on Industrial Informatics*, vol. 16, no. 7, pp. 4670–4680, 2020.

[19] S. Bouktif, A. Fiaz, A. Ouni, and M. A. Serhani, "Multi-sequence LSTM-RNN deep learning and metaheuristics for electric load forecasting," *Energies*, vol. 13, no. 2, p. 391, 2020.

[20] J. Du, C. M. Vong, and C. L. P. Chen, "Novel efficient RNN and LSTM-like architectures: recurrent and gated broad learning systems and their applications for text classification," *IEEE Transactions on Cybernetics*, vol. 51, no. 3, pp. 1586–1597, 2021.

[21] B. Zhao, X. Li, and X. Lu, "TTH-RNN: tensor-train hierarchical recurrent neural network for video summarization," *IEEE Transactions on Industrial Electronics*, vol. 68, no. 4, pp. 3629–3637, 2021.

[22] D. Kollias and S. Zafeiriou, "Exploiting multi-cnn features in cnn-rnn based dimensional emotion recognition on the omg in-the-wild dataset," *IEEE Transactions on Affective Computing*, vol. 12, no. 3, pp. 595–606, 2021.

[23] H. K. Ahn and N. Park, "Deep RNN-based photovoltaic power short-term forecast using power IoT sensors," *Energies*, vol. 14, no. 2, p. 436, 2021.

[24] B. Zhao, X. Li, and X. Lu, "CAM-RNN: Co-attention model based RNN for video captioning," *IEEE Transactions on Image Processing*, vol. 28, no. 11, pp. 5552–5565, 2019.

[25] F. Ofli, R. Chaudhry, G. Kurillo, R. Vidal, and R. Bajcsy, "Sequence of the most informative joints (SMIJ): a new representation for human skeletal action recognition," *Journal of Visual Communication and Image Representation*, vol. 25, no. 1, pp. 24–38, 2014.

Research Article

Statistical Characterization and Modeling of Radio Frequency Signal Propagation in Mobile Broadband Cellular Next Generation Wireless Networks

Joseph Isabona [iD],[1] **Lanlege Louis Ibitome,**[2] **Agbotiname Lucky Imoize** [iD],[3,4] **Udit Mamodiya** [iD],[5] **Ankit Kumar** [iD],[6] **Montaser M. Hassan** [iD],[7] **and Isaac Kweku Boakye** [iD][8]

[1]*Department of Physics, Federal University Lokoja, Lokoja 260101, Nigeria*
[2]*Department of Mathematical Sciences, Federal University Lokoja, Lokoja 260101, Nigeria*
[3]*Department of Electrical and Electronics Engineering, Faculty of Engineering, University of Lagos, Akoka, Lagos 100213, Nigeria*
[4]*Department of Electrical Engineering and Information Technology, Institute of Digital Communication, Ruhr University, Bochum 44801, Germany*
[5]*Department of Electrical Engineering, PIET-AICTE Idea Lab, Poornima Institute of Engineering and Technology, Jaipur, Rajasthan, India*
[6]*Department of Computer Engineering and Applications, GLA University Mathura, Mathura, Uttar Pradesh 281406, India*
[7]*Department of Biology, College of Science, Taif University, P.O. Box 11099, Taif 21944, Saudi Arabia*
[8]*Kwame Nkrumah University of Science and Technology (KNUST), Kumasi, Ghana*

Correspondence should be addressed to Isaac Kweku Boakye; ikboakye3@st.knust.edu.gh

An accurate assessment of the spatial and temporal radio frequency channel characteristics is essential for complex signal processing and cellular network optimization. Current research has employed numerous models to figure out how much signal propagation loss occurs along the propagation paths. However, there are issues in finding the right model for a particular terrain because these models are not universally applicable. By employing the lognormal function and the Maximum Likelihood model, a hybrid probabilistic statistical distribution model was evolved. Three LTE cell site locations in Port Harcourt, Nigeria, were used to create a hybrid model that describes the functional stochastic signal propagation loss in the area. The evaluated Maximum Likelihood model accurately estimates the relevant wireless channel properties based on observed field data. The minor square regression approach and the proposed hybrid parameter estimation methodology are compared. When it comes to estimating standard deviation errors as well as the root mean square errors, the ML-based approach consistently outperforms the least square regression model. Finally, the proposed hybrid probabilistic statistical distribution model would be useful for mobile broadband network planning in related wireless propagation conditions.

1. Introduction

Adequate knowledge of spatial radio frequency channel parameters is critical to cellular network engineering [1–4]. Accurate estimation of the network parameters is necessary for estimating the location probability and shadow margin computations, aiding effective network planning and optimization processes [5–9]. The work in [5] investigated macrocell path loss prediction employing artificial intelligence techniques. On the measurements of radio field strength and pathloss determination in UMTS networks, Isabona et al. [6] characterized the signal propagation loss in typical 3G wireless networks. In the built-up area of South-South Nigeria, Isabona and Peter [7] described signal propagation loss based on field measurements at 1.9 GHz. In [8], the authors presented radio frequency measurements and capacity analysis for industrial indoor environments. The work presented focuses on measurements campaign,

including field testing, modeling, and a comparative analysis of multifrequency band propagation characteristics for cellular networks. By using experimental and simulated propagation data, estimating the spatial and temporal radio frequency channel parameters is key to addressing the proliferating issues in complex signal processing, cellular network systems design, and optimization [10–14].

In order to address the problem of determining the most suitable model for a specific environment, several parameter estimation approaches have been exploited recently [15–20]. Specifically, the work in [15] examined transmit power estimation focusing on the signal strength of the wireless network with cooperative receiver nodes using the Maximum Likelihood (ML) estimation [21, 22]. The authors applied the experimental findings to validate the explored ML estimation. In [16], the authors investigated the Maximum Likelihood estimation combined with signal statistics to determine the performance of intensity-modulated fibre optic links.

In related work, the authors in [17] reported realistic predictive modeling of stochastic path attenuation losses in wireless channels over microcellular urban, suburban, and rural terrains using probability distribution functions. Their study revealed that the normal distribution was most suitable for the statistical predictive modeling of signal path loss data. Similar predictive analyses have been reported [18–20]. Specifically, the work in [18] presented a study on empirical path loss models to accurately predict TV signals for secondary users. The authors of the work in [19] posed and answered a question on why is shadow fading lognormal. In [20], the authors investigated the fading characteristics of wireless channels on a high-speed railway in hilly terrain. In [23–25], the least square and absolute deviation regression methods were applied to estimate the parameters of the deployed radio frequency channel measurements from different wireless propagation environments. In particular, the work in [23] reported an experimental study of UMTS radio signal propagation characteristics, employing field measurements in the GSM band. In [24], the authors presented RF propagation measurement and modeling to facilitate network planning of outdoor wireless local area networks operating in the 2.4 GHz band.

Similarly, the work in [25] examined path loss propagation prediction and optimization, employing the popular Hata model at 800 MHz in an urban area. In a similar study, Gentile et al. [26] proposed a suitable methodology for benchmarking radio-frequency channel sounders through a system model. The current contribution exploited an efficient parameter-based ML estimation model combined with the lognormal distribution function to estimate spatial variations of wireless propagated signals. The study focused on practical field tests performed on a commercial mobile broadband network. The findings of this work demonstrated that the proposed ML-based model estimates the relevant wireless channel parameters for the tested environments, in comparison with the measured data, with minimal errors. The main contributions of the paper are outlined as follows:

(i) An efficient parameter-based ML estimation model combined with the lognormal distribution function to estimate spatial variations of wireless propagated signals is proposed

(ii) The performance of the proposed hybrid parameter estimation model compared with the least square regression method was examined

(iii) The cumulative hazard plots of propagation loss distribution of ML and LS models with the measurement obtained from different site locations were demonstrated

(iv) The mean prediction error with ML and LS estimated parameters on measured pathloss loss data were determined

The remainder of this paper is organized as follows: in Section 2, the preliminaries are highlighted briefly. Section 3 gives an overview of the simulated and experimental measurements and analyses. Section 4 presents the results and discussions. Finally, Section 5 provides a concise conclusion to the paper.

2. Materials and Methods

This section briefs the measurement campaign, signal propagation model, and maximum-likelihood estimators.

2.1. Measurements Campaign and Signal Propagation Modeling.
The measurement campaign was conducted in the built-up areas of Port-Harcourt, Nigeria. The tested 4G LTE network operates at 1900 MHz. Field measurements were taken using drive test tools in and around the investigated environment [27–29]. Real-time 4G LTE signal strength obtained from the evolved base station (eNodeBs) was processed and analyzed in MATLAB. In particular, the Reference Signal Received Power (RSRP) was extracted from the logged files and processed similarly to earlier works [30–32]. According to Rappaport [33], the experimental received signal power and propagation loss are logarithmically related to the propagation distances, d_i, and transmit power P_{TX} is defined by the following equation:

$$P_{\mathrm{dBm},i} = P_{TX} - L_{\mathrm{off}} - 10\alpha \log_{10}(d_i) - X_i, \tag{1}$$

where X_i and L_{off} express the location-specific fading and offset parameters, respectively. Equation (1) describes the signal propagation loss model. Specifically, it is assumed that L_{off} can be precisely achieved using a small reference measurement number. In the model, the shadow fading parameter X_i is assumed to be a specific random variable such that $X_i \sim N(0, \sigma^2)$. The key attenuation model parameters such as α and σ^2 are derived relative to their dependence on the actual wireless propagation environment [27, 29, 34, 35].

2.2. Maximum Likelihood Estimators.
The Maximum Likelihood (ML) estimation is an indispensable and effective channel parameter estimation method that finds practical application in signal processing [36–39]. The ML method can be deployed to examine the behaviour of channel data

parameters. This study employs the likelihood function [40–42] to determine the ML estimation parameters in the measured pathloss data. Specifically, the likelihood function of the lognormal distribution for P_i $(i = 1, 2, 3, \ldots, n)$ dataset is achievable by considering the product of the probability densities expressed in equations (2) to (6):

$$f\left(\frac{P, \theta}{\mu, \omega^2}\right) = \prod_{i=1}^{n}\left[f\left(\frac{P_i}{\mu, \omega^2}\right)\right], \tag{2}$$

$$= \prod_{i=1}^{n}\left(\left(2\pi\omega^2\right)^{-1/2} P_i^{-1} \exp\left[\frac{-(\ln P_i - \mu)^2}{2\omega^2}\right]\right), \tag{3}$$

$$= \left(2\pi\omega^2\right)^{-1/2} \prod_{i=1}^{n}\left(P_i^{-1} \exp\left[\sum_{i=1}^{n} \frac{-(\ln P_i - \mu)^2}{2\omega^2}\right]\right), \tag{4}$$

$f(\cdot)$ signifies the lognormal distribution with parameters:

$$\widehat{\omega} = c\omega, c := \frac{10}{\ln(10)}, \tag{5}$$

and

$$\mu_i = cP_{\text{TX}} - L_{\text{off}} - 10\alpha \log_{10}(d_i). \tag{6}$$

The lognormal distribution log-likelihood function for P_i $(i = 1, 2, 3, \ldots, n)$ dataset can be obtained by exploring the natural log of the likelihood function (7) to (11):

$$L\left(\frac{P}{\mu, \omega^2}\right) = \ln\left(\left(2\pi\omega^2\right)^{-1/2} \prod_{i=1}^{n} P_i^{-1} \exp\left[\sum_{i=1}^{n} \frac{-(\ln P_i - \mu)^2}{2\omega^2}\right]\right), \tag{7}$$

$$= -\frac{n}{2}\ln\left(2\pi\omega^2\right) - \sum_{i=1}^{n} \ln P_i - \frac{\sum_{i=1}^{n} -(\ln P_i - \mu)^2}{2\omega^2}, \tag{8}$$

$$= -\frac{n}{2}\ln\left(2\pi\omega^2\right) - \sum_{i=1}^{n} \ln P_i - \frac{\sum_{i=1}^{n} -\left(\ln\left(P_i\right)^2 - 2\ln P_i\mu + \mu^2\right)}{2\omega^2}, \tag{9}$$

$$= -\frac{n}{2}\ln\left(2\pi\omega^2\right) - \sum_{i=1}^{n} \ln P_i - \frac{\sum_{i=1}^{n} \ln\left(P_i\right)^2}{2\omega^2} + \frac{\sum_{i=1}^{n} \ln P_i\mu}{2\omega^2} - \frac{\sum_{i=1}^{n} \ln \mu^2}{2\omega^2}, \tag{10}$$

$$= -\frac{n}{2}\ln\left(2\pi\omega^2\right) - \sum_{i=1}^{n} \ln P_i - \frac{\sum_{i=1}^{n} \ln\left(P_i\right)^2}{2\omega^2} + \frac{\sum_{i=1}^{n} \ln P_i\mu}{\omega^2} - \frac{n\mu}{2\omega^2}. \tag{11}$$

The next step is to find μ and ω^2, which maximize $L(P/\mu, \omega^2)$. Thus, for μ, we have the following equation:

$$\frac{\delta L}{\delta \mu} = \frac{\sum_{i=1}^{n} \ln P_i\mu}{\omega^2} - \frac{2n\mu}{2\omega^2} = 0. \tag{12}$$

Equation (11) also implies that equations (13) and (14) hold:

$$\frac{n\mu}{\omega^2} = \frac{\sum_{i=1}^{n} \ln P_i\mu}{\omega^2}. \tag{13}$$

So

$$\mu = \sum_{i=1}^{n} \ln P_i/n. \tag{14}$$

Similarly, to find ω^2, which maximize $L(P/\mu, \omega^2)$, according to (15) to (17):

$$\frac{\delta L}{\delta \omega^2} = -\frac{n}{2}\frac{1}{\sigma^2} - \frac{\sum_{i=1}^{n} (\ln P_i - \mu)^2 \sum_{i=1}^{n} (\ln P_i - \mu)^2}{2}\left(-\omega^2\right)^{-2}, \tag{15}$$

$$= -\frac{n}{2\sigma^2} - \frac{\sum_{i=1}^{n} (\ln P_i - \mu)^2}{2\left(\omega^2\right)^2} = 0, \tag{16}$$

$$-\frac{n}{2\sigma^2} = \frac{\sum_{i=1}^{n} (\ln P_i - \mu)^2}{2\omega^4}. \tag{17}$$

Equation (17) implies the definitions in (18) and (19):

$$n = \frac{\sum_{i=1}^{n} (\ln P_i - \mu)^2}{\omega^2}, \tag{18}$$

and

$$\omega^2 = \frac{\sum_{i=1}^{n} (\ln P_i - \mu)^2}{n}. \tag{19}$$

By applying the expression in equations (15) and (19) can also be written as follows:

$$\omega^2 = \frac{\sum_{i=1}^{n} \left(\ln P_i - \sum_{i=1}^{n} \ln P_i/n\right)^2}{n}. \tag{20}$$

Therefore, the ML estimation model parameters are defined in (21): $\mu = \sum_{i=1}^{n} \ln P_i/n$ and

$$\omega = \sqrt{\frac{\sum_{i=1}^{n} \left(\ln X_i - \sum_{i=1}^{n} \ln P_i/n\right)^2}{n}}. \tag{21}$$

3. Results and Discussions

The results of the characterized parameters and predictive analysis of the propagation loss data using the ML estimate approach are briefed. The parameters of the pathloss data obtained via the least square (LS) regression estimation are provided for deductive comparison [15, 16]. The cumulative hazard plots are presented in Figures 1–3. Table 1 shows the measured loss estimated parameters and their estimation accuracies using the two approaches. The cumulative hazard plots are employed to visually examine the ML and LS models and their distributive prediction and reliability on the measured propagation loss. From the plotted mean prediction graphs of Figures 4–9 and the summarized prediction results in Table 2, it is evident that the ML estimation is superior to the LS approach. In Table 2, for
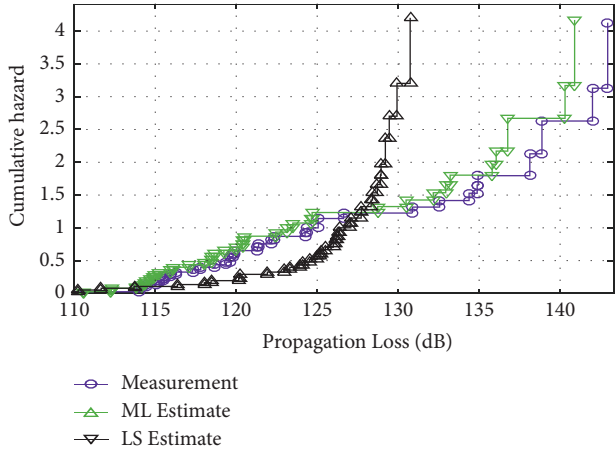
Figure 1: Cumulative hazard plots of propagation loss distribution of ML and LS models with the measurement obtained from site location 1.

Table 1: Estimated propagation loss parameters with the ML and LS models.

	Model estimated loss parameters	μ	ω	α
Site 1	ML	134.3	7.48	2.6
	LS	134.2	6.17	2.0
Site 2	ML	123.5	7.45	2.6
	LS	123.5	5.81	1.4
Site 3	ML	123.8	9.12	2.8
	LS	123.8	5.77	2.2
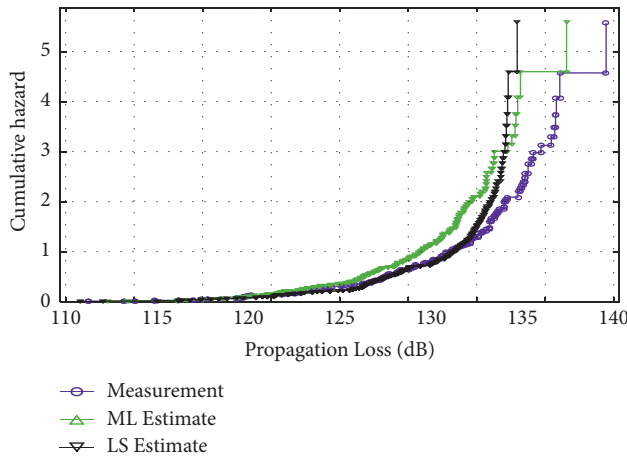
Figure 2: Cumulative hazard plots of propagation loss distribution of ML and LS models with the measurement obtained from site location 2.

instance, employing the mean absolute error (MAE), mean percentage error (MAPE), root mean square error (RMSE), and standard deviation error (SDE) statistics, the ML model, attains 1.82, 3.97, 1.99, and 0.79, respectively, in site location 1. In contrast, the LS model achieved 2.70, 11.85, 3.44, and 2.13, respectively. The ML posed similar parameter estimation and prediction performance over the LS approach, as revealed in Table 2 for site locations 1 and 2.
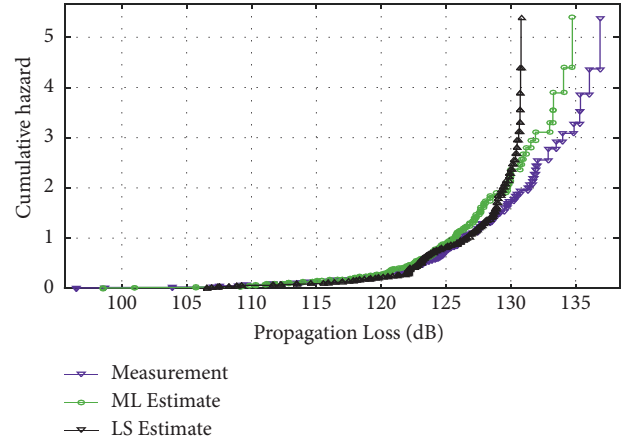
Figure 3: Cumulative hazard plots of propagation loss distribution of ML and LS models with the measurement obtained from site location 3.
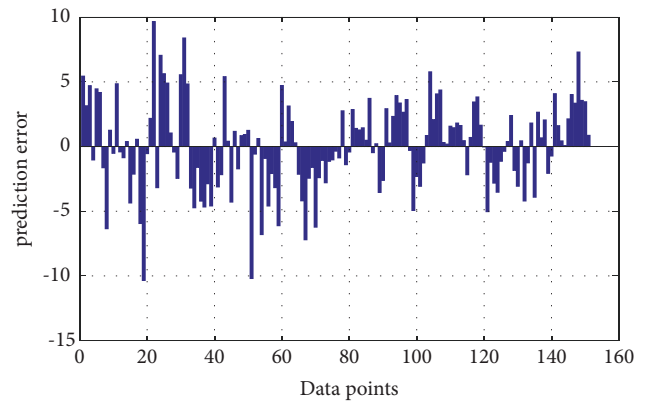
Figure 4: Mean prediction error with ML estimated parameters on measured loss data obtained from site location 1.
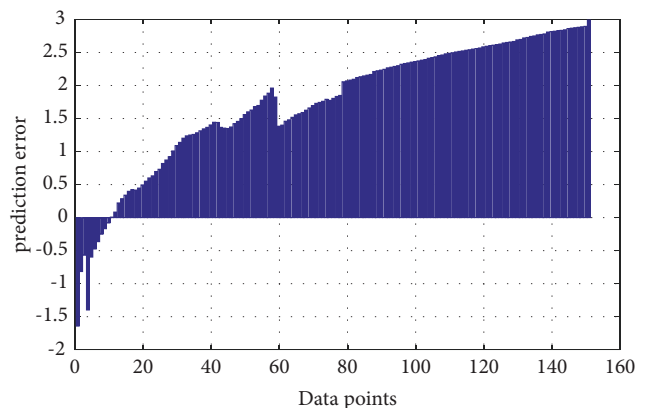
Figure 5: Mean prediction error with LS estimated parameters on measured loss data obtained from site location 1.

Figures 10–12 show exponential CDF plots to demonstrate the accuracy attained by the ML approach in estimating (predicting) the measured path loss values acquired over three study locations. It can be found from the three graphs that the ML-based estimation closely maps the
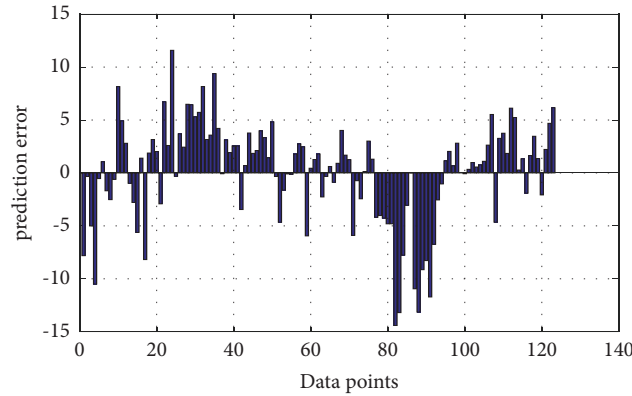
FIGURE 6: Mean prediction error with ML estimated parameters on measured loss data obtained from site location 2.
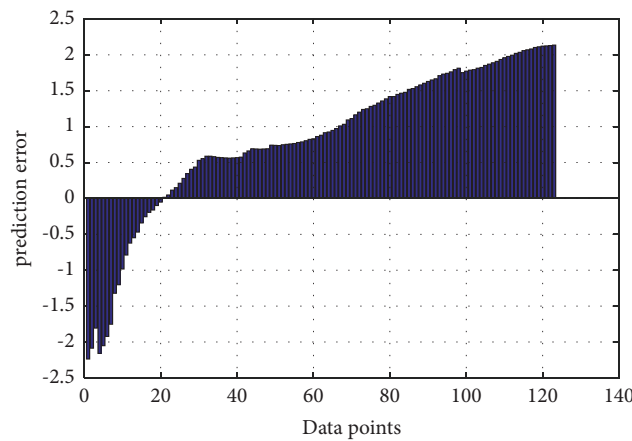
FIGURE 7: Mean prediction error with LS estimated parameters on measured loss data obtained from site location 2.
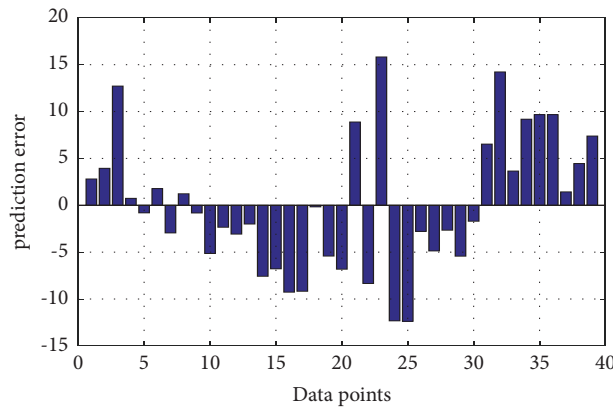
FIGURE 8: Mean prediction error with ML estimated parameters on measured loss data obtained from site location 3.

measured path loss values up to 70% each before deviations. In contrast, the LS-based approach could only accurately predict 30–50% of the measured path loss values sample. The prediction error attained by engaging the ML-based and ML-based estimation approaches is quantitively defined in Table 3.
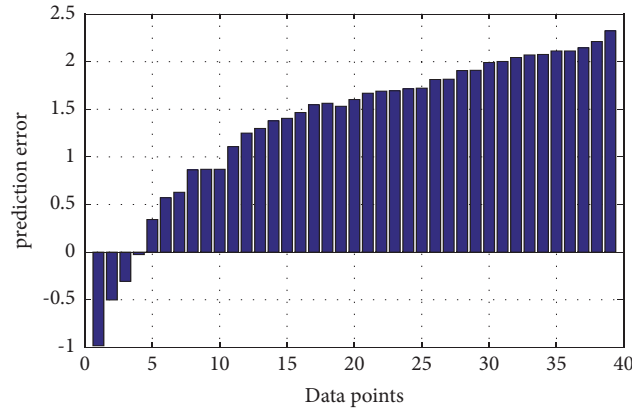
FIGURE 9: Mean prediction error with LS estimated parameters on measured loss data obtained from site location 3.

TABLE 2: Estimated propagation loss parameters with ML and LS models using standard metrics.

	Model and loss estimation error	MAE	MRE	RMSE	SDE
Site 1	ML	1.82	3.97	1.99	0.79
	LS	2.70	11.8	3.44	2.13
Site 2	ML	1.18	0.95	1.34	0.63
	LS	3.51	2.86	4.69	3.11
Site 3	ML	1.46	3.75	1.58	0.59
	LS	5.81	14.9	7.11	4.10
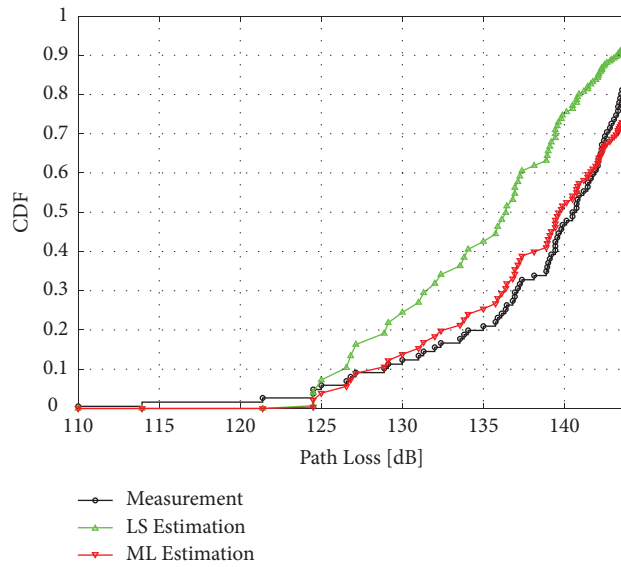
FIGURE 10: Path prediction attained with LS-based estimation and ML-based estimation approaches from site location 1.
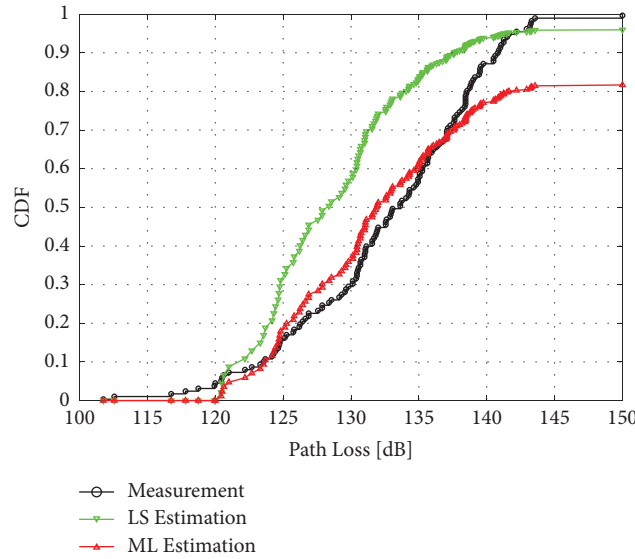
FIGURE 11: Path prediction attained with LS-based estimation and ML-based estimation approaches from site location 2.
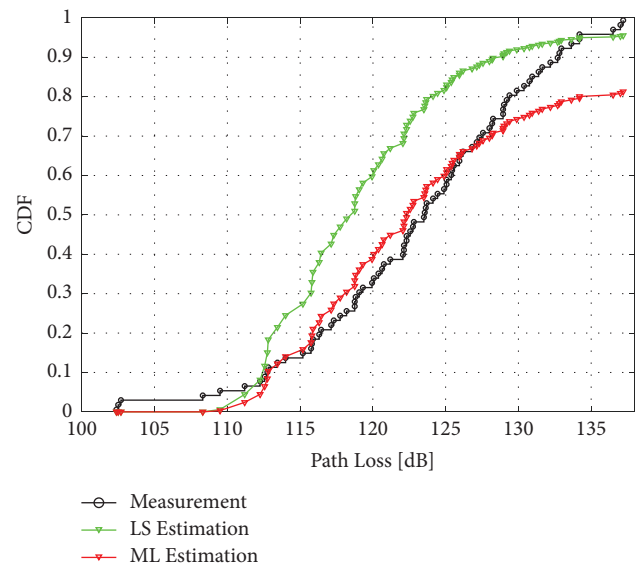
FIGURE 12: Path prediction attained with LS-based estimation and ML-based estimation approaches from site location 3.

TABLE 3: Precision estimation accuracy attained by LS-based estimation and ML-based estimation at different study locations.

Location	Locations	MAE	MRE	STE	RMSE
	1	0.169126	11.39	0.0966802	0.19481
LS-based estimation	2	0.174385	12.17	0.1007700	0.201407
	3	0.164623	10.92	0.0964925	0.190818
	1	0.0604279	1.58	0.0457335	0.0726338
ML-based estimation	2	0.0558125	1.42	0.0401722	0.0687666
	3	0.0539799	1.39	0.0413426	0.067993

4. Conclusions

This study considers parameter estimation for spatial variations of a radio frequency channel based on experimental measurements derived from an operational 4G LTE broadband network. The work developed a combined maximum-likelihood estimation model and a lognormal distribution function. The explored ML-based model reliably estimates the specified wireless channel parameters compared with measured field data for the investigated environments. In order to test the validity of the proposed model, standard statistical metrics were employed for

benchmarking. Regarding the mean absolute error (MAE), Mean percentage error (MAPE), root mean square error (RMSE), and standard deviation error (SDE) statistics, the ML model approach attains 1.82, 3.97, 1.99, and 0.79 in site location 1. In contrast, the LS model achieved 2.70, 11.85, 3.44, and 2.13 values, respectively, for the same site location. Similar parameter estimation and prediction performance of the ML method over the LS approach are demonstrated for site locations 1 and 2. Future work would focus on optimizing the parameters of the proposed hybrid model for optimal performance in a related wireless propagation environment.

Data Availability

The data that support the findings of this study are available from the corresponding author upon reasonable request.

Ethical Approval

This article does not contain any studies with human participants or animals performed by any of the authors.

Conflicts of Interest

The authors declare that they have no conflicts of interest.

Acknowledgments

References

[1] M. R. Akdeniz, Y. Liu, M. K. Samimi et al., "Millimeter wave channel modeling and cellular capacity evaluation," *IEEE Journal on Selected Areas in Communications*, vol. 32, no. 6, pp. 1164–1179, 2014.

[2] D. Vasisht, S. Kumar, H. Rahul, and D. Katabi, "Eliminating channel feedback in next-generation cellular networks," in *Proceedings of the 2016 ACM SIGCOMM Conference*, New York, NY, USA, August 2016.

[3] B. H. Fleury, M. Tschudin, R. Heddergott, D. Dahlhaus, and K. Ingeman Pedersen, "Channel parameter estimation in mobile radio environments using the SAGE algorithm," *IEEE Journal on Selected Areas in Communications*, vol. 17, no. 3, pp. 434–450, 1999.

[4] A. Richter, "Estimation of Radio Channel Parameters," *Models and Algorithms*, vol. 19, no. 4, 2005.

[5] A. U. Usman, O. U. Okereke, and E. E. Omizegba, "Macrocell path loss prediction using artificial intelligence techniques," *International Journal of Electronics*, vol. 101, no. 4, pp. 500–515, 2014.

[6] J. Isabona, C. C. Konyeha, C. B. Chinule, and G. P. Isaiah, "Radio field strength propagation data and pathloss

calculation methods in UMTS network," *Advances in Physics Theories and Applications*, vol. 21, pp. 54–68, 2013.

[7] J. Isabona and I. G. Peter, "CDMA2000 radio measurements at 1.9 GHz and comparison of propagation models in three built-up cities of SouthSouth-South, Nigeria," *Am. J. Eng. Res*, vol. 2, no. 05, pp. 96–106, 2013.

[8] Y. Ai, M. Cheffena, and Q. Li, "Radio frequency measurements and capacity analysis for industrial indoor environments," in *Proceedings of the 2015 9th European Conference on Antennas and Propagation (EuCAP)*, Lisbon, Portugal, April 2015.

[9] H. Xu, C. Shi, W. Zhang, and Y. Yang, "Field testing, modeling and comparison of multi frequency band propagation characteristics for cellular networks," in *Proceedings of the 2016 IEEE International Conference on Communications (ICC)*, Kuala Lumpur, Malaysia, May 2016.

[10] A. R. Mishra, *Fundamentals of Cellular Network Planning and Optimisation*, John Wiley & Sons, Hoboken, New Jersey, United States, 2018.

[11] S. O. Ajose and A. L. Imoize, "Propagation measurements and modelling at 1800 MHz in Lagos Nigeria," *International Journal of Wireless and Mobile Computing*, vol. 6, no. 2, pp. 165–174, 2013.

[12] A. L. Imoize, E. M. Otuokere, S. O. Ajose, and A. O. Adegbenro, "Experimental validation of a best-fit model for predicting radio wave propagation through vegetation," *Arid Zo. J. Eng. Technol. Environ*, vol. 15, pp. 172–186, 2019.

[13] A. L. Imoize, A. E. Ibhaze, P. O. Nwosu, and S. O. Ajose, "Determination of best-fit propagation models for pathloss prediction of a 4G LTE network in suburban and urban areas of lagos, Nigeria," *West Indian J. Eng*, vol. 41, no. 2, pp. 13–21, 2019.

[14] A. L. Imoize and A. I. Oseni, "Investigation and pathloss modeling of fourth generation long term evolution network along major highways in Lagos Nigeria," *IFE Journal of Science*, vol. 21, no. 1, pp. 39–60, 2019.

[15] X.-L. Hu, P.-H. Ho, and L. Peng, "Performance analysis of maximum likelihood estimation for transmit power based on signal strength model," *Journal of Sensor and Actuator Networks*, vol. 7, no. 3, p. 38, 2018.

[16] N. Alić, G. C. Papen, R. E. Saperstein, L. B. Milstein, and Y. Fainman, "Signal statistics and maximum likelihood sequence estimation in intensity modulated fiber optic links containing a single optical preamplifier," *Optics Express*, vol. 13, no. 12, pp. 4568–4579, 2005.

[17] C. I. Abiodun and J. S. Ojo, "Determination of probability distribution function for modelling path loss for wireless channels applications over micro-cellular environments of Ondo State, Southwestern Nigeria," *World Sci. News*, vol. 118, pp. 74–88, 2019.

[18] N. Faruk, A. Ayeni, and Y. A. Adediran, "On the study of empirical path loss models for accurate prediction of TV signal for secondary users," *Progress In Electromagnetics Research B*, vol. 49, pp. 155–176, 2013.

[19] J. Salo, L. Vuokko, and P. Vainikainen, "Why is shadow fading lognormal?" in *Proccedings of the International Symposium on Wireless Personal Multimedia Communications*, Aalborg, Denmark, September 2005.

[20] F. Luan, Y. Zhang, L. Xiao, C. Zhou, and S. Zhou, "Fading characteristics of wireless channel on high-speed railway in hilly terrain scenario," *International Journal of Antennas and Propagation*, vol. 2013, pp. 1–9, Article ID 378407, 2013.

[21] C. Gustafson, T. Abbas, D. Bolin, and F. Tufvesson, "Statistical modeling and estimation of censored pathloss data," *IEEE*

Wireless Communications Letters, vol. 4, no. 5, pp. 569–572, 2015.

[22] R. Sari and H. Zayyani, "RSS localization using unknown statistical path loss exponent model," *IEEE Communications Letters*, vol. 22, no. 9, pp. 1830–1833, 2018.

[23] J. Isabona, "Experimental study of UMTS radio signal propagation characteristics by field measurement," *Department of Basic Sciences Benson Idahosa University PMB*, vol. 2, no. 07, pp. 99–106, 2013.

[24] J. Isabona and K. Obahiagbon, "RF propagation measurement and modelling to support adept planning of outdoor wireless local area networks in 2.4 GHz Band," *Am. J. Eng. Res*, vol. 3, no. 1, pp. 258–267, 2014.

[25] J. Isabona Joseph and C. C. Konyeha, "Urban area path loss propagation prediction and optimisation using Hata model at 800MHz," *IOSR Journal of Applied Physics*, vol. 3, no. 4, pp. 8–18, 2013.

[26] C. Gentile, A. F. Molisch, J. Chuang et al., "Methodology for benchmarking radio-frequency channel sounders through a system model," *IEEE Transactions on Wireless Communications*, vol. 19, no. 10, pp. 6504–6519, 2020.

[27] J. Isabona, R. Kehinde, A. L. Imoize, S. Ojo, and N. Faruk, "Large-scale signal attenuation and shadow fading measurement and modelling for efficient wireless network design and management," in *Proceedings of the 2022 IEEE Nigeria 4th International Conference on Disruptive Technologies for Sustainable Development (NIGERCON)*, Lagos, Nigeria, April 2022.

[28] S. Ojo, A. Imoize, and D. Alienyi, "Radial basis function neural network path loss prediction model for LTE networks in multitransmitter signal propagation environments," *International Journal of Communication Systems*, vol. 34, no. 3, pp. 1–26, 2021.

[29] J. Isabona, A. L. Imoize, S. Ojo et al., "Development of a multilayer perceptron neural network for optimal predictive modeling in urban microcellular radio environments," *Applied Sciences*, vol. 12, no. 11, p. 5713, 2022.

[30] A. L. Imoize and A. I. Dosunmu, "Path loss characterization of long term evolution network for," *Jordan J. Electr. Eng*, vol. 4, no. 2, pp. 114–128, 2018.

[31] A. L. Imoize and O. D. Adegbite, "Measurements-based performance analysis of a 4G LTE network in and around shopping malls and campus environments in lagos Nigeria," *Arid Zo. J. Eng. Technol. Environ*, vol. 14, no. 2, pp. 208–225, 2018.

[32] A. E. Ibhaze, A. L. Imoize, S. O. Ajose, S. N. John, C. U. Ndujiuba, and F. E. Idachaba, "An empirical propagation model for path loss prediction at 2100MHz in a dense urban environment," *Indian Journal of Science and Technology*, vol. 10, no. 5, pp. 1–9, 2017.

[33] T. S. Rappaport, *Wireless Communications: Principles and Applications*, Prentice-Hall, Upper Saddle River, New Jersey, 2nd ed edition, 2002.

[34] T. S. Rappaport, F. Gutierrez, E. Ben-Dor, J. N. Murdock, Y. Qiao, and J. I. Tamir, "Broadband millimeter-wave propagation measurements and models using adaptive-beam antennas for outdoor urban cellular communications," *IEEE Transactions on Antennas and Propagation*, vol. 61, no. 4, pp. 1850–1859, 2013.

[35] J. Isabona, A. L. Imoize, P. Rawat et al., "Realistic prognostic modeling of specific attenuation due to rain at microwave frequency for tropical climate region," *Wireless Communications and Mobile Computing*, vol. 2022, Article ID 8209256, 10 pages, 2022.

[36] D. G. Kleinbaum and M. Klein, "Maximum likelihood techniques: an overview," *Logist. Regres*, vol. 101, pp. 103–127, 2010.

[37] A. E. Waadt, C. Kocks, S. Wang, G. H. Bruck, and P. Jung, "Maximum likelihood localization estimation based on received signal strength," in *Proceedings of the 2010 3rd International Symposium on Applied Sciences in Biomedical and Communication Technologies (ISABEL 2010)*, Rome, Italy, November 2010.

[38] Y. T. Chan, B. H. Lee, R. Inkol, and F. Chan, "Received signal strength localization with an unknown path loss exponent," in *Proceedings of the 2011 24th Canadian Conference on Electrical and Computer Engineering (CCECE)*, pp. 000456 -000459, Niagara Falls, ON, Canada, May 2011.

[39] I. Valera, B. T. Sieskul, and J. Míguez, "On the maximum likelihood estimation of the ToA under an imperfect path loss exponent," *EURASIP Journal on Wireless Communications and Networking*, vol. 2013, no. 1, pp. 1–21, 2013.

[40] G. Jacinto, P. A. Filipe, and C. A. Braumann, "Weighted maximum likelihood estimation for individual growth models," *Optimization*, vol. 71, no. 11, pp. 3295–3311, 2022.

[41] R. Orellana, G. Bittner, R. Carvajal, and J. C. Agüero, "Maximum Likelihood estimation for non-minimum-phase noise transfer function with Gaussian mixture noise distribution," *Automatica*, vol. 135, Article ID 109937, 2022.

[42] C. Cheng, S. Liu, H. Wu, and Y. Zhang, "An Efficient Maximum-likelihood-like Algorithm for Near-Field Coherent Source Localization," *IEEE Transactions on Antennas and Propagation*, vol. 70, no. 7, pp. 6111–6116, 2022.

Retraction

Retracted: Hypoxia-Induced Nestin Regulates Viability and Metabolism of Lung Cancer by Targeting Transcriptional Factor Nrf2, STAT3, and SOX2

Computational Intelligence and Neuroscience

This article has been retracted by Hindawi following an investigation undertaken by the publisher [1]. This investigation has uncovered evidence of one or more of the following indicators of systematic manipulation of the publication process:

(1) Discrepancies in scope

(2) Discrepancies in the description of the research reported

(3) Discrepancies between the availability of data and the research described

(4) Inappropriate citations

(5) Incoherent, meaningless and/or irrelevant content included in the article

(6) Peer-review manipulation

The presence of these indicators undermines our confidence in the integrity of the article's content and we cannot, therefore, vouch for its reliability. Please note that this notice is intended solely to alert readers that the content of this article is unreliable. We have not investigated whether authors were aware of or involved in the systematic manipulation of the publication process.

Wiley and Hindawi regrets that the usual quality checks did not identify these issues before publication and have since put additional measures in place to safeguard research integrity.

We wish to credit our own Research Integrity and Research Publishing teams and anonymous and named external researchers and research integrity experts for contributing to this investigation.

The corresponding author, as the representative of all authors, has been given the opportunity to register their agreement or disagreement to this retraction. We have kept a record of any response received.

References

[1] Y. Liu, X. Zhang, T. Jiang, and N. Du, "Hypoxia-Induced Nestin Regulates Viability and Metabolism of Lung Cancer by Targeting Transcriptional Factor Nrf2, STAT3, and SOX2," *Computational Intelligence and Neuroscience*, vol. 2022, Article ID 9811905, 7 pages, 2022.

Research Article

Hypoxia-Induced Nestin Regulates Viability and Metabolism of Lung Cancer by Targeting Transcriptional Factor Nrf2, STAT3, and SOX2

Yongshi Liu,[1] Xinglin Zhang,[2] Tao Jiang [1] and Ning Du [3]

[1]*Department of Thoracic Surgery, Tangdu Hospital, Air Force Medical University, Xi'an, Shaanxi, China*
[2]*Department of Oncology, Qingdao Municipal Hospital, Qingdao, Shandong, China*
[3]*Department of Thoracic Surgery, The First Affiliated Hospital of Xi'an Jiaotong University, Xi'an, Shaanxi, China*

Correspondence should be addressed to Tao Jiang; jiangtaochest@163.com and Ning Du; andrewdu@xjtufh.edu.cn

Objective. To investigate hypoxia-induced Nestin regulates lung cancer viability and metabolism by targeting transcription factors Nrf2, STAT3, and SOX2. *Methods.* Eighty-four cases of nonsmall cell lung cancer (nonsmall cell lung cancer, NSCLC), which had been treated from June 2020 to February 2021, were randomly selected from our clinicopathology database. Immunohisto-chemical staining of collected tissue cells was performed to assess the expression patterns of Nestin, STAT3, Nrf2, and SOX2. Data were quantified and statistically analyzed using one-way and two-way ANOVA tests with $P < 0.05$. *Results.* Clinicopathological findings showed significant differences in lymph node metastasis, tissue differentiation, and histology on induction of Nestin expression; Nestin expression correlated with STAT3, Nrf2, and SOX2 expression.Nestin/STAT3/SOX2/Nrf2 are involved in angiogenesis and lung cancer development. *Conclusion.* Hypoxia-induced Nestin promotes the progression of nonsmall lung cancer cells by targeting the downstream transcription factors STAT3, Nrf2, and SOX2.

1. Introduction

According to the Global Cancer Survey, approximately 1.8 million people will die from lung cancer in 2020 [1]. Primary bronchial lung cancer is currently the fastest growing tumor in terms of incidence and mortality, and it is clinically classified into small cell lung cancer (SCLC) and nonsmall cell lung cancer (NSCLC) according to the pathological pattern, of which NSCLC accounts for about 80% of the total incidence of lung cancer. NSCLC accounts for about 80% of the total incidence of lung cancer, and the symptoms of NSCLC invasion and metastasis have received more and more attention and research in recent years [2]. Compared with SCLC, NSCLC is relatively slow to spread and me-tastasize, but most patients already have organ metastasis at the time of diagnosis and are prone to irreversible migration to bone and central nervous system, resulting in poor prognosis and reduced 5-year survival rate of NSCLC

patients [3]. The transcription factors Nrf2, STAT3, and SOX2 are multifunctional proteins [4], and several studies have shown that the abnormal expression of Nrf2, STAT3, and SOX2 can play a regulatory role in tumor proliferation and metastasis by interacting with different protein cofac-tors, including NSCLC, however, the role of Nrf2, STAT3, and SOX2 in NSCLC is still not well studied. The mecha-nisms of Nrf2, STAT3, and SOX2 in NSCLC are not well studied, and further research is needed.

Nestin is a plastic cytoskeletal protein whose expression may vary with the functional state of the cell and is widely used as a marker for neuronal cells derived from embryonic stem cells (hES cells) and induced pluripotent stem cells (iPS cells). Nestin expression in tumor cells has been reported to result in chemoresistance in hepatocellular carcinoma cell lines and radioresistance in nasopharyngeal carcinoma cell lines [5, 6]. Previously, Nestin has been reported to be as-sociated with neuroendocrine features and involved in

malignant phenotypes including cell growth. Other investigations have also shown that Nestin is regulated by certain transcription factors to achieve its biological functions [7]. Transcriptional signaling transmitters and activators (STAT) include a family of proteins consisting of the latent cell membrane or intracellular transcription factors, including cellular signaling pathways induced by extrinsic and intrinsic stimuli. Among other activators, Nestin has been shown to be activated by STAT proteins, particularly the STAT3 protein. Moreover, STAT3 activation ultimately leads to the expression or inhibition of several functional genes such as cell proliferation, angiogenesis, inflammation, and apoptosis [8]. Subsequently, STAT3 activation promotes the regulation of signaling pathways directly related to the sex determination region Y) box 2 (SOX2) promoter, leading to Sox2 expression and Nestin expression [9]. Other transcription factors, such as nuclear respiratory factor 2 (Nrf2) are now considered to be key players in the regulation of gene transcription implicated in various cellular functions and cancer development and progression [10].

Studies [11] have demonstrated that Nestin expression can be induced by hypoxia and that the increase in Nestin is regulated in part by hypoxia-inducible factor 1-alpha (HIF-1) and vascular endothelial growth factor (VEGF). Recently, it was demonstrated [12] that severe hypoxia (1% oxygen) enhances the expression of stem cell markers, including Nestin and Sox2 glioma stemlike cells. Although Nestin is expressed in various malignancies, little is known about its role in lung cancer cells. Several studies have shown Nestin expression in nonsmall cell lung cancer (NSCLC), and they all suggest that Nestin is significantly associated with poor differentiation [13]. However, to date, few studies have investigated the mechanistic model of hypoxia-induced Nestin regulation in NSCLC.

Based on this, we explored how induction of Nestin allows to promote the progression of NSCLC cells by targeting transcription factors Nrf2, STAT3, and SOX2. We first report the following.

2. Materials and Methods

2.1. Study Population.
In this study, 84 cases of NSCLC (cell line A549 and H1299) were randomly selected from our tissue database from patients who had been treated in our Thoracic Department from June 2020 to February 2021. Included patients, had not received any treatment form, chemotherapy or radio chemotherapy. Additional patient information was attained by reviewing their preoperative and perioperative medical records, contact details, and/or written agreements. All participating patients provided a written form consent in accordance with the institution of ethics committee of medical sciences and were approved by the hospital ethical committee. Histopathological studies were performed on the collected samples using hematoxylin and eosin staining, while histological staining was determined according to WHO classification [14]. The size of the tumor and the number and location of metastatic lymph nodes were obtained from the pathology report.

2.2. Immunohistochemical Staining and Assessment.
Collected sample tissues were immunohistochemically stained with the streptavidin-peroxidase method, and each tissue was deparaffinized, rehydrated, and incubated with fresh 3% methanolic hydrogen peroxide for 15 minutes. The samples were then rinsed with phosphate buffered saline (PBS); antigen was carried out at 100°C in the microwave for 15 minutes in 0.01 mol/L of sodium citrate buffer (pH 6.0). Nonspecific binding was inhibited with normal goat serum for 15 minutes at room temperature then, incubated at 4°C overnight with several antibodies (Table 1). After rinsing with PBS, the slides were then incubated for 10 mins at room temperature with biotin-conjugated secondary antibodies, then incubated with streptavidin-conjugated peroxide solution for 10 minutes. Using 39-diaminobenzidine tetrachloride, sections were stained for 3–5 minutes. Subsequently, tissues were stained with Mayer's hematoxylin, dehydrated, and mounted, negative controls were prepared substituting PBS for primary antibody.

In this study, both cytoplasmic and nucleic staining on Nestin were recorded as positive. Intensity of Nestin expression was scored numerically as, negative = 0, light = 1, moderate = 3, and intense = 3.

2.3. Cell Culture.
Human nonsmall cell lung cancer (hNSCLS) were cultured in a medium supplemented with 10% (vol/vol) FBS, 100 U/ml penicillin, and 100 μg/ml streptomycin, and incubated at 37°C in humidified environment with 5% CO_2.

2.4. Western Blotting.
Using the RIPA buffer, the Cell lysates were prepared for immunoblotting, then they were supplemented with protease inhibitor cocktail (Roche). After, the lysates were centrifuged at $12,000 \times g$ for 10 mins at 4°C for debris removal. Then, the protein concentration was assessed using the BCA Protein assay kit (Thermo). 20 μg of the investigated protein was denatured and resolved using the SDS/PAGE, the target proteins were immunoblotted with antibodies.

2.5. Hypoxia Studies.
In this study NSCLC cells were plated at 5000 cells/cm^2 in a 12-well plates and replaced after 24 hrs with preconditioned media from different Oxygen tensions (21% or 1%). At ambient oxygen tension (21%), cells were cultured in a standard humidified incubators at 37°C mixed with 5% CO_2. At 1% oxygen tension, NSCLC cells were cultured in a humidified incubators at 37°C mixed with 5% CO_2, 1% Oxygen tension was reduced with supplemented Nitrogen based on default parameters (using the Heracell 1590, Thermo Fisher USA).

2.6. PCR Analysis.
RNA was purified using the RNeasy Mini Kit (Qiagen), thereafter, samples were transcribed using the using the Qunatitect Reverse Transcription Kit (Qiagen). qPCR NSCLC cell samples were performed, with parameters; 42 cycles of DNA AMPLIFICATION at 94°C for 30 sec, 56–68°C for 30 sec and 72°C for 30 sec.

TABLE 1: Relationship of the Nestin expression in hNSCLC with clinical and pathological factors.

	Patients	NESTIN-low, n (%)	NESTIN-high, n (%)	P (value)
Sex				
Female	25	17 (54.0)	8 (46.0)	0.548
Male	33	18 (43.9)	15 (56.1)	
Age (y)				
≤60	36	20 (44.7)	16 (55.3)	0.298
>60	22	12 (58.7)	10 (41.3)	
Smoking				
Yes	34	28 (60.7)	6 (39.3)	0.155
No	24	14 (33.3)	10 (66.7)	
Diffrentitian				
Good	23	15 (67.3)	8 (32.7)	0.047
Moderate	17	8 (34.5)	9 (63.5)	
Poor	18	12 (67.4)	4 (32.6)	
TNM stage				
I	33	15 (61.7)	18 (38.3)	0.189
II	12	7 (56.0)	5 (43.0)	
III	13	6 (45.9)	7 (56.1)	
Histology				
Adenocarcinoma	29	19 (53.8)	10 (46.2)	0.003
Squamous cell carcinoma	26	13 (50.3)	13 (49.7)	
Large cell carinoma	3	1 (50.0)	2 (50.0)	
Lymph node metastasis				
N0	23	14 (72.2)	9 (27.8)	0.009
N1	20	9 (61.3)	11 (38.7)	
N2	15	10 (78.9)	5 (21.1)	
MVD expression				
High	30	19 (64.9)	11 (35.1)	0.22
Low	22	14 (56.9)	8 (43.1)	
Lvd expresssion				
High	34	20 (48.3)	14 (51.7)	0.874
Low	24	13 (73.6)	9 (26.4)	
VEGF expression				
High	29	15 (61.9)	14 (38.1)	0.754
Low	29	18 (40.0)	11 (60.0)	
COX-2 expression				
High	28	17 (68.3)	11 (31.7)	0.269
Low	30	22 (62.0)	8 (38.0)	

2.7. Statistical Analysis. Data were presented as the mean-± standard deviation (SD), and the error bars represent standard error of the mean. Statistical analysis of means was performed using one-way and two-way ANOVA. Probability level of $P < 0.05$ was considered as statistically significant.

3. Results

3.1. Basic Clinic Information and Tumor Characteristics. Thirty-three male and twenty-five female patients diagnosed with NSCLC, treated with curative surgical resection were enrolled in this study with a mean age range of 57.5 ± 10 years (range 36–77 years). 29 cases of lung adenocarcinoma, 26 cases of squamous cell carcinoma, and 3 cases of large cell carcinoma were observed amongst the patients. There were 33, 17, and 18 cases with good, moderate, and poor differentiation, respectively, and the observed cases were classified according to the TNM staging system of the

International Union Against Cancer (2002), and the cases were classified as stage I ($n = 33$), stage II ($n = 12$), and stage II ($n = 13$) [15]. Thirty-five of these patients had lymph node metastases, and information was obtained for 90% (52/58) of the patients analyzed after 4 years of followup. Other clinical characteristics of the study sample are shown in Table 1.

3.2. Hypoxic Environment Induced Nestin Expression in hLSCs. There was a significant increase in Nestin mRNA expression in hNSCLC at 24 hr postincubation in 1% O_2 in comparison to cell incubated at 21% O_2 (Figure 1(a)). An increasing pattern was marked by a significant decrease at 48 hr. Nestin protein levels were significantly greater in 1% O_2 at both 6 and 24 hrs (Figure 1(b)). Notable increase in Nestin was recorded at 6 and 24 hrs, at which this rise achieved statistical significance (Figure 1(b)). This result suggest that Nestin mRNA and protein levels are increased under hypoxic conditions.

(a)

(b)
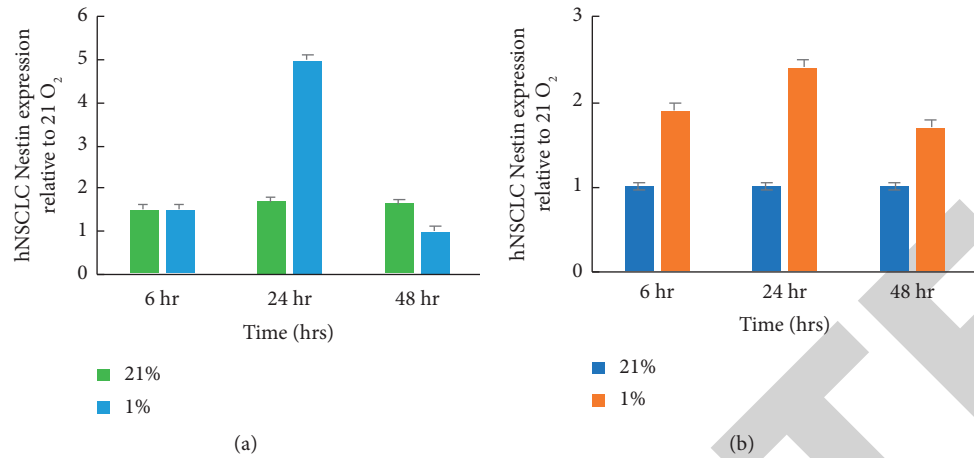
Figure 1: Hypoxia conditions promote nestin expression in hNSCLC. *Note.* (a) qPCR analysis of Nestin expression at 6, 24, and 48 hr, cultured 21% and 0% O_2; ($P < 0.05$). (b) Quantification of Nestin protein expression in hNSCLC cultured at 21% and 0% O_2. Bars represent mean protein expression normalized.
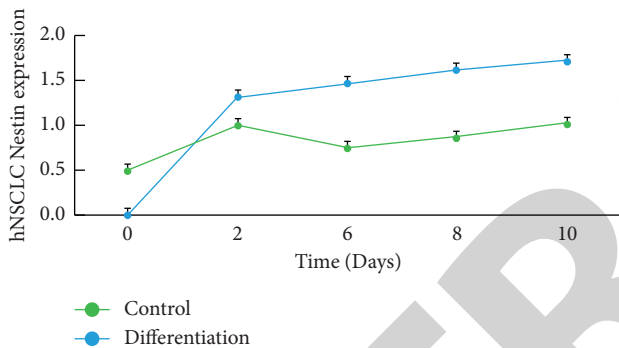
Figure 2: Effects of time in human nonsmall lung cancer media on Nestin expression. *Note.* Bars represent mean nestin expression normalized.
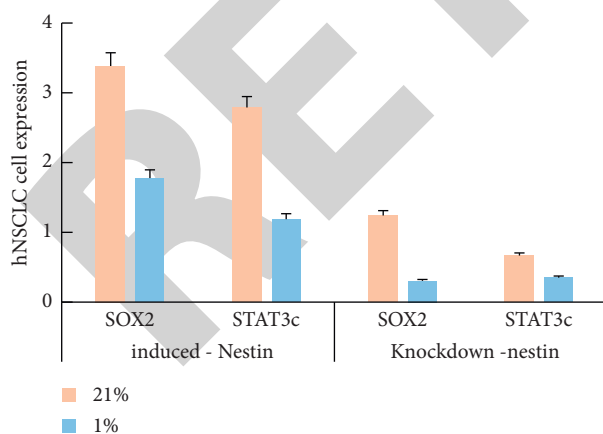
Figure 3: Nestin regulation analysis by the STAT3 protein expression through an intermediate SOX2. *Note.* Mean protein expression is represented by blue and orange bars in the graph, shows an 1% and 21% Oxygen content in both Nestin-induced and Nestin-knockdown environments.

3.3. Nestin Expression Is Maintained during hNSCLC Differentiation.
To verify the clinicopathological findings of hNSCLC in correlation with nestin expression, cell differentiation was assessed qualitatively. In hNSCLC medium, the increase in staining over time showed a different degree of cell differentiation, consistent with the clinicopathological recordings in Table 1. Statistically, nestin expression was significantly different from controls in hNSCLCs induced to differentiate (Figure 2), but not significantly different in terms of time progression within 10 days.

3.4. STAT3 Regulates Nestin Expression via SOX2.
To confirm the regulation of the SOX2 promoter by STA3 under Nestin-induced conditions, we introduced STAT3c cells into hNSCLC. These were lysed 48h after transfection, and SOX2 expression was analyzed (Figure 3). We observed that STAT3c successfully induced SOX2 expression in NSCLC cells. Suggesting that SOX2 regulates is an intermediary for STAT3 regulation of Nestin expression.

3.5. Nestin Expression Activates the Nrf2 Transcription Factor.
The Nrf2 transcription factor is known to regulate the antioxidant defense system. In this study we found that Nestin expression regulates the hNSCLCs through targeting the Nrf2 signaling pathway. To analyze the relationship between Nrf2 and Nestin, NSCLC cells were treated with pivaloyl hydroquinone (tBHQ) and sulfathionine (SF) to analyze the activation of Nrf2. Previous studies have shown that a decrease in Nestin expression decreases the expression of several transcription factors that are targets of Nrf2, such as CAT, GPX1/4, SOD1/2, GCLC/M, HO-1, and NQO1. To investigate this hypothesis, we immunoprecipitated hNSCLC cells with ARE luciferase. Our results showed an increase in Nestin expression induced by hypoxic conditions, which increased the expression of NQO1, GCLM, and HO-1 (Figure 4). The results showed that tBHQ and SF enhanced the protein levels of Nrf2 in both cell lines as compared with the control. Moreover, the transcription
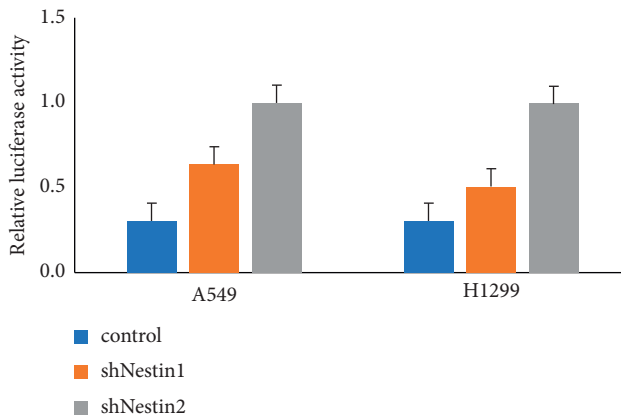
Figure 4: Luciferase assay to investigate the effect of Nestin on cellular antioxidant activity mediated in the Nrf2-ARE pathway. Note: hNSCLS cells with and without Nestin knockdown were transfected with ARE reporter gene plasmid. Results showed a fold change of luciferase activity.
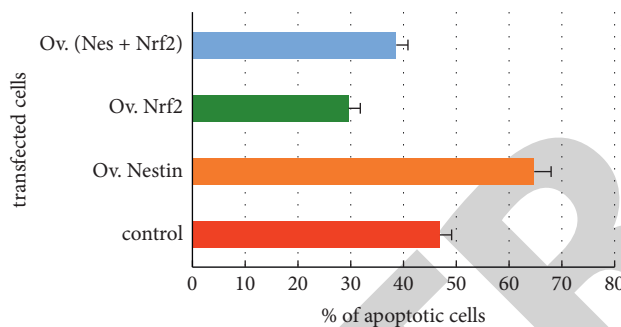
Figure 5: Nestin and Nrf2 increase the resistance to antioxidant capacity. Note: Statistical evaluation of overexpressed Nestin and Nrf2 A549 cells. Bars represent percentage of apoptotic cells, data is defined as the means $\pm$ SD, $P < 0.05$ considered statistically significant.

of downstream genes were enhanced. These results suggest that the Nestin expression induced by hypoxic conditions regulate the Nrf2 expression.

3.6. Antioxidant Capacity Is Enhanced by Nestin and Nrf2. To determine the role of Nrf2 in Nestin-induced environment in response to oxidative stress, we used overexpression plasmid transfection to alter the expression levels of Nrf2 and Nestin in hNCSLC cells (Figure 5), and we obtained that Nestin maintains redox homeostasis in NSCLC cells by regulating antioxidant capacity. The cells were stimulated with H_2O_2 at 48h after transfection. Overexpressed Nrf2 enhanced the resistance of Nestin-knockdown cells to H_2O_2-induced toxicity. Furthermore, the suppression of Nrf2 increased the sensitivity of Nestin-overexpressing cell to H_2O_2-induced toxicity. Overall, these results showed that overexpressed induced Nestin by hypoxic conditions in association with expression of Nrf2 increase the resistance of Nestin to antioxidative stress.

3.7. Nestin, SOX2, STAT3, And Nrf2 Expression in hNSCLC. There were significant differences between primary and metastatic tumor cells throughout the sections, with 12 of 25 (48%) and 3 of 6, STAT3 was not expressed in either cell; whereas 12% and 16% of primary and metastatic tumor cells, respectively, showed positive expression of Nrf2, were positive for Nestin expression, and none of the cells tested positive for SOX2. Interestingly, when Nestin was combined with all the three transcription factors, 40% and 33% of both the primary and metastatic tumor cells tested positive. Proposing a significant relationship of the three in whole section cell growth. Similar trends were observed in the tissue microarray, except the fact SOX2 had increased positive cells, 12.8% and 7.8% in the primary and metastatic tumor cells. Summation the tumor cells that tested positive in different cells in shown in Table 2.

4. Discussion

Lung cancer has a poor prognosis and its death rate is the highest among all malignant tumors [5]. Nonsmall cell lung cancer is a common subtype of lung cancer, and platinum-based chemotherapy is still the main treatment for NSCLC patients [16]. In recent years, cell therapy and gene therapy have also been used to treat NSCLC, but their efficacy is still not significant, and the combination of high metastasis rate to other parts of the body in the early stage of NSCLC and the tendency of drug resistance during treatment are clinical characteristics that make the treatment of NSCLC patients unsatisfactory [17]. Despite the rapid development of surgical procedures, radiotherapy, targeted therapies, and immunotherapy, most patients diagnosed with NSCLC have already missed the prime time for treatment, so the search for efficient treatments, the discussion of the evolutionary mechanism and developmental process of NSCLC, and the appropriate interventions for precancerous lesions are the hot topics in the modern research direction of lung cancer treatment [18]. Of particular importance is the significant relationship between hypoxia-induced activation of the Nestin transduction pathway and the formation, drug resistance, recurrence, and poor prognosis of NSCLC [19].

In the present study, we first confirmed the increased Nestin expression in hNSCLC under hypoxic conditions using two oxygen parameters (O2 at 21% and 1%) associated with increased time. In 1% oxygen, Nestin levels increased at both 6 and 24 hours, peaking at 48 hours, which confirms previous studies that hypoxic conditions induce Nestin expression in cancer tumor cells, in this case lung cancer cells [20]. In support of this phenomenon, hypoxic conditions have been shown to enhance the protumorigenic effects of procollagen lysine hydroxylase 1 (PLOD1) [21]. Studies [22] have shown that Nestin has a common marker for pluripotent stem cells, which is dysregulated in tissue damage and cancer progression. To assess the molecular function of Nestin in lung cancer cells, we analyzed the relationship of Nestin expression with downstream transcription factors, and we demonstrated that Nestin is regulated by STAT3 transcription factor through SOX2 protein.

Table 2: Nestin, Sox2, STA3, and Nrf2 immunoreactivity in human nonsmall cell lung cancer.

	Whole section		Tissue microarrays	
	Primary (%)	Metastitic (%)	Primary (%)	Metastic (%)
NESTIN	12 (48)	3 (50)	17 (16.8)	5 (13.2)
SOX2	0	0	13 (12.8)	3 (7.8)
NRF2	3 (12)	1 (16)	0	3 (7.8)
STAT3	0	0	15 (14.8)	4 (10.5)
COMBINED	10 (40)	2 (33)	45 (44.5)	22 (57.9)
NEITHER	0	0	11 (10.8)	0
TOTAL	25	6	101	38

We further investigated the expression relationship of Nestin with another downstream transcription factor and observed that Nestin expression also regulates Nrf2 expression. To understand the induced expression of Nestin and its downstream regulation, we performed whole section and microarray expression analysis on primary and metastatic lung cancer tumor cells. In this regard, we conclude that Nestin regulates the metabolism and viability of human lung cancer cells by combining the regulatory patterns of SOX2, STAT3, and Nrf2. Although previous studies have demonstrated this regulatory pattern, only a few studies have confirmed it in human lung cancer cells [23, 24]. Furthermore, the regulatory mechanism of Nestin still requires further experiments. In this study, we found that Nestin expression levels correlated with the expression of Nrf2 TFs. Studies [25] have recently revealed the role of Nestin in different types of cancer, and they explained that Nestin, as a marker of microvascular density, is a reliable prognostic factor for neoplastic malignancies. The study [26] also reported that SOX2 is a signal transducer and activator of STAT3 and Nestin in a model of inhibition of glioblastoma multiforme (GMB). In their study [27], they showed that Nestin and SOX2 were coexpressed in human melanoma tissues, which subsequently triggered STAT3 expression. This result raises the possibility that Nestin/SOX2/STAT3/Nrf2 may confer greater clinical virulence, which is consistent with previous studies [28, 29].

However, our study has some shortcomings; the prognostic value of inducible Nestin in lung cancer was not estimated in several clinical samples, and only a few patients and their cell samples were included in this study. In addition, the follow-up period was not extended.

5. Conclusion

In summary, we conclude that hypoxia-induced Nestin targets STAT3, SOX2, and Nrf2, induces their expression, and leads to increased metastatic spread in hNSCLC. Although our study has some limitations, it also provides some clinical basis that the goal of saving the lives of NSCLC patients and prolonging their survival will eventually be achieved.

Data Availability

The data used to support the findings of this study are available from the corresponding author upon request.

Conflicts of Interest

The authors declare that there are no conflicts of interest.

Authors' Contributions

Yongshi Liu and Xinglin Zhang both authors contributed equally to this work and should be considered as equal first coauthors.

Acknowledgments

References

[1] H. Sung, J. Ferlay, R. L. Siegel et al., "Global cancer statistics 2020: GLOBOCAN estimates of incidence and mortality worldwide for 36 cancers in 185 countries," CA: A Cancer Journal for Clinicians, vol. 71, no. 3, pp. 209–249, 2021.

[2] A. Agliano, A. Calvo, and C. Box, "The challenge of targeting cancer stem cells to halt metastasis," Seminars in Cancer Biology, vol. 44, pp. 25–42, 2017.

[3] C. R. Arnold, J. Mangesius, I. I. Skvortsova, and U. Ganswindt, "The role of cancer stem cells in radiation resistance," Frontiers in Oncology, vol. 10, p. 164, 2020.

[4] K. Sone, K. Maeno, A. Masaki et al., "Nestin expression affects resistance to chemotherapy and clinical outcome in small cell lung cancer," Frontiers in Oncology, vol. 10, p. 1367, 2020.

[5] G. Jaramillo-Rangel, M.-d.-L. Chávez-Briones, A. Ancer-Arellano, and M. Ortega-Martínez, "Nestin-expressing cells in the lung: the bad and the good parts," Cells, vol. 10, no. 12, p. 3413, 2021.

[6] T. Das, A. Kamle, A. Kumar, and S. Chakravarty, "Hypoxia induced sex-difference in zebrafish brain proteome profile reveals the crucial role of H3K9me3 in recovery from acute hypoxia," Frontiers in Genetics, vol. 12, Article ID 635904, 2021.

[7] A. Wong, E. Ghassemi, and C. E. Yellowley, "Nestin expression in mesenchymal stromal cells: regulation by hypoxia and osteogenesis," BMC Veterinary Research, vol. 10, no. 1, pp. 173–179, 2014.

[8] S. He, J. Lin, L. Lin, Y. Xu, and J. Feng, "Shikonin-mediated inhibition of nestin affects hypoxia-induced proliferation of pulmonary artery smooth muscle cells," Molecular Medicine Reports, vol. 18, no. 3, pp. 3476–3482, 2018.

[9] M. Nishikawa, A. Inoue, T. Ohnishi et al., "Hypoxia-induced phenotypic transition from highly invasive to less invasive tumors in glioma stem-like cells: significance of CD44 and osteopontin as therapeutic targets in glioblastoma," Translational Oncology, vol. 14, no. 8, Article ID 101137, 2021.

[10] Z. Chen, T. Wang, H. Luo et al., "Expression of nestin in lymph node metastasis and lymphangiogenesis in non-small cell lung cancer patients," Human Pathology, vol. 41, no. 5, pp. 737–744, 2010.

[11] Y. Lin, Z. Song, and Z. Xi, "The anticancer potency of artemisinin and its derivatives," SPR, vol. 1, no. 2, pp. 43–51, 2021.

[12] J. A. Barta, C. A. Powell, and J. P. Wisnivesky, "Global epidemiology of lung cancer," Annals of Global Health, vol. 85, no. 1, p. 8, 2019.

[13] W. D. Travis, E. Brambilla, A. G. Nicholson et al., "The 2015 world health organization classification of lung tumors: impact of genetic, clinical and radiologic advances since the 2004

Retraction

Retracted: Urban Landscaping Landscape Design and Maintenance Management Method Based on Multisource Big Data Fusion

Computational Intelligence and Neuroscience

This article has been retracted by Hindawi following an investigation undertaken by the publisher [1]. This investigation has uncovered evidence of one or more of the following indicators of systematic manipulation of the publication process:

(1) Discrepancies in scope

(2) Discrepancies in the description of the research reported

(3) Discrepancies between the availability of data and the research described

(4) Inappropriate citations

(5) Incoherent, meaningless and/or irrelevant content included in the article

(6) Peer-review manipulation

The presence of these indicators undermines our confidence in the integrity of the article's content and we cannot, therefore, vouch for its reliability. Please note that this notice is intended solely to alert readers that the content of this article is unreliable. We have not investigated whether authors were aware of or involved in the systematic manipulation of the publication process.

Wiley and Hindawi regrets that the usual quality checks did not identify these issues before publication and have since put additional measures in place to safeguard research integrity.

We wish to credit our own Research Integrity and Research Publishing teams and anonymous and named external researchers and research integrity experts for contributing to this investigation.

The corresponding author, as the representative of all authors, has been given the opportunity to register their agreement or disagreement to this retraction. We have kept a record of any response received.

References

[1] L. Zhu, "Urban Landscaping Landscape Design and Maintenance Management Method Based on Multisource Big Data Fusion," *Computational Intelligence and Neuroscience*, vol. 2022, Article ID 1353668, 8 pages, 2022.

Research Article

Urban Landscaping Landscape Design and Maintenance Management Method Based on Multisource Big Data Fusion

Lijuan Zhu

Zhengzhou University of Aeronautics, Henan, Zhengzhou 450046, China

Correspondence should be addressed to Lijuan Zhu; lijuanzhu1031@zua.edu.cn

In the process of continuous urbanization construction, the construction scale of urban landscaping projects is getting larger. At the same time, the design and the maintenance of the management is becoming more important. Recently, the rocketing development of the ternary world of many people, machines, and things has triggered the generation of multisource fusion data and the development of artificial intelligence technology, and the world has entered the era of multisource big data intelligence. Multisource data refer to the fusion of multiple types of data with effective characteristic information, which has richer, more comprehensive, more detailed, and more effective information than a single data source, and can provide high-quality data sources for various complex problems. Therefore, more effective data can be provided for the definition of urban fringe areas. From the moment Google's AlphaGo defeated Go world champion Li Shishi, the chess game has been occupied by AI, setting off an upsurge in the study, research, and application of AI technology. Colleges and universities around the world have followed suit and set up AI-related majors. Deep learning is one of the cutting-edge technologies in the field of artificial intelligence. It is a method to solve complex real-life problems by extracting effective information from the data and mining key features on the basis of a large amount of learning and computing data.

1. Introduction

Landscaping landscape design is a thinking process and planning strategy for people with relevant professional knowledge of architecture, plants, aesthetics, literature, etc. to consciously transform the natural environment on the basis of traditional garden theory. Specifically speaking, this is the procedure of building a beautiful and natural environment as well as the living and recreational environment within the scope of geography, employing the garden art and engineering techniques, or over transforming terrain, planting plants, creating buildings, and arranging garden roads. Through landscape design, the environment has aesthetic appreciation value, daily use function, and can ensure ecologically sustainable development [1].

The construction of urban garden landscapes in various places has become a very important content in urban construction. Whether urban landscape planning can adapt to the development and requirements of urban construction,

and how to meet the needs of urban residents, will become an important measure of "livability" [2]. As a kind of human landscape, the urban garden landscape is a complex natural landscape and artificial landscape. To achieve the ideal realm of "living in a poetic place," the ideal realm of "original" urban landscape must be carried out, and an "original" urban landscape design must be carried out to maximize the value of the landscape [3]. Under the background of advocating a conservation-oriented society and a harmonious society, both urban landscape and small and medium-sized town landscape construction should take regionality as the most basic principle and explore the design methods of preserving culture, continuing history, and saving resources.

In landscape design, we should obtain a larger green area and a better landscape design effect with less investment [4]. Therefore, the original ecological elements should be fully respected in the design, and the original terrain, vegetation, and other elements should be used as much as possible to achieve the design purpose. Interpret the site from the

regional scale, analyze the landscape characteristics of the existing urban built-up area and the relationship between the site and the surrounding environment, and grasp the context and direction of development. The comprehensive site analysis includes the analysis of the natural elements, regional characteristics, and cultural landscape of the site. The comprehensive analysis of the site is actually a process of finding and interpreting the landscape and reading the Earth. On the basis of a full investigation of various elements, a comprehensive analysis is carried out, and favorable factors, unfavorable factors, and development potentials are proposed. A detailed site analysis can effectively provide guidance for planning. For example, in reality, in expressing the mountain and rock scenery, the original stones and plants on the site can be used and modified in the later stage to make the original scenery more in line with the design idea.

Urban landscape protection design must follow the protection of natural landscape, and strictly speaking, it is ecological design. Eco-city natural relics contain representative samples of biological communities and landscapes, and the animal and plant species, habitats, and landforms in them are of significance for conservation, education, recreation, and popular science. According to different management purposes, it can be further divided into ecological protection type, ecological tourism type, ecological science popularization type, and so on. In urban landscape design and construction, biodiversity is a factor that must be considered. The urban landscape is an indispensable part of people's life and production. In urban landscape design, the positive and negative impacts of landscape design on biodiversity and the ecological environment must be considered. The protection design of the architectural landscape must fully consider the optimal use of resources. In the overall design of the city, the rational use of resources is the most important. Replacing all the old to meet the new requirements is wasteful and expensive, destroying entire cities or even a region. We must break the balance somewhere, take the scientific concept of development as the guide, combine the local reality, and at the same time refer to the experience of other places, and do a good job in the protection of the urban landscape.

The multisource data fusion method is originated in the 1960s. It refers to the technology of using relevant means to integrate all the information obtained from investigation and analysis, evaluate the information uniformly, and finally obtain unified information. The purpose of this technology is to synthesize various different data information, absorb the characteristics of different data sources, and then extract unified, better, and richer information than single data. Compared with the single data source model, the multisource data model has more original information and is better in data inference. Dana argues that, in many disciplines, information can be obtained from a variety of sources, including different types of measurement instruments, different measurement techniques, and different experimental setups. Due to the complexity of some natural courses, it is not possible for a single exploring method to present an all-rounded comprehension of them. In natural

life, we humans perceive things through various senses. We have hearing, sight, smell, taste, etc. to perceive everything in the world. Various senses in our body acquire information about a phenomenon, and then, each sense transmits the acquired information to the brain, and finally, the brain integrates the information transmitted by various sensory parts to make judgments about things. Covers specific information in the area, and finally, transmits this information to the owner of the network. At present, the number of samples involved in most data fusion literature is relatively small. In large sensor networks, due to a large number of sensor nodes, if each sensor node carries a large amount of data, processing data from all sensors is a big task, facing a huge amount of computation.

2. Materials and Methods

Foreign scholars have a wide range of research fields on the fusion of multisource datasets. After collecting data from different nodes, we must consider whether the data are affected specifically by each node before modeling the data. Since data sets from different sources may have problems such as distribution shifts and inconsistent measurement standards, it is not possible to directly integrate all data together. Due to the problems of distribution shift and nonuniform measurement standards in the datasets from different sources, it is not possible to directly integrate all the data together. At present, most statistical machine learning research has proposed some algorithms to solve the distribution shift or perform data fusion [6, 7]. For example, Ben-David and Schuller pointed out that domain adaptation problems involving data set or covariate transfer should first align the data distribution for further data analysis [8]. Such algorithms usually suffer from bias in the sampling process, which is generally solved by weighting [9]. The literature on domain adaptation focuses on using a certain type of algorithm to solve the problem of differences between nodes before fusing the data, and after eliminating the differences between different data sets, is it significant to fuse the data together? Zhou et al. considered the integration of data sets from two different places, established a linear regression model in the case of small samples, and proposed hypothesis testing in the case of small samples. And combined with real datasets, it is demonstrated that fusing together similar datasets from multiple sites improves the statistical power of the model [10]. Zhou et al. used a graphical model approach to address the problem of distribution transfer in different datasets and proposed a hypothesis test under which conditions such datasets can be fused or analyzed. And using the support vector machine method, combined with the Alzheimer's disease dataset, the classification problem of the fused dataset is considered. Due to the particularity of some diseases, the number of patients is relatively small, and the amount of related data is also small [11]. Dana Lahat et al. proposed a multimodal data fusion method to fuse datasets obtained by different means [12]. D. L. Hall compares multisensor data fusion with single sensor data fusion and believes that multisensor data fusion will have more advantages in data accuracy and practical application. In

addition, in terms of information presentation and expression, multisource and multimodal data also increase robustness. For example, audio does not need a line of sight, and video is not afraid of environmental noise. Therefore, when there are high requirements for information quality, such as the high requirements for accuracy of medical diagnosis and the comprehensive requirements of meteorological prediction for data, the fusion and integration of multisource data are an important basis for improving the quality of data analysis. Domestic research on multisource data fusion started relatively late, but it has developed rapidly in the past two years. Fang Kuangnan and Zhao Mengmi selected data from two sources, rural and urban, and proposed a logistic regression model based on multisource data fusion for personal credit scoring. The results of the study show that the prediction effect of the integrated model is better than that of the independent dataset model [13]. Xiong Lifang and Zhen Feng used Baidu index to obtain user attention data among cities in the Yangtze River Delta and analyzed the temporal and spatial evolution characteristics of cities in the Yangtze River Delta by simulating urban information flow [14]. Shi Lina used the five-year road passenger and freight volume data of 133 counties in two provinces and one city in the Yangtze River Delta for analysis and judged the changes and grades of node cities through the spatial connection reflected by road passenger and freight volumes [15].

Compared with the traditional way of obtaining data through research, the technology of big data is featured by the large volume, timely and microscopic information. With the emergence of big data sources such as social media, online media, and mobile communications, the application of big data has broken through the space, and the shackles of the time category, the laws of human behavior, and the social attributes of the garden environment have been paid more attention by researchers [16]. The research objects cover the landscape architecture environment of various types and scales, such as urban green space, ecological service facilities, and scenic spots [17]. Through computer software and algorithms and other technologies to analyze mobile phone positioning data, map service POI data, social network data, traffic sensor data, and other open data, to solve space quality assessment, greenway planning, location and route selection, and green space usage rules and related issues such as the assessment of influencing factors. With the breaking down of big data acquisition barriers and the maturity of data mining and processing technologies, the precision and accuracy of big data analysis will be significantly improved [18].

3. Results and Discussion

3.1. 3D Urban Garden Landscape Generation.
Texture path selection is quite important in improving the vraisemblance of the texture. In the process of the 3D garden landscape, the problems are disguised as the best path in the condition of multiconvergence [19].

The paper will get rooted in the practical problems and explicit the spatial scale. The weighing adjacency which can express the best problem range will be given. In this process, the characteristic points on each path of the whole graph were marked with the optimal problem scale for simulated ants, and the individual ants were marked [20–23].

The pheromone should be updated after the ants traverse a complete cycle to avoid the problem, which can be changed by the following formula:

$$\tau_{ij}(t+n) = (1-\rho) \cdot \tau_{ij}(t) + \Delta\tau_{ij}(t), \tag{1}$$

$$\Delta\tau_{ij}(t) = \sum_{k=1}^{m} \Delta\tau_{ij}^{k}(t). \tag{2}$$

The fixed information pheromone volatility element is indicated by p, and the total number of the setting ant colonies which is optimized by the scale of the problems is shown as m. Basically, if the value of m is even higher, the possibility of the best results will be better acquired. The update process is

$$\Delta\tau_{ij}^{k} = \begin{cases} Q/C^K, & \text{Path}\,(i, j)\text{Be traversed by ants}, \\ 0, & \text{Other circumstances}. \end{cases} \tag{3}$$

3.2. Information Fusion Model Construction.
GA takes the fitness function as the evolutionary target which is assumed that the population size is N, the individual in the population is FI, $F(F_i)$ represents the individual fitness value, and the selection probability P_i is calculated as follows:

$$P_i = \frac{F(f_i)}{\sum_{i=1}^{N} F(f_i)}. \tag{4}$$

First calculate the cumulative probability Pi:

$$P_i = \sum_{i=1}^{N} p_i, \quad i = 1, 2, \ldots, N. \tag{5}$$

In order to prevent premature convergence, the adaptive P_c and P_d methods are used. P_c and P_d are changed according to the adaptive function of the solution. The process is as follows:

$$P_c = \begin{cases} (f_{\max} - f')(f_{\max} - f_{\text{avg}}), & f' > f_{\text{avg}}, \\ 1, & f \le f_{\text{avg}}, \end{cases}$$
$$P_d = \begin{cases} (f_{\max} - f)(f_{\max} - f_{\text{avg}}), & f > f_{\text{avg}}, \\ 1, & f \le f_{\text{avg}}. \end{cases} \tag{6}$$

The experiment uses an arithmetic crossover method to ensure that the resulting offspring are located between the chromosomes of the two parents. In fact, the arithmetic intersection is to perform the following linear combination of random two points x_1 and x_2 in the solution space D.

$$\alpha x_1 + (1-\alpha)x_2, \quad \alpha \in [0, 1]. \tag{7}$$

According to this feature, assuming that x_1 and x_2 represent the parent chromosomes of the crossover calculation, the generated offspring are

$$\begin{cases} x_1' = \alpha x_1 + (1-\alpha)x_2, \\ x_2' = \alpha x_2 + (1-\alpha)x_1. \end{cases} \tag{8}$$

Chromosomes are encoded by real numbers, and the mutation process is as follows:

$$\begin{cases} x_1 = x^{\min} - \left| \dfrac{x^{\min} \times P_d \times f}{f_{\max}} \right|, \\[3mm] x_2 = x^{\max} - \left| \dfrac{x^{\max} \times P_d \times f}{f_{\max}} \right|. \end{cases} \tag{9}$$

The BP neural network uses a three-layer architecture as shown in Figure 1.

The forward computing input is the network output of the output layer, and the input of the JTH node in the hidden layer is

$$\text{net}_j = \sum_i W_{ji} o_i + \theta_j. \tag{10}$$

Among them, o_i is the node input of the input layer i, and W_{ji} is the connection weight between the hidden layer node j and the input layer node i.

The output analytical expression of the hidden layer node j is described as

$$\alpha_j = \frac{1}{1 + \exp(\text{net}_j)}. \tag{11}$$

The input of the output layer node k is

$$y_k = \sum_i V_{kj} a_j. \tag{12}$$

Among them, V is the connection weight between the output layer node k and the hidden layer node j.

On this basis, the network deviation function is defined as follows:

$$E = \frac{1}{2} \sum_k (t_k - y_k)^2. \tag{13}$$

Among them, t_k is the expected output, y_k is the actual output, and k is the number of output layer nodes.

The core idea of the BP algorithm is "save the previously calculated results, and then use them for the next calculation, and find the iterative relationship between them, so as to greatly save the computational cost." The essence of the gradient descent method is to calculate the parameters corresponding to the minimum value of the objective function in the form of iteration. (The objective function is the corresponding error function in deep learning and machine learning.) The core essence of the standard BP algorithm is a kind of optimized algorithm which shows a decreasing grad. And this will lead to oscillations during the learning course and the slowing down in the convergence speed. It is also important to pick up the influencing learning factors. The thesis will take the experiment steps repeatedly till the expected requirement about the accuracy is reached.
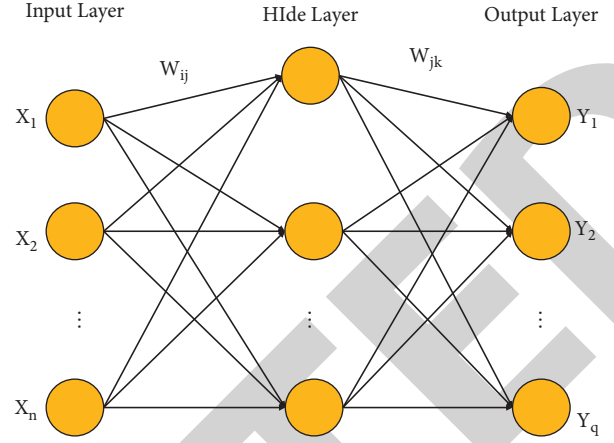
FIGURE 1: BP neural network architecture diagram.

The training of the BP network is finished, the collected data from the remote sensor will be dealt with in blocks, and the information integration will be on the way. The model based on the information integration of the genetic neural network is presented in Figure 2.

3.3. AHP and Neural Network Landscape Design Effect Evaluation Method

(1) Build an ED system for the landscape design. Expert system is an intelligent computer program system, which contains a large number of expert-level knowledge and experience in a certain field. It can apply artificial intelligence technology and computer technology to reason and judge according to the knowledge and experience in the system and simulate the decision-making process of human experts, so as to solve those complex problems that need human experts to deal with.

(2) Determine the weight of the landscape design evaluation index using the analytic hierarchy process.

(3) Collect landscape design evaluation sample data v, use experts to score landscape design evaluation results, and form a landscape design evaluation index sample set.

(4) The number of input nodes of the BP neural network is determined by the number of landscape design evaluation indicators, the landscape design evaluation effect is used as the output of the BP neural network, and the number of hidden nodes of the BP neural network is determined according to a certain formula, thereby establishing the BP neural network topology.

(5) The related parameters of the BP neural network will be restarted.

(6) Employ BP neural network to learn the training samples of landscape design evaluation, and determine the optimal parameters with the accuracy of landscape design evaluation as the training goal.
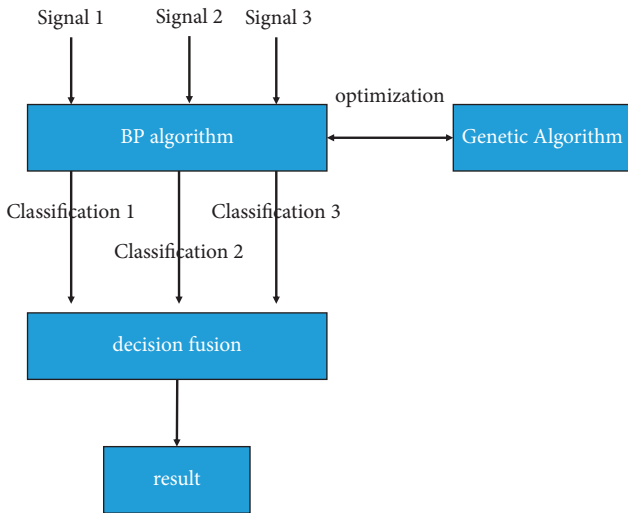
Figure 2: Schematic diagram of the information fusion model.

(7) Build a landscape design evaluation model according to the optimal parameters, and use the landscape design evaluation test samples to test the performance of the model.

Based on the above, the specific process of landscape design evaluation of AHP and neural network is shown in Figure 3.

4. Analysis of Experimental Results

4.1. Analysis of the Model Stability. If the head of the sensor cluster is not changed, with the increasing of the number of the damaged notes, the possibility that the damaged notes turn into the clusters will present a liner rise. Therefore, the probability of it will be regarded as the index of the stability of the model. Figure 4 shows the ending results.

4.2. Analysis of Energy Consumption. As for the information storage and processing, the real number encoding is employed to decrease the consumption of the node information storage. In this experiment, there are 110 nodes in numbers that make up the sensor network lying in the landscape area, and the numbers are distributed in the scope of 110 m × 110 m, which can be presented in Figure 5.

4.2.1. Setting of the Test Environment. In order to test the landscape design evaluation performance of AHP and neural network, specific experiments are used to test their performance. The evaluation environment is shown in Table 1.

4.2.2. Test Object. For the results of 50 landscape design plans, the scores are given by many experts in the same working field who have ranked them in terms of indicators and their experience. The grade will be shown in Figure 6.

From Figure 6, it can be found that the scoring results of different landscape design results are different, showing that
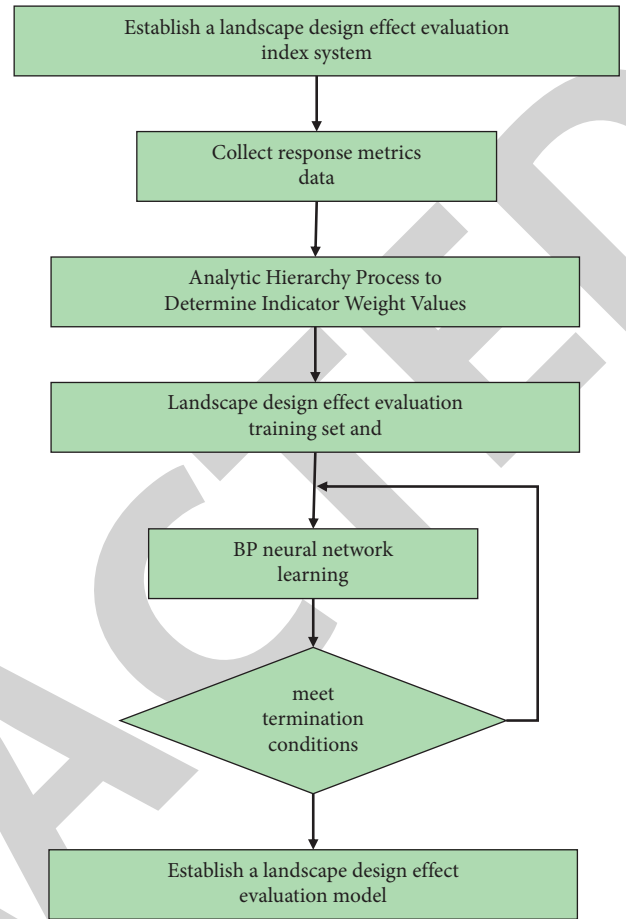
Figure 3: The landscape design evaluation process of AHP and neural network.
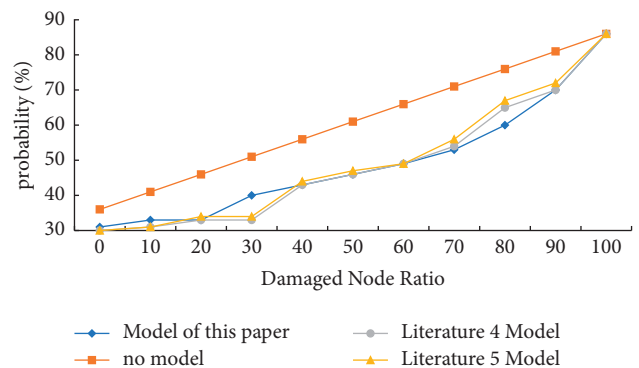
Figure 4: Possibility of damaged nodes leading to cluster heads.

the landscape design effects are featured by the certain randomness.

4.2.3. Comparison of the Evaluation Accuracy of the Landscape Index Layer. 10 schemes about the design were selected as test samples at random, and the rest ones were used as the training sample ones. Each method was tested for 5 times to reflect the objectiveness of the experimental
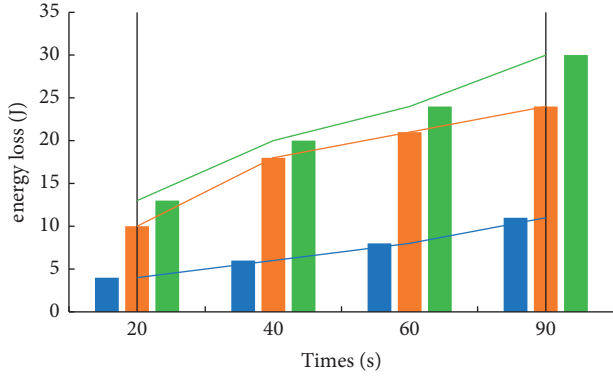
Figure 5: Comparison of information fusion energy consumption of three different models.

Table 1: Settings of the test environment.

Type of environment	Parameter	Parameter value
Hardware environment	CPU	AMD 3.0 GHz
	RAM	16 GB
	Hard disk	1000 GB SDD
	Network card	1000 M
Software environment	Operating system	Win 10
	Programming tools	VC 6.0++
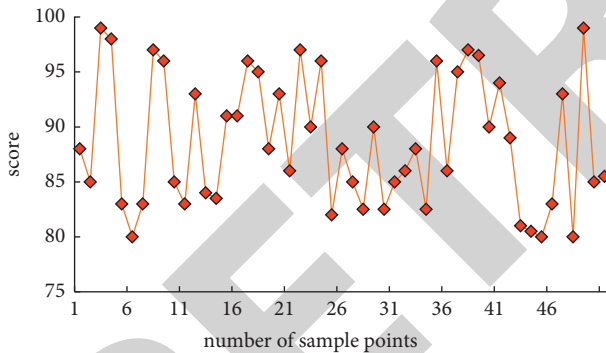
Figure 6: Score values of 50 landscape design effects.

results. The accuracy of landscape design effect evaluation is demonstrated in Figure 7.

Through the comparison in Figure 7, it can be known that the average accuracy of the method in this paper is 91.52%, the average accuracy of landscape design effect evaluation of AHP is 84.20%, and the average accuracy of landscape design effect evaluation of BP neural network is 86.3%. Compared with the comparison method, the evaluation error of the landscape design effect of the method in this paper is greatly reduced. This is mainly because the method of this paper integrates the advantages of the analytic hierarchy process and neural network and solves the defect of the large error of the current landscape design effect evaluation, which verifies the superiority of the landscape design effect evaluation method in this thesis.
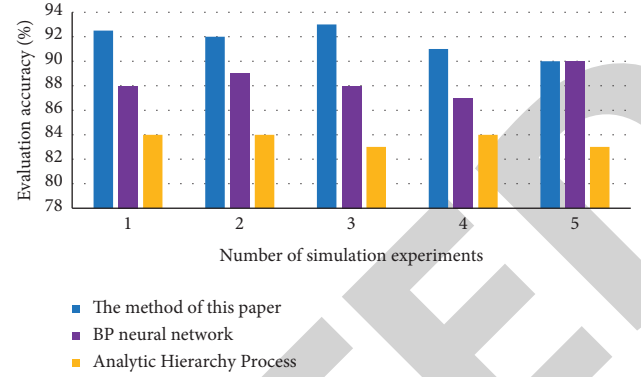
Figure 7: Comparison of the accuracy of landscape design effect assessment by different methods.

4.2.4. Comparison of Evaluation Efficiency of Landscape Index Layer. The landscape design effect evaluation time of 5 simulation tests for each method is counted, and the results are shown in Figure 8.

It can be seen from Figure 8 that the evaluation time of the landscape design effect of the method in this paper is significantly less than that of the comparison method, which overcomes the shortcomings of the current low efficiency of landscape design effect evaluation and improves the speed.

4.3. Urban Landscape Maintenance Management Methods. The completion of garden green space does not mean the completion of the garden landscape "three planting, seven breeding." We should ensure the sustainability and long-term effectiveness of garden greening and not only do one-time greening projects. If the maintenance work is not done well, the garden landscape built at a great cost cannot be maintained well, and some will soon show grassland degradation, tree death, and overgrown weeds. Therefore, landscape maintenance should implement scientific and standardized scientific maintenance and management. Among many plants, how their later growth conditions are closely related to their conservation and management methods. The general method is basically similar for each region, but for different regions, different types of plants grow in different environments, and the maintenance methods are different. Therefore, in terms of plant maintenance methods, scientific maintenance methods should be selected according to their functions, environment, climate, and soil. For example, climbing plants have different watering levels under different climatic conditions, and the same hedgerows are trimmed in different environments. All are different. Figure 9 shows the pattern indicators that need to be considered when maintaining and managing urban landscapes.

Plant conservation in the urban environment is not a task that can be accomplished at one time, and long-term and short-term planning must be made according to the urban space, environment, and function. Think carefully about which plants to take and what measures to take. The improvement of plant landscape maintenance can be improved from the following aspects.
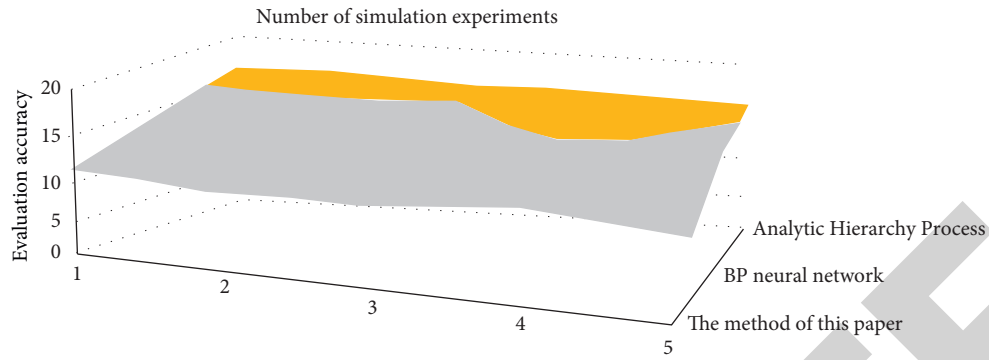
FIGURE 8: Comparison of landscape design effect assessment time for different methods.
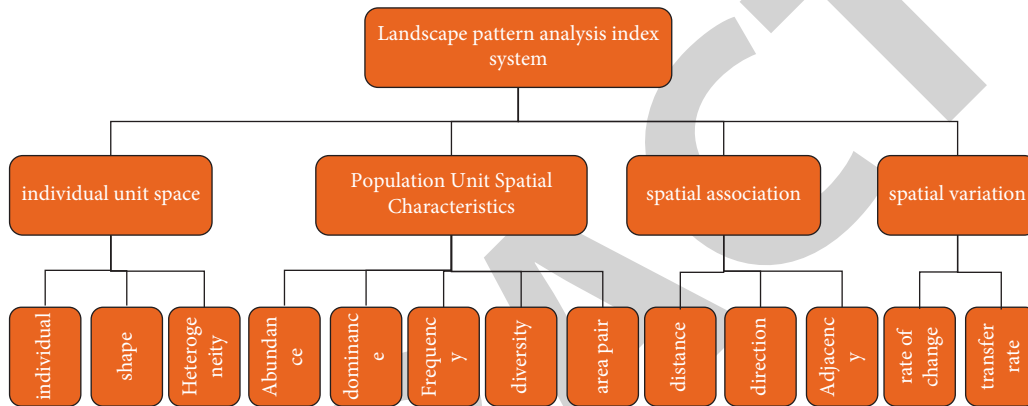
FIGURE 9: Analysis of the urban landscape pattern index system.

One is plant selection and configuration optimization. Plant selection should be suitable for trees in the right place, and on this basis, try to increase plant species, and appropriately introduce exotic plant landscape varieties to enrich the levels and types of green plant landscapes. It is necessary to use vines with climbing ability and good growth from multiple angles. The optimization of plant configuration can increase colorful flowering shrubs, and the lower layer should be combined with drought-tolerant, shallow-rooted succulent herbs. According to the features of Nanjing's urban environment, the plant landscape mostly chooses plants that can reduce noise and have strong adaptability. In terms of plant configuration and maintenance, it is necessary to choose a method that adapts to local conditions, choose native plants as much as possible, pay attention to the matching of plant varieties, and use artistic and aesthetic methods and means to create a comfortable plant landscape.

The second is to establish the concept of overall development from the perspective of long-term planning of plant landscapes and reserve certain planning, three-dimensional and green spaces. The maintenance and management of landscaping must strengthen the scientific management and planning of landscaping projects and strictly follow the norms. Nanjing is a famous ancient cultural capital. Considering the large number of cultural heritages here, the development of Nanjing's ancient culture and the inheritance of new cultures should also be considered, and the cultural heritage spirit of plant landscapes can be added. As an important case of plant landscape design, it is perfectly combined with urban beautification and road greening.

Third, the plant landscape design should fully consider the urban function. Taking the urban road function as an example, different types of road green space and plant landscape need to be combined with specific road functions to configure plants. For example, the three-dimensional greening plant configuration in the traffic island can increase the plants with strong orientation and permeability, which can be used as a guide to guide the plants to choose some plants that do not affect the line of sight. In the plant landscape design of the city square, considering its bearing capacity and the surrounding traffic flow lines, it can be combined with the specific square function, scale, and surrounding environment design, combined with the main body of the square, and the plant configuration can be reasonably arranged to form a transparent and open space.

5. Conclusion

Landscaping landscape design is a thinking process and planning strategy for people with relevant professional knowledge of architecture, plants, aesthetics, literature, etc. to consciously transform the natural environment on the basis of traditional garden theory. Through landscape design, the environment has aesthetic appreciation value, daily

Retraction

Retracted: Mutual Trust Influence on the Correlation between the Quality of Corporate Internal Control and the Accounting Information Quality Using Deep Learning Assessment

Computational Intelligence and Neuroscience

This article has been retracted by Hindawi following an investigation undertaken by the publisher [1]. This investigation has uncovered evidence of one or more of the following indicators of systematic manipulation of the publication process:

(1) Discrepancies in scope

(2) Discrepancies in the description of the research reported

(3) Discrepancies between the availability of data and the research described

(4) Inappropriate citations

(5) Incoherent, meaningless and/or irrelevant content included in the article

(6) Peer-review manipulation

The presence of these indicators undermines our confidence in the integrity of the article's content and we cannot, therefore, vouch for its reliability. Please note that this notice is intended solely to alert readers that the content of this article is unreliable. We have not investigated whether authors were aware of or involved in the systematic manipulation of the publication process.

Wiley and Hindawi regrets that the usual quality checks did not identify these issues before publication and have since put additional measures in place to safeguard research integrity.

We wish to credit our own Research Integrity and Research Publishing teams and anonymous and named external researchers and research integrity experts for contributing to this investigation.

The corresponding author, as the representative of all authors, has been given the opportunity to register their agreement or disagreement to this retraction. We have kept a record of any response received.

References

[1] Y. Zhao, "Mutual Trust Influence on the Correlation between the Quality of Corporate Internal Control and the Accounting Information Quality Using Deep Learning Assessment," *Computational Intelligence and Neuroscience*, vol. 2022, Article ID 8257880, 10 pages, 2022.

Research Article

Mutual Trust Influence on the Correlation between the Quality of Corporate Internal Control and the Accounting Information Quality Using Deep Learning Assessment

Ying Zhao (ORCID)

School of Accounting, Sias University, Xinzheng, Henan 451100, China

Correspondence should be addressed to Ying Zhao; 10754@sias.edu.cn

There is a close correlation between internal control and accounting information quality in the process of enterprise management, and this correlation drives the effect of internal control on accounting information quality, thus forming the effect that internal control optimization promotes accounting information quality optimization. This paper firstly gives a brief description of internal control and accounting information quality and then evaluates the correlation between internal control and accounting information quality based on deep learning and proposes a specific modeling method. Through the correlation and promotion of internal control and enterprise accounting information quality, the optimization of enterprise accounting information quality is achieved. And in combination with the actual case analysis, it is found that the method of this paper can achieve 92% accuracy of correlation analysis, and the analysis is more efficient.

1. Introduction

At the beginning of the twenty-first century, a series of financial fraud and audit failure cases broke out in the global capital market one after another, such as Enron, WorldCom, and Yinguangxia. In 2019, the Chinese market even broke out the financial fraud cases of Kangmei Pharmaceutical and Kangde Xin one after another [1]. These cases have shocked stockholders while also triggering discussions in the community about the effectiveness of external audit work and reflecting deficiencies in the government's development of accounting standards, the industry's regulation, and companies' internal corporate governance. These deficiencies—lack of internal management mechanism and lack of external supervision mechanism—are the causes of SOEs' surplus management behavior [2], and good internal control and external audit happen to be the means of internal management and external supervision of the company. In July 2002, the Sarbanes-Oxley Act was enacted in the United States to strengthen the regulation of the accounting profession and to improve the accuracy and reliability of

corporate disclosures, which emphasized the importance of internal control systems [3]. Since 2008, the Chinese regulatory authorities have promulgated a series of rules and regulations, collectively known as the "One Standard and Three Guidelines," to strengthen the daily management of enterprises and improve their internal control. These regulations have opened a new period of comprehensive construction of internal control systems for Chinese enterprises [4].

The Audit Office in the "Thirteenth Five-Year Plan national audit work development plan" proposed to promote the vitality of the state-owned economy, to promote enterprise reform, and to achieve full audit coverage of enterprises; the audit objective is to promote the quality and efficiency of enterprises: (1) comprehensive audit of state-owned capital investment and operation companies; (2) at least one audit of state-owned and state-owned capital-dominated enterprises within five years, focusing on the authenticity, integrity, and value preservation and appreciation of state-owned assets within and outside the enterprise, assets, liabilities, profit and loss, major investment

decisions and investment performance, development potential and risk potential, corporate governance and internal control of the enterprise, and the compliance with relevant national laws and regulations; (3) paying attention to the implementation of major national policies and measures by enterprises. From this document, it can be seen that the current government audit of enterprise audits focuses on three aspects; one is related to enterprise performance, such as attention to the allocation and operational efficiency of capital and investment performance; the second is related to the quality of accounting information, such as the authenticity and integrity of assets and assets and liabilities profit and loss; the third is related to the internal control of enterprises, such as corporate governance, internal control, and compliance with laws and regulations. The third is related to the internal control of enterprises, such as corporate governance, internal control, and compliance with laws and regulations.

According to the principal-agent theory, the principal, who has the ownership, and the agent, who has the management, have conflicting interests, and the principal cannot fully supervise the agent, and the agent has the motivation and ability to harm the interests of the enterprise for his own benefit, thus giving rise to the principal-agent problem. Among them, information asymmetry is one of the causes of this problem. High quality accounting information in financial reports can effectively alleviate the agency problem caused by information asymmetry. Accounting information, as a carrier of the business status, reflects the efficiency and effectiveness of the business operation. For internal and external stakeholders, they can use the accounting information to understand the real business situation of the enterprise and use it as a basis to make decisions such as investment and disinvestment. Then it is especially important for users of financial statements to obtain a true and reliable financial report.

In the process of obtaining true and reliable financial reports, internal control and external audit of enterprises play an important role. Internal controls aim to provide reasonable assurance that the financial reports provided by the company are true and reliable, and their quality profoundly affects the quality of accounting information of the company. In addition, internal control can also play a key role in preventing fraud, addressing operational risks, and safeguarding the company's property [5].

2. Related Work

As an indispensable part of modern corporate governance system, the role of internal control system has been highly recognized in the capital market. Internal control, as a management activity within an enterprise, controls the generation and transmission of accounting information. Theoretically, ensuring the quality of corporate accounting information is one of the core objectives of the internal control system, and effective internal control can improve corporate management, increase efficiency and effectiveness, and improve the quality of corporate accounting

information, thus promoting the long-term stable development of the enterprise [6].

According to scholars, internal control is the first line of defense for companies against financial reporting misstatements [7], and safeguarding the truthfulness of corporate accounting information and asset security is the main line of the continuous development of internal control theory, and some even consider the issue of the relevance of internal control effectiveness to the quality of corporate accounting information as the fundamental topic of internal control theory research [8], which is related to the vitality and development direction of internal control.

The following contradictory views on the relationship between internal control and accounting information quality have been found through previous studies. Most foreign scholars take SOX as the research event to explore the changes in the quality of corporate accounting information before and after the implementation of the Act. The SOX Act mandates companies to evaluate and disclose their internal controls by legislation. For example, [9] classifies companies into those with corporate-level internal control deficiencies and those with effective implementation of internal control systems. A controlled study found that companies with internal control deficiencies at the corporate-level exhibited more robust accounting information after the enactment of SOX, but there was no significant difference in the robustness of accounting between companies with internal control deficiencies at the operational level and companies with effective internal controls. For example, [10] studied 4441 companies' financial data before and after the Act and found that companies were more prudent before the implementation of the Act, as evidenced by later recognition of earnings and earlier recognition of losses.

Our scholars [11] and others found that high quality internal control does not imply high quality accounting surplus, the quality of surplus did not improve significantly when firms improved the quality of internal control, and the quality of accounting information did not improve significantly even when firms disclosed internal control evaluation reports in a timely manner. Further, [12] verified whether internal control affects different business relationships differently by classifying firms' business relationships into supplier-relationship type and customer relationship type. They found that the higher the quality of internal control, the less positive the surplus management, and there is no significant change in negative surplus management in the supplier-relationship type of business. In other business relationships, high quality internal controls did not have a significant inhibitory effect on surplus management. Some scholars even found that although high quality internal control inhibits accrual surplus management by executives, it invariably leads to more insidious true surplus management [13].

And most domestic and foreign scholars have found that corporate internal controls significantly and positively affect the quality of accounting information. On the foreign side, scholars' studies have suggested that high quality internal controls can improve the quality of a firm's accruals,

improve the robustness of accounting information, and reduce the firm's surplus management [14].

On the domestic side, some scholars point out that the primary factor affecting the quality of accounting information in a firm is the internal control environment [15], but the power structure within the firm affects the relationship between the two [16]. The first is that internal control only exerts an improving effect on accounting information quality when the power of corporate executives is not concentrated; second, if executive power is further divided into structural power, reputational power, political power, and expert power, they find that structural power reduces the inhibitory effect of internal control on surplus management, but expert power and reputational power reinforce that inhibitory effect, while political power has no significant effect. Reference [17] found that the more rational the corporate governance arrangement and the higher the quality of internal control, the higher the quality of accounting information disclosed by the firm, where internal control positively moderates the effect of corporate governance on the improvement of the quality of disclosed accounting information. Reference [18] investigated the relationship between the effectiveness of internal control, firm quality, and the quality of the firm's financial reporting and found that there is a correlation between them. Reference [19] further found that high quality internal control significantly improved the value relevance of accounting surplus, although surplus persistence did not significantly improve when the quality of internal control improved; reference [20] proposed a similar conclusion that higher internal control effectiveness was accompanied by better comparability of accounting information, but the enhancement effect was worse for state-owned firms compared to non-state-owned firms. Literature [21] contradicts the findings of [22], which used 2007–2008 financial accounting data of Chinese A-share listed companies and found that firms without internal control deficiencies have significantly higher robustness of accounting information and accrual quality than those with deficiencies. Similarly, [23] contradicts the findings of [24], where they found that internal control effectiveness is significantly and negatively related to the degree of surplus management activities. Furthermore, [25] pointed out that although internal control can be effective in improving the quality of accounting information of a firm, not all elements, specifically the five elements, exert a significant positive effect on the quality of accounting information of a firm.

3. Methodology

3.1. Measurements of ICQ.
The main evaluation methods of ICQ in academia are divided into three types: first, the results of internal control audit reports issued after audit by firms are used as proxy variables; second, questionnaires are conducted on relevant personnel of enterprises to evaluate whether the internal control of enterprises is properly designed and effectively implemented based on their scores; third, based on the data of relevant information disclosed by listed companies, experts and scholars build their own. Third, according to

the information disclosed by listed companies, experts and scholars have established their own index system. First, listed companies may not be willing to disclose internal audit reports, so they cannot evaluate their advantages; on this basis, some scholars believe that nondisclosure is sufficient to prove that there are some defects in internal control, which can be determined by disclosing variables 0–1. Secondly, the questionnaire survey for individual enterprises is suitable for case analysis, but not for empirical analysis of the overall situation.

3.2. Measurement of Accounting Information Quality.
As mentioned earlier, there are two main models for measuring the quality of accounting information at home and abroad. The first model is to find proxy variables of accounting information quality such as the degree of surplus management; the second model is to use multiple indicators using models to calculate them together.

The accrual principle, which is the basis of accounting measurement for modern enterprises, requires enterprises to account for and measure realized revenues and expenses that should be borne, regardless of whether they are actually received or paid, as revenues and expenses for the current period. Therefore, under this principle, the surplus of an enterprise can be divided into two parts according to whether it is received or paid. One is the net cash flow from operating activities, which measures the portion of earnings that the company can actually capture, while the profits recorded in the form of receivables and thus not actually captured by the company are accrued profits. The accrued profit is divided into a manipulable part and a nonmanipulable part according to whether the company can manipulate it or not. For the former, depending on the risk appetite of the enterprise, the enterprise can choose different accounting policies to manipulate this part; for example, in order to increase the book profit, the enterprise can adjust to reduce the amount of bad debt accrual of accounts receivable and underaccount for the resulting bad debt loss to achieve the purpose of whitewashing the statement. For the nonmanipulable part, it is difficult to be manipulated by enterprises due to the constraints of accounting treatment.

Based on the fact that the quality of accounting information is measured to some extent by the value of manipulable accrued profits accumulated over a certain period of time, then the level of accounting information quality of an enterprise is reflected by the measurement of manipulable accrued profits. The smaller the amount of the manipulable portion, the higher the quality of the enterprise's accounting information. Academics currently measure manipulable accrued profits mainly by using the accrued profit separation method, under which scholars have developed numerous models to measure the degree of corporate surplus management, such as the modified Jones model, the Dechow-Dichev model, and the Lu Jianqiao model. In this paper, the Jones model modified by cross section is used to calculate manipulable accrued profit, which reflects the quality of accounting information of the company. The meanings of each indicator of the cross-sectional Jones model are shown in Table 1.

Table 1: Meaning of each index of the cross-sectional Jones model.

Variable symbol	Chinese name
$TA_{i,t}/ATA_{i,t}$	Average total assets
$TA_{i,t}$	Accrued profit
$\Delta REV_{i,t}$	Change in operating income
$\Delta REC_{i,t}$	Change in accounts receivable
$PPE_{i,t}$	Fixed assets

Firstly, the regression of (1) by industry by year is calculated as $\alpha_0, \alpha_1, \alpha_2$, and the rest are classified according to the primary industry code. Here manufacturing industry is classified according to the secondary industry code of the SEC, and the rest are classified according to the primary industry code, and the industries with less than 10 classifications are excluded, and then the OLS estimates as $\alpha_0, \alpha_1, \alpha_2$ are substituted into formula (2) to calculate the nonmanipulable surplus of the enterprise, and then the nonmanipulable surplus is brought into formula (3) to calculate the manipulable surplus of the enterprise, and the absolute value (DA) is taken as a measure of the quality of accounting information; that is, the larger the absolute value, the worse the quality of accounting information.

$$\frac{TA_{i,t}}{ATA_{i,t-1}} = \alpha_0 \times \frac{1}{ATA_{i,t-1}} + \alpha_1 \times \frac{\Delta REV_{i,t}}{ATA_{i,t-1}} + \alpha_2 \times \frac{PPE_{i,t}}{ATA_{i,t-1}} + \varepsilon_{i,t}, \tag{1}$$

$$\text{NDA} = a_0 \times \frac{1}{ATA_{i,t-1}} + a_1 \times \frac{\Delta REV_{i,t} - \Delta REC_{i,t}}{ATA_{i,t-1}} + a_2 \times \frac{PPE_{i,t}}{ATA_{i,t-1}}, \tag{2}$$

$$\text{Da} = \frac{TA_{i,t}}{ATA_{i,t-1}} - \text{NDA}. \tag{3}$$

The correlation between the ICQ and the AIP is very complex, and the situation of "one multifunction" is more common in actual enterprise planning. For a project attribute, it has one main purpose, but at the same time it has several functions and may improve the AIP to different degrees, which makes the correspondence between project attribute investment and AIP difficult to determine. Therefore, based on the historical data of enterprises, this paper takes project attribute investment as the input of NN and AIP improvement as the output of NN and establishes a deep confidence network model to explore the intrinsic connection between enterprise ICQ and AIP.

3.3. DBN Model. The DBN model consists of several layers of Restricted Boltzmann Machine (RBM). An RBM contains visible and hidden layers, each layer consists of several neurons, and its structure is shown in Figure 1. In the RBM structure, neurons are interconnected between the visible and hidden layers, but there are no connections between neurons within each layer. The visible layer of the RBM
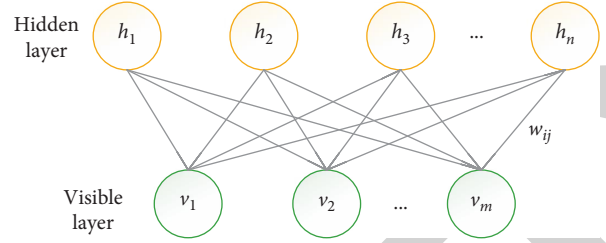
Figure 1: RBM model.

satisfies the Bernoulli distribution or Gaussian distribution, while the hidden layer is the invisible feature detected and satisfies the Bernoulli distribution. The visible and hidden layers are connected by a symmetric weight matrix with probabilities satisfying the Boltzmann distribution.

When v_i, h_j are given, the conditional probability distribution is

$$\begin{cases} P(h_j = 1|v; \theta) = \sigma\left(\sum_{i=1}^m w_{ij}v_i + a_i\right), \\ P(v_j = 1|h; \theta) = \sigma\left(\sum_{j=1}^n w_{ij}h_j + b_j\right), \end{cases} \tag{4}$$

where $\theta = w_{ij}$ is the connection weight between v_i and h_j; a_i and b_j are the parameters of the RBM model; v_i is the i th neuron of the visible layer, corresponding to the investment of the i th item attribute; h_j is the j th neuron of the hidden layer; m, n are the number of neurons in the visible and hidden layers, respectively; a_i and b_j are the unit biases of the visible and hidden layers, respectively.

The visible and hidden layers are independent of each other, and the conditional probability of h on v is

$$\sigma(x) = \frac{1}{(1 + e^{-x})}. \tag{5}$$

Given 1 set of defined training sets $\{V^c | c\{1, 2, 3 \dots c\}\}$, the training objective is to maximize the log-likelihood function of the established model, and by calculating the gradient of the likelihood function, the weight update formula of the RBM can be obtained.

$$\Delta w_{ij} = \varepsilon\left(E_{\text{data}}(v_i h_j) - E_{\text{model}}(v_i h_j)\right), \tag{6}$$

where E_{data} is the expected output of the observation layer, and E_{model} is the expected output on the probability distribution of the model.

The DBN model consisting of multiple RBMs stacked bottom-up is shown in Figure 2. This deep confidence network is divided into 2 layers, the bottom DBN pretraining model and the top backpropagation (BP) fine-tuning model, respectively.

3.4. Model Training Method. The traditional neural network uses BP algorithm to train the network, but with the increase of the number of hidden layers, the BP algorithm has the problems of gradient being gradually sparse and easy to converge to the local minimum. DBN based on deep
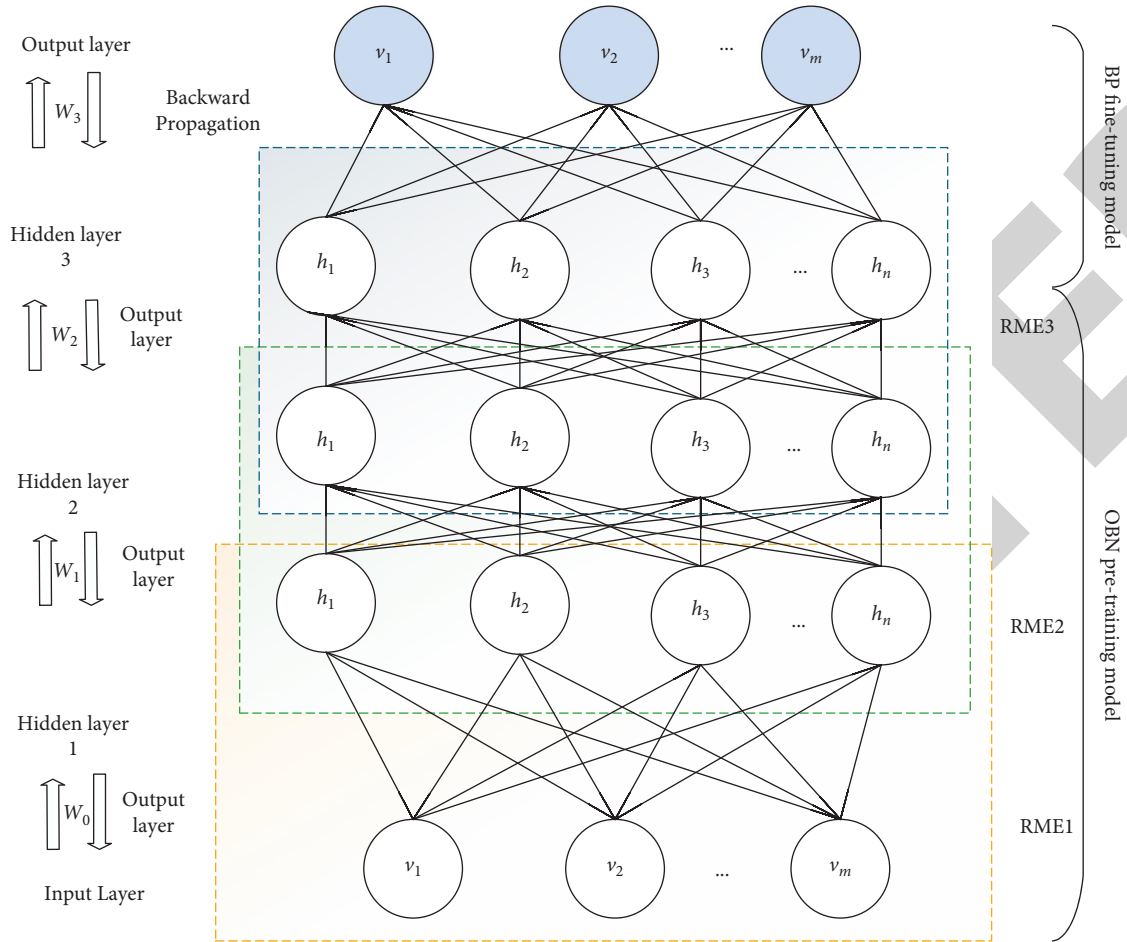
Figure 2: DBN-based model for analyzing the correlation between the ICQ and the AIP.

learning can better solve the problems of BP algorithm by pretraining and fine-tuning the network parameters, which is divided into the following 2 steps.

3.4.1. Pretraining. Train each layer of the network separately and unsupervised, and use the output of the upper layer as the input of the lower layer to ensure that as much information as possible is retained when the feature vectors are mapped to different feature spaces.

3.4.2. Fine-Tuning. The BP network is set up in the last layer of the DBN to receive the output of the RBM as its input, and the network is trained in a supervised manner to achieve top-down fine-tuning of the parameters.

Each layer of the RBM network can only ensure that the weights within its own layer map optimally to the feature vectors in that layer, so the BP network also propagates the deviation information from the top down to each layer of the RBM, fine-tuning the whole DBN network. The whole training process can be regarded as the initialization of the weights of the deep BP network, thus overcoming the disadvantage of the BP network of randomly selecting the initial values and falling into the local optimum, and the training time and convergence speed are significantly improved.

4. Case Study

Taking enterprises as an example, 17 local and municipal enterprises participating in AIP investment from 2018 to 2022 and the real design attributes of data are selected as data input and output models for network parameter training. To verify the authenticity and accuracy of the DBN model, the actual data of 17 local and municipal enterprises in 2022 were used. From the ICQ and AIP enterprise evaluation index system, the neurons are corresponding to 7 different ICQ enterprises. The neurons in the output layer are corresponding to 8 AIP, and the number is 1–8.

4.1. DBN Model Parameter Determination. The depth of model structure and parameter research will affect the learning time and prediction error of the model. To optimize the learning effect, variable control method is used to compare and optimize the hidden layer of DBN model. At the same time, the mean absolute error (MAPE) is introduced to evaluate the prediction accuracy of DBN model.

$$\text{MAPE} = \frac{1}{np} \sum_{i=1}^{n} \sum_{j=1}^{p} \left| \frac{y_{ij} - \widehat{y}_{ij}}{y_{ij}} \right| \times 100\%. \tag{7}$$

From Table 2, when the number of hidden layers is 4, MAPE = 9.1%, and the model has the highest accuracy. As hidden layers increases, the prediction error of the model first increases and then decreases, and "overfitting" occurs. And the number of neurons was selected as shown in Table 3.

From Table 3, when the number of hidden layer neurons is 128, MAPE = 8.2% and the model prediction error is the smallest.

4.2. Method Validation. To verify the validity of the DBN-based model, the maximum relative error is introduced, which can be expressed as follows:

$$\Delta A = \max_j \left\{ \left| \frac{y_j - \widehat{y}_j}{y_j} \right| \times 100\%, \quad j = 1, 2 \dots p \right\}, \tag{8}$$

where ΔA is the maximum relative error.

The ICQ in cities A, B, and C in 2022 was selected as input and the AIP value as output. The predicted value of each AIP is obtained by adding the actual value of the previous year's index and the predicted index improvement value, and comparing the deviation between the actual and predicted values, the results are shown in Figures 3–5.

From Figures 3 and 4, the predicted values of AIP for cities A, B, and C under the DBN model are basically consistent with the actual values, and the maximum relative errors are 9.45%, 13.21%, and 11.58%, respectively. The maximum relative error corresponds to the AIP for city B, with actual and predicted values of 23.2% and 26%, respectively, and the absolute error is only 2.8%, which has a small impact on the evaluation results of the enterprises. At the same time, considering the deviation of historical data of enterprises and the variability of development level among municipalities, the accuracy of evaluation results of different municipalities under DBN model varies slightly.

4.3. Analysis of Correlation between the ICQ and the AIP. Based on the theoretical analysis of the sensitivity of enterprise ICQ and AIP, the impact of changes in ICQ on the quality of each accounting information is analyzed by taking a city enterprise as an example, and the results are shown in Figures 5 and 6.

The results of Figures 5 and 6 show that, with the improvement of the internal control index of enterprises, the impact on the quality of accounting information is becoming more and more obvious. Therefore, when an enterprise implements internal control, it should select the projects that need to be improved according to the development of the enterprise and carry out targeted management of the projects according to the established ICQ and AIP matching analysis model.

4.3.1. Analysis of the Empirical Results of the Relevance of ICQ and AIP. According to the regression results, the F-value of model 6 equation is 217.3 and the corresponding P value is less than the significance level of 0.01, which means that the equation of model 6 is valid. The corresponding P

Table 2: Effect of #hidden layers on the accuracy of the model.

Hidden layers	MAPE (%)	Training time (s)
2	11.2	55
3	10.4	176
4	9.2	789
5	9.6	439
6	10.8	608
7	12.4	701

Table 3: Effect of #neurons in the hidden layer on the accuracy of the model.

Number of hidden layers	MAPE (%)	Training time (s)
32	10.5	32
64	9.2	286
128	8.1	988
256	9.6	2047
512	10.5	7072

value is less than the significance level 0.01, which indicates that the effect of internal control index ICQ on accounting information quality SYN is statistically significant, and furthermore, the coefficient value is 0.067, which means that internal control quality is significantly and positively related to accounting information quality, and the higher the internal control index ICQ, the higher the accounting information quality SYN. As the size of the company LNSIZE and the number of years of establishment OLD increase, the quality of accounting information SYN rises. Hypothesis H1 holds. The correlation analysis is shown in Table 4.

4.3.2. Analysis of the Empirical Results on the Relevance of AIP and AIP. According to the regression results of model 7, the F-value of model 7 equation is 217.3, and the corresponding P value is less than the meaningful level of 0.01, indicating that model 7 equation is effective. The VIF value of all variables in the model is less than 10, which can detect the lack of consistency between variables within the validity of the model. ABSDA detected that AIP was negative 4.26 and P was less than 0.01. It is worth noting that the experiment is statistically significant, with a value of −7005. And the correlation results are shown in Figure 7.

4.3.3. Analysis of the Empirical Results on the Effect of AIP as a Mediating Variable on Internal Control and AIP. The above model test shows that the F-value of model 8 equation is 210.6, which corresponds to a P value significantly lower than 0.01, which means that the hypothesis of the model is valid. The adjusted R-squared is 0.373, which indicates that the model 8 hypothesis also actually exists. The corresponding P value is less than 0.01, which means that the intermediate ABSDA variable has a very significant impact on the overall development of AIP and also means that the intermediate ABSDA variable has a significant impact on AIP syn. At the same time, model 8 notes that the internal control level of ICQ is quite high, indicating that this intermediate effect is completely indirect. The regression results are shown in Table 5.
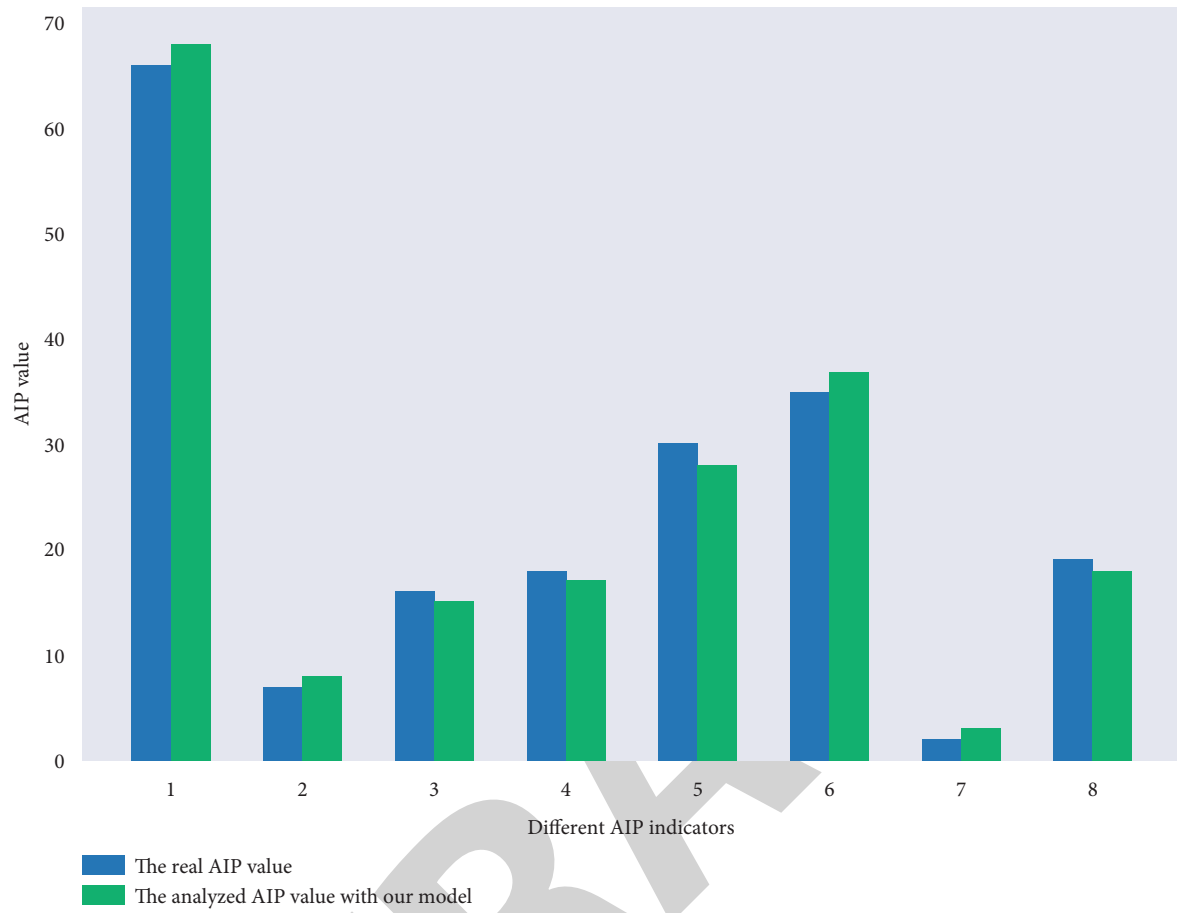
Figure 3: Comparison of actual and predicted values of the AIP in city A.
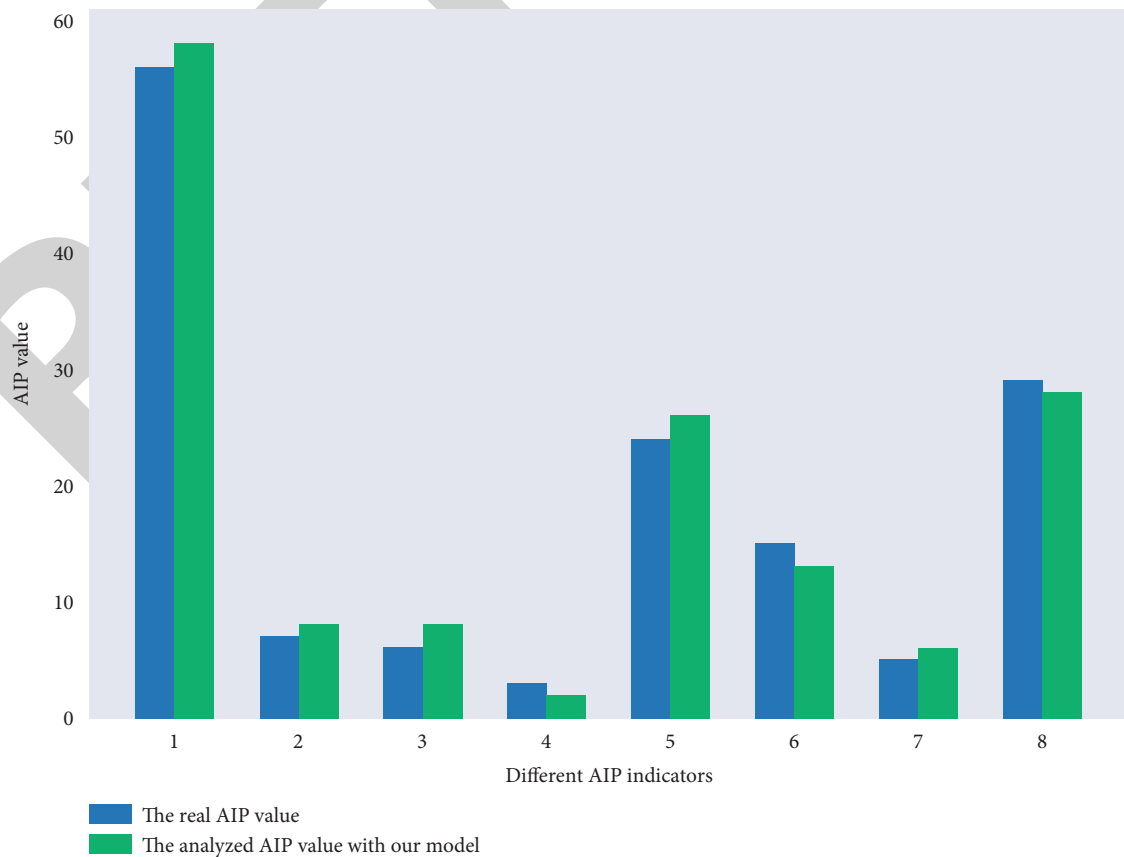
Figure 4: Comparison of actual and predicted values of AIP in city B.
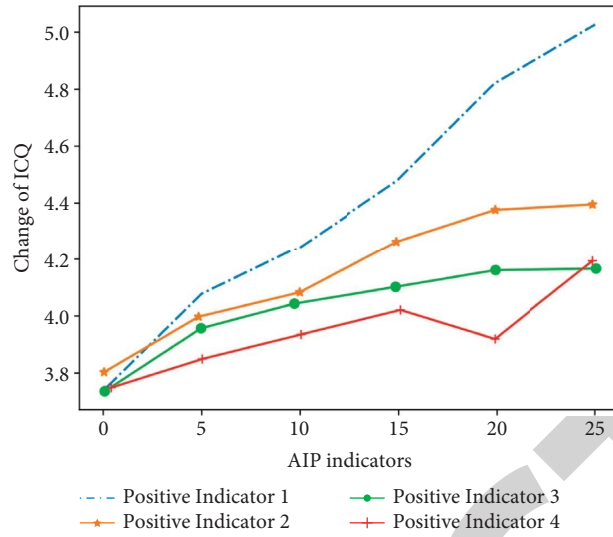
Figure 5: The impact of changes in the ICQ on each positive AIP indicators.
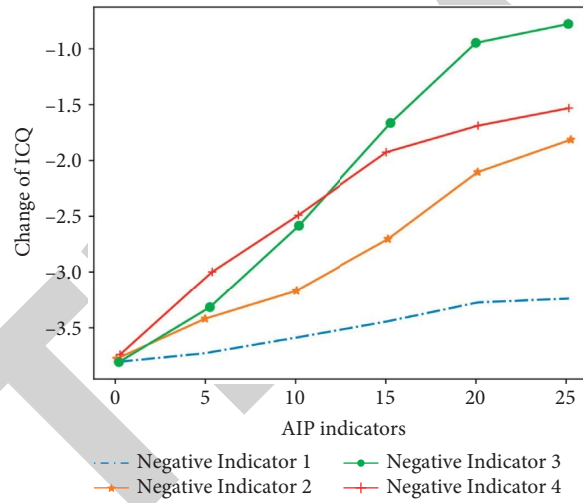
Figure 6: The impact of changes in the ICQ on each negative AIP indicators.

Table 4: Correlation analysis.

	SYN	ABSDA	ICQ	LEV	INSIZE	MB	TOP1	INST	OLD
SYN	1	−0.042 **	0.041 **	0.046 **	0.155 **	−0.105 **	0.015	0.056 **	0.082 **
ABSDA	−0.042 **	1	0.025 **	0.074 **	−0.033 **	0.072 **	−0.023 **	−0.062 **	0.034 **
ICQ	0.041 **	0.025 **	1	0.022 **	0.205 **	−0.047 **	0.103 **	0.148 **	−0.018 **
LEV	0.045 **	0.072 **	0.024 **	1	0.532 **	−0.413 **	0.108 **	0.213 **	0.145 **
INSIZE	0.155 **	−0.033 **	0.205 **	0.532 **	1	−0.539 **	0.255 **	0.427 **	0.099 **
MB	−0.106 **	0.072 **	−0.045 **	−0.413 **	−0.537 **	1	−0.088 **	−0.152 **	−0.096 **
TOP1	0.015	−0.023 **	0.101 **	0.108 **	0.255 **	−0.088 **	1	0.505 **	−0.065 **
INST	0.056 **	−0.062 **	0.148 **	0.211 **	0.425 **	−0.152 **	0.505 **	1	0.082 **
OLD	0.082 **	0.036 **	−0.018	0.145 **	0.099 **	−0.094 **	−0.065 **	0.082 **	1

** Correlation is significant at the 0.01 level (2-tailed).
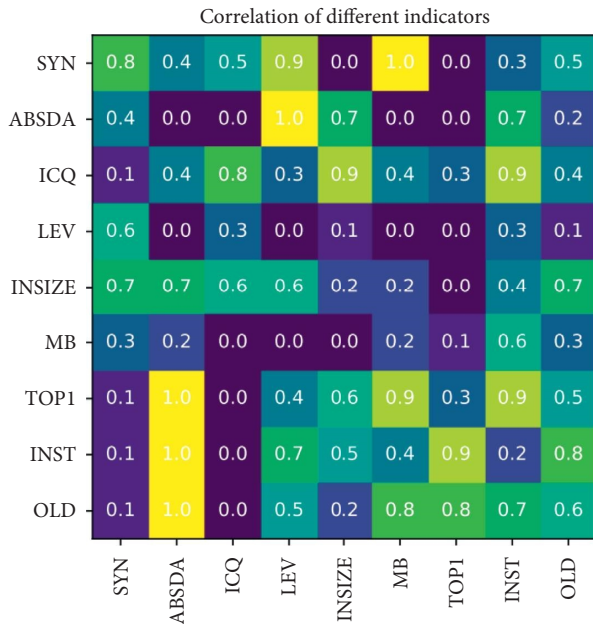
Figure 7: Correlation results of different indictors.

Table 5: Regression results.

	Hypothesis 1	Hypothesis 2	Hypothesis 3
	SYN	SYN	SYN
ICQ	0.068 ***		0.071 ***
	(4.15)		(4.35)
LEV	−0.472 ***	−0.472 ***	−0.442 ***
	(−6.66)	(−6.65)	(−6.20)
LNSIZE	0.065 ***	0.075 ***	0.064 ***
	(5.12)	(5.99)	(4.98)
MB	−0.097 ***	−0.092 ***	−0.095 ***
	(−15.02)	(−14.48)	(−14.67)
TOP1	0.111	0.125	0.116
	(1.25)	(1.38)	(1.33)
INST	−0.166 ***	−0.168 ***	−0.183 ***
	(−2.65)	(−2.68)	(−2.92)
OLD	0.006 ***	0.006 ***	0.006 ***
	(3.08)	(3.04)	(3.12)
ABSDA		−0.705 ***	−0.735 ***
		(−4.26)	(−4.47)
CONS	−2.546 ***	−2.281 ***	−2.489 ***
	(−8.68)	(−7.87)	(−8.46)
R^2	0.376	0.376	0.377
ADJ R^2	0.372	0.372	0.373
F	217.5 ***	274.5 ***	210.6 ***

5. Conclusion

The discussion on the quality of accounting information from the perspective of internal control is an important strategic planning issue and management planning direction for the economy and enterprises at a certain stage of development. From the perspective of internal control, the optimization of enterprise accounting information quality can be carried out as follows: optimization of internal control system and governance structure, optimization of internal accounting control system and accounting function, optimization of personnel control, etc. In the face of the ever-changing market economy, the optimization of accounting information quality with good internal control planning is an important way to realize enterprise efficiency and management innovation.

Data Availability

The experimental data used to support the findings of this study can be obtained from the corresponding author upon request.

Conflicts of Interest

The authors declared that they have no conflicts of interest regarding this work.

References

[1] M. Luo, "Enterprise internal control and accounting information quality," *Journal of Financial Risk Management*, vol. 6, no. 1, pp. 16–26, 2017.

[2] S. Mulyani and E. D. P. Arum, "The influence of manager competency and internal control effectiveness toward AIP," *International Journal of Applied Business and Economic Research*, vol. 14, no. 1, pp. 181–190, 2022.

[3] S. D. Setyaningsih, S. Mulyani, B. Akbar, and I. Farida, "Implementation and performance of accounting information systems, internal control and organizational culture in the quality of financial information," *Utopía y Praxis Latinoamericana: revista internacional de filosofía iberoamericana y teoría social*, vol. 1, pp. 222–236, 2021.

[4] A. Susanto, "The effect of internal control on accounting information system," *International Business Management*, vol. 10, no. 23, pp. 5523–5529, 2022.

[5] Di Wu, Y. Lei, M. He, C. Zhang, and Li Ji, "Deep reinforcement learning-based path control and optimization for unmanned ships," *Wireless Communications and Mobile Computing*, vol. 2022, pp. 1–8, Article ID 7135043, 2022.

[6] S. P. Teru, I. Idoku, and J. T. Ndeyati, "A review of the impact of accounting information system for effective internal control on firm performance," *Indian Journal of Finance and Banking*, vol. 1, no. 2, pp. 52–59, 2017.

[7] H. Rashedi and T. Dargahi, "How influence the accounting information systems ICQ on financial reporting quality," *JMDMA*, vol. 2, no. 5, pp. 33–45, 2019.

[8] G. Cai, Y. Fang, J. Wen, S. Mumtaz, Y. Song, and V. Frascolla, "Multi-carrier M-ary DCSK system with code index modulation: an efficient solution for chaotic communications," *IEEE Journal of Selected Topics in Signal Processing*, vol. 13, no. 6, pp. 1375–1386, 2019.

[9] K. Chandra, A. S. Marcano, S. Mumtaz, R. V. Prasad, and H. L. Christiansen, "Unveiling capacity gains in ultradense networks: using mm-wave NOMA," *IEEE Vehicular Technology Magazine*, vol. 13, no. 2, pp. 75–83, June 2018.

[10] S. D. Anggadini, "The effect of top management support and internal control of the accounting information systems quality and its implications on the accounting information quality," *Information Management and Business Review*, vol. 7, no. 3, pp. 93–102, 2015.

[11] S. Palanisamy, B. Thangaraju, O. I. Khalaf, Y. Alotaibi, S. Alghamdi, and F. Alassery, "A novel approach of design and analysis of a hexagonal fractal antenna array (HFAA) for next-

Retraction

Retracted: Study on the Relationship between Unexplained Recurrent Abortion and HLA-DQ Gene Polymorphism

Computational Intelligence and Neuroscience

This article has been retracted by Hindawi following an investigation undertaken by the publisher [1]. This investigation has uncovered evidence of one or more of the following indicators of systematic manipulation of the publication process:

(1) Discrepancies in scope

(2) Discrepancies in the description of the research reported

(3) Discrepancies between the availability of data and the research described

(4) Inappropriate citations

(5) Incoherent, meaningless and/or irrelevant content included in the article

(6) Peer-review manipulation

The presence of these indicators undermines our confidence in the integrity of the article's content and we cannot, therefore, vouch for its reliability. Please note that this notice is intended solely to alert readers that the content of this article is unreliable. We have not investigated whether authors were aware of or involved in the systematic manipulation of the publication process.

In addition, our investigation has also shown that one or more of the following human-subject reporting requirements has not been met in this article: ethical approval by an Institutional Review Board (IRB) committee or equivalent, patient/participant consent to participate, and/or agreement to publish patient/participant details (where relevant).

Wiley and Hindawi regrets that the usual quality checks did not identify these issues before publication and have since put additional measures in place to safeguard research integrity.

We wish to credit our own Research Integrity and Research Publishing teams and anonymous and named external researchers and research integrity experts for contributing to this investigation.

The corresponding author, as the representative of all authors, has been given the opportunity to register their agreement or disagreement to this retraction. We have kept a record of any response received.

References

[1] J. Tang, J. Zhu, L. Shu, X. Huang, and S. Ma, "Study on the Relationship between Unexplained Recurrent Abortion and HLA-DQ Gene Polymorphism," *Computational Intelligence and Neuroscience*, vol. 2022, Article ID 8005538, 5 pages, 2022.

Research Article

Study on the Relationship between Unexplained Recurrent Abortion and HLA-DQ Gene Polymorphism

Jie Tang,[1] Jichao Zhu,[2] Longwen Shu,[1] Xiaohong Huang,[1] and Siming Ma [1]

[1]*Department of Obstetrics and Gynecology, Huzhou Central Hospital, Huzhou 313000, China*
[2]*Department of Laboratory Medicine, Huzhou Central Hospital, Huzhou 313000, China*

Correspondence should be addressed to Siming Ma; masiming@stu.ahu.edu.cn

Objective. The study aimed to investigate the relationship between human leukocyte antigen (HLA-DQB1) gene variants and recurrent miscarriage. *Methods*. HLA-DQ gene polymorphisms (PCR-SSP) were detected in 50 couples with recurrent miscarriage (URSA group) and 30 couples with normal births (control group) using sequence-specific primer-guided polymerase chain reaction. *Results*. The frequency of the DQB1*0303 allele in the URSA group (21.50%) was substantially higher than that of the control group (11.67%) ($P = 0.0260$ 0.05, RR = 1.754); however, the frequency of the DQB1*0302 allele in the URSA group (4.00%) was substantially lower than that of the control pair (10.00%) ($P = 0.0318$ 0.05, RR = 0.400); the frequency of sharing one allele was 46.00% (23/50) in the URSA group and 0.00% (0/30) in the normal control group; the frequency of sharing two alleles was 40.00% (2/50) in the URSA group and 43.33% (13/30) in the normal control group, with no significant difference between the two groups. *Conclusion*. For the Zhejiang population, HLA-DQB1*0303 may be a susceptibility gene for recurrent miscarriage, while HLA-DQB1*0302 may be protective against recurrent miscarriage, especially for women.

1. Introduction

Recurrent spontaneous abortion (RSA) is a complex condition. Although it is defined nationally as 3 or more pregnancy losses, most experts believe that 2 spontaneous abortions should be taken seriously and evaluated because the likelihood of recurrent spontaneous abortion is similar to that of 3 [1]. RSA is defined by the American Society for Reproductive Medicine as two or more failed pregnancies occur within 20 weeks [2], with early miscarriages occurring before 12 weeks of gestation and late miscarriages occurring between 12 and 20 weeks of gestation [3], while the incidence of RSA in women of childbearing age is 3%–5% and the incidence of spontaneous abortion in repeat pregnancies in patients with RSA is as high as 70%–80% [4]. The etiology of RSA is complex and diverse, and in addition to genetic, anatomical abnormalities, endocrine disorders, infections, autoimmunity, sperm quality, lifestyle, psychosomatic, and environmental factors, the etiology of 50%–75% of RSA is still unknown [5]. The literature [6] shows that a significant

proportion of recurrent spontaneous abortions are associated with immune factors. The HLA gene system is the most complex polymorphic system known in humans, and it has an important influence on the way the human immune system is regulated. The DQB1 allele polymorphism in the HLA-II class system is relatively high and has been shown to be significantly associated with recurrent abortions [7]. Considering the role of the HLA gene system in recurrent spontaneous abortion and its ethnic and geographical differences [8], the aim of this study was to investigate the role of the HLA gene system in recurrent spontaneous abortion by examining HLA-DQB1 gene polymorphisms in couples presenting with unexplained recurrent spontaneous abortion in Zhejiang province.

2. Material and Methods

2.1. Research Subjects. Fifty women who suffered from recurrent abortion were selected from October 2017 to February 2019 in Huzhou Central Hospital. All cases were

selected after detailed history collection and auxiliary examination, and the following conditions were met at the same time: ① Two or more times of primary spontaneous abortion occurred continuously (2–10 times), and the last time occurred within 1 year; ② the bilateral chromosomes of the couple were normal; ③ the woman had no anatomical deformity of the reproductive tract, and abnormal internal secretion was excluded from the determination of the endocrine hormone level; ④ there was no infection in the reproductive system; ⑤ the results of autoimmune antibodies such as antiphospholipid antibodies were negative; ⑥ regular testing revealed that the male spouse's sperm was healthy. In the control group, 30 healthy expectant and postpartum women and their husbands who were hospitalized to the Obstetrics Department of Huzhou Central Hospital for delivery and underwent physical examination between November 2017 and March 2019 were chosen at random. There was no history of spontaneous abortion, stillbirth, coinfection, or autoimmune diseases in the control group. All the subjects were from Zhejiang province.

2.2. Research Methods. 200 ul of EDTA anticoagulated whole blood was collected, and DNA was extracted using a DNA extraction kit at a concentration of 40–90 ng/uL and 1.7–2.0 at 260D/280D d. The HLA-DQB l locus was genotyped in strict accordance with the operating procedures of Tianjin Xiupeng Biotechnology Development Co., Ltd., and the results were interpreted by automatic analysis software. The review approach used PCR-SBT or sequence-based PCR typing.

2.3. Statistical Method. The frequencies of each allele were calculated by Microsoft Office Excel2003, with the analytic program SPSS17.0. The HLA-DQBl gene frequencies between the URSA group and the control group were compared using the chi-square test. The difference was statistically significant at $P < 0.05$. A relative risk calculation was made.

3. Result

3.1. Frequency Distribution of HLA-DQB1 Alleles. As shown in Table 1, the frequency of the HLA-DQB1*0303 allele was 21.50% (43/200) in the URSA group and 11.67% (14/120) in the normal control group; the prevalence of the HLA-DQB1*0303 allele was substantially higher in the URSA group than in the normal control group, $\chi^2 = 4.954$, $P = 0.026$, and the frequency of the HLA-DQB1*0302 frequency was 4.00% (8/200) in the URSA group and 10.00% (12/120) in the normal control group, $\chi^2 = 4.608$, $P = 0.032$, histogram in Figure 1; as shown in Table 2, the HLA-DQB1*0302 allele was significantly less frequent in the URSA female group with a frequency of 4.00% (4/100). The frequency was 13.33% (8/60) in the normal control female group, $\chi^2 = 4.709$, $P = 0.030$, and there were no significant differences in the frequencies of other alleles ($P > 0.05$); the bar graphs are shown in Figure 2.

3.2. Sharing Rate of the HLA-DQB1 Allele between Couples. The frequency of sharing one allele was 46.00% (23/50) in the URSA couple group and 43.33% (13/30) in the normal control group, with no significant difference between these two groups, and the frequency of sharing two alleles was 40.00% (2/50) in the URSA couple group and 0.00% (0/30) in the normal control group. Table 3 shows that there were no significant differences, and the bars are shown in Figure 3.

4. Discussion

4.1. Polymorphisms and Characteristics of the HLA-DQB1 Gene. Since the discovery of the first human leukocyte antigen Mac (HLA-A2) by French physician Dausset in 1958, research on HLA has developed rapidly [9]. HLA is located in region 21.3 of the short arm of chromosome 6, with a length of 4100 kb, and is by far the most polymorphic system known in humans, accounting for about 0.1% of the genes in the human genome [10]. The gene structure of this region has the following characteristics: (1) the region with the highest concentration and abundance of genes related to immune function, with 39.8% of gene products being immune among 128 functional genes; (2) the region with the highest gene density, with an average of one gene per 16 kb; (3) the region with the strongest polymorphism; (4) the region with the closest relationship to disease. In 1991, Bodmer classified HLA into three categories, namely, HLA-I genes including HLA-A, B, C, E, F, and G. HLA-II genes consist of six subunits, including HLA-DR, DQ, DP, DNA, DOB, and DM [11]. The HLA-III gene region mainly encodes complement-related genes, such as C2, C4A, C4B, and BF. In DQ of the HLA-II gene subregion, there are two pairs of α and β genes, of which, α1 and β1 domains are polymorphic sites and HLA-DQB1 is located in the β1 domain. A major function of the HLA-II gene is to present antigens and activate T lymphocytes, which are mostly present on the surface of dendritic cells, macrophages, B lymphocytes, activated T lymphocytes, and other cells. The distribution of HLA is ethnic and regional, and the genetic characteristics of HLA gene frequencies vary among different ethnic and regional populations [12].

4.2. HLA Gene System and Immunity. The HLA gene system has a major impact on the way the human immune system is regulated. The literature [13] showed that whether the body responds to antigenic substances and the intensity of the response is genetically controlled. The HLA class II gene region contains immune response regulatory genes. Due to the different peptide structures of the molecules encoded by HLA-II genes, their ability to bind different antigenic peptides and stimulate Th cells is different, so the expression of genes in the immune response is different. The non-T cell surface stimulation of autologous mixed lymphocytes in response to AMLR is determined by HLA-DQ in one of the HLA-II molecules. AMLR is a regulatory mechanism between immune cells in vivo, maintaining immune homeostasis. Thus, by activating AMLR, HLA-II-like molecules can influence immunological control. Despite the fact that the

Table 1: Frequency distribution of HLA-DQB1 alleles in 50 URSA couples and 30 normal fertile couples.

HLA-DQB1 genotypes	Couples in the URSA group (n = 200)		Couples in the normal group (n = 120)		χ^2 value	P value
	Times	Frequency (%)	Times	Frequency (%)		
0301	49	24.50	31	25.83	0.0711	0.7897
0303	43	21.50	14	11.67	4.9541	0.026
0201	17	8.50	16	13.33	1.9671	0.1607
0501	18	9.00	14	11.67	0.5926	0.4414
0302	8	4.00	12	10.00	4.6081	0.0318
0202	10	5.00	5	4.17	0.1166	0.7328
0602	10	5.00	11	9.17	2.1231	0.1451
0401	10	5.00	6	5.00	0	1
0603	7	3.50	6	5.00	0.3169	0.5735
0503	6	3.00	3	2.50	0.0686	0.7934
0402	1	0.50	1	1.83	0.1342	0.7141
Total genotype	179		119			
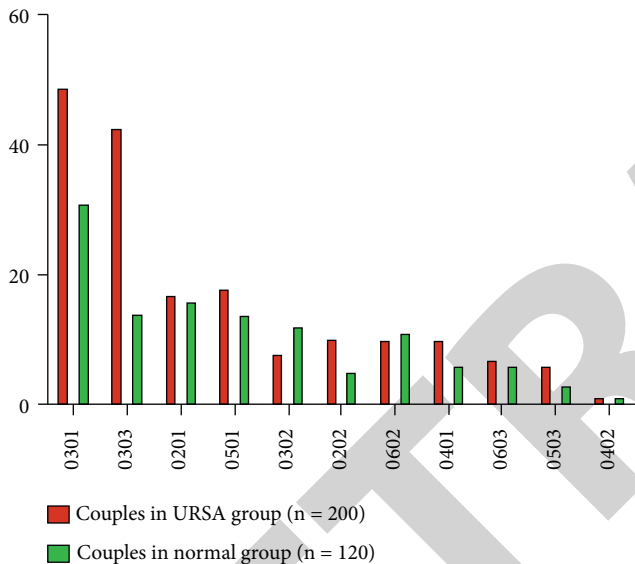
Figure 1: Frequency distribution of HLA-DQB1 alleles in 50 URSA couples and 30 normal fertile couples.

fetus is a semiallogeneic transplant of the mother, the immune response of the mother during pregnancy can protect the fetus from rejection. However, the literature [14] has demonstrated that several tolerance mechanisms limit the maternal immune response during normal pregnancy. The literature [15] showed that in couples with unexplained recurrent spontaneous abortions, HLA molecules are thought to have played an important role at the maternal-fetal interface. Fetal blood enters the maternal circulation when exchanging blood with the mother through the placenta, and the maternal immune system is able to recognize paternal HLA antigens carried by the blood; excessive sharing of HLA antigens between the couple can lead to insufficient production of blocking antibodies and finally to recurrent miscarriage. The literature [16] suggests that excessive sharing of HLA antigens between couples can lead to low maternal responsiveness to paternal antigens, which is an important mechanism leading to recurrent miscarriage. The literature [17] suggests that antipaternal HLA antibodies

may not be harmful in healthy pregnancies but rather may even be beneficial. However, the literature [18] suggests that maternal HLA antibodies are detrimental to pregnancy in couples with recurrent miscarriage.

4.3. Undiagnosed Recurrent Miscarriage and HLA-DQB1 Gene Polymorphism. In this study, 50 couples with URSA and 30 couples with normal births were studied. The results showed that HLA-DQB1*0303 may be a susceptibility gene for recurrent miscarriage and that HLA-DQB1*0302 may play a protective role against recurrent miscarriage, especially in women. Studies in the literature [19] suggest that DQB1*03 : 03 : 02 is a susceptibility gene for recurrent miscarriage in South India, and the inconsistent results may be due to regional and ethnic differences in HLA. A study in the literature [20] showed that the number of couples sharing two HLA alleles for recurrent pregnancy loss was less than those sharing one allele and those not sharing, and the rate of HLA allele sharing did not correlate with recurrent miscarriage. The results of this study showed that there was no significant difference in the frequency of sharing one allele between URSA couples and normal controls, nor was there a significant difference in the frequency of sharing two alleles between URSA couples and normal controls. The results of this study also show a lack of association between the rate of HLA allele sharing and unexplained recurrent miscarriage. In addition, it needs to be compared with epidemiological data on the population distribution of HLA-DQB1 in China. The literature [18] on the distribution of HLA-DQB1 polymorphisms in South and North China showed that the distribution of HLA-DQB1*02, 05, 0601, 0602, and 0603 in the Chinese population was different between North and South. The literature [21] reported that HLA-DQB1*0303, 0302 did not differ significantly between North and South China. However, few studies have examined the distribution of HLA-DQB1 allele polymorphisms in Zhejiang. Due to the vast geographical area and many ethnic groups in China, the sample data of HLA-DQB1 in unexplained recurrent miscarriage need to be expanded and epidemiological data need to be improved.

Table 2: Frequency distributions of HLA-DQB1 alleles in 50 URSA females and 30 fertile females.

HLA-DQB1 genotypes	Females in the URSA group (n = 100)		Females in the normal group (n = 60)		χ^2 value	P value
	Times	Frequency (%)	Times	Frequency (%)		
0301	25	25.00	15	25.00	0	1
0303	21	21.00	7	11.67	2.2631	0.1325
0201	11	11.00	8	13.33	0.1951	0.6587
0501	10	10.00	6	10.00	0	1
0602	7	7.00	5	8.33	0.0961	0.7566
0401	5	5.00	3	5.00	0	1
0302	4	4.00	8	13.33	4.7091	0.03
0603	4	4.00	5	8.33	1.3261	0,2494
0402	1	1.00	1	1.67	0.135	0.7133
0202	2	2.00	1	1.67	0.2265	0.8804
Total genotype	90		59			
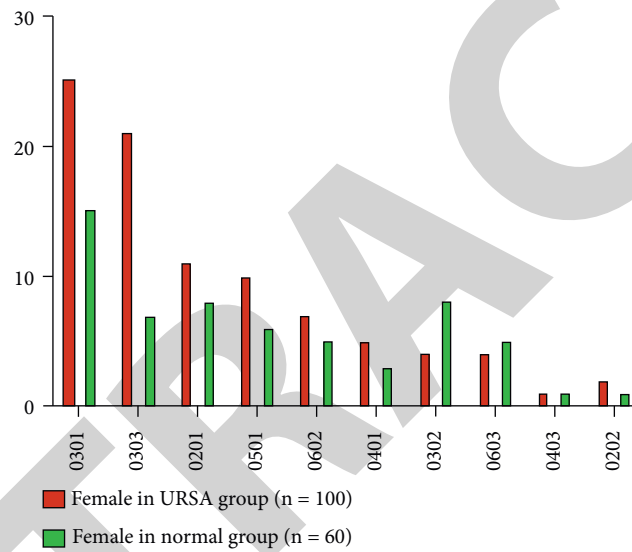
Figure 2: Frequency distributions of HLA-DQB1 alleles in 50 URSA females and 30 fertile females.

Table 3: Comparison of the number of shared HLA-DQB1 alleles between 50 URSA couples and 30 fertile couples.

Allelic genes	URSA group (n = 50)		Normal group (n = 30)		χ^2 value	P value
	Times	Frequency (%)	Times	Frequency (%)		
Share 1 allelic gene	23	46.00	13	43.33	0.0539	0.8165
Share 2 allelic genes	2	4.00	0	0.00	1.2311	0.2673
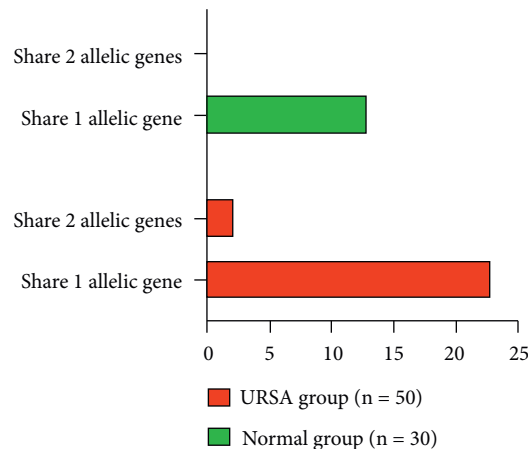
Figure 3: Comparison of the number of shared HLA-DQB1 alleles between 50 URSA couples and 30 fertile couples.

Retraction

Retracted: Analysis of Therapeutic Effect of Elderly Patients with Severe Heart Failure Based on LSTM Neural Model

Computational Intelligence and Neuroscience

This article has been retracted by Hindawi following an investigation undertaken by the publisher [1]. This investigation has uncovered evidence of one or more of the following indicators of systematic manipulation of the publication process:

(1) Discrepancies in scope

(2) Discrepancies in the description of the research reported

(3) Discrepancies between the availability of data and the research described

(4) Inappropriate citations

(5) Incoherent, meaningless and/or irrelevant content included in the article

(6) Peer-review manipulation

The presence of these indicators undermines our confidence in the integrity of the article's content and we cannot, therefore, vouch for its reliability. Please note that this notice is intended solely to alert readers that the content of this article is unreliable. We have not investigated whether authors were aware of or involved in the systematic manipulation of the publication process.

In addition, our investigation has also shown that one or more of the following human-subject reporting requirements has not been met in this article: ethical approval by an Institutional Review Board (IRB) committee or equivalent, patient/participant consent to participate, and/or agreement to publish patient/participant details (where relevant).

Wiley and Hindawi regrets that the usual quality checks did not identify these issues before publication and have since put additional measures in place to safeguard research integrity.

We wish to credit our own Research Integrity and Research Publishing teams and anonymous and named external researchers and research integrity experts for contributing to this investigation.

The corresponding author, as the representative of all authors, has been given the opportunity to register their agreement or disagreement to this retraction. We have kept a record of any response received.

References

[1] S. Chen and S. He, "Analysis of Therapeutic Effect of Elderly Patients with Severe Heart Failure Based on LSTM Neural Model," *Computational Intelligence and Neuroscience*, vol. 2022, Article ID 7250791, 10 pages, 2022.

Hindawi

Research Article

Analysis of Therapeutic Effect of Elderly Patients with Severe Heart Failure Based on LSTM Neural Model

Shunhong Chen and Shoudu He [ORCID]

Department of Emergency, Affiliated Hospital of Gansu University of Chinese Medicine, Lanzhou 730000, Gansu, China

Correspondence should be addressed to Shoudu He; hesd4521@stu.cpu.edu.cn

In recent years, cardiovascular-related diseases have become the "number one killer" threatening human life and health and have received much attention. The timely and accurate detection and diagnosis of arrhythmias and heart failure are relatively common heart diseases, which are of great social value and research significance in improving people's quality of life by providing early treatment or intervention for those who are at risk. Based on this, this paper proposes a deep learning network architecture based on the combination of long- and short-term memory networks and deep residual neural networks for the automatic detection of heart failure. A total of 60 elderly patients with severe heart failure treated in the emergency department of our hospital from August 2019 to August 2021 were selected as the sample subjects of this study. The treatment outcomes and prognostic quality of life of the two groups of patients were compared and analyzed. Based on the unbiased test method, the accuracy of the proposed method on the authoritative open continuous heart rate database PhysioNet was 99.67% (data length 500), 98.84% (data length 1000), and 96.63% (data length 2000). This indicates that the network model can well extract the high-dimensional features of continuous heart rate and improve the accuracy of the classification model. The LSTM neural model proposed in this paper may be able to provide richer information on heart health status for portable ECG detection systems, which have very important clinical value and social significance.

1. Introduction

Population aging has always been a major social issue in China, and the results of the seventh census show that the total population of the country will be about 1.44 billion by the end of 2020, of which 18.7% will be 60 years old and above and 13.5% will be 65 years old and above [1], and the number of people suffering from cardiovascular diseases is increasing as the process of aging and urbanization accelerates, especially in the low-age and low-income groups. The potential risk factors for cardiovascular diseases show rapid growth and individual aggregation. Based on previous surveys, the report estimates that the number of people suffering from cardiovascular diseases in China has reached 290 million [2]. It is expected that the number of cardiovascular diseases will continue to show a rapid increase in the next decade [3].

There is more than one risk factor for cardiovascular disease, and most of the cases are due to the long-term superposition of several adverse factors that interact with each other, so we cannot make a one-sided analysis. Especially in recent years, it has been found that atmospheric pollution is also one of the risk factors for the development of cardiovascular diseases, especially PM2.5 as the main pathogenic component of particulate matter (PM), which has a closer relationship with cardiovascular diseases [4]. Since 2004, the average annual growth rate of total hospitalization costs for cardiovascular diseases alone has been much higher than the growth rate of gross domestic product (GDP) in the same period [5]. In summary, the prevention and treatment of cardiovascular diseases have become an important part of public health construction in China and have attracted the attention of the state and society.

In addition, the elderly are prone to diseases specific to this population and various complications and organ failure. The course of heart failure is shown in Figure 1. In addition, heart failure in the elderly has the following characteristics: the more women there are, the more the HFPEF is (also known as diastolic heart failure), the more patients have weakness, comorbidity and cognitive impairment, poor treatment outcomes, and mortality and hospitalization rates remain constant for years [6]. It is difficult to translate "evidence-based medical information" directly into evidence for the treatment of heart failure in the elderly because elderly patients with heart failure, particularly mental retardation, frailty, and comorbidities, fall under the exclusion criteria of clinical trials and have little evidence-based medical evidence. As a result, the prevention and treatment of elderly patients with heart failure are more complex and specific.

Studies have shown that heart failure can be detected based on quantitative indicators of continuous heart rate [7]. It was found that the standard deviation of continuous heart rate (SDNN) could be used to predict the risk of death in patients with heart failure [8]. Since then, researchers have been trying to identify heart failure patients by analyzing continuous heart rates. In recent years, deep learning algorithms have been continuously applied in various fields such as image recognition, speech analysis, and natural language processing with remarkable results [9]. Among the many deep learning models, the deep residual network (RESNET) [10] is particularly outstanding and is rapidly becoming one of the most popular network frameworks for various computer vision tasks. In this paper, we identify heart failure based on the deep residual network architecture and short-term continuous heart rate signals to effectively improve the accuracy and real-time performance of heart failure detection, help heart failure patients self-manage, improve survival and quality of life, and lay the foundation for more accurate and convenient heart health monitoring in the future.

2. Related Work

After more than 100 years of development, ECG testing equipment is now gradually improved, not only in terms of its shrinking size but also in terms of its clear recording and anti interference ability. In recent years, with the emergence and development of intelligent computers, people have also started to think whether they can use the power of computers to assist physicians in the observation and analysis of ECGs. Computer-Aided Diagnosis (CAD) system not only effectively solves the problem of subjective consciousness uncertainty that may occur during the analysis and diagnosis of ECG signals by doctors but also enhances the efficiency of doctors, which is of great practical significance to clinical work.

Among the machine learning algorithms, support vector machine (SVM) is one of the most frequently used methods for arrhythmia classification [11]. It has been reported that the 1-v-l (one-versus-one) SVM algorithm was used to

classify ECG data and a high recognition rate is obtained. The authors in [12, 13] used the SVM classifier for the classification of six arrhythmias based on the ECG signal features extracted by the wavelet transform method and achieved an accuracy of 99.68%. Reference [14] et al. used the particle swarm optimization (PSO) algorithm to optimize the generalization performance of the SVM classifier and applied the system to the automatic classification of ECG signals and proved that the SVM approach outperformed other traditional classification algorithms, such as k-nearest neighbor (KNN) and radial basis function (RBF) neural networks. Reference [15] et al. then adopted a maximum voting strategy to hierarchically use SVM classifiers, thus improving the classification effect of SVM. Besides, some researchers also proposed a novel kernel function that significantly improved the final classification accuracy. However, the study also compared the classification results of the SVM-based algorithm with those of a deep learning network architecture based on a combination of long-term and short-term memory networks and deep residual neural networks and found that although the SVM algorithm outperformed the MLP method in terms of training time, the deep learning network architecture based on a combination of long-term and short-term memory networks and deep residual neural networks performed better in terms of accuracy, sensitivity, and so on. The performance is much better.

With the successful application of deep learning in other fields, more and more scholars have tried to use deep learning algorithms to solve practical problems in the field of ECG signal analysis [16]. Deep learning is an "end-to-end" approach, which makes predictions directly from raw data and can cope with a wider range of classification tasks. It can also improve the effectiveness of the learning process in the context of big data. Reference [17] in 2017 used Convolutional Neural Network for arrhythmia diagnosis based on single-lead ECG signals, which trained -a 34-layer convolutional neural network to detect arrhythmias in ECG time series of arbitrary length. Reference [18] et al. performed the classification of ECG signals based on deep neural networks, and the whole classification network was built using the current popular TensorFlow and Google toolboxes for the network. Reference [19], on the other hand, performed ECG signal classification based on the Alex Net deep learning architecture and achieved an average correct rate of 92%.

In summary, the relevance of deep learning network architectures based on a combination of long-term and short-term memory networks and deep residual neural networks to heart failure has been generally recognized by researchers, and the detection of heart failure using statistical methods or traditional machine learning methods has achieved some results, but there is still room for further improvement. The organic combination of deep learning and expert experience will be an important direction in this field in the future, and deep learning will also be the next hot spot for conducting heart failure diagnosis research due to its ability to extract high-dimensional features.
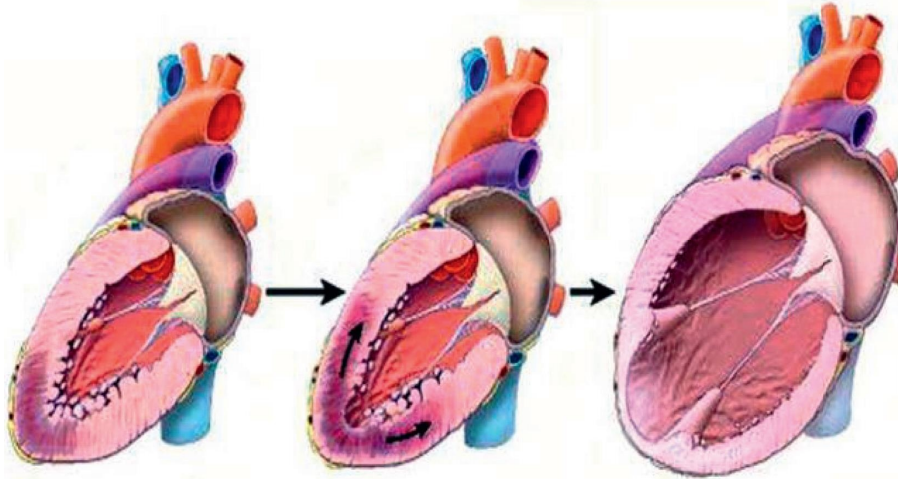
FIGURE 1: Heart failure process.

3. Experimental Data

The experimental data for this study were obtained from PhysioNet, an internationally recognized open-source database, which is divided into a clinical database and a waveform database. The waveform database contains continuous records of physiological signals in various noncritical care settings. In this study, we used the bidmc congestive heart failure database (bidmc-chf), the MIT-BIH normal sinus rhythm (NSR), and the fantasy database (FD).

The bidmc heart failure database included continuous ECG data of 15 patients with severe heart failure (NYHA grade 3-4), including 11 men aged 22 to 71 and 4 women aged 54 to 63; MIT-BIH normal sinus rhythm database includes continuous ECG data of 18 healthy people, including 5 men aged 26 to 45 and 13 women aged 20 to 50. The Fantasia database includes the physiological characteristics data of 20 young people (21 to 34 years old) and 20 elderly healthy subjects (68 to 85 years old) who have been strictly screened after 2 hours of rest. In this study, we first divide the database into a training set and a test set according to the subject's file information. The purpose of this is to ensure that the data in the test set never appear in the training stage and prevent the impact of overfitting on the algorithm evaluation. Then, the continuous heart rate data in the data set are divided into equal-length data with 500, 1000, and 2000 continuous heartbeats. Table 1 summarizes the number of samples obtained from the above three databases after data segmentation. Table 2 shows the information of subjects in the test set (there are many subjects in the training set, which are not listed here). Figure 2 shows the schematic diagram of two kinds of continuous heart rate signals when the division length is 500 heartbeats.

4. Deep Network Structure

4.1. DBN Model. The DBN model consists of several layers of Restricted Boltzmann Machine (RBM) stacked on top of each other. An RBM contains visible and hidden layers, each

TABLE 1: Sample size of different databases.

Database	Split length		
	500	1000	2000
BIDMC-CHF	3214	1607	803
NSR	3579	1793	869
FD	500	250	125

TABLE 2: Information of subjects in the test set.

Subject information		Split length		
54,F,#11	50,F,#19830			
63,M,#13	38,F,#19140	686	339	164
61,M#14	34,M,#19093			

layer consists of several neurons, and its structure is shown in Figure 3. In the RBM structure, neurons are interconnected between the visible and hidden layers, but there are no connections between neurons within each layer. The visible layer of the RBM satisfies the Bernoulli distribution or Gaussian distribution, while the hidden layer is the invisible feature detected and satisfies the Bernoulli distribution. The visible and hidden layers are connected by a symmetric weight matrix with probabilities satisfying the Boltzmann distribution.

For 1 set of values of (v, h) at a given state, assuming that both visible and hidden layer neurons obey Bernoulli distribution, the energy function can be expressed as

$$E(v, h, \theta) = -\sum_{i=1}^{m} \sum_{j=1}^{n} w_{ij} v_i h_j - \sum_{i=1}^{m} a_i v_i - \sum_{j=1}^{n} b_j h_j, \quad (1)$$

where $\theta = w_{ij}$ is the connection weight between v_i and h_j; a_i and b_j are the parameters of the RBM model; v_i is the i th neuron of the visible layer, corresponding to the investment of the i th item attribute; h_j is the j th neuron of the hidden layer; m and n are the number of neurons in the visible and hidden layers, respectively; and a_i and b_j are the unit biases of the visible and hidden layers, respectively.

(a)

(b)
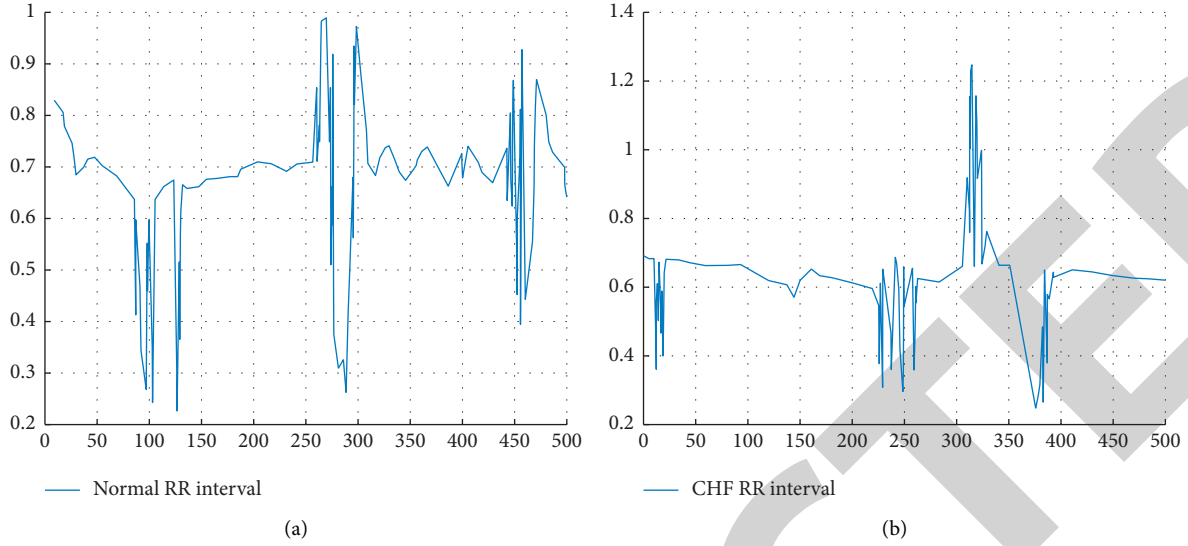
FIGURE 2: Two types of data when the sample length is 500 heartbeats.
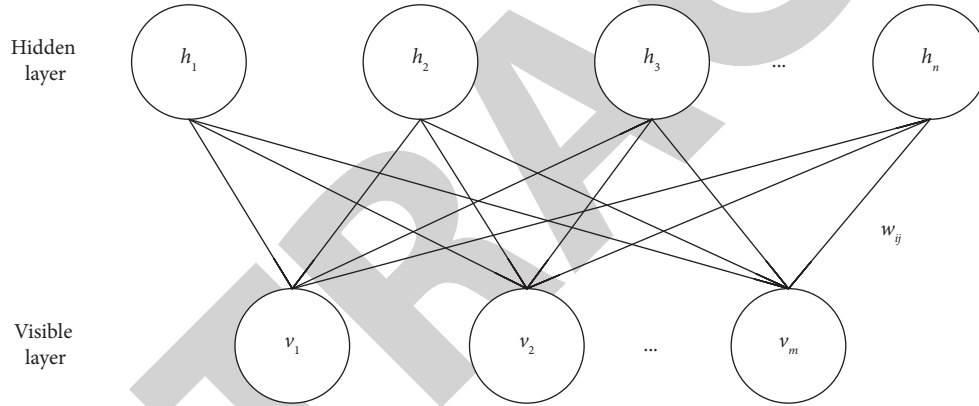
FIGURE 3: RBM model.

The visible and hidden layers are independent of each other, and the conditional probability of h on v is

$$P(h|v) = \prod_j P(h|v). \tag{2}$$

When v_i and h_j are given, the conditional probability distribution can be calculated as

$$\begin{cases} P(h_j = 1|v; \theta) = \sigma\left(\sum_{i=1}^{m} w_{ij}v_i + a_i\right), \\ P(v_j = 1|h; \theta) = \sigma\left(\sum_{j=1}^{n} w_{ij}h_j + b_j\right). \end{cases} \tag{3}$$

The excitation function σ is chosen as the Sigmoid function.

$$\sigma(x) = \frac{1}{(1 + e^{-x})}. \tag{4}$$

Given 1 set of defined training sets $\{V^c|c\{1, 2, 3 \ldots c\}\}$, the training objective is to maximize the log-likelihood function of the established model, and by calculating the gradient of the likelihood function, the weight update formula of the RBM can be obtained.

$$\Delta w_{ij} = \varepsilon\left(E_{\text{data}}(v_i h_j) - E_{\text{model}}(v_i h_j)\right), \tag{5}$$

where ε is the learning rate; E_{data} is the expected output of the input data of the observation layer; and E_{model} is the expected output on the probability distribution of the model.

The DBN model consisting of multiple RBMs stacked bottom-up is shown in Figure 4. This deep confidence network is divided into 2 layers, the bottom DBN pre-training model and the top back propagation (BP) fine-tuning model, respectively.

4.2. Model Training Method. The traditional neural network uses the BP algorithm to train the network, but with the increase of the number of hidden layers, the BP algorithm has the problems of gradient gradually sparse and easy to converge to the local minimum. DBN based on deep learning can better solve the problems of the BP algorithm by pretraining and fine-tuning the network parameters, which is divided into the following 2 steps.
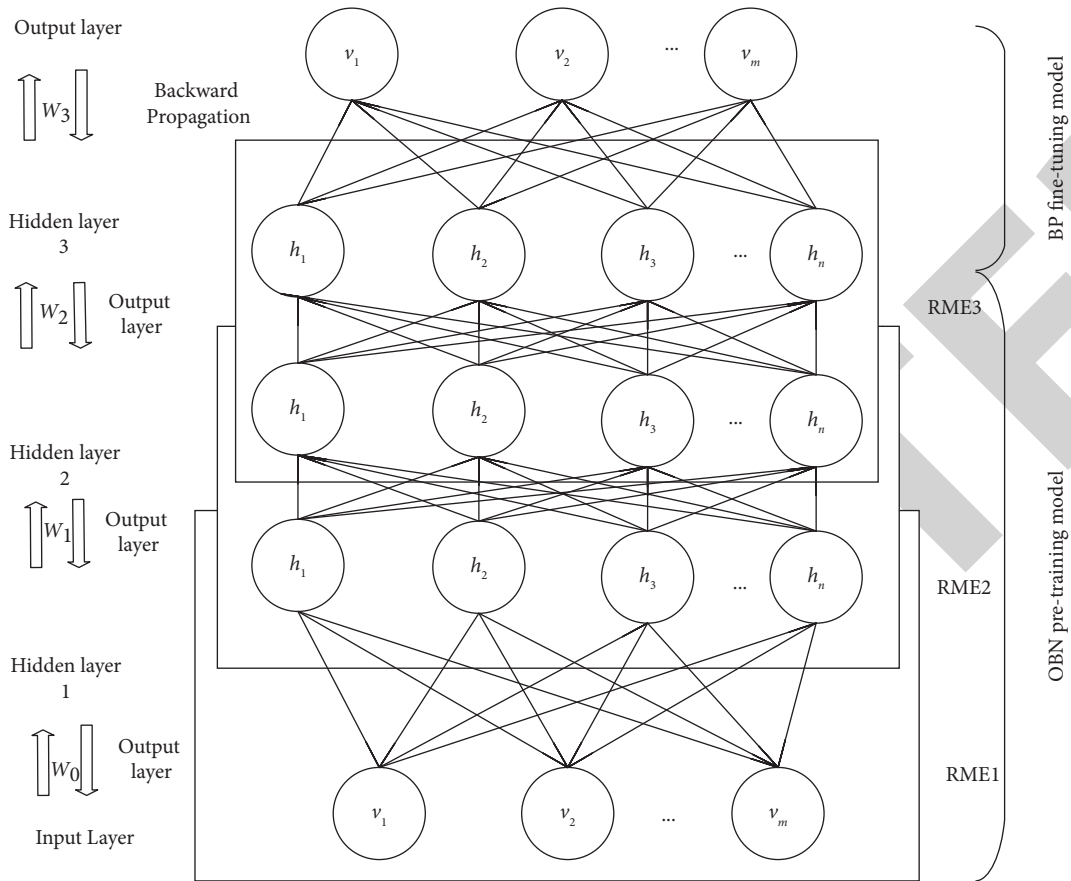
Figure 4: DBN.

4.2.1. Pretraining. Each layer of the network is trained separately and unsupervised, and the output of the upper layer is used as the input of the lower layer to ensure that as much information as possible is retained when the feature vectors are mapped to different feature spaces.

4.3. Fine-Tuning. The BP network is set up in the last layer of the DBN to receive the output of the RBM as its input, and the network is trained in a supervised manner to achieve top-down fine-tuning of the parameters.

Each layer of the RBM network can only ensure that the weights within its layer map optimally to the feature vectors in that layer, so the BP network also propagates the deviation information from the top-down to each layer of the RBM, fine-tuning the whole DBN network. The whole training process can be regarded as the initialization of the weights of the deep BP network, thus overcoming the disadvantage of the BP network of randomly selecting the initial values and falling into the local optimum, and the training time and convergence speed are significantly improved.

The residual network, a convolutional neural network proposed by four scholars from Microsoft Research, won the ImageNet Large Scale Visual Recognition Challenge (ILSVRC) in 2015 for image classification [20]. The residual network is characterized by its ease of optimization and its ability to improve accuracy by adding considerable depth. Its internal residual block uses jump connections to alleviate the gradient disappearance problem associated with increasing depth in deep neural networks and has been used with good results in practical applications. As shown in Tables 1 and 2, it directly skips one or more layers, thus introducing the data output of the previous layers to the input part of the later data layers.

The emergence of deep residual network structure effectively solves the degradation problem in deep learning because the residual network learns the residual function $f(x) = H(x) - x$ rather than $H(x)$. Although the two forms of objective functions can approximate the required function in principle, the difficulty of learning is not the same. In fact, after a lot of practical verification, the deep residual network has higher accuracy than other networks, such as VGGNet and GoogleNet.

4.4. Heart Failure Diagnosis Based on Deep Residual Network. As described above, the continuous heart rate signal itself is a time series signal, which has both spatial information and temporal information. Therefore, based on the deep residual network, we introduce long short-term memory (LSTM) units to extract the features of time series more effectively. As shown in Figure 5, the prototype of long-term and short-term memory units is a recurrent neural network (RNN). It improves the processing of time information of long-term time series by adding an input gate, memory gate, and

forgetting gate. LSTM network is very suitable for classification, processing, and prediction tasks based on time series data and has been successfully applied in the fields of tourism time prediction and music generation. As shown in Figure 6, in this study, we use the LSTM network to replace the convolution network between residual blocks. We choose adaptive moment estimation (Adam) as the optimizer, and its parameter is set to the learning rate of 0.001, $\beta 1 = 0.9$, and $\beta 2 = 0.999$. Figure 7 is our deep learning model architecture based on LSTM.

5. Experimental Results and Analysis

5.1. Evaluating Indicator. In this study, we used accuracy, sensitivity, and specificity as validation indicators. The specific definitions are as follows:

$$Se = \frac{TP}{TP + FN} \text{specificity},$$

$$Sp = \frac{TN}{TN + FP} \text{accuracy}, \qquad (6)$$

$$Acc = \frac{TN + FP}{TP + FN + TN + FP}.$$

It should be noted that in medical diagnosis, sensitivity refers to the ability of the algorithm to correctly detect patients with a certain disease, while specificity refers to the ability of the algorithm to correctly identify people without a disease.

5.2. Experimental Result. In practical clinical application, whether a model is mature and effective mainly depends on whether it can make accurate and reliable detection when facing patients. Therefore, in this study, we use the unbiased test to evaluate the effectiveness of the algorithm. Table 3 shows the performance of this method on the unbiased test set.

Compared with the traditional heart failure recognition algorithm, the heart failure recognition algorithm based on deep learning can extract reliable features in high-dimensional space without manual operation and avoid possible human errors. Deep learning system finds the distributed feature representation of data by combining low-level features, so as to form a more abstract feature representation.

Figure 8 shows that after heart failure and cure, this method has two advantages. First, heart failure is detected based on the residual neural network. The decision system based on this method can automatically obtain useful information from all data, rather than manual data dimensionality reduction through feature extraction. This can preserve the useful information of the data to the greatest extent and avoid potential errors; Secondly, we modify the network architecture based on the LSTM network unit to make the model more suitable for the classification of time series signals. However, this study also has some limitations. Firstly, this study did not carry out multiclassification identification of heart failure with different severity and did not deeply discuss the effect of heart failure drugs on the
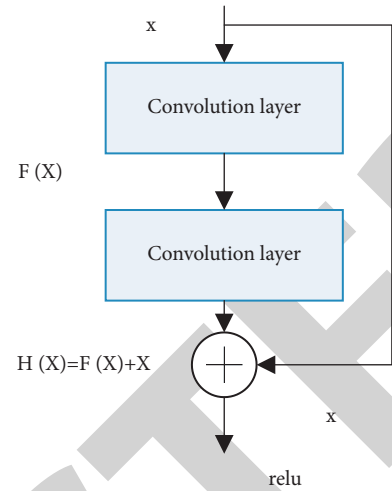
Figure 5: Schematic diagram of the residual building block.

continuous heart rate of subjects in the database. Secondly, this method needs big data to train the model to obtain the best performance, and the calculation consumption of the modified network model based on LSTM in the training stage is low.

6. Case Analysis

6.1. General Information. A total of 60 elderly patients with severe heart failure treated in the emergency department of our hospital from August 2019 to August 2021 were selected as the sample objects of this study. The selected patients were randomly divided into 30 patients in the control group who received only ordinary treatment and 30 patients in the observation group who received combined treatment. There were 19 male patients and 11 female patients in the control group, aged 49–71 years, with an average age of (61.3 ± 7.1) years. There were 17 male patients and 13 female patients in the observation group, aged 48–80 years, with an average age of (62.1 ± 6.9) years.

6.2. Observation Index. The treatment efficiency of the two groups was compared and analyzed. The higher the score, the higher the patient's score, and the better the quality of life.

7. Results

It can be seen from Table 4 that compared with the control group only receiving routine treatment, the curative effect of the observation group receiving combined treatment intervention is better, which is statistically significant $(P < 0.05)$.

It can be seen from Table 5 that the prognosis and quality of life of patients in the observation group treated with combination therapy are significantly better than those in the control group treated only with routine therapy, and the difference between the two groups is statistically significant $(P < 0.05)$.
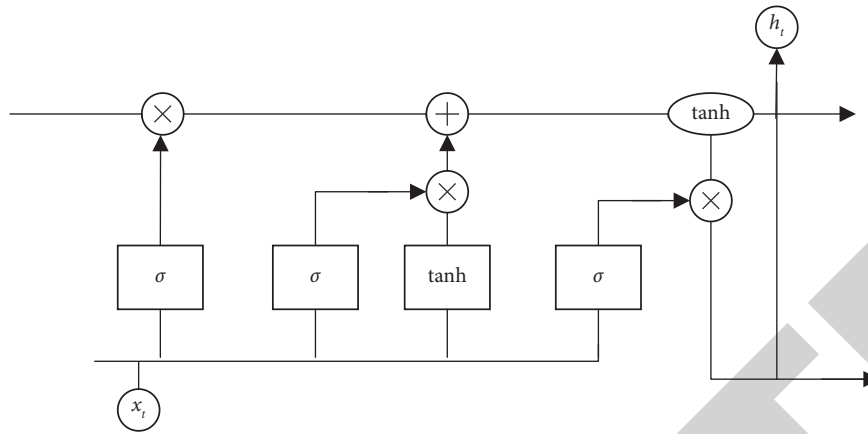
FIGURE 6: LSTM cell structure.
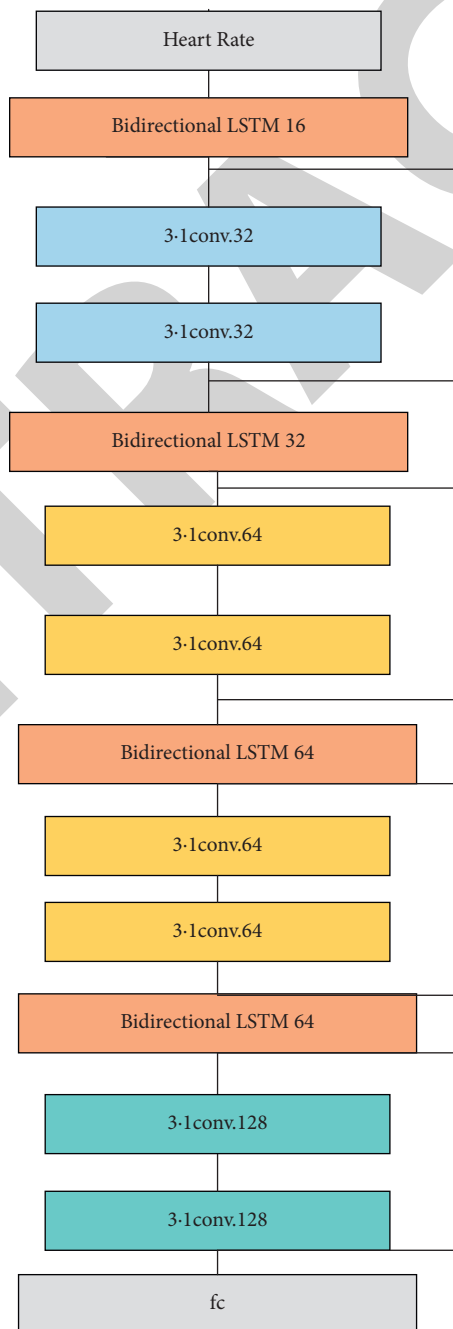
FIGURE 7: Deep network architecture.

TABLE 3: Performance on unbiased test sets.

Signal length	Accuracy (%)	Sensitivity (%)	Specificity (%)
500	99.67	99.34	100
1000	98.84	97.53	100
2000	96.63	100	93.64
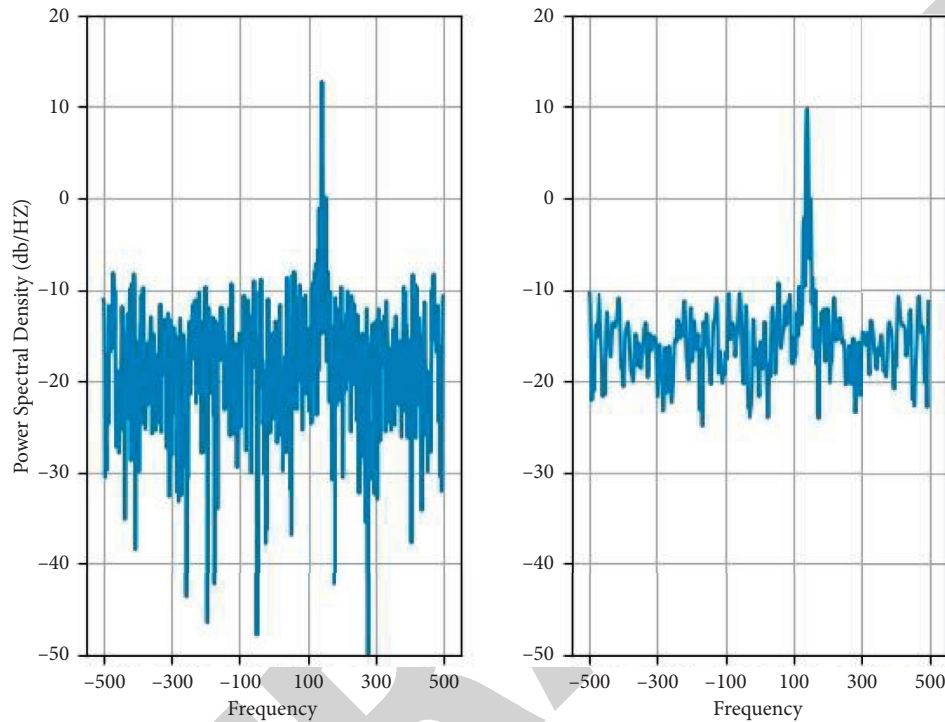
FIGURE 8: Heart failure and post cure.

TABLE 4: Comparison of treatment effectiveness between the two groups.

Group	Number of cases	Remarkable effect	Effective	Invalid	Effective rate (%)
Control group	30	16	4	10	20 (66.67)
Observation group	30	26	4	1	29 (96.67)
x^2	-	-	-	-	9.017
P	-	-	-	-	0.003

TABLE 5: Comparison of quality of life scores between the two groups.

Group	Number of cases	Physiological function	Psychological function	Social function	Total score
Control group	30	48.62 ± 8.32	60.41 ± 11.71	61.64 ± 9.32	58.75 ± 6.32
Observation group	30	60.69 ± 8.19	75.36 ± 10.57	76.95 ± 9.53	68.33 ± 8.58
T	-	5.663	5.191	6.291	4.924
P	-	0.000	0.000	0.000	0.000

8. Discussion

The main cause of severe heart failure is the myocardial strain caused by the patient's cardiomyopathy, myocardial infarction, and other hemodynamics with a large load, which changes the structural properties of the patient's myocardial function, and finally leads to the change of a cardiac function. Patients often show dyspnea and fatigue in the clinic, which not only reduces the quality of life of patients but also poses a threat to their life, health, and safety of

patients. Therefore, timely and effective treatment for patients with severe heart failure is of positive significance to ensure the life safety of patients. During routine treatment, as β Metoprolol, a receptor blocker, can reduce blood pressure and control the patient's heart rate [21], which can effectively control the catecholamines secreted in the patient's body and slow down the myocardial damage, but it can not effectively improve the level of LVEF and fundamentally treat the heart problems of patients with heart failure. The addition of irbesartan hydrochlorothiazide on

the basis of ordinary treatment can greatly improve the therapeutic effect. Irbesartan hydrochlorothiazide is an angiotensin II receptor inhibitor, which can effectively inhibit the activity of angiotensin, so as to reduce the incidence of hypokalemia and improve the actual treatment effect. Combined with the survey and research results, the treatment effective rate of the observation group was 96.67%, while that of the control group was 66.67%, and the quality of life score of the observation group was significantly higher than that of the control group ($P < 0.05$).

To sum up, in the treatment of elderly patients with severe heart failure, metoprolol combined with erbesar is more effective, can effectively improve the clinical symptoms and improve the quality of life of patients, and is worthy of popularization and application.

9. Conclusions

The proposed method is evaluated based on three open-source databases and four input data of different lengths. The results show that the accuracy of this method reaches 99.67%, 98.84%, and 96.63%, respectively, when the length is 500, 1000, and 2000. Heart failure detection using continuous heart rate is very important for medical and healthcare applications, especially for wearable devices such as smartwatches and bracelets. In the next step, we will deploy this model to healthcare applications as an auxiliary means for daily monitoring of patients with heart failure and try to add an attention mechanism to further improve the accuracy.

Data Availability

The experimental data used to support the findings of this study are available from the corresponding author upon request.

Conflicts of Interest

The authors declare that they have no conflicts of interest regarding this work.

References

[1] G. Y. Yeh, E. P. Mccarthy, P. M. Wayne et al., *Archives of Internal Medicine*, vol. 171, no. 8, pp. 750–757, 2011.

[2] V. Agrawal, B. Rai, J. Fellows, and P. A. McCullough, "In-hospital outcomes with thrombolytic therapy in patients with renal dysfunction presenting with acute ischaemic stroke," *Nephrology Dialysis Transplantation*, vol. 25, no. 4, pp. 1150–1157, 2010.

[3] A. D. M. Soeiro, A. D. Ruppert, M. Canzian, V. L. Capelozzi, and J. C. V. Serrano, "Postmortem diagnosis of acute myocardial infarction in patients with acute respiratory failure: demographics, etiologic and pulmonary histologic analysis," *Clinics*, vol. 67, no. 3, 2012.

[4] O. Bajenaru, F. Antochi, R. Balasa et al., "VTE-NEURO study group. Assessment of venous thromboembolism prophylaxis in neurological patients with restricted mobility - VTE-NEURO study," *Maedica*, vol. 9, no. 1, pp. 6–14, 2014.

[5] M. A. Oyama, J. E. Rush, E. A. Rozanski et al., "Assessment of serum N-terminal pro-B-type natriuretic peptide concentration for differentiation of congestive heart failure from primary respiratory tract disease as the cause of respiratory signs in dogs," *Journal of the American Veterinary Medical Association*, vol. 235, no. 11, pp. 1319–1325, 2009.

[6] A. Fuhlbrigge, D. Peden, A. J. Apter et al., "Asthma outcomes: e," *The Journal of Allergy and Clinical Immunology*, vol. 129, no. 3, pp. S34–S48, 2012.

[7] A. S. Dincq, S. Lessire, J. Douxfils, J. M. Dogne, M. Gourdin, and F Mullier, "Management of non-vitamin K antagonist oral anticoagulants in the perioperative setting," *BioMed Research International*, vol. 2014, p. 1, Article ID 385014, 2014.

[8] A. Misra, K. Maybury, and T. A. Eltigani, "Late erythema after photodynamic therapy to the face," *Plastic and Reconstructive Surgery*, vol. 117, no. 7, pp. 2522-2523, 2006.

[9] V. K. Puppala, O. Dickinson, and D. G. Benditt, "Syncope: classification and risk stratification," *Journal of Cardiology*, vol. 63, no. 3, pp. 171–177, 2014.

[10] A. Branthomme, R. Benamouzig, B. Bejou, T. Coste, J. Rautureau, and B. Huet, "Inappropriateness of hospital days and causes of failure in a Gastroenterology and Internal Medicine ward," *Gastroenterologie Clinique et Biologique*, vol. 26, no. 1, pp. 29–37, 2002.

[11] E. Andrès, S. Talha, M. Hajjam, J. Hajjam, S. Erve, and A. Hajjam, "Experimentation of 2.0 telemedicine in elderly patients with chronic heart failure: a study prospective in 175 patients," *European Journal of Internal Medicine*, vol. 51, pp. e11–e12, 2018.

[12] L. Tait, A. K. Roalfe, J. Mant et al., "The REFER (REFer for EchocaRdiogram) protocol: a prospective validation of a clinical decision rule, NT-proBNP, or their combination, in the diagnosis of heart failure in primary care. Rationale and design," *BMC Cardiovascular Disorders*, vol. 12, no. 1, p. 97, 2012.

[13] D. Iacob, A. Butnariu, D. C. Leucuta, G. Samasca, D. Deleanu, and I. Lupan, "Evaluation of NT-proBNP in children with heart failure younger than 3 years old," *Romanian Journal of Internal Medicine*, vol. 55, no. 2, pp. 69–74, 2017.

[14] E. Lambrinou, F. Kalogirou, D. Lamnisos, and P. Sourtzi, "Effectiveness of heart failure management programmes with nurse-led discharge planning in reducing re-admissions: a systematic review and meta-analysis," *International Journal of Nursing Studies*, vol. 49, no. 5, pp. 610–624, 2012.

[15] K. M. Stanek, J. Gunstad, R. H. Paul et al., "Longitudinal cognitive performance in older adults with cardiovascular disease: evidence for improvement in heart failure," *Journal of Cardiovascular Nursing*, vol. 24, no. 3, pp. 192–197, 2009.

[16] M. K. Kim, B. Kim, J. Y. Lee et al., "Tissue Doppler-derived E/e' ratio as a parameter for assessing diastolic heart failure and as a predictor of mortality in patients with chronic kidney disease," *The Korean Journal of Internal Medicine*, vol. 28, no. 1, pp. 35–44, 2013.

[17] H. Li, D. Zeng, L. Chen, Q. Chen, M. Wang, and C. Zhang, "Immune multipath reliable transmission with fault tolerance in wireless sensor networks," in *Proceedings of the International Conference on Bio-Inspired Computing: Theories and Applications*, pp. 513–517, Springer, Singapore, January 2016.

[18] I. Chung, A. Choudhury, J. Patel, and G. Y. H. Lip, "Soluble CD40L, platelet surface CD40L and total platelet CD40L in congestive heart failure: relationship to platelet volume, mass and granularity," *Journal of Internal Medicine*, vol. 263, no. 3, pp. 313–321, 2008.

Retraction

Retracted: Impact of Diabetic Nephropathy on Pulmonary Function and Clinical Outcomes

Computational Intelligence and Neuroscience

This article has been retracted by Hindawi following an investigation undertaken by the publisher [1]. This investigation has uncovered evidence of one or more of the following indicators of systematic manipulation of the publication process:

(1) Discrepancies in scope

(2) Discrepancies in the description of the research reported

(3) Discrepancies between the availability of data and the research described

(4) Inappropriate citations

(5) Incoherent, meaningless and/or irrelevant content included in the article

(6) Peer-review manipulation

The presence of these indicators undermines our confidence in the integrity of the article's content and we cannot, therefore, vouch for its reliability. Please note that this notice is intended solely to alert readers that the content of this article is unreliable. We have not investigated whether authors were aware of or involved in the systematic manipulation of the publication process.

Wiley and Hindawi regrets that the usual quality checks did not identify these issues before publication and have since put additional measures in place to safeguard research integrity.

We wish to credit our own Research Integrity and Research Publishing teams and anonymous and named external researchers and research integrity experts for contributing to this investigation.

The corresponding author, as the representative of all authors, has been given the opportunity to register their agreement or disagreement to this retraction. We have kept a record of any response received.

References

[1] C. Niu, L. Liu, Y. Li, and X. Li, "Impact of Diabetic Nephropathy on Pulmonary Function and Clinical Outcomes," *Computational Intelligence and Neuroscience*, vol. 2022, Article ID 8164034, 11 pages, 2022.

Research Article

Impact of Diabetic Nephropathy on Pulmonary Function and Clinical Outcomes

Chunbo Niu,[1] **Lu Liu,**[1] **Yang Li,**[2] **and Xiaoqi Li** ®[2]

[1]*First School of Clinical Medical to Gansu University of Chinese Medicine, Lanzhou 730000, China*
[2]*Department of Respiration and Critical Medicine in Cadre Ward, Gansu Provincial Hospital, Lanzhou 730000, China*

Correspondence should be addressed to Xiaoqi Li; lixiaoqi@gszy.edu.cn

Objective. The main objective is to study the effect of diabetic nephropathy on pulmonary function and clinical outcomes. *Methods*. The method is to retrospectively analyze patients with diabetic nephropathy (DN) in our hospital from April 2018 to March 2022 as study subjects. The differences in baseline data, serum indicators, renal function indicators, and pulmonary function of patients at different clinical stages were analyzed and then explored. Finally, logistic regression was used to analyze the risk factors affecting patients' clinical outcomes and to evaluate the diagnostic effects. *Results*. Baseline information (age, disease duration, BMI, and systolic and diastolic blood pressure), serum indicators (HbA1c, FBG, 2hPG, TG, TC, and LDLC), renal function indicators (CysC, BUN, and Scr), and pulmonary function (TLC, VC, FEV1, FEV1/FVC, MVV, MEF25, MEF50 MEF75, DLCO, and DLCO/VA) were significantly different ($P < 0.01$); multiple logistic regression analysis showed that SBP, HbA1c, FBG, 2hPG, BUN, Scr, TLC, VC, FEV1/FVC, MVV, DLCO, and DLCO/VA were all key factors in the development of clinical outcomes in DN ($P < 0.05$). ROC analysis showed that all of these important factors had an AUC greater than 0.75 for the diagnosis of DN with high sensitivity and specificity. *Conclusion*. Serum and renal function indices of DN patients gradually increased with stage, accompanied by a decrease in pulmonary ventilation, and diffusion function; SBP, HbA1c, FBG, 2hPG, BUN, Scr, TLC, VC, FEV1/FVC, MVV, DLCO, and DLCO/VA were all key factors affecting the clinical outcome of DN; controlling blood glucose, lipids, improving pulmonary ventilation, and diffusion function can better prevent the occurrence and worsening of DN.

1. Introduction

Diabetic nephropathy (DN) is a diabetic (DM) lesion involving the kidneys, and approximately 40% of patients develop this microvascular complication, greatly increasing morbidity and mortality in DM patients [1]. DN is a progressive disease with a decades-long course that is irreversible once patients enter the clinical proteinuria phase, eventually leading to end-stage renal disease [2]. In clinical practice, the proportion of patients with end-stage renal disease has increased rapidly in the last decade [3, 4]. Currently, the diagnosis of DN is based on persistent high proteinuria and decreased glomerular filtration rate (GFR) [5, 6]. Given the complex pathogenesis of DN, there is no curative therapy, and most patients require

renal replacement therapy [7]. Diabetic nephropathy is one of the most common microvascular complications, and the lung is a relatively microvascular and collagen-rich organ and therefore vulnerable to diabetic microangiopathy and histone nonglycosylation [2, 8]. Alterations in microvascular ultrastructure regulate the thickening of the alveolar capillary endothelial cell matrix, which in turn affects pulmonary ventilation and pulmonary diffusion function [9]. Therefore, assessing pulmonary function in patients with DN can lead to better prevention and treatment.

DN is a complex disease influenced by several factors, including susceptibility factors (age, gender, race and family history, smoking and alcohol consumption, etc.), primary factors (hyperglycemia, dyslipidemia), and secondary factors

(hypertension, obesity, etc.) [10, 11]. There was a nonlinear and significant correlation between HbA1c levels as an indicator of glycemic control and susceptibility to microvascular complications in DM [12]. Therefore, exploring key factors for the development of DN would be beneficial for designing better DN prevention and treatment programs.

Based on this, this study used statistical analysis to investigate the impact of diabetic nephropathy on pulmonary function and clinical outcomes and to screen the main influencing factors of clinical outcomes, aiming to provide a laboratory basis for early diagnosis as well as prevention and treatment of the disease. The study is reported as follows.

2. Materials and Methods

2.1. Research Objects. A total of 183 children diagnosed with DN in the hospital from April 2018 to March 2022 were recruited as research objects. DM was diagnosed with a random blood glucose (2hPG) ≥ 11.0 mmol/L, fasting blood glucose (FBG) ≥ 7.0 mmol/L, and 2-hour blood glucose (2hPG) ≥ 11.0 mmol/L. DN was defined as more than 2 urinary albumin excretion rates (AER) greater than 20 μg/min and exclusion of ketoacidosis, exercise, urinary tract infections, and other renal diseases.

DN staging criteria (Mogensen staging) were as follows: Stage III: microalbuminuria (early diabetic nephropathy), patients with approximately normal GFR and irreversible renal disease. Stage IV: massive proteinuria, urinary protein >0.5 g/d, late GFR down to 20. Stage V: renal failure, GFR <20, extensive glomerulosclerosis, and rapid deterioration of renal function until renal failure occurs.

Inclusion criteria were as follows: all patients met the diagnostic criteria for DN, aged 18–80 years old, and who had completed all index examinations and complete clinical data upon admission. Patients who had been treated with glucose-lowering, antihypertensive, and lipid-lowering drugs within the last month, patients with kidney damage such as urinary tract infections, nephritis, and renal vascular stenosis, and patients with combined cardiovascular and cerebrovascular diseases, tumours, and immune system diseases were excluded. The study was approved by the hospital ethics committee, and all patients signed an informed consent form.

2.2. Methods

2.2.1. Serum and Renal Function. Fasting blood samples from patients with DN were collected using EDTA anticoagulation tubes (fasting for at least 8 hours) and centrifuged for 15 minutes at room temperature. The serum was carefully separated and packed into centrifuge tubes and then stored in a refrigerator at 80 degrees. Serum AER, glycosylated hemoglobin (HbA1c), FBG, 22hPG, triglyceride (TG), total cholesterol (TC), and low density lipoprotein (LDLC) were detected by enzyme-linked immunosorbent assay (ELISA). At the same time, renal function indexes, cystatin C (CysC), urea nitrogen (BUN), and serum creatinine (Scr) were measured. In addition, the baseline data of patients with DN were collected, including age, gender,

course of the disease, smoking history, drinking history, BMI, systolic blood pressure (SBP), and diastolic blood pressure (DBP).

2.2.2. Detection of Pulmonary Function Index. A spirometer was used to measure the pulmonary function parameters of DN patients, total lung volume (TLC), lung volume (VC), exertional expiratory volume in 1 second (FEV1), exertional expiratory volume in 1 second rate (FEV1/FVC), maximum ventilation volume (MVV), maximum expiratory flow in 25% of lung volume (MEF50), 50% (MEF50), 75% (MEF75), exhaled gas 25%–75% mean flow rate of lung volume (MEF25-75), lung carbon monoxide dispersion (DLCO), and carbon monoxide dispersion per alveolar volume (DLCO/VA). The instrument was calibrated before use, and each item was repeated 3 times to obtain the maximum value of the desired curve. All tests were done at 8–10 points and performed by the same operator.

2.2.3. Statistical Processing. SPSS 22.0 software was used for statistical processing and analysis. The counting data from baseline data were expressed as percentages (n%), and χ^2 test was conducted. The measurement data such as different indicators were expressed as mean ± standard deviation ($\overline{x} \pm s$) using the t-test, with $P < 0.05$ indicating a statistically significant difference. GraphPad Prism 9 software was used to visualise the results of the statistical analysis. Multiple logistic regression was used to perform risk factor analysis for clinical outcomes in DN. ROC curves were used to analyze the predictive outcomes of the included indicators in DN clinical outcomes, with an AUC >0.75 indicating accurate results.m

3. Results

3.1. Baseline Data for DN Patients with Different Stages. Baseline data on age, gender, disease duration, smoking history, alcohol history, BMI, systolic blood pressure (SBP), and diastolic blood pressure (DBP) of DN patients are shown in Table 1 and Figure 1. 65 cases of stage III, 93 cases of stage IV, and 25 cases of stage V were obtained based on staging. Statistical analysis revealed significant differences in age, disease duration, BMI, and SBP between patients with stage IV and V DN compared to stage III, and DBP was also significantly different in patients with stage IV DN compared to stage III ($P < 0.05$). In addition, there were significant differences in SBP indicators between DN patients with stage IV and stage V. However, there were no significant differences in gender ($P = 0.44$), smoking ($P = 0.74$), and alcohol consumption ($P = 0.81$) among DN patients with stage IV. This suggests that age, disease duration, BMI, SBP, and DBP may influence the development of DN.

3.2. Serum and Renal Function Indicators in DN Patients with Different Stages. To further investigate the changes in indicators in different stages of DN, we mainly measured

TABLE 1: Comparison of baseline data for DN patients with different stages.

Grouping		III stage	IV stage	V stage	P value
N		65	93	25	—
Age		55.14 ± 4.84	63.10 ± 6.59	65.00 ± 3.27	<0.01[b]
Course of disease		10.60 ± 2.84	13.37 ± 2.87	13.80 ± 3.37	<0.01[b]
Gender	Male (n%)	36 (55%)	51 (55%)	14 (52%)	0.44[a]
	Female (n%)	19 (45%)	42 (45%)	11 (48%)	
Smoking	Yes	36 (55%)	55 (59%)	15 (60%)	0.74[a]
	No	19 (45%)	38 (41%)	10 (40%)	
Alcohol	Yes	46 (71%)	70 (75%)	18 (72%)	0.81[a]
	No	19 (29%)	23 (25%)	7 (28%)	
BMI (kg/m^2)		23.65 ± 1.02	24.23 ± 0.93	24.19 ± 1.10	<0.01[b]
Systolic blood pressure (mmHg)		140.00 ± 3.22	144.51 ± 5.41	152.44 ± 6.24	<0.01[b]
Diastolic blood pressure (mmHg)		80.00 ± 3.08	81.60 ± 3.88	83.44 ± 3.38	<0.01[b]

(a)

(b)
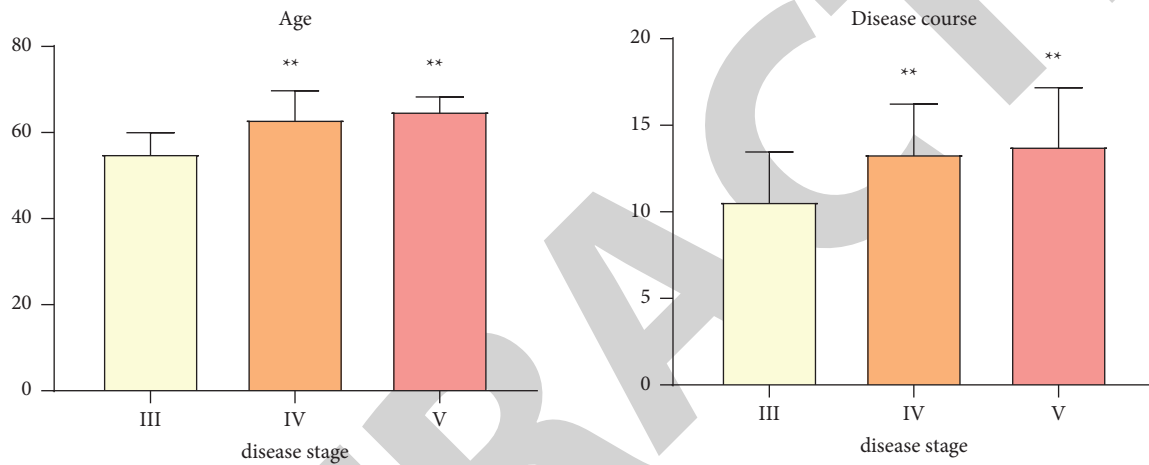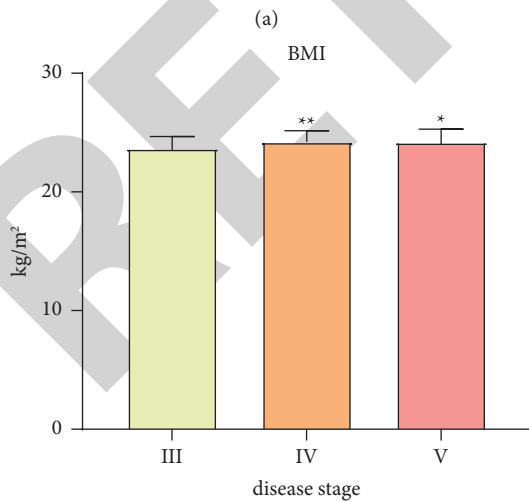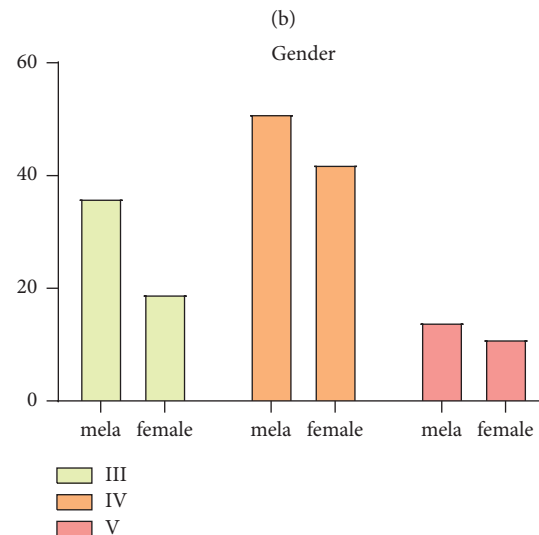
(c)

(d)

FIGURE 1: Continued.

(e)

(f)

(g)
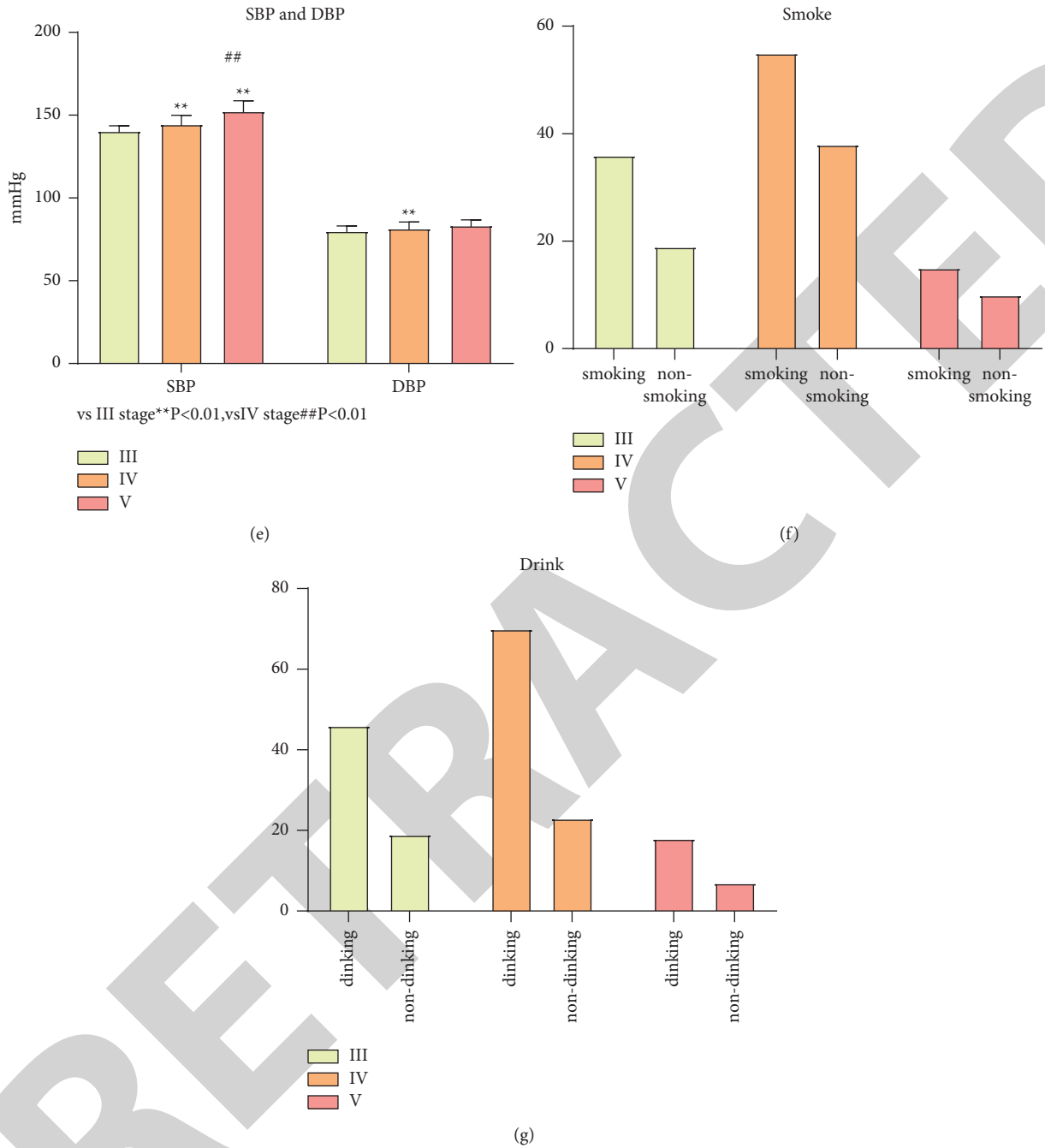
Figure 1: Comparison of baseline data for DN patients with different stages.

serum indicators (HbA1c, FBG, 2hPG, TG, TC, and LDLC) and renal function indicators (CysC, BUN, and Scr). As shown in Table 2 and Figure 2, the indicators of HbA1c, FBG, 2hPG, TG, TC, and LDLC were significantly higher in patients with stage IV and V DN than in patients with stage III ($P < 0.5$); the indicators of HbA1c, FBG, 2hPG, TG, TC, and LDLC were also significantly higher in patients with stage V DN than in patients with stage IV; similarly, the indicators of renal function CysC, BUN, and Scr also showed the same results. In conclusion, serum indicators HbA1c, FBG, 2hPG, TG, TC, and LDLC and renal function

indicators CysC, BUN, and Scr may be key markers for DN staging.

3.3. Pulmonary Function Indicators for DN Patients with Different Stages. To examine the cumulative lung profile of DN, we similarly tested pulmonary function indicators (TLC, VC, FEV1, FEV1/FVC, MVV, MEF25, MEF50, MEF75, MEF25-75, DLCO, and DLCO/VA) in patients with different stages of DN, and the results were shown in Table 3 and Figure 3. The statistical results showed that TLC, VC,

TABLE 2: Serum and renal function indicators in DN patients with different stages.

Group	Stage III	Stage IV	Stage V	P value
Glycosylated hemoglobin (mmol/L)	7.35 ± 0.08	8.65 ± 0.14	9.42 ± 0.12	<0.01[b]
Fasting blood glucose (mmol/L)	7.86 ± 0.63	8.86 ± 0.51	9.19 ± 0.57	<0.01[b]
2-hour blood glucose (mmol/L)	12.66 ± 0.23	13.67 ± 0.22	14.66 ± 0.30	<0.01[b]
Triglyceride (mmol/L)	2.59 ± 0.20	3.34 ± 0.16	3.61 ± 0.20	<0.01[b]
Total cholesterol (mmol/L)	4.56 ± 0.23	5.05 ± 0.27	5.44 ± 0.29	<0.01[b]
Low density lipoprotein (mmol/L)	2.60 ± 0.18	3.35 ± 0.29	4.20 ± 0.33	<0.01[b]
Cystatin C (mg/L)	1.85 ± 0.07	2.46 ± 0.17	3.38 ± 0.20	<0.01[b]
Urea nitrogen (mmol/L)	6.71 ± 0.57	8.69 ± 0.47	12.74 ± 0.56	<0.01[b]
Serum creatinine (μ mol/L)	88.91 ± 4.90	120.16 ± 5.11	136.20 ± 4.73	<0.01[b]

(a)

(b)

(c)

(d)
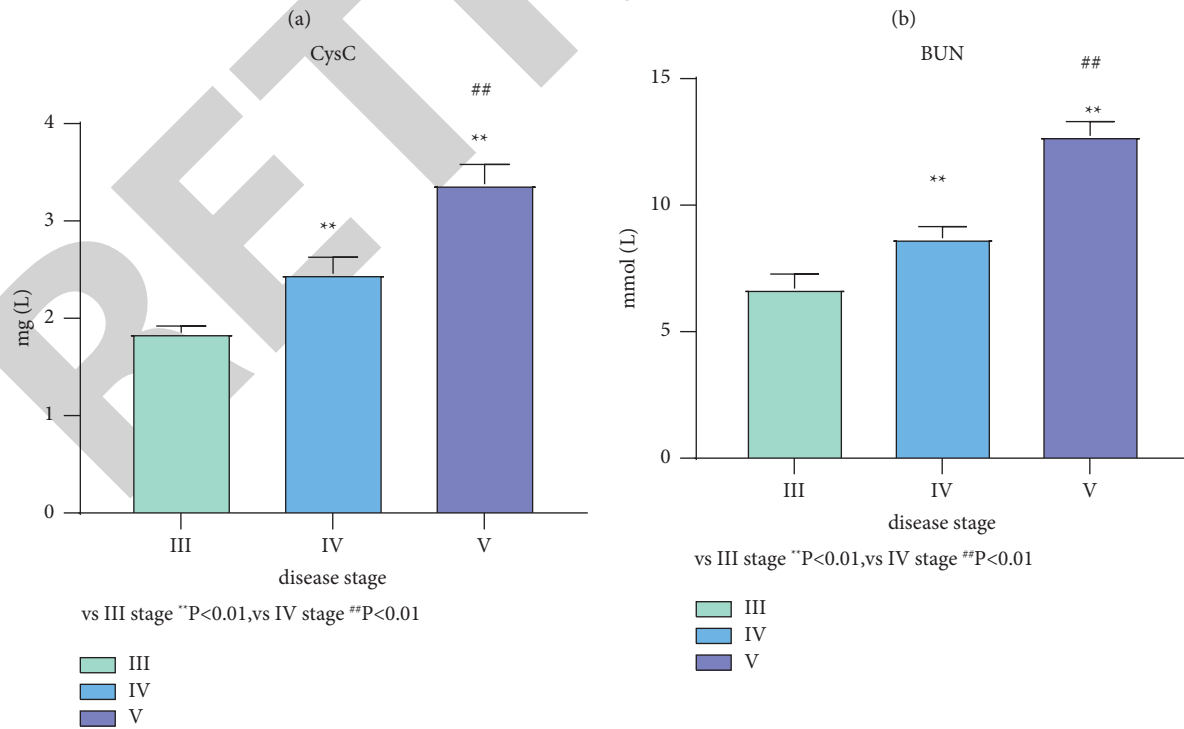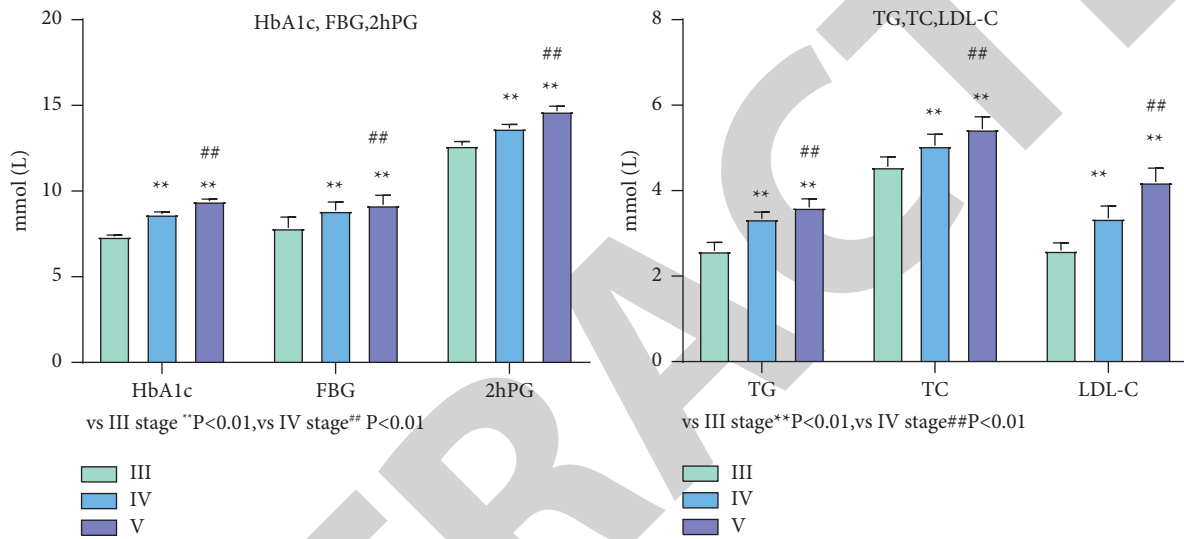
FIGURE 2: Continued.

(e)
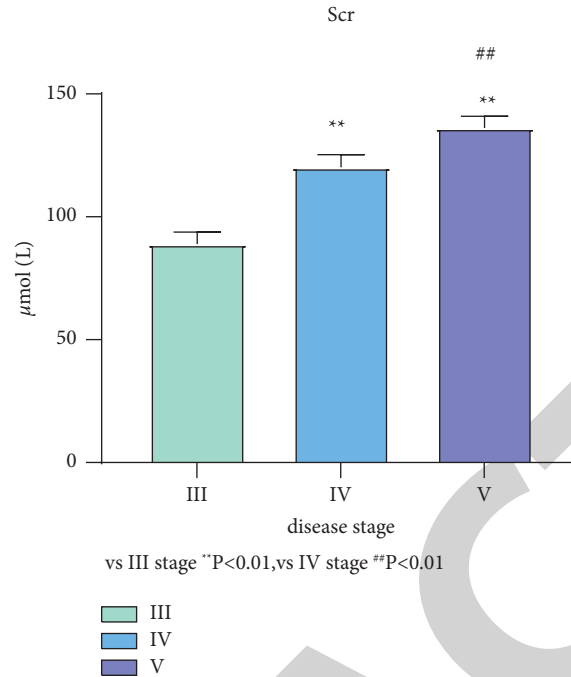
Figure 2: Serum and renal function indicators in DN patients with different stages.

FEV1, FEV1/FVC, MVV, MEF25, MEF50, MEF75, MEF25-75, DLCO, and DLCO/VA were significantly higher in DN patients with IV stage and V stage compared to those with III stage ($P < 0.01$), and each index was also significantly higher in DN patients with V stage compared to those with IV stage ($P < 0.01$). This suggests that the involvement of the lungs in DN correlates with the different stages of the disease and that the higher the stage, the more severe the impairment in lung ventilation and diffusion function.

3.4. Comparison of Indicators for DN Patients with Different Clinical Outcomes. To explore the influence of each index on the clinical outcome of patients with DN, the differences in baseline data (age, course of disease, gender, smoking history, drinking history, BMI, and systolic and diastolic blood pressure), serum indexes (HbA1c, FBG, 2hPG, TG, TC, and LDLC), renal function indexes (CysC, BUN, and Scr), and pulmonary function (TLC, VC, FEV1, FEV1/FVC, MVV, MEF25, MEF50, MEF75, MEF25-75, DLCO, and DLCO/VA) were also analyzed. As shown in Table 4, all indicators were significantly different ($P < 0.01$) for both occurring and nonoccurring clinical outcome events, except for gender ($P = 0.77$), with higher baseline profile levels, serum and renal function indicator levels for occurring outcome events, and lower for pulmonary function indicators. It is suggested that age, disease duration, history of smoking, history of alcohol consumption, BMI, systolic blood pressure, diastolic blood pressure, serum, renal function, and pulmonary function may be risk factors for clinical resolution in patients with DN.

3.5. Key Factors in Clinical Outcomes for DN Patients. To further screen for key factors predisposing to clinical outcomes, we used logistic regression to analyze the correlation between baseline data, serum indices, renal function indices, and pulmonary function and clinical outcomes. The results (Table 5 and Figure 4) showed that SBP [EXP(B) (95% CI) = 1.135 (1.014–1.270), $P = 0.028$], glycemic index HbA1c [(95% CI) = 1.755 (1.007–2.311), $P = 0.016$], FBG [EXP(B) (95% CI) = 2.082 (1.762–3.688), $P = 0.033$], and 2hPG [EXP(B) (95% CI) = 1.638 (1.293–2.547), $P = 0.038$] BUN [EXP(B) (95% CI) = 1.189 (1.049–3.455), $P = 0.025$], and ScrEXP(B) (95% CI) = 1.956 (1.157–3.065), $P = 0.041$] could significantly improve the incidence of clinical outcomes.

Translated withhttps://www.DeepL.com/Translator(free version), TLC[EXP(B) (95% CI) = 0.818 (0.716–0.935), $P = 0.003$], VC[EXP(B) (95% CI) = 0.873 (0.778–0.965), $P = 0.037$], FEV1/FVC [EXP(B) (95% CI) = 0.868 (0.713–0.957), $P = 0.016$], MVV[EXP(B) (95%CI) = 0.833 (0.794–0.969), $P = 0.049$], DLCO [EXP(B) (95%CI) = 0.901 (0.755–0.987), $P = 0.043$], and DLCO/VA [EXP(B) (95%CI) = 0.805 (0.625–0.938), $P = 0.044$]. It can significantly reduce the risk of clinical outcome events. To sum up, SBP, serum indexes (HbA1c, FBG, and 2hPG), renal function indexes (BUN and Scr), and pulmonary function (TLC, VC, FEV1/FVC, MVV, DLCO, and DLCO/VA) may be the key factors affecting the occurrence of clinical outcome in DN.

3.6. Predictive Assessment of Key Factors for Clinical Outcomes in DN Patients. To further assess the efficacy of key factors affecting clinical outcomes in DN, we plotted ROC curves

TABLE 3: Pulmonary function indicators.

Group	III stage	IV stage	V stage	P Value
Total lung volume	102.90 ± 3.74	95.40 ± 4.55	87.24 ± 5.47	<0.01[b]
Vital capacity	101.40 ± 2.26	94.34 ± 1.76	77.13 ± 3.68	<0.01[b]
FEV1	97.13 ± 1.42	89.61 ± 2.01	76.74 ± 2.94	<0.01[b]
Forced expiratory volume 1 second rate	99.14 ± 1.93	91.25 ± 3.02	85.64 ± 2.03	<0.01[b]
MVC	98.46 ± 2.04	90.99 ± 1.34	86.83 ± 1.53	<0.01[b]
25% MMEF	98.66 ± 1.92	90.51 ± 3.13	86.42 ± 3.08	<0.01[b]
50% MMEF	96.56 ± 1.95	91.70 ± 1.91	85.21 ± 1.04	<0.01[b]
75% MMEF.	94.47 ± 1.68	89.61 ± 1.97	84.32 ± 1.85	<0.01[b]
Exhaled gas average flow of 25%–75% lung volume	95.48 ± 1.79	90.91 ± 2.04	86.17 ± 1.19	<0.01[b]
Carbon monoxide diffusion capacity	95.64 ± 2.70	87.59 ± 1.39	75.54 ± 2.54	<0.01[b]
DLCO per unit alveolar volume	94.11 ± 1.62	86.69 ± 2.10	82.30 ± 2.85	<0.01[b]

vs III stage **P<0.01,vs IV stage ##P<0.01

III
IV
V

(a)

vs III stage **P<0.01,vs IV stage ##P<0.01

III
IV
V

(b)

vs III stage **P<0.01, vs IV stage ##P<0.01

III
IV
V

(c)
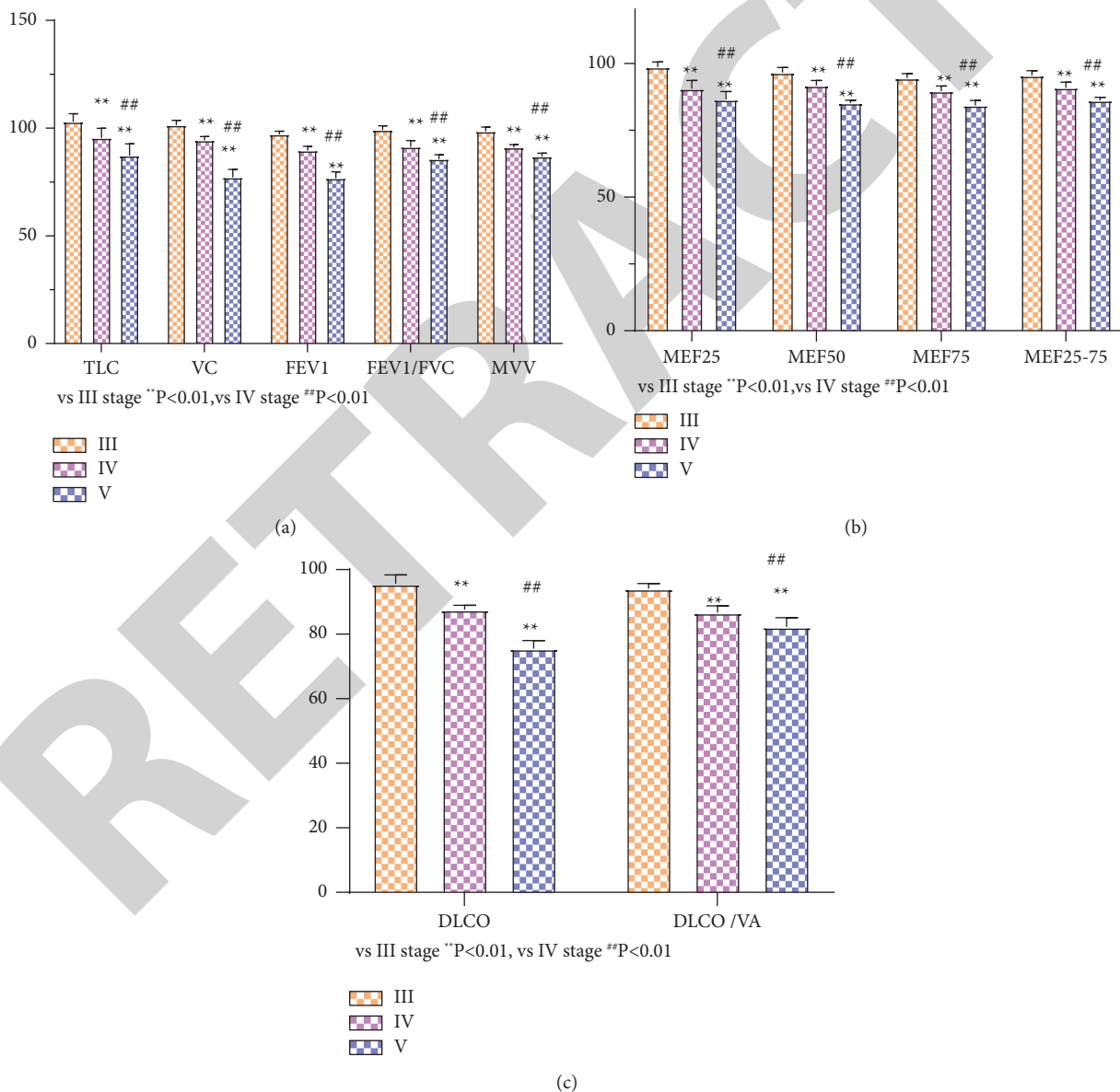
FIGURE 3: Pulmonary function indicators for patients with different stages of DN.

TABLE 4: Comparison of pathological data of patients with different clinical outcomes.

Group	No ending event	Ending event	Statistical data	P value
Age	59.30 ± 5.95	67.10 ± 7.24	6.33	<0.01[b]
Course of disease	11.80 ± 2.91	15.90 ± 3.04	7.01	<0.01[b]
Gender (male)	84 (59%)	17 (57%)	0.29	0.77[a]
Smoking history	79 (53%)	27 (90%)	5.80	<0.01[a]
History of drinking	106 (69%)	28 (93%)	4.33	<0.01[a]
BMI	23.70 ± 0.86	25.40 ± 0.61	10.32	<0.01[b]
SBP	143.00 ± 5.36	150.00 ± 6.08	6.40	<0.01[b]
DBP	80.30 ± 3.12	86.60 ± 1.67	10.75	<0.01[b]
HbA1c	8.22 ± 0.74	8.68 ± 0.75	3.106	<0.01[b]
FBG	8.39 ± 0.71	9.38 ± 0.42	7.38	<0.01[b]
2hPG	13.30 ± 0.60	13.9 ± 0.61	4.99	<0.01[b]
TG	3.05 ± 0.42	3.47 ± 0.34	5.15	<0.01[b]
TC	4.84 ± 0.35	5.38 ± 0.32	7.83	<0.01[b]
LDLC	3.10 ± 0.53	3.71 ± 0.61	5.62	<0.01[b]
CysC	2.30 ± 0.46	2.74 ± 0.60	4.54	<0.01[b]
BUN	8.25 ± 1.80	10.00 ± 2.18	4.70	<0.01[b]
Scr	109.00 ± 17.50	123.00 ± 16.70	4.04	<0.01[b]
TLC	98.40 ± 5.93	89.40 ± 5.87	7.61	<0.01[b]
VC	95.70 ± 7.09	88.40 ± 9.55	4.85	<0.01[b]
FEV1	91.50 ± 6.04	85.50 ± 8.08	4.69	<0.01[b]
FEV1/FVC	93.70 ± 4.39	89.60 ± 5.26	4.52	<0.01[b]
MVV	93.70 ± 4.86	89.70 ± 3.72	4.27	<0.01[b]
MEF25	93.20 ± 3.87	88.30 ± 5.08	6.00	<0.01[b]
MEF50	91.30 ± 3.53	89.00 ± 3.43	3.28	<0.01[b]
MEF75	93.20 ± 3.87	87.01 ± 3.27	8.20	<0.01[b]
MEF25-75	92.60 ± 3.31	88.30 ± 2.84	6.65	<0.01[b]
DLCO	89.80 ± 6.23	84.10 ± 7.27	4.46	<0.01[b]
DLCO/VA	89.50 ± 4.33	84.60 ± 4.55	5.62	<0.01[b]

for each factor versus clinical outcomes. The analysis results (Table 6 and Figure 5) showed that SBP [AUC (95%CI) = 0.80 (0.72–0.88)], HbA1c [AUC (95%CI) = 0.76 (0.67–0.86)], FBG [AUC (95%CI) = 0.90 (0.85–0.95)], 2hPG [AUC (95%CI) = 0.80 (0.71–0.89)], BUN [AUC (95%CI) = 0.79 (0.70–0.88)], Scr [AUC (95%CI) = 0.78 (0.69–0.87)], TLC [AUC (95%CI) = 0.86 (0.79–0.93)], VC[AUC (95% CI) = 0.78 (0.69–0.87)], FEV1/FVC [AUC (95%CI) = 0.75 (0.65–0.83)], MVV [AUC (95%CI) = 0.79 (0.70–0.88)], DLCO [AUC (95%CI) = 0.77 (0.67–0.86)], and DLCO/VA [AUC (95%CI) = 0.80 (0.70–0.89)] had high sensitivity and specificity, which can accurately predict the occurrence of clinical outcomes in DN.

4. Discussion

Abnormalities in blood glucose, blood pressure, and renal function affect the development and progression of DN [13]. Hyperglycemia is the initiator and facilitator of DN [14]. The literature [15] found that enhanced glycemic control (HbA1 ≤ 6.5%) significantly reduced proteinuria, decreased the deterioration of renal function, and reduced the risk of end-stage renal disease (ESRD). The literature [16] found that hyperglycemia promotes apoptosis and induces loss of MCs function, that is, low baseline renal function and rapid decline in renal function, and hypertension is likewise a risk factor for the development of DN. Stimulation of the renin–angiotensin–aldosterone system, volume expansion due to increased renal sodium reabsorption, and reduction

of vasoactive substances have been implicated [17]. The literature [18] found that DM rats had a significantly increased urinary albumin to creatinine ratio, enlarged glomeruli, and decreased levels of transforming growth factor-β and type IV collagen, with oxidative stress and inflammation. In addition, stage I obesity 1.36 (95% CI 1.10–1.67), stage II obesity 1.43 (95% CI 1.16 CI 1.78), and stage III obesity 1.32 (95% CI 1.05 color 1.66) significantly increased the risk of DN compared to normal BMI. The literature [19] found that cystatin C, a 13 kDa cysteine protease inhibitor, could be used as a biomarker for reduced GFR and early DN. This study also found that age, disease duration, BMI, systolic and diastolic blood pressure, serum markers (HbA1c, FBG, 2hPG, TG, TC, and LDLC), and renal function markers (CysC, BUN, and Scr) increased significantly with increasing clinical stage in patients with DN. Meanwhile, elevated levels of SBP, HbA1c, FBG, 2hPG, BUN, and Scr were significantly and positively correlated with the clinical outcome of DN, which may be a key factor affecting the clinical outcome of DN.

Abnormalities in pulmonary ventilation and diffusion function are associated with the development of DN [20]. DN poses a significant impairment of the pulmonary function indicators FEV1 and FVC, and this impairment is significantly associated with an increased rate of abnormal proteinuria (urinary protein/urinary creatinine ratio) [21]. The literature [22, 23] found that DLCO can be used as a predictor of pulmonary microangiopathy and that somatic variation in DLCO is a useful noninvasive test for

TABLE 5: Analysis of key factors for clinical outcomes of DN.

Variables	B	S.E	Wals	df	Sig.	Exp (B)	95% CI of EXP(B)	
							Lower limit	Upper limit
Age	0.045	0.051	0.787	1	0.375	1.046	0.947	1.155
Course of disease	0.088	0.087	1.026	1	0.311	1.092	0.921	1.295
BMI	0.247	0.283	0.757	1	0.384	1.280	0.734	2.230
Gender	0.295	0.552	0.285	1	0.594	1.342	0.455	3.961
Smoking	−0.184	0.548	0.113	1	0.737	1.202	0.411	3.517
Alcohol	−0.519	0.592	0.767	1	0.381	0.595	0.186	1.901
SBP	0.126	0.057	4.842	1	0.028	1.135	1.014	1.270
DBP	0.031	0.073	0.177	1	0.674	1.031	0.893	1.191
HbA1c	0.128	0.039	5.914	1	0.016	1.755	1.007	2.311
FBG	0.033	0.053	7.046	1	0.033	2.082	1.762	3.688
2hPG	0.187	0.029	8.764	1	0.038	1.683	1.293	2.547
TG	0.239	1.557	0.024	1	0.878	1.270	0.060	26.865
TC	0.867	0.960	0.815	1	0.367	2.379	0.362	15.622
LDLC	0.095	1.022	0.009	1	0.926	0.909	0.123	6.742
CysC	0.592	1.683	0.124	1	0.725	0.553	0.020	14.984
BUN	0.073	0.044	6.101	1	0.025	1.189	1.049	3.455
Scr	0.045	0.055	8.667	1	0.041	1.956	1.157	3.065
TLC	−0.200	0.068	8.655	1	0.003	0.818	0.716	0.935
VC	−0.228	0.014	6.059	1	0.037	0.873	0.778	0.965
FEV1	−0.095	0.126	0.574	1	0.449	0.909	0.710	1.163
FEV1/FVC	−0.242	0.073	4.988	1	0.016	0.868	0.713	0.957
MVV	−0.225	0.082	4.474	1	0.049	0.833	0.794	0.969
MEF25	−0.121	0.097	1.578	1	0.209	0.886	0.733	1.070
MEF50	0.108	0.160	0.454	1	0.501	1.114	0.814	1.523
MEF75	−0.009	0.150	0.003	1	0.955	0.991	0.738	1.331
MEF25-75	−0.144	0.143	1.019	1	0.313	1.155	0.873	1.527
DLCO	−0.301	0.084	4.578	1	0.043	0.901	0.755	0.987
DLCO/VA	−0.217	0.090	4.803	1	0.044	0.805	0.625	0.938

	Pvalue	Exp (B)	
SBP	0.028	1.135 (1.014- 1.270)	
HbA1c	0.016	1.755 (1.007- 2.311)	
FBG	0.033	2.082 (1.762- 3.688)	
2hPG	0.038	2.683 (1.293- 2.547)	
BUN	0.025	1.189 (1.049- 3.455)	
Scr	0.041	1.956 (1.157- 3.065)	
TLC	0.003	0.818 (0.716- 0.935)	
VC	0.037	0.873 (0.778- 0.965)	
FEV1/FVC	0.016	0.868 (0.713- 0.957)	
MVV	0.049	0.833 (0.794- 0.956)	
DLCO	0.043	0.901 (0.755- 0.987)	
DLCO/VA	0.044	0.805 (0.625- 0.938)	
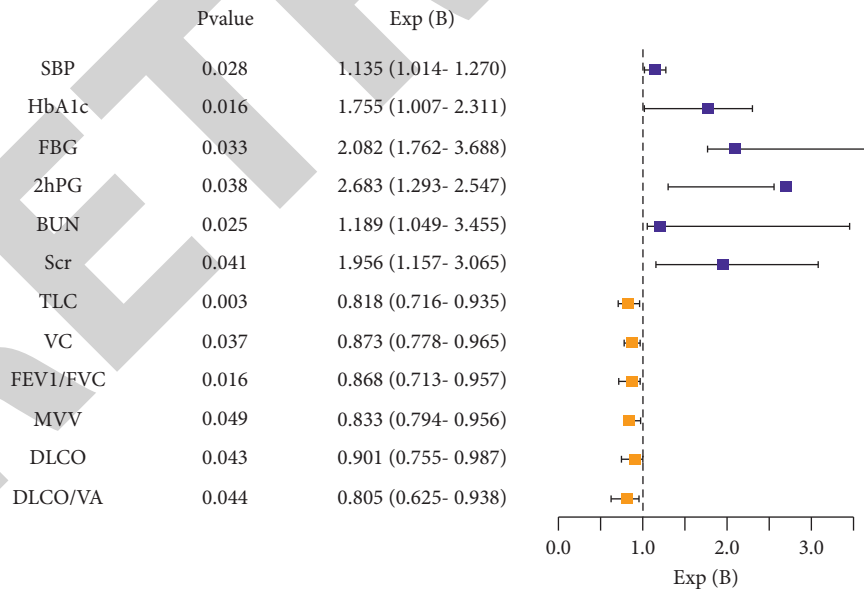
FIGURE 4: Forest plot of key risk factors for the development of clinical outcomes in DN.

identifying pulmonary microangiopathy in patients with T2DM. As the results of this study showed, pulmonary function indices (TLC, VC, FEV1, FEV1/FVC, MVV, MEF25, MEF50, MEF75, MEF25-75, DLCO, and DLCO/VA) decreased significantly with increasing clinical stage. Decreases in the pulmonary function indices TLC, VC, FEV1/FVC, MVV, DLCO, and DLCO/VA were significantly associated with the occurrence of clinical outcome and could be a key factor in the diagnosis of DN clinical outcome.

Table 6: Results of ROC curve analysis of factors affecting clinical outcomes.

Index	AUC (95%CI)	Sensitivity	Specificity	P Value	Standard error
SBP	0.80 (0.72–0.88)	0.97	0.87	<0.01	0.041
HbA1c	0.76 (0.67–0.86)	0.87	0.75	<0.01	0.047
FBG	0.90 (0.85–0.95)	0.97	0.90	<0.01	0.025
2hPG	0.80 (0.71–0.89)	0.93	0.88	<0.01	0.047
BUN	0.79 (0.70–0.88)	0.89	0.86	<0.01	0.047
Scr	0.78 (0.69–0.87)	0.86	0.93	<0.01	0.047
TLC	0.86 (0.79–0.93)	0.95	0.88	<0.01	0.034
VC	0.78 (0.69–0.87)	0.98	0.83	<0.01	0.047
FEV1/FVC	0.75 (0.65–0.83)	0.86	0.89	<0.01	0.049
MVV	0.79 (0.70–0.88)	0.88	0.86	<0.01	0.047
DLCO	0.77 (0.67–0.86)	0.91	0.89	<0.01	0.048
DLCO/VA	0.80 (0.70–0.89)	0.93	0.90	<0.01	0.047

(a)

(b)
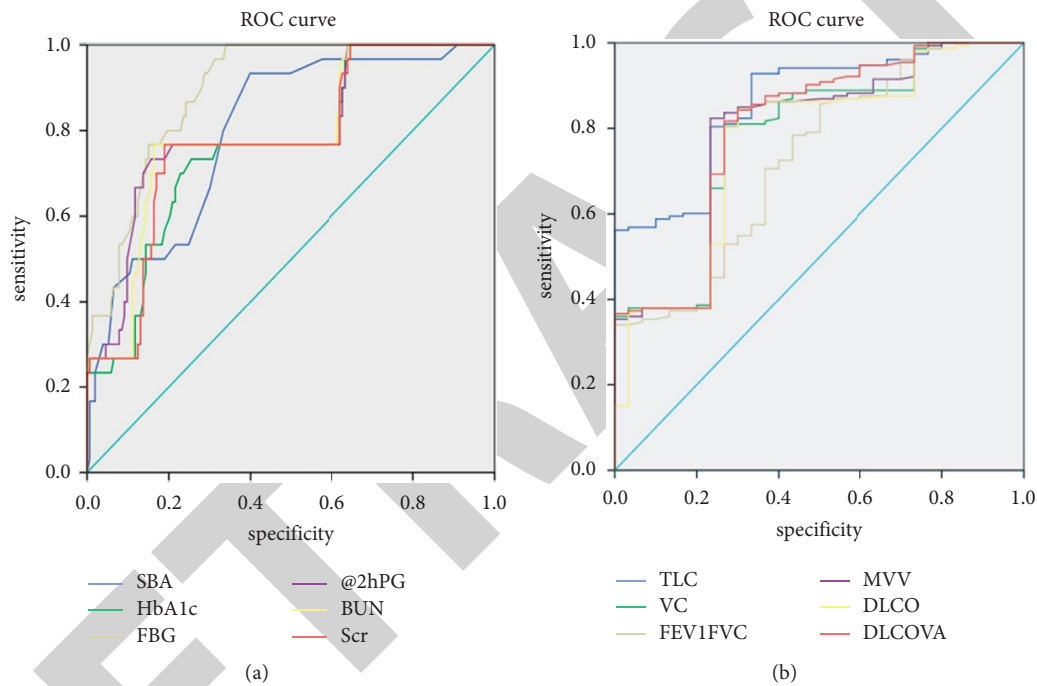
Figure 5: ROC curve of key factors influencing clinical outcomes.

This study only preliminarily explored the impact of DN on lung function and clinical outcomes at the clinical level, while the mechanisms of DN itself are extremely complex in terms of occurrence and treatment. In subsequent studies, a large number of animal and cellular experiments are needed to explore the regulatory mechanisms of various factors and provide protocols for the personalized prevention and treatment of DN.

5. Conclusion

This study used statistical analysis to investigate the effects of diabetic nephropathy on pulmonary function and clinical outcomes and screened key influencing factors on clinical outcomes. Preliminarily, we obtained that controlling blood glucose, blood pressure, and improving pulmonary ventilation and diffusion function can better prevent the occurrence and deterioration of DN, which is a retrospective study, but

this study is a retrospective study and has a small sample size, and a prospective design of a large sample size and multicenter study is needed to verify the correctness of the findings.

Data Availability

The data used to support the findings of this study are available from the corresponding author upon request.

Conflicts of Interest

The authors declare that they have no conflicts of interest.

Acknowledgments

Retraction

Retracted: Cloud Statistics of Accounting Informatization Based on Statistics Mining

Computational Intelligence and Neuroscience

This article has been retracted by Hindawi following an investigation undertaken by the publisher [1]. This investigation has uncovered evidence of one or more of the following indicators of systematic manipulation of the publication process:

(1) Discrepancies in scope

(2) Discrepancies in the description of the research reported

(3) Discrepancies between the availability of data and the research described

(4) Inappropriate citations

(5) Incoherent, meaningless and/or irrelevant content included in the article

(6) Peer-review manipulation

The presence of these indicators undermines our confidence in the integrity of the article's content and we cannot, therefore, vouch for its reliability. Please note that this notice is intended solely to alert readers that the content of this article is unreliable. We have not investigated whether authors were aware of or involved in the systematic manipulation of the publication process.

Wiley and Hindawi regrets that the usual quality checks did not identify these issues before publication and have since put additional measures in place to safeguard research integrity.

We wish to credit our own Research Integrity and Research Publishing teams and anonymous and named external researchers and research integrity experts for contributing to this investigation.

The corresponding author, as the representative of all authors, has been given the opportunity to register their agreement or disagreement to this retraction. We have kept a record of any response received.

References

[1] T. Jin, B. Zhang, and Z. Yang, "Cloud Statistics of Accounting Informatization Based on Statistics Mining," *Computational Intelligence and Neuroscience*, vol. 2022, Article ID 3493678, 10 pages, 2022.

Research Article

Cloud Statistics of Accounting Informatization Based on Statistics Mining

Taolan Jin [ID],[1] **Bo Zhang,**[2] **and Zhi Yang**[3]

[1]*School of Economics and Management, Nanjing Vocational University of Industry Technology, Nanjing, Jiangsu 210000, China*
[2]*State Grid Taizhou Power Supply Company, Taizhou, Jiangsu 210000, China*
[3]*ZTE Nanjing R&D Center, Nanjing, Jiangsu 210000, China*

Correspondence should be addressed to Taolan Jin; 19401182@masu.edu.cn

With the rapid development of information technology, the amount of all kinds of data information is increasing rapidly. As an important means to collect, store, and manage massive data, and then analyze and predict the habits and characteristics of certain groups of people and even the development trend of a certain industry, big data technology provides a comprehensive strategic basis for management decision makers that the traditional processing mode cannot match. Contemporary management accounting serves the whole process of enterprise internal control, so it will produce a large number of various data. With the explosive growth of network data and the increasing scale of database, more and more people begin to study data mining, and the classification algorithm, as the key technology in data mining, has also received extensive attention. In order to further improve the information technology level of enterprise management accounting and increase the depth of information application, many enterprises began to pay more attention to data mining, and through deep data mining, the depth and breadth of enterprise data analysis were improved. In the research of data and accounting informatization, data mining technology accounts for about 50% of informatization, which is the way for future development. With the advent of the information age, the dependence of enterprises on information technology in the process of accounting management has been further improved. If enterprises want to achieve better development in the information age, they need to pay more attention to the information technology of management accounting and improve the application ability of enterprise staff in information.

1. Introduction

There are many classify algorithms. This study will focus on the decision tree, Bayesian, genetic, artificial neural network, and classify algorithms based on association rules. To construct a management accounting working method system based on statistics mining, we must first make clear the adaptability of statistics mining to management accounting and the central link between statistics mining methods and ideas in management accounting. Statistics mining is an in-depth analysis of the relationship between statistics, finding the relationship between different statistics, then analyzing the business situation of enterprises, finding the problems in business operation, and promoting the overall improvement of financial analysis and decision-making level of

enterprises. In statistics analysis technology, statistics classification algorithm has become more and more important. With the deepening of statistics analysis research, more and more statistics classify algorithms have been proposed. A crucial step in statistics classify is to construct a statistics classifier, which is used to accurately classify some unknown types of statistics [1]. In the past, the construction of accounting informatization required the purchase of a large number of hardwares and softwares, and regular maintenance and upgrading also consumed huge costs. Many aspects required a lot of manpower and material support, which increased the operating costs of enterprises. Statistics classify algorithm is the core content of big statistics mining. Its main function is to extract valuable knowledge and message through a large number of operations on massive

disordered statistics, analyze the characteristics of all kinds of message, and provide statistics basis for researchers to further predict a certain trend. With the advent of the era of big statistics, the number of statistics that enterprises need to account is also rising, which virtually aggravates the work intensity and difficulty of accountants. As a product of the mature development of the Internet, cloud computing has sufficient network storage space. Cloud computing is a new computing mode based on shared resources, which has developed rapidly in recent years [2, 3]. Cloud storage technology is its core sub-function. Through RAC, networking, or multitiered file storage system, a mass storage device is gathered together through app software to work together, providing convenient and low-cost mass storage services. In the era of big statistics, with the changing development trend of accounting work, the amount of statistics involved in accounting work is increasing, and the difficulty of statistics calculation and analysis is getting higher and higher, which naturally brings great impact to the accounting work of enterprises. Statistics mining is to extract useful knowledge and value from a large number of statistics, which is the inevitable outcome of the development of statisticsbase technology. Statistics mining has been widely used in retail, finance, insurance, medicine, communication, and other fields. Classify is one of the most important technologies in statistics mining, and many algorithms have been proposed so far. Classify is a technology that constructs a classifier according to the characteristics of statistics sets and uses the classifier to assign categories to samples of unknown categories [4].

The goal of accounting is to provide message support for the internal management and control of enterprises. The ultimate goal of the management accounting staff to collect and summarize all kinds of message is to analyze the future production and operation situation of the enterprise based on the past production and operation results, so as to provide support for the strategic decision of the enterprise. The app of statistics mining depends on the message technology of management accounting. Through message technology, the comprehensiveness and depth of statistics can be improved, the financial analysis ability of enterprises can be improved, and the financial management level of enterprises can be improved. With the advent of the statistics era and the development of cloud service technology, the investment in hardware and software in the early stage has been saved to a great extent, and a few computers are often needed, which greatly saves the cost of enterprises. With the wide app of statistics mining technology, statistics classify algorithms are constantly emerging and gradually optimized, among which the classical classify algorithms are decision tree classify algorithm, naive Bayes algorithm, support vector machine classify algorithm, artificial neural network classify algorithm, etc [5].

This study also uses a variety of research methods in its research. In the research of statistics mining, the principle model diagram and algorithm formula are established to study and analyze it. In the research of accounting informatization cloud statistics, the corresponding statistics graph is established to analyze and explain it.

The main contributions of this study are:

(1) In this study, an algorithm formula is established to explain the research.

(2) In the research of statistics mining in this study, a model diagram is established for analysis.

(3) In the research, this study thinks that under the premise of statistics mining, accounting informatization can develop better and better.

The rest of this study is arranged: The second part introduces the related work to make a brief analysis of its research. The third part analyzes and explains the statistics mining. The fourth part analyzes and introduces the accounting informatization. The fifth part summarizes the full text.

2. Related Work

As popular technologies such as cloud storage and cloud computing have greatly met the growing demand for storage and computing power, security and privacy issues have become a concern of people. Cloud storage service providers are not completely trustworthy, and the integrity of user statistics may be destroyed due to improper management or insufficient security capability, while bit rot, disk controller error, and tape failure may also cause the integrity of user statistics to be destroyed. Scalability and fast scalability. It can improve the efficiency of accounting when it is applied to the internal accounting work of enterprises. In the process of enterprise management accounting message processing, it is necessary to apply statistics mining technology to carry out statistics analysis, so as to provide reliable statistics support for management accounting, and provide reliable guarantee for the development of enterprises and the improvement of message processing ability. Accounting is a form of accounting work that takes the internal management and control of enterprises as its main service object. Because there is a fundamental difference between financial accounting and financial accounting in the service object, the message that management accounting pays attention to and collects is often not only limited to the single financial message, but also the reflected content is not only the post-reaction and supervision of the enterprise's operating results. Statisticsbase-based knowledge discovery is a computer technology proposed with the rapid development of artificial intelligence and statisticsbase. It searches the hidden useful message from a large amount of statistics by some algorithm, and many fields such as machine learning, pattern recognition, statistics, knowledge acquisition, intelligent statisticsbase, expert system, and high-performance computing are closely related to this technology.

Chen put forward the concept of Merkle Hash Tree, which is a means to greatly reduce the cost of computing hashes for large-scale statistics structures [6]. A short message signature scheme proposed by Hu, Chen, and Ling, compared with RSA and DSA signature schemes, under the same security condition with a modulus of 1024 bits, the BLS signature has a shorter number of signatures [7]. Zheng

proposal makes up for the shortage that the Bayesian classify algorithm needs a large number of samples [8]. Shi et al. put forward several improved Bayesian classify algorithms, among which semi-naive Bayesian algorithm, candidate compressed Bayesian network construction algorithm, TAN algorithm, and other effective methods can reduce autonomy [9]. Yunyang et al. proposed a CBA classify method. CBA algorithm is mainly composed of two workflows [10]. Yang proposed a sentinel-based statistics recoverability proof mechanism, which can not only verify the integrity of the statistics on the remote node, but also recover the original statistics to a certain extent if the statistics are damaged [11].

3. Research on Statistics Mining Technology

3.1. Statistics Mining Technology. The core purpose of statistics mining is to find interesting parts of statistics message, and interpret statistics message from the perspectives of its evolution trend and composition mode. Statistics mining is a key step in knowledge discovery based on statisticsbase, and the knowledge learning stage is usually called statistics mining. For continuous attributes, when each internal node searches for its optimal splitting standard, it is necessary to sort the training set according to the value of the attribute, and sorting is a waste of time. Decision tree classify is an inductive learning method, which predicts a group of random and disordered sample statistics in a tree structure. Decision tree classify algorithm can intuitively reflect the problems and key problems encountered by decision-making classes in each decision-making stage, and is composed of root nodes, internal nodes, leaf nodes, and directed edge nodes. At present, the classical classify algorithms in the stage of big statistics analysis and statistics mining mainly include decision tree, naive Bayes, support vector machine, neural network classify algorithm, and so on. Among the decision tree classify algorithms, the non-C4.5 algorithm is typical, but with the development of computer technology and message technology, 4C5 algorithm can't meet the increasingly complex statistics classify algorithms. Therefore, in order to adapt to the processing of large-scale statistics sets, different classify methods have their own characteristics, and the problems that need to be dealt with are not the same [12]. SL IQ algorithm adopts presorting technology to eliminate the need of sorting statistics sets at each node of decision tree. Decision tree classify algorithm is one of the inductive learning algorithms, which mainly refers to the classify rules that infer "tree" structure from a series of irregular and unordered sample statistics message to predict. Compared with traditional statistics classify algorithms such as statistical methods and neural network methods, decision tree classify algorithm has many obvious advantages. For example, the statistics classify rules of decision tree classify algorithm are simple and clear, easy to understand, and difficult to make mistakes in actual operation. By analyzing and summarizing case sets, the decision tree has the ability of multi-concept learning, which is easy to use and has a wide range of apps [13, 14]. Decision tree algorithm is a better choice when classifying large-scale

case statistics represented by unstructured attribute-value pairs. At present, ID3, C4.5, SLIQ and SPRINT are the most commonly used decision tree learning algorithms. In the research, the corresponding model diagrams are established to analyze and explain them, as shown in Figures 1 and 2.

The data mining principle model diagram in Figure 1 further illustrates the application principle of its data mining, and also guides the research of its data mining algorithm. Big statistics mining technology is mainly a process of collecting and dividing statistics messages from massive message statistics according to a specified attribute, and gradually acquiring and accumulating some effective message. As the product of the development of network message technology in the era of big statistics, statistics mining technology mainly involves artificial intelligence, statisticsbase, statistics, and so on. In cloud storage, the schemes for verifying statistics integrity can be divided into statistics holding proof mechanism and statistics recoverability proof mechanism according to whether fault-tolerant preprocessing is applied to the statistics. According to the specific research of classify algorithm, the correlation between the effectiveness of classify algorithm and the characteristics of statistics is strong, and the statistics have vacancy value, loud noise, and dispersion. Part of the statistics has continuous attribute characteristics; Some statistics are scattered and mixed. The process of classifier construction is generally divided into two steps: training and testing. In the training stage, the characteristics of the training statistics set are analyzed, and an accurate description or model of the corresponding statistics set is generated for each category. In the test phase, the test is classified by using the description or model of the category, and its classify accuracy is tested. Generally, the cost of the testing phase is much lower than that of the training phase [15, 16]. Big statistics, as an abstract concept, is simply the mining and integration of massive statistics message. These statistics types are diverse, the statistics volume is huge, the value density is low, and the growth rate is fast. Only by reasonable statistics mining and statistical analysis can the app value behind them be discovered. With the development of production in various industries, a large amount of statistics will be produced every day. Through big statistics technology, this message has a subtle influence on people's current life and even the development of a certain industry.

3.2. Research on Statistics Mining Algorithm. The decision tree classify algorithm can intuitively show the problems and key points of decision-making classes in different periods in the whole decision-making process. The decision tree consists of root nodes, internal nodes, leaf nodes, and directed edges connecting nodes. The root node is unique, it represents a group of classified samples, while the internal group represents the attribute of the object, while the terminal node represents the result of the classify. The algorithm starts from the root node, selects the corresponding attribute value from top to bottom, sends the branch to the corresponding node, and repeats this step until the final node and category of the path are stored in the leaf node.
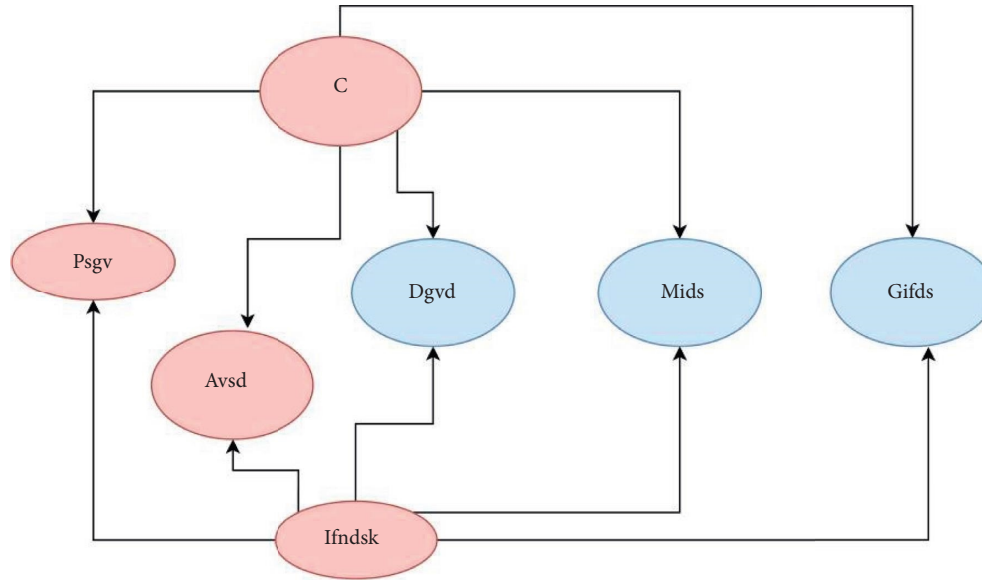
FIGURE 1: Model diagram of statistics mining sorting principle.
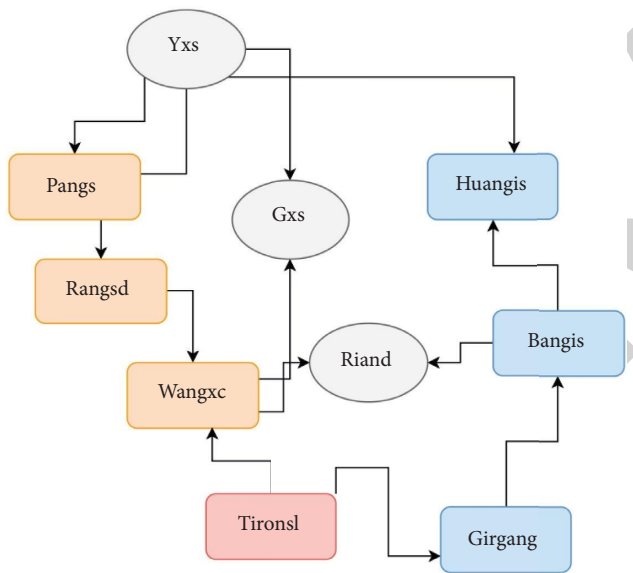
FIGURE 2: Statistics mining classify decision analysis model diagram.

Each branch of the decision tree corresponds to a classify rule, so the decision tree classify algorithm can finally output an easy-to-understand rule set. Although the decision tree statistics classify algorithm has many advantages, it also has many disadvantages. Because the decision tree determines the statistics analysis process, in the process of statistics classify, especially in the process of tree construction, it is inevitable to scan and sort the statistics several times in sequence, which will inevitably lead to the whole statistics analysis process becomes slow. Bayes classify algorithm is put forward based on the Bayes formula, and it is an algorithm that uses the knowledge of probability statistics to classify. When the prior probability and class conditional probability are known, the classify algorithm calculates the probability that a given sample with unknown class belongs

to each class by Bayes theorem, and selects the class with the highest probability as the determined class of the sample. Li algorithm is improved in many aspects based on 4C5 algorithm technology, and it also adopts sorting technology and breadth-first strategy technology, which makes SLIQ algorithm technology have good scalability for increasing the number of records and attributes to a certain extent. In the research algorithm, corresponding calculation formulas are established to analyze them, such as formulas (1)–(5).

$$1^3 \left(-\overline{\Gamma}\right)N = \left\{ 1^7 \left(X\right) Y k_\Gamma \begin{pmatrix} l_- \\ 1 \end{pmatrix}, \right. \tag{1}$$

$$\bigcap_J = c_{i_\infty^{1-\infty-x}} \left(y \prod_{t=0}^{11} 1 \right), x_t |y|, \tag{2}$$

$$P^m_{(i^c|u)\infty p(1t)_{a-1}^{\Pi_p} C} x^{41c/3}, \tag{3}$$

$$D^n \left(1, 11, 1L \ldots 1k, \left(J = pkc\right) \frac{1}{1!} \right)^1, \tag{4}$$

$$n_C = \operatorname*{Res}_{\partial\varphi} \cdot 3\beta Q_-^{2+2^\beta} Q + \beta. \tag{5}$$

Because of the characteristics of C45 algorithm, the structure of decision tree is completed according to the depth-first strategy, so every key node must be analyzed in the process of statistics classify and analysis, and the efficiency is extremely low [17, 18]. However, after the breadth-first strategy technology is adopted, it is only necessary to scan each attribute list once for each layer, and the optimal splitting criteria can be found for each leaf node in the current decision tree. The naive Bayesian algorithm is relatively stable, and it will not have a great impact on the classify results because of the different characteristics of the

statistics itself. The stronger the independence between naive Bayesian statistics, the more accurate the classify results. However, we need to pay attention to the premise that the classify algorithm needs to be based on the conditional independence hypothesis, which is an ideal state. In practical app, there will be links between statistics attributes, which will reduce the classify accuracy, so the effect of this method is often difficult to reach the theoretical maximum. It is to improve the ability of statistics processing and increase the value of statistics. From a technical point of view, the relationship between big statistics and cloud computing is inseparable like the front and back of a coin. The existence of big statistics can't be handled by a single computer, so it must be implemented in a multitiered architecture, and massive statistics can be mined in a multitiered way. However, it must rely on cloud computing's multitiered processing and cloud storage virtualization technology. With the advent of the cloud era, big statistics has gradually gained more attention.

SPRIN algorithm has made corresponding changes to the statistics analysis structure of decision tree algorithm, especially deleting the list of statistics categories that need to be stored in memory in SLI Q algorithm, and instead merging the list of statistics categories into the attribute list of each statistics number. The advantage of this method is that when analyzing a large number of statistics, it can avoid repeated statistics analysis when traversing each attribute list to find the optimal splitting standard of the current node. In the process of building a decision tree, the most time-consuming operations are the statistical calculation of the category distribution message of the statistics set belonging to each non-terminal node and the splitting of the statistics set by using splitting criteria. Both operations are realized by UDF in M IND. Genetic algorithm is an efficient search and random optimization algorithm that evolved from the theory of biological evolution. It is an important breakthrough in the combination of natural science and computer algorithm. With the help of the principle of natural evolution, the algorithm transforms the process of solving problems into the process of finding chromosomes with high fitness according to the genes on chromosomes. This algorithm combines the advantages of directional search and random search, so it has good global search ability, and avoids the disadvantage that most optimization methods are easy to fall into local optimum. The algorithm combines random search with directional search, which makes it have better global optimization performance, and overcomes the defect that the traditional optimal solution is difficult to achieve local optimization [19–21]. Like nature, genetic algorithms can solve problems without knowing them. Its main job is to evaluate all the chromosomes generated in the algorithm, and select the corresponding chromosomes according to their fitness, so that the chromosomes are easier to reproduce. Although the rise of statistics mining research is initiated by researchers in the field of statisticsbase, most of the algorithms proposed so far have not made use of the related technologies of statisticsbase, and it is difficult for statistics mining apps to integrate with statisticsbase systems. This problem has become one of the key issues in this

field. In the research of its algorithms, we have once again established its algorithm formulas to analyze and explain them, such as formulas(6)–(9).

$$TC_u \bar{\text{i}}_-^{\sigma-1^\beta X_1 - \mathbb{R}_2 + J_{31} x'}, \tag{6}$$

$$TS\Sigma'_{K+\zeta}: T_{.11}^L = 5JK_{11}, \tag{7}$$

$$-\bar{l}|_1^y x = 4t g_1 \lambda_1 f \delta \text{i}^{x_2 + \cdots} + \mu_2, \tag{8}$$

$$n_{C,x} = \frac{1^{r/2}}{1} = \text{i} \cdot T \ker\phi. \tag{9}$$

MIND uses the typical decision tree construction method to build the classifier. The specific steps are similar to SLIQ. The main difference is that it uses the UDF method and SQL statement provided by statisticsbase to construct the tree. Simply put, at each level of the tree, a dimension table is established for each attribute, and the number of each value of each attribute belonging to each category and the node number to which it belongs are stored. CBA algorithm mainly constructs classifier by finding association rules in training set. The classical algorithm Aprio ri is used to discover association rules, which is effective for discovering association rules hidden in a large number of transaction records. At the same time, statistics mining does not artificially limit and exclude the types of statistics to be analyzed. Whether it is financial statistics or non-financial statistics that can be analyzed by accounting subjects, or even non-statistics message, statistics mining does not exclude it. Therefore, statistics mining has strong adaptability to management accounting in two aspects: purpose and object. The method of statistics mining can determine the correlation among all kinds of message through the parameter estimation results of regression analysis, multi-factor variance analysis, and other methods, thus making it possible to identify the influencing factors of the message that managers care about. Genetic algorithm doesn't need to know something about the problem when solving it. Its task is only to evaluate all chromosomes produced in the process of algorithm, and then to screen chromosomes according to the fitness value, among which chromosomes with high fitness value have a greater chance of reproducing the next generation [22–24].

4. Research on Accounting Message Statistics

4.1. Statistics Mining Management Accounting Message Processing Research. With the development of message technology, financial sharing has good technical conditions. The development of the Internet can realize the sharing of enterprise financial statistics, which has a positive impact on improving the timeliness of financial statistics in enterprise accounting message systems. Cloud computing is an important part of multitiered computing. Specifically, it decomposes huge statistics computing and processing programs into countless small programs, and then processes and analyzes them through a system composed of multiple

servers, and feeds back the results of the small programs to users. In the early days of cloud computing, it was also a simple multitiered computing task distribution and integrated computing results. Message management cannot be separated from advanced software and hardware facilities. Therefore, we should first strengthen the construction and improvement of basic management facilities, transform the existing library resources in the library into digital message content through the professional library materials input program, and upload it to the designated library resources platform, so that people can quickly search and download it on the platform. In the message platform, the financial statistics of each region of the enterprise is comprehensively managed, so that the financial statistics can appear on the financial sharing platform in time after it happens, so that the financial personnel can handle the accounts in time after obtaining the relevant statistics, which plays a positive role in improving the timeliness of the financial statistics message in the enterprise accounting message system. In the process of applying the management accounting message system, we should further expand the scope of message processing, help enterprises realize the overall "messagization", and incorporate the operation statistics of other departments into the accounting message system, so as to realize the supervision and management of the whole enterprise and improve the management effect of the accounting message system. In the research, statistics graphs are established for analysis and interpretation, as shown in Figures 3 and 4.

According to the survey, although some libraries have introduced advanced library message management equipment and set up related intelligent message management platforms at this stage, due to the huge number of books and materials in their collections, there is a problem that the reform of message management mode is incomplete, and most of the books and materials in their collections are still not entered into the message management platform, but kept in traditional paper books. At present, the development of human society has entered the stage of comprehensive informatization, and batch message processing, rapid message transmission and message sharing have become the keywords of the development of the times. It indicates the coming of the era of big statistics. In the process of installation, testing, and operation of accounting message software, a certain amount of capital investment is also needed, which will test the professional ability of financial staff. In the later stage, it is still necessary to upgrade the equipment maintenance software to promote the smooth operation of accounting message construction. Therefore, the continuous cost consumption will aggravate the burden on enterprises, while the traditional accounting message business process is still relatively complicated. The theoretical basis and ideas that statistics mining relies on the process of message selection and trend analysis come from statistics. Among the collected message, it is one of the core ideas of statistics mining to select samples to guess the characteristics of the population and check whether the observed samples belong to the same category as the known population. During the implementation of enterprise management accounting informatization, it is necessary to

ensure the reliability and timeliness of the original statistics in order to dig the statistics message deeply. The timeliness of financial work has a very important impact on the level of work and users of financial reports, and the untimely transmission of original statistics has become an important reason that affects the informatization level of enterprise management accounting. In the research, the corresponding statistics graphs are established for analysis and interpretation, as shown in Figures 5 and 6.

When enterprises carry out management accounting work, in the process of message processing, it is necessary to compare the budget statistics, so as to better discover the problems in operation and carry out financial management by mining the differences between the statistics. Enterprise informatization should be applied to budget management, and the management and control of enterprise financial work should be strengthened according to budget statistics. Management accounting message processing based on statistics mining needs to comprehensively improve the depth and breadth of financial statistics, and ensuring the integrity of statistics is an important condition for developing statistics mining and improving message processing ability. The final result of the statistics mining process will be able to provide a powerful help to the core function of management accounting-forecasting. In the management accounting work, the forecast can be divided into two parts: the forecast of the change scale of the existing situation, the forecast of various risks, and the change probability of other uncertain factors. It promotes the internal and external sharing of resources. In the past message environment, although the enterprise supply chain system can share statistics and messages in many aspects, such as production, sales, and finance, and its limitations are still very obvious. Cloud computing technology includes a series of message, such as financial business warehousing, in the platform, breaking down the barriers between various departments, and making the work message of departments no longer presented in the form of message islands, becoming more open and transparent, and sharing internal resources is also an effective supervision for enterprise accounting message.

4.2. Research on Accounting Informatization Strategy.
Paying attention to the integration and classify of message is one of the optimization strategies to better promote the development of enterprise accounting informatization by using cloud computing technology in the era of big statistics. According to the above analysis, in the current era, the accounting work of enterprises is already facing a huge amount of message, and it is undoubtedly a huge challenge for accountants to complete the processing and processing of various statistics message in a fixed time. Therefore, it is even more necessary to use advanced message technology to classify and sort out the limited financial accounting message inside enterprises and reduce the statistics risks outside enterprises. In order to complete the message collection, analysis, and calculation more conveniently, it is necessary to use the message platform and cloud computing technology to create a more comprehensive and rich enterprise

FIGURE 3: Message statistics analysis statistics diagram.
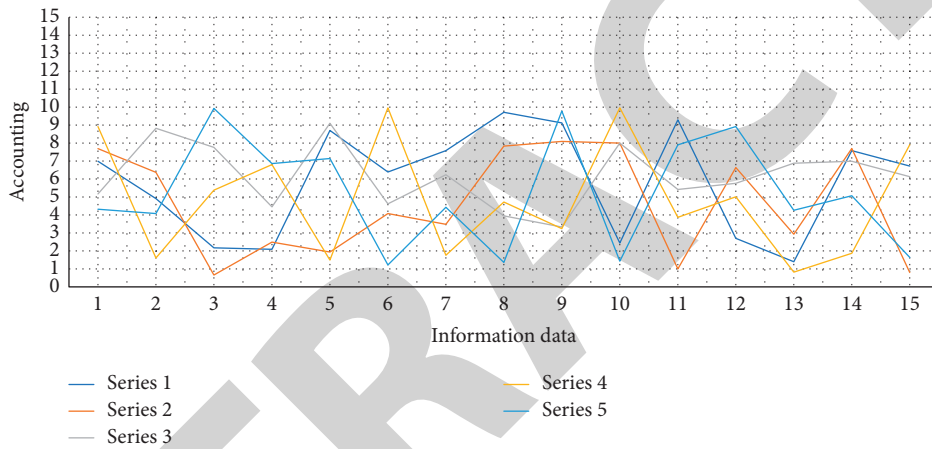
FIGURE 4: Message statistics accounting management analysis diagram.
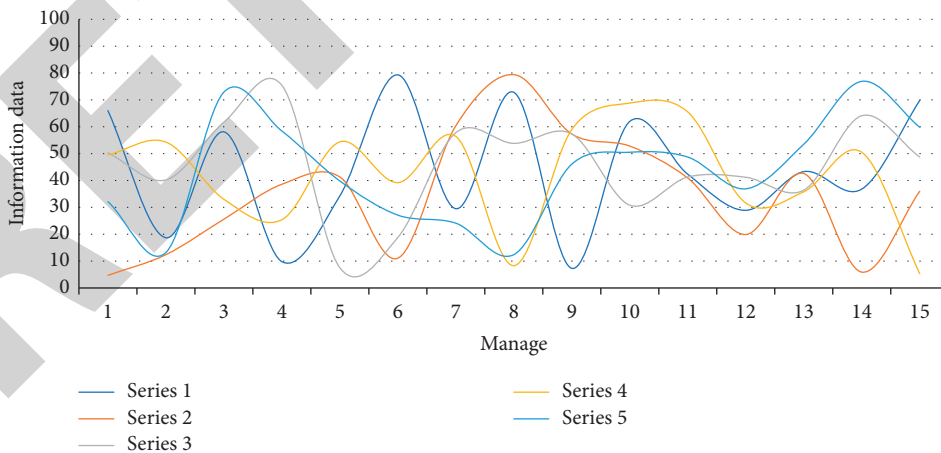
FIGURE 5: Statistics map of management accounting informatization (1).

accounting message. In the process of perfecting the management system and system, we can't ignore the improvement of the comprehensive quality of the library management team. First, it is necessary to improve the professional skills of relevant staff, so as to ensure that every staff involved in message management of books and materials can master the operation methods of infrastructure, understand the functions and functions of message management system, and correctly realize the important significance of message management for the management of
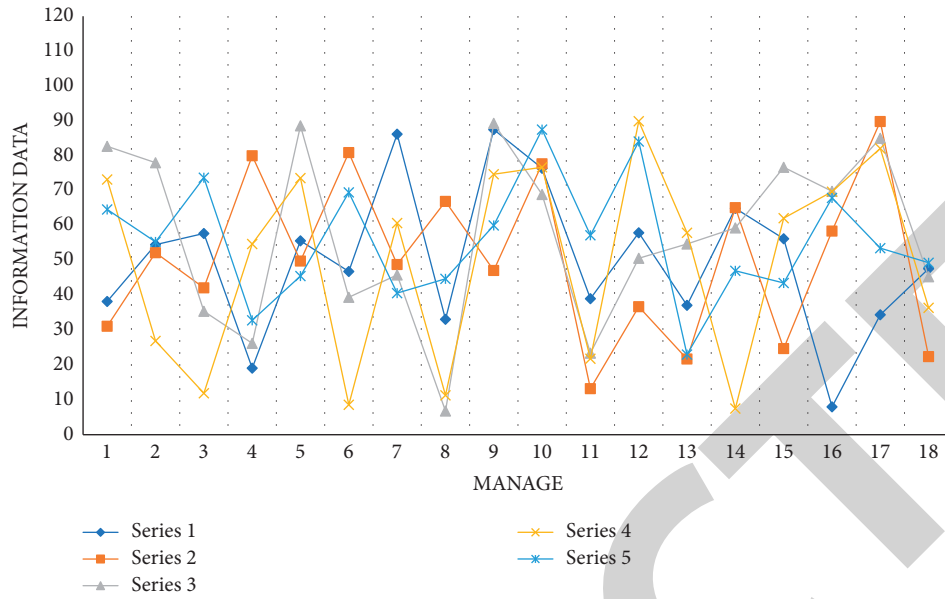
FIGURE 6: Statistics map of management accounting informatization (2).
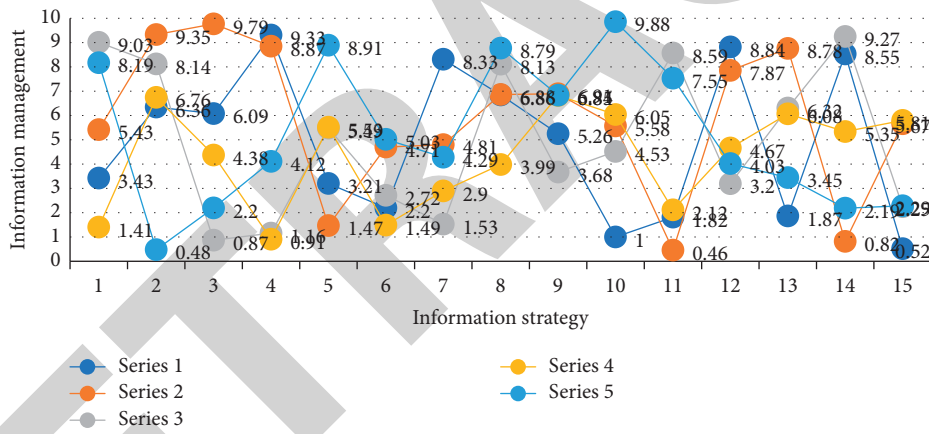
FIGURE 7: Statistics map of accounting message management decision-making.

books and materials. The core function of accounting lies in the supervision and feedback of the existing work results of each process of enterprise management, and the prediction of the long-term changes in enterprise management. In this context, the role of statistics mining will be greatly strengthened. For the management accounting analysis of certain messages, the main functions of statistics mining are cost change analysis, activity-based value analysis, market forecast, and market segmentation. In the research, a statistics map is established to analyze and explain it, as shown in Figure 7.

The management decision of accounting informatization in Figure 7 accounts for about 90% of the whole accounting informatization. Budget is an important part of enterprise's prior management, and it plays a positive role in improving management accounting message processing ability and operation ability. Therefore, in the process of management

accounting message processing based on statistics mining, enterprises should incorporate the budget work into the accounting message system of enterprises, use accounting software to analyze the business situation of enterprises, formulate a scientific and reasonable budget in combination with the future development strategy of enterprises, improve the budget management level of enterprises, and narrow the difference between budget and actual statistics. As a manager, you should keep abreast of the development of your own industry and related industries, update your ideas in time, and know the latest trends. In the era of big statistics, the better app of cloud computing technology to the internal financial and accounting management of enterprises needs to improve relevant laws and regulations to ensure the message security. Facing the general trend of message management, we should dare to try, dare to break the traditional model in the past, pay attention to the

development of technology and personnel, and realize the development of accounting messages.

5. Summary

In the era of big statistics, the emergence of cloud computing technology has brought more possibilities for enterprise accounting informatization, but at the same time, a series of risks still exist. How to seize the opportunity to deal with risks and challenges is still an important problem that every enterprise is facing in the era of big statistics. Systematically studying the classify algorithm of statistics mining will help us to know the advantages and disadvantages of the decision tree classify algorithm, naive Bayes classify algorithm, support vector machine classify algorithm and neural network classify algorithm, as well as their applicable scenarios, and make targeted optimization and improvement on their shortcomings. Big statistics technology and cloud computing technology bring a lot of convenience to the development of accounting informatization, which not only reduces the cost and improves efficiency, but also realizes the sharing of resources, and has great development prospects. With the advent of the era of big statistics, the importance of statistics classify algorithm will become more and more obvious, and the characteristics of algorithms such as execution speed, scalability, and intelligibility of output results will become the trend of statistical analysis. In the process of applying statistics mining to management accounting message processing, enterprises need to pay more attention to the level of financial personnel, improve the level of financial informatization, and provide a human resource foundation for better development of financial informatization.

Data Availability

The figures used to support the findings of this study are included in the article.

Conflicts of Interest

The authors declare that they have no conflicts of interest.

References

[1] S. H. Liao, P. H. Chu, and P. Y. Hsiao, "Data mining techniques and applications – a decade review from 2000 to 2011," *Expert Systems with Applications*, vol. 39, no. 12, Article ID 11303, 2012.

[2] D. T. Larose, "Statistics mining: methods and models," *Technometrics*, vol. 49, no. 4, p. 500, 2007.

[3] S. R. Joseph, H. Hlomani, and K. Letsholo, "Statistics mining algorithms: an overview," *Neuroscience*, vol. 12, no. 3, pp. 719–743, 2016.

[4] S. Busygin, O. Prokopyev, and P. M. Pardalos, "Biclustering in data mining," *Computers & Operations Research*, vol. 35, no. 9, pp. 2964–2987, 2008.

[5] R. Leslie, "Clustering for statistics mining: a statistics recovery approach," *Psychometrika*, vol. 20, no. 6, p. 6, 2007.

[6] W. S. Chen and Y. K. Du, "Using neural networks and data mining techniques for the financial distress prediction model," *Expert Systems with Applications*, vol. 36, no. 2, pp. 4075–4086, 2009.

[7] Y. Hu, J. Chen, and X. Ling, "Research on architecture and technology of statistics mining platform in cloud computing," *Wireless Internet Technology*, vol. 30, no. 54, p. 2, 2018.

[8] Li Zheng, "Analysis of the construction of accounting message processing mode in the era of big statistics," *Wireless Personal Communications*, vol. 20, no. 56, p. 3, 2018.

[9] S. Shi, L. Xu, H. Dong et al., "Research on data pre-deployment in information service flow of digital ocean cloud computing," *Acta Oceanologica Sinica*, vol. 33, no. 9, pp. 82–92, 2014.

[10] L. Yunyang and YuHao, "Research on statistics security technology based on cloud storage," *Science of the Total Environment*, vol. 20, no. 23, p. 23, 2018.

[11] Z. H. Yang and Pan, "Research on electronic commerce message management system based on statistics mining," *Agro Food Ind Hi Tec*, vol. 201, no. 2, p. 39, 2017.

[12] Y. Zou, "Statistics analysis and processing of massive network traffic based on cloud computing and research on its key algorithms," *Wireless Personal Communications*, vol. 208, no. 2, p. 12, 2018.

[13] S. Lee, K. Choi, and D. Yoo, "Predicting the insolvency of SMEs using technological feasibility assessment information and data mining techniques," *Sustainability*, vol. 12, no. 23, p. 9790, 2020.

[14] A. Zhygalova, "Perceived value of cloud based message systems," *Case: Accounting Message Systems.*vol. 2013, no. 21, p. 2, 2013.

[15] S. Zhang, "Coping strategies research on accounting message risks based on cloud computing environments," in *Measurement and Intelligent Materials*vol. 2016, no. 3, , p. 2, Atlantis Press, 2016.

[16] C. Brandas, O. Megan, and O. Didraga, "Global perspectives on accounting information systems: mobile and cloud approach," *Procedia Economics and Finance*, vol. 20, no. 3, pp. 88–93, 2015.

[17] N. Zhao, "Research on accounting messageization construction of administrative institutions based on cloud platform," *Modern Message Technology*, vol. 2018, no. 4, p. 56, 2018.

[18] F. Marsintauli, E. Novianti, R. P. Situmorang, and F. D. F. Djoniputri, "An analysis on the implementation of cloud accounting to the accounting process," *Accounting*, vol. 2021, no. 2, pp. 747–754, 2021.

[19] L. J. Jiao, "Research on modern accounting development under the "Internet plus" era," *The Journal of Shandong Agriculture and Engineering University*, vol. 2, no. 3, p. 34, 2019.

[20] Z. K. Hou, H. L. Cheng, S. W. Sun, J. Chen, D. Q. Qi, and Z. B. Liu, "Crack propagation and hydraulic fracturing in different lithologies," *Applied Geophysics*, vol. 16, no. 2, pp. 243–251, 2019.

[21] J. Han, H. Cheng, Y. Shi, L. Wang, Y. Song, and W. Zhnag, "Connectivity analysis and application of fracture cave carbonate reservoir in Tazhong," *Science Technology and Engineering*, vol. 16, no. 5, pp. 147–152, 2016.

[22] H. Cheng, J. Wei, and Z. Cheng, "Study on Sedimentary Facies and Reservoir Characteristics of Paleogene sandstone in

Retraction

Retracted: Effects of Gemcitabine and Oxaliplatin Combined with Apatinib on Immune Function and Levels of SIL-2R and sicAM-1 in Patients with Gallbladder Cancer

Computational Intelligence and Neuroscience

This article has been retracted by Hindawi following an investigation undertaken by the publisher [1]. This investigation has uncovered evidence of one or more of the following indicators of systematic manipulation of the publication process:

(1) Discrepancies in scope

(2) Discrepancies in the description of the research reported

(3) Discrepancies between the availability of data and the research described

(4) Inappropriate citations

(5) Incoherent, meaningless and/or irrelevant content included in the article

(6) Peer-review manipulation

The presence of these indicators undermines our confidence in the integrity of the article's content and we cannot, therefore, vouch for its reliability. Please note that this notice is intended solely to alert readers that the content of this article is unreliable. We have not investigated whether authors were aware of or involved in the systematic manipulation of the publication process.

Wiley and Hindawi regrets that the usual quality checks did not identify these issues before publication and have since put additional measures in place to safeguard research integrity.

We wish to credit our own Research Integrity and Research Publishing teams and anonymous and named external researchers and research integrity experts for contributing to this investigation.

The corresponding author, as the representative of all authors, has been given the opportunity to register their agreement or disagreement to this retraction. We have kept a record of any response received.

References

[1] L. Qu, K. Li, K. Liu, and W. Hu, "Effects of Gemcitabine and Oxaliplatin Combined with Apatinib on Immune Function and Levels of SIL-2R and SicAM-1 in Patients with Gallbladder Cancer," *Computational Intelligence and Neuroscience*, vol. 2022, Article ID 4959840, 8 pages, 2022.

Research Article

Effects of Gemcitabine and Oxaliplatin Combined with Apatinib on Immune Function and Levels of SIL-2R and sicAM-1 in Patients with Gallbladder Cancer

Linlin Qu, Kun Li, Kui Liu, and Weiyu Hu ![ORCID icon]

Department of Hepatopancreatobiliary Surgery, The Affiliated Hospital of Qingdao University, Qingdao 266000, China

Correspondence should be addressed to Weiyu Hu; huweiyucn@qdu.edu.cn

Objective. The aim of this study was to determine how gemcitabine, oxaliplatin combination, and apatinib affect immune function and SIL-2R and sicAM-1 levels in patients with gallbladder cancer. *Methods*. Retrospective analysis of 116 patients with gallbladder cancer treated at our institution between February 2019 and February 2021. The patients were randomly divided into control and study groups, with 58 patients in each group. The study group received the combination of apatinib and the control group received gemcitabine and oxaliplatin. Immune function, serum tumor markers, short-term efficacy, survival measures, and incidence of adverse events were monitored and compared between the two groups. *Results*. CD3+, CD4+, CD4+/CD8+, and NK levels were significantly higher in both groups after treatment, while CD8+ levels were significantly lower; levels of sicAM-1, sicAM-1 (VEGF), and CEA were greatly reduced in both groups after treatment; there were significant differences between the study and control groups in terms of rr46.55% and DCR84.48%; at one year after treatment, the survival rate in the study group increased from 67.24% in the control group to 79.31%, with an increase in both PFs and 0S. Compared with the control group, the incidence of hypertension and myelosuppression, neutropenia, proteinuria, and hand-foot syndrome were lower in the study group ($P < 0.05$). All differences were statistically significant. *Conclusion*. In the treatment of gallbladder cancer, the use of gemcitabine and oxaliplatin combined with apatinib can effectively control the progression of patients' disease.

1. Introduction

Gallbladder cancer is a relatively common malignant tumor of the biliary system in clinical practice, with insidious onset, rapid tumor growth, and high malignancy, which is a great threat to patients' lives [1]. The occurrence of gallbladder cancer is related to various risk factors, such as gallbladder stones, bile duct inflammation, and obesity, but the exact etiology is still unclear [2, 3]. In the process of continuous in-depth clinical research on gallbladder cancer, the treatment methods about gallbladder cancer have been continuously improved, and the treatment effect of gallbladder cancer has been significantly enhanced [4, 5]. Due to the high malignancy of gallbladder cancer, chemotherapy can directly kill tumor cells [6, 7]. Gemcitabine, oxaliplatin, and apatinib all have significant effects on the treatment of tumors [8, 9]. Gemcitabine has a strong broad-spectrum antitumor activity

and a unique mechanism of action and is widely used in the treatment of malignant tumors in clinical practice; oxaliplatin has the advantage of significant effects and few adverse effects; and apatinib is able to antagonize vascular endothelial growth factor receptor 2 (VEGFR-2) and can effectively promote apoptosis of tumor cells. In this paper, the efficacy of gemcitabine and oxaliplatin combined with apatinib in the treatment of gallbladder cancer is analyzed and reported as follows.

2. Material and Methods

2.1. General Material. Patients with gallbladder cancer admitted to our hospital between February 2019 and January 2021 were randomly divided into two groups: 23 males and 35 females in the control group, aged 42–76 years; 58 patients in the study group, with a mean age of 56.08 years and

TABLE 1: Comparison of immune index levels.

Group	Period	Observation group (n = 58)	Control group (n = 58)
CD3+(%)	Before	47.92 ± 9.56	47.85 ± 9.58
	After	54.83 ± 11.97*	62.97 ± 12.74*#
CD4+(%)	Before	35.86 ± 6.98	35.87 ± 6.84
	After	40.15 ± 7.57*	48.97 ± 8.12*#
CD8+(%)	Before	25.12 ± 6.42	25.13 ± 6.48
	After	22.97 ± 5.14*	16.89 ± 4.23*#
CD4+/CD8+	Before	1.33 ± 0.29	1.35 ± 0.26
	After	1.58 ± 0.34*	1.89 ± 0.52*#
NK(%)	Before	16.89 ± 4.16	17.23 ± 4.39
	After	32.76 ± 6.98*	37.89 ± 7.42*#

a mean disease duration of 15.09 months (see Table 1), with a performance status (ECOG) score of 1 in 11 cases, 2 in 20 cases, 3 in 27 cases, and tumor patients 1 case with score 4 and TNM stage [10] (tumor node metastasis grading). A total of 17 cases of stage III and 41 cases of stage IV were found; in the study group, there were 24 males and 34 females, with ages ranging from 41 to 77 years, mean age (57.12 ± 4.25) years, and duration of disease (15.12 ± 2.01) months. Scores of ECOG: 12 cases were 1, 20 cases were 2, and 26 cases were 3. 15 cases were classified as stage III according to TNM, and 43 cases were stage IV. The differences between the two groups in terms of gender, age, and disease duration were not statistically significant. The control group was given gemcitabine and oxaliplatin, while the experimental group added apatinib to the control group. The medical ethics committee of the hospital has approved the study.

2.2. Criteria of Inclusion and Exclusion. Inclusion criteria were ① Compliance with the guidelines of the Biliary Surgery Group of the Chinese Medical Association for the diagnosis of gallbladder cancer [11]; ② confirmed by cell immunology, imaging examination, and pathological biopsy of gallbladder cancer; ③ aged 18–80 years old, with the first gallbladder cancer; ④ ECOG score of 1–3; TNM stage of stage III–IV; ⑤ estimated survival time >3 months, which could not be treated by previous surgery or drugs; ⑥ have the solid lesions that can be measured (the diameter of the lesions in the spiral CT examination is ≥10 mm); ⑦ patients and members of their families get an explanation of the study's goals, and they sign an informed consent form as a proof of their agreement.

Exclusion criteria were ① Patients with injury or dysfunction of heart and blood vessels and other organs; ② patients with obvious gastrointestinal bleeding, including local ulcer, hematochezia and hematemesis within two months, and patients with occult blood in stool; ③ patients with primary gastric cancer without surgical resection, who are often considered to have massive gastrointestinal bleeding without examination; ④ there are no other diseases of the gallbladder, such as gangrenous cholecystitis, gallbladder atrophy, and diffuse stones; ⑤ abnormal coagulation function, allergic to research drugs; ⑥ accompanied by cognitive impairment and mental disorders; ⑦ poor

compliance, recently participated in other clinical drug researchers.

2.3. Research Methods. After admission, the patients underwent relevant examinations, including laboratory, cytology, imaging, and pathological examination, and were given basic treatment, including analgesia, sedation, anti-inflammatory, anti-infection, and nutritional support. Gemcitabine and oxaliplatin were used in the control group: 1000mg/m2 gemcitabine (Jiangsu Hausen Pharmaceutical Group Co. Ltd. Chinese medicine standard word H20030104) was dissolved in 100 ml of 0.9% normal saline for 30 minutes, once/week, 3 weeks/course, and then entered a course after one week's rest; 85 mg/m^2 oxaliabine Fireseuskaby (Wuhan) Pharmaceutical Co. intravenous instillation for 2.5~3 hours, 2 weeks/time, 2 weeks/course of treatment, one week of intermediate rest, and then enter a course of treatment for 4 months. Following this, apatinib, a drug manufactured by Jiangsu Hengrui Pharmaceutical Co. Ltd. and given in warm water, 500 mg/time, once a day, 30 minutes after meals, and for two courses of treatment was administered to the research group. Testing for gastrointestinal, liver, and kidney functions should be done as soon as possible if side effects such as nausea and vomiting occur during chemotherapy. If the white blood cell level is abnormally increased, the electrocardiogram, liver, and kidney function shall be monitored regularly; if the white blood cell level is abnormally decreased, the granulocyte colony stimulating factor treatment shall be implemented; and if bone marrow suppression occurs, the hematopoietic factor shall be injected.

2.4. Observational Indicators. ① Immune function measurement: Flow cytometry (Nexcelom Bioscience Company, USA) identified T cell subsets, in peripheral venous blood before and 2 months after the natural killer cell. ② Evaluation of sICAM-1, vascular endothelial growth factor, and carcinoembryonic antigen before and after therapy was conducted. A nocturnal blood sample was taken from the patient and then centrifuged in the morning. For cold storage, the supernatant was gathered. In this research, flow cytometry was used to measure sIL-2R and sICAM-1 levels. Shanghai BRahman State Biotechnology Co. Ltd. provided the kit, and the double antibody Sandwich method was used to measure VEGF and CEA levels. Operate in line with the instructions provided in the package.③ Clinical treatment effect: complete response (CR): complete tissue disappeared completely without tumor enhancement >4 weeks; partial response (PR): a reduction in lesion tissue of at least 50% and a duration of at least four weeks are required; stable disease (SD): lesions on the largest scale dropped by 50% or rose by 25%, but no new lesions formed; progressive disease (PD): lesion tissue grew by more than 25%, or a new lesion was discovered. Disease control rate (DCR) = (CR + PR + SD) cases/total cases x 100%; objective response rate (RR) = (CR + PR) cases/total cases 100%. ④ Survival indicators: follow-up (outpatient, SMS, telephone, etc.) and record the survival indicators of the two groups during one
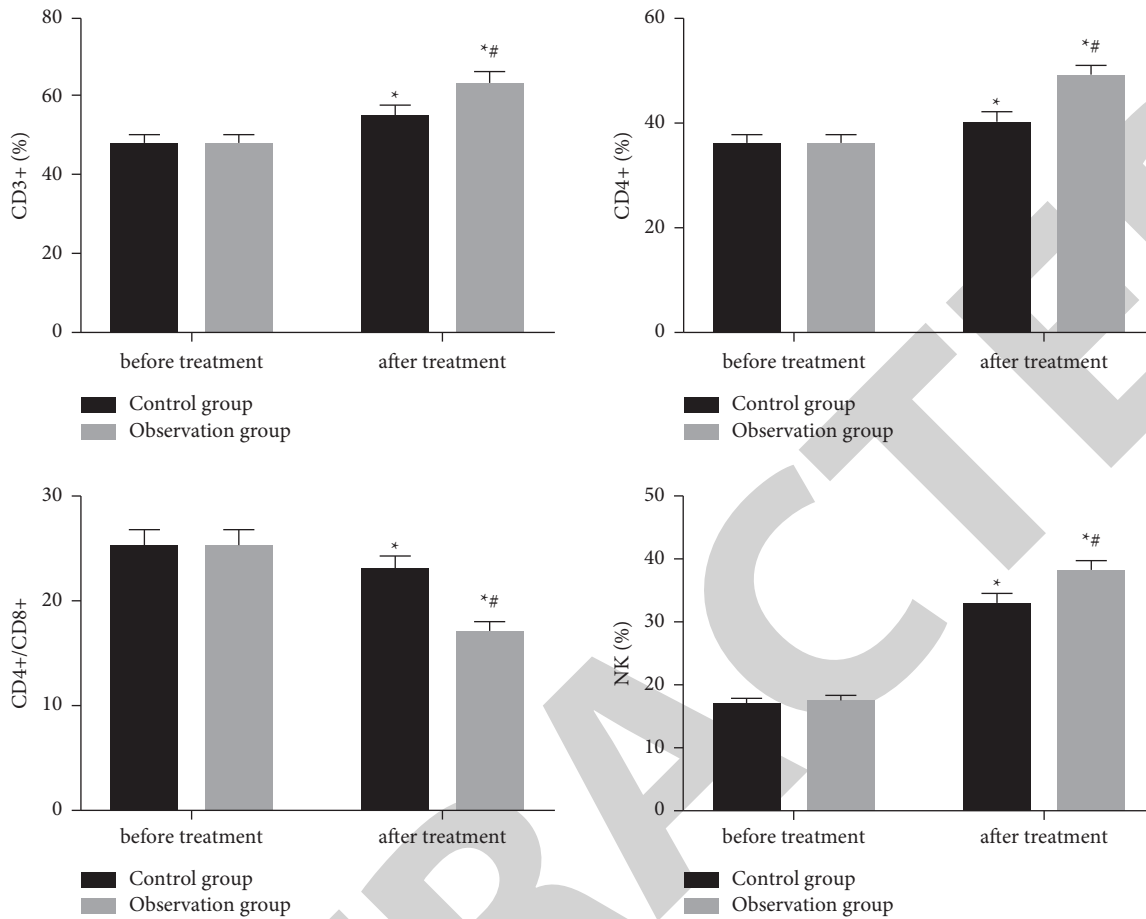
FIGURE 1: Comparison of immune index levels.

year, including survival rate, survival time, progression-free survival (progression-free survival,PFs), and overall survival (0 s). Survival was the cumulative survival ratio after the first year of follow-up. The PFs and 0 s reflect the amount of time elapsed between the time of enrollment and the time of death or the last follow-up, respectively. ⑤ Adverse reactions: patients experienced hypertension, neutropenia, and proteinuria as well as bone marrow suppression and hand-foot syndrome throughout therapy and follow-up.

2.5. Statistical Treatment. Using SPSS 24.0 statistical software, *t*-tests were employed to compare groups, and measurement data according to a normal distribution was presented as ±. For comparisons between groups, enumeration data were reported in terms of number of cases and percentages (*n* and %), and a *P* < 0.05 denotes statistically significant differences.

3. Outcome

3.1. Comparison of Immune Function. Immunological parameters were not significantly different before treatment. There was a striking increase in CD3+, CD4+, CD4+/CD8+, and NK in NK cells and a striking decrease in CD8+ in NK cells. CD3+, CD4+/CD8, and NK levels in the study group

were significantly higher than CD4+/CD8+ levels in the control group; see Table 1 and Figure 1.

3.2. Comparison of Serum Tumor Markers. In the comparison of serum tumor markers, the levels of sIL-2R, sICAM-1, VEGF, and CEA were flatly lower in the control group than in the study group as shown in Table 2 and Figure 2.

3.3. Comparison of Clinical Therapeutic Effects. In terms of clinical efficacy, the RR after treatment was 46.55% higher and the DCR was 84.48% higher in the study group than in the control group, and the differences were statistically significant as shown in Table 3 and Figure 3.

3.4. Comparison of Survival Indicators. In the comparison of survival indicators, the one year survival rate after treatment was 79.31% higher in the study group than in the control group (*P* < 67.24%), which is remarkable. Table 4 and Figure 4 show that the survival time, PFs, and 0 s were longer in the study group than in the control group.

3.5. Comparison of Adverse Reaction Rates. In the comparison of the incidence of adverse reactions, hypertension and myelosuppression were lower in the study group, but the

Table 2: Comparison of serum tumor markers.

Group	Period	Observation group (n = 58)	Control group (n = 58)
sIL-2R (IU/ml)	Before	763.02 ± 136.24	760.91 ± 135.43
	After	649.14 ± 115.68*	528.32 ± 93.61*#
sICAM-1 (μg/l)	Before	513.21 ± 145.76	516.86 ± 148.97
	After	359.42 ± 112.64*	218.54 ± 79.36*#
VEGF (ng/ml)	Before	570.43 ± 106.94	573.54 ± 109.83
	After	403.21 ± 84.55*	238.17 ± 69.31*#
CEA (ng/ml)	Before	38.20 ± 10.93	38.41 ± 10.89
	After	23.01 ± 8.06*	15.73 ± 4.88*#
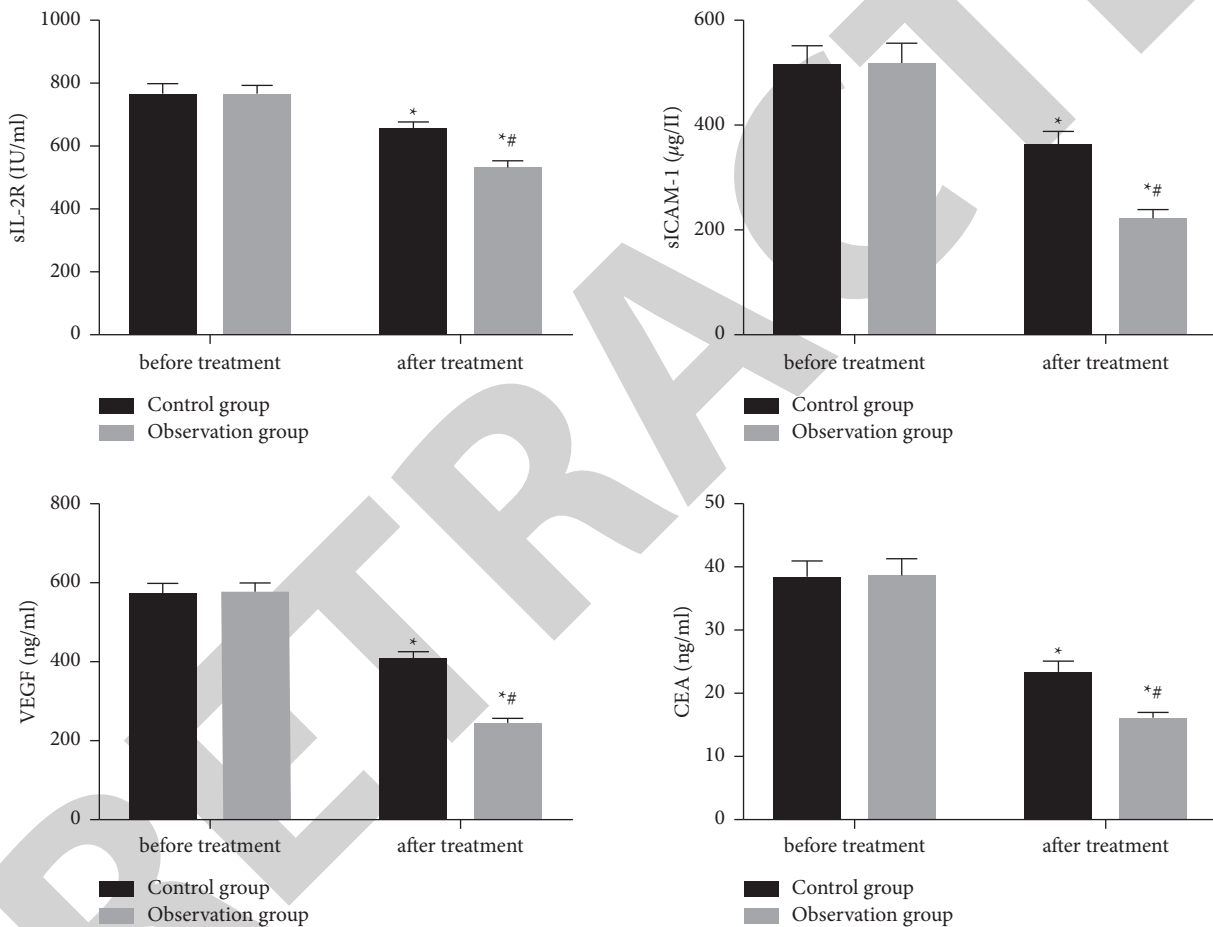
Figure 2: Comparison of serum tumor markers.

Table 3: Comparison of clinical efficacy.

Group	Observation group (n = 58)	Control group (n = 58)	χ^2 index	P index
CR	3(5.17)	8(13.79)	—	—
PR	11(18.97)	19(32.76)	—	—
SD	27(46.55)	22(37.93)	—	—
PD	17(29.31)	9(15.52)	—	—
RR	24.14%	46.55%	0.786	0.012
DCR	70.69%	84.48%	1.023	0.005

differences were not statistically significant. Neutropenia, proteinuria, and hand-foot syndrome were quite rare in the study group as shown in Table 5 and Figure 5.

4. Discussion

The main treatment modality for malignant tumors is comprehensive treatment, and radical resection is the only way to treat patients with gallbladder cancer with the
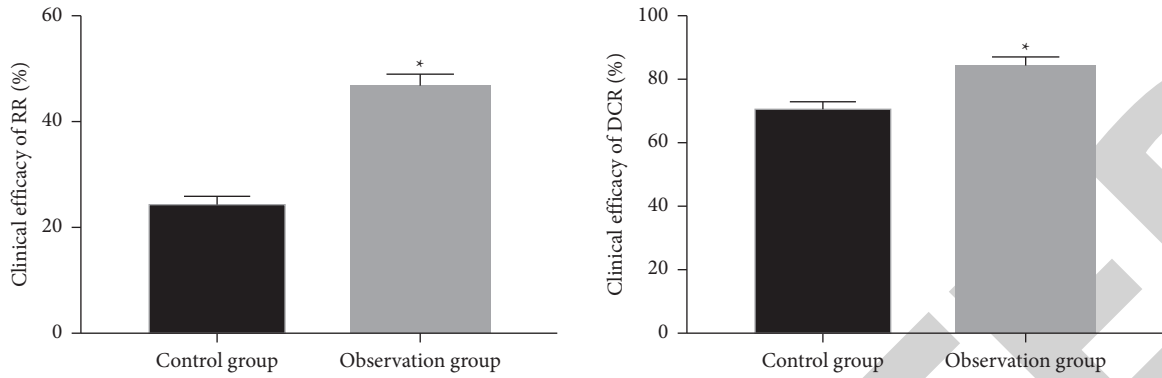
FIGURE 3: Comparison of clinical efficacy.

TABLE 4: Comparison of survival indicators.

Group	Observation group (n = 58)	Control group (n = 58)	Statistical index	P index
Survival rate	39(67.24)	46(79.31)	0.201	0.014
Time (months)	8.15 ± 1.23	10.93 ± 1.26	4.303	0.021
PFs (months)	4.96 ± 1.15	5.43 ± 1.08	5.133	0.004
0s (months)	7.85 ± 1.04	9.53 ± 1.23	2.854	0.038
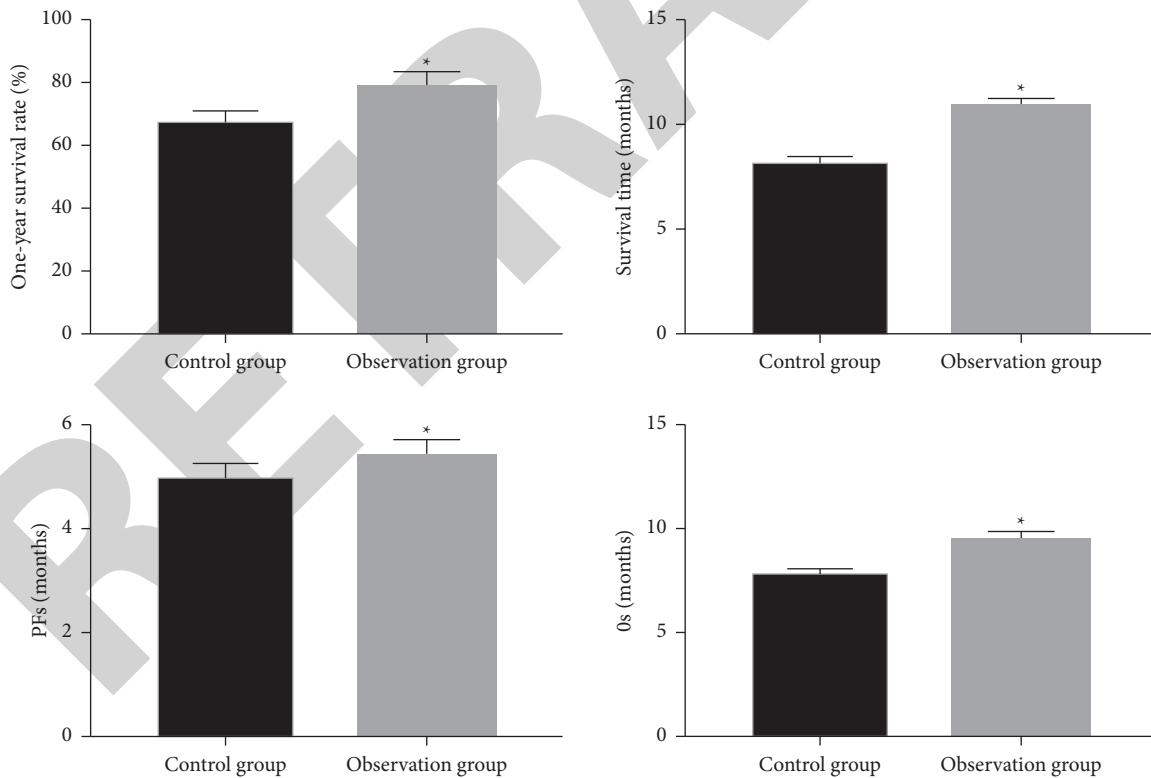
FIGURE 4: Comparison of survival indicators.

possibility of cure [12]. Patients with gallbladder cancer need to undergo surgical exploration first, and resection at an early stage can effectively prolong the survival time of patients [13]. However, in actual clinical practice, many patients with gallbladder cancer are diagnosed in the middle and late stages because of the early manifestations of the disease and the rapid growth of the tumor, and the tumor cells have already invaded the plasma membrane, resulting in metastases in the liver and peritoneum [14]. Patients with advanced gallbladder

TABLE 5: Comparison of the incidence of adverse reactions.

Group	Observation group (n = 58)	Control group (n = 58)	χ^2 index	P index
Hypertension	11(18.97)	7(12.07)	5.402	0.340
Neutropenia	5(8.62)	1(1.72)	0.185	0.018
Proteinuria	7(12.07)	3(5.17)	0.892	0.006
Bone marrow depression	8(13.79)	3(5.17)	0.418	0.522
Hand-foot syndrome	6(10.34)	5(8.62)	0.322	0.023
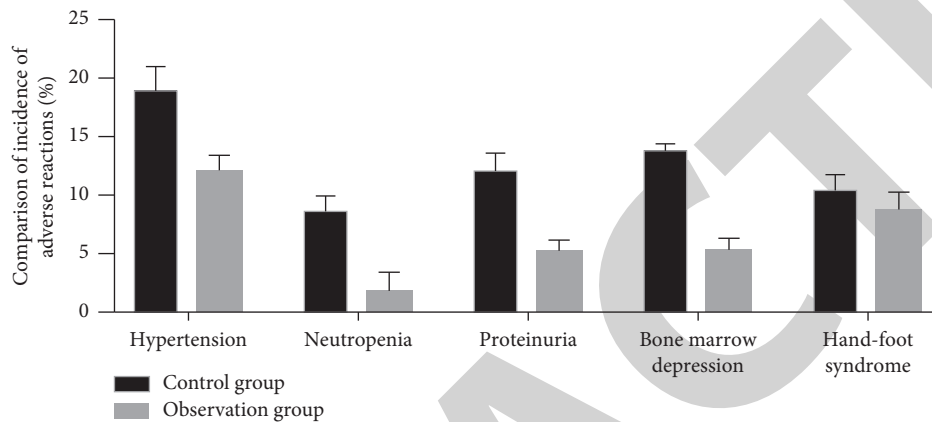
FIGURE 5: Comparison of the incidence of adverse reactions.

cancer have long operation time, large resection area, high surgical risk, and many postoperative complications [15]. Therefore, chemotherapy has become the main treatment modality for this group of patients. Among them, gemcitabine, oxaliplatin, and apatinib as chemotherapy drugs have different anticancer effects and mechanisms, which can amazingly promote apoptosis of diseased tissues to inhibit the growth and metabolism of tumor cells [16]. Currently, the anticancer mechanisms and effects of gemcitabine, oxaliplatin, and apatinib are frequently studied at home and abroad, while the effects of gemcitabine, oxaliplatin, and apatinib on immune function, sIL-2R, and sICAM-1 are still relatively limited [17]. In this study, gemcitabine and oxaliplatin combined with apatinib significantly inhibited tumor vascular growth, improved somatic cell immune function, alleviated sIL-2R, and sICAM-1 levels, improved short-term treatment effects and survival time, and controlled the occurrence of adverse effects.

When cancer cells invade the gallbladder, immune function is suppressed, allowing the growth and development of tumor vascular cells, and increasing the activity of tumor biomarkers. This leads to a dramatic decrease in CD3 +, CD4 +, CD4 +/CD8 +, and NK levels, an increase in CD8 + and a decrease in anticancer and anti-infective capacity. The literature[18] treats breast cancer patients with gemcitabine, which interferes with the expression of VEGF and its receptor in cancer cells by engaging the AKT pathway, thereby promoting apoptosis of tumor cells. Consistent with previous studies, gemcitabine, oxaliplatin, and apatinib have been shown to improve immune function, inhibit tumor cell activity,

and reduce the activity and expression of serum tumor markers in patients with gallbladder cancer [19]. As a nucleoside analogue, gemcitabine can effectively affect DNA synthesis during tumor cell metabolism and induce apoptosis in cancer cells. Oxaliplatin, a third-generation anticancer drug, has similar effects to gemcitabine and is involved in the growth and proliferation of tumor cell DNA. Apatinib, as a VEGFR-2 tyrosine kinase inhibitor, can effectively bind to the VEGF receptor, inhibit its expression in tumor cells, and interfere with the growth, metabolism, and proliferation of tumor blood vessels. It can also regulate the activity of tumor markers, such as sIL-2R and sICAM-1, whose synergistic effects can alleviate cancer cell-induced immune disorders, promote body immune regulation, improve immune function, and enhance therapeutic efficacy.

Chemotherapy and targeted drugs are often used to treat patients with biliary tract cancer. Among them, chemotherapeutic drugs have a strong suppressive effect on the body's immune system and are prone to adverse reactions and drug resistance, which affect prognosis and safety. In recent years, there has been an explosion of research on targeted drugs. The positive effects of cancer treatment have become more pronounced and the side effects have been greatly reduced. The literature [20] demonstrated that oxaliplatin and apatinib, adjuvant therapy for patients with locally advanced biliary tract cancer can significantly improve DCR and therapeutic benefits and enhance anticancer activity. Apatinib was safe and effective, and no deaths were reported. The literature [21] showed that gemcitabine, oxaliplatin, and apatinib significantly improved the short- and long-term outcomes and reduced the incidence of

adverse effects in patients with biliary cancer. This finding is consistent with a previous study by [22] et al. Improved treatment outcomes and increased overall survival time have been shown in patients with gallbladder cancer in a manner that is both very safe and within the tolerable range of possible side effects [23].

There are certain limitations in this study, mainly including limited sample size, deviation of the study results from actual clinical data, which affects the reliability of the study report; insufficient time to assess the long-term effectiveness and resistance to treatment; and failure to consider the effects of drug treatment on other immune mechanisms. Expanding the sample size, extending the follow-up period, and studying different mechanisms of action are important to improve the feasibility and scientific validity of the study results.

The combination of gemcitabine, oxaliplatin, and apatinib has been shown to enhance immune function, limit the proliferation and spread of tumor vascular cells, and attenuate the expression of sIL-2R and sICAM-1 in patients with gallbladder cancer. This is a safe and effective treatment for advanced gallbladder cancer, and it presents a new idea for clinical trials.

Data Availability

The data used to support the findings of this study are available from the corresponding author upon request.

Conflicts of Interest

The authors declare that they have no conflicts of interest.

Acknowledgments

References

[1] W. Wan, B. Zheng, and W. Sun, "Adjuvant therapy in the treatment of resected nonmetastatic gallbladder cancer of stage II-IV: a generalized propensity score analysis," *Oncology Research and Treatment*, vol. 44, no. 7-8, pp. 390–399, 2021.

[2] I. Siraj and P. S. Bharti, "3D printing process: a review of recent research," *Science Progress and Research*, vol. 1, no. 3, pp. 127–137, 2021.

[3] A. Lugo, G. Peveri, and S. Gallus, "Should we consider gallbladder cancer a new smoking-related cancer? A comprehensive meta," *International Journal of Cancer*, vol. 15, no. 12, pp. 3304–3311, 2020.

[4] T. Yamashita, K. Kato, and S. Fujihara, "Anti-diabetic drug metformin inhibits cell proliferation and tumor growth in gallbladder cancer via G0/G1 cell cycle arrest," *Anti-Cancer Drugs*, vol. 31, no. 3, pp. 231–240, 2020.

[5] D. Jwabc, D. Xnabc, S. Sheng et al., "Phosphorylation at Ser10 triggered p27 degradation and promoted gallbladder carcinoma cell migration and invasion by regulating stathmin1 under glucose deficiency," *Cellular Signalling*, vol. 80, no. 4, pp. 109923–109925, 2021.

[6] A. Shahabaz and M. Afzal, "Implementation of high dose rate brachytherapy in cancer treatment," *Science Progress and Research*, vol. 1, no. 3, pp. 77–106, 2021.

[7] Q. D. Shen, L. Wang, and H. Y. Zhu, "Gemcitabine, oxaliplatin and dexamethasone (GemDOx) as salvage therapy for relapsed or refractory diffuse large B-cell lymphoma and peripheral T-cell lymphoma," *Journal of Cancer*, vol. 12, no. 1, pp. 163–169, 2021.

[8] M. Leonard and B. Williams, "Usage of social media twitter in the intervention of diabetes mellitus," *Science Progress and Research*, vol. 1, no. 3, pp. 63–69, 2021.

[9] X. Lv, J. Chen, and T. Yi, "The efficacy and safety of low-dose Apatinib in the management of stage IV luminal-type breast cancer: a case report and literature review," *Anti-Cancer Drugs*, vol. 32, no. 8, pp. 773–778, 2021.

[10] B. J. Giantonio, P. J. Catalano, and N. J. Meropol, "Bevacizumab in combination with oxaliplatin, fluorouracil, and leucovorin (FOLFOX4) for previously treated metastatic colorectal cancer: results from the eastern cooperative oncology group study E3200," *Journal of Clinical Oncology*, vol. 25, no. 12, pp. 1539–1544, 2007.

[11] K. Kitamura, D. Shida, and S. Sekine, "Comparison of model fit and discriminatory ability of the 8th edition of the tumor-node-metastasis classification and the 9th edition of the Japanese classification to identify stage III colorectal cancer," *International Journal of Clinical Oncology*, vol. 26, no. 9, pp. 1671–1678, 2021.

[12] Z. G. Xue, F. Cao, A. Li, and F. Li, *Zhonghua Wai Ke Za Zhi*, vol. 59, no. 8, pp. 672–678, 2021.

[13] L. Seymour, J. Bogaerts, and A. Perrone, "iRECIST: guidelines for response criteria for use in trials testing immunotherapeutics," pp. e143–152, 2017.

[14] B. Ouyang, N. Pan, and H. Zhang, "miR-146b-5p inhibits tumorigenesis and metastasis of gallbladder cancer by targeting toll-like receptor 4 via the nuclear factor-κB pathway," *Oncology Reports*, vol. 45, no. 4, pp. 15–19, 2021.

[15] Y. L. Cai, Y. X. Lin, and X. Z. Xiong, "Postsurgical radiotherapy in stage IIIB gallbladder cancer patients with one to three lymph nodes metastases: a propensity score matching analysis," *The American Journal of Surgery*, vol. 221, no. 3, pp. 642–648, 2021.

[16] Y. H. Choi, "A high monocyte-to-lymphocyte ratio predicts poor prognosis in patients with advanced gallbladder cancer receiving chemotherapy," *Cancer Epidemiology, Biomarkers & Prevention*, vol. 28, no. 6, pp. 1045–1051, 2019.

[17] P. García, C. Bizama, and L. Rosa, "Functional and genomic characterization of three novel cell lines derived from a metastatic gallbladder cancer tumor," *Biological Research*, vol. 15, no. 1, pp. 13–17, 2020.

[18] W. A. Dik and M. Heron, *The Netherlands Journal of Medicine*, vol. 78, no. 5, pp. 220–231, 2020.

[19] L. Fisher, "Retraction: gemcitabine aggravates miR-199a-5p-mediated breast cancer cell apoptosis by promoting VEGFA downregulation via inactivating the AKT signaling pathway," *RSC Advances*, vol. 11, no. 23, pp. 2930–2937, 2021.

[20] N. F. Maroufi, M. R. Rashidi, V. Vahedian, M. Akbarzadeh, A. Fattahi, and M. Nouri, "Therapeutic potentials of Apatinib in cancer treatment: possible mechanisms and clinical relevance," *Life Sciences*, vol. 241, no. 15, pp. 117106–117117, 2019.

[21] J. H. Rao, C. Wu, H. Zhang, and D. WangLuChengChen, "Efficacy and biomarker analysis of neoadjuvant carrizumab

Retraction

Retracted: Analytical Study of Financial Accounting and Management Trends Based on the Internet Era

Computational Intelligence and Neuroscience

This article has been retracted by Hindawi following an investigation undertaken by the publisher [1]. This investigation has uncovered evidence of one or more of the following indicators of systematic manipulation of the publication process:

(1) Discrepancies in scope

(2) Discrepancies in the description of the research reported

(3) Discrepancies between the availability of data and the research described

(4) Inappropriate citations

(5) Incoherent, meaningless and/or irrelevant content included in the article

(6) Peer-review manipulation

The presence of these indicators undermines our confidence in the integrity of the article's content and we cannot, therefore, vouch for its reliability. Please note that this notice is intended solely to alert readers that the content of this article is unreliable. We have not investigated whether authors were aware of or involved in the systematic manipulation of the publication process.

Wiley and Hindawi regrets that the usual quality checks did not identify these issues before publication and have since put additional measures in place to safeguard research integrity.

We wish to credit our own Research Integrity and Research Publishing teams and anonymous and named external researchers and research integrity experts for contributing to this investigation.

The corresponding author, as the representative of all authors, has been given the opportunity to register their agreement or disagreement to this retraction. We have kept a record of any response received.

References

[1] Q. Li, "Analytical Study of Financial Accounting and Management Trends Based on the Internet Era," *Computational Intelligence and Neuroscience*, vol. 2022, Article ID 5922614, 11 pages, 2022.

Research Article

Analytical Study of Financial Accounting and Management Trends Based on the Internet Era

Qin Li (ID)

College of Accountancy, Shanxi Technology and Business College, Taiyuan 030000, Shanxi, China

Correspondence should be addressed to Qin Li; liqin@poers.edu.pl

With the development of Internet technology and computer technology, the network has provided convenience to enterprises while putting forward new requirements for the development of the accounting industry. The combination of traditional financial accounting methods and computerized information technology enables accurate and rapid transmission of financial data. At the same time, the application of network technology optimizes the financial accounting process of enterprises and greatly improves the efficiency of accounting work and accountants can devote more time and energy to the analysis of enterprise financial information. However, with the application of Internet technology, the change in financial accounting has also generated new problems. The article focuses on the topic of financial accounting; first, it briefly introduces the development history of financial accounting and the Internet; second, it discusses the changes in accounting work mode and its characteristics under the network environment and analyzes the advantages and problems of combining network technology and financial accounting; and finally, it puts forward the countermeasures to solve the "Internet+" era financial accounting work for the current situation. Finally, the countermeasures to solve the financial accounting work in the era of "Internet+" are proposed to improve the professional ability of financial personnel.

1. Introduction

Compared with the previous enterprise financial management work, financial management in the Internet era has distinct advantages, which effectively expands the scope of enterprise financial management and allows comprehensive supervision of the entire financial management work [1]. In the Internet era, corporate financial management generates more information and requires rapid transmission of information in a short period of time [2]. If they want to meet the development needs of the times, enterprises need to have a clear understanding and awareness of the importance of financial and accounting management work to innovate the working model (Figure 1). At the same time, enterprises also need to improve the dissemination of financial information and manage financial accounting information in a diversified way, which can not only effectively improve the efficiency of enterprise financial management, but also optimize the working environment comprehensively [3]. In the

Internet era, intelligence has become the main direction of enterprise financial management work, which is an important basis for enterprise financial management in the Internet era and an inevitable trend of the market economy, which can not only effectively improve the market competitiveness of enterprises, but also facilitate the implementation of scientific management by relevant financial and accounting departments and lay a solid foundation for the efficient development of financial accounting [4]. Therefore, in the Internet era, enterprises need to pay more attention to the informationization and intelligence of financial accounting management, fully meet the development trend of the times, and actively promote the development of enterprises [5].

Nowadays, China has entered the Internet era, and the vigorous development of the Internet has directly changed the financial accounting management work, significantly improved the management quality of financial accounting, and the content involved in financial accounting has become

FIGURE 1: New model of financial accounting.

more extensive [6]. For this reason, relevant personnel must deeply analyze the financial accounting management trends in the Internet era in order to do their jobs well.

1.1. Expanded Scope of Financial Management. In the Internet era, the management efficiency of enterprises has been significantly improved, and the financial accounting management mode has been changed [7]. The most significant change is that it extends the scope of financial management and enriches the work of financial management. For example, the use of the Internet not only enables direct procurement and management but also the ability to discipline suppliers and later sales to ensure the integrity of management [8].

1.2. Improving the Timeliness of Financial Management. Real-time and timeliness are the most significant advantages of Internet technology, so for financial accounting management work, it is also necessary to improve the speed of information transmission to help users get accurate information [9]. Financial and accounting management pays more attention to the timeliness of information, and the existence of Internet technology helps meet this need effectively [10]. The use of Internet technology enables financial management to be more timely and changes the method of communication, increasing communication and exchange between personnel [11]. For example, the use of the Internet makes it possible to lay out the relevant work content and to monitor the implementation of the work; the use of the Internet also makes it possible to give feedback to the company on specific work situations, significantly improving efficiency [12].

1.3. Orderly Operation within the Enterprise. Financial accounting management work in the Internet era can deliver financial information in a timely manner and make financial management work more flexible and orderly [13]. Financial accounting management work is the focus of enterprise management. In enterprise financial accounting management, it is difficult to achieve obvious management effects if we still rely on the older way to implement management. At this time, the use of Internet technology can manage the financial and business work scientifically and ensure the orderliness of the internal operation of the enterprise.

At present, China is in the era of intensified economic globalization and extremely rapid transmission of information, and the competition among enterprises is increasingly fierce. In the face of the increasingly competitive market environment, leaders need to conduct enterprise management not only to consider the traditional factors of competition between enterprises, but also to start from the management level, relying on strong and excellent financial management to help managers to make appropriate corporate decisions [14]. Therefore, real-time and comprehensive financial management information plays a pivotal role for managers to make decisions.

2. Related Work

Financial accounting is a branch of business accounting that, together with management accounting, forms the two main areas of business accounting, known as "traditional accounting" because it follows traditional manual accounting records, and therefore also known as "external reporting accounting" because it focuses on the business external stakeholders' decision-making needs and financial reporting outside the enterprise [15]. Financial accounting is an economic management activity that is carried out through comprehensive and systematic accounting and monitoring of the financial flows carried out by the enterprise, with the main purpose of providing economic information about the financial position and profitability of the enterprise to external investors, creditors and relevant government agencies that have an economic interest in the enterprise (refer to Figure 2).

Financial accounting plays a pivotal role in enterprise management and can provide useful information to decision-makers through various accounting procedures, actively participate in the management decisions of the enterprise, improve the efficiency of production and operation activities of the enterprise, and promote the healthy and normal development of the market economy. Therefore, financial accounting is crucial and indispensable in the course of the development of enterprises [16].

The Internet was born in the 1960s and 1970s as a large global network consisting of a series of common protocols [17]. As the economy grew, the development of the Internet accelerated, and by the 1980s and 1990s, it had matured, become more sophisticated, and gradually began to spread around the world [18]. Throughout the early development of the Internet, fundamental changes occurred almost every decade [19]. In China, the adoption of the Internet began around 1994 [20].

With the increasing popularity of mobile Internet, cloud computing, big data, and other technologies, human beings have stepped into the Internet era. Whether it is attendance records and online shopping, daily commuting to and from work, or software used in daily work, Internet technology is necessary [21]. It can be seen that technology has a decisive influence on the development of society, and the

Figure 2: Traditional financial accounting.

development of network technology will continue to push human society into a new era.

By applying Internet technology to financial accounting and management, the transport linkage of computer data and automatic calculation of data are realized, which in turn improves the accuracy of financial data in a comprehensive manner [22]. In addition, with the support of Internet technology, workers effectively enhance the degree of information sharing in daily financial accounting or management and create good conditions for the smooth implementation of financial supervision [23]. For example, in daily work, when workers need relevant financial information, they can quickly obtain the required information with the help of information sharing. Although Internet technology has improved the efficiency and quality of financial accounting and management work, the content of financial accounting and management work in the new era is gradually diversified and complicated [24].

With the gradual diversification of financial management content, the financial management staff of institutions can fully understand the importance of this work and continuously improve their Internet technology and financial management knowledge and skills to better meet the needs of the real work, and then give full play to the maximum value of financial management work [25].

3. Methodology

3.1. Basic Model. An accounting information system (AIS) is a system that incorporates all accounting information. AIS is an important application of computer technology in the field of accounting; the generation of AIS brings accounting from the original era of manual bookkeeping to the era of machine bookkeeping, realizing computerization of accounting is an important reform in accounting practice. Its essence is the use of computers for an accounting information system.

The mechanism of its role is that the accounting information system first collects some of the data produced by the front-end business process that meet the definition of accounting, then carries out corresponding accounting processing according to these accounting data, completes accounting, generates accounting information, and finally, managers use this accounting information to make business decisions. Analysis and organization of the role mechanism of AIS is shown in Figure 3.

In this article, "whether the accounting information system can realize the sharing of business and financial data" is taken as the mark of the division between traditional and financial integration accounting information systems; from this perspective, the traditional accounting information system has gone through five rounds of evolution, as shown in Figure 4.

Although the accounting information system in the first 4 stages could also record some business information, the content of the recording was very limited, and business information still needed to be transferred between business and finance departments through paper-based original vouchers. Compared with the first 4 stages, the most significant feature of this stage is that the front-end business module is incorporated into the AIS, which helps the AIS record not only the business data conforming to the accounting definition, but also other types of business data so that the AIS system provides managers with richer data and enables managers to see the original business picture more intuitively through the system.

Through the above 5 stages of development of an accounting information system, we can see that the traditional accounting information system mainly solves 2 problems: first, for the paperless bookkeeping vouchers, accounting personnel use computers instead of manual bookkeeping; second, recognizing that business data play a very important role in enterprise management, business department data and financial data are integrated into the accounting information system, so that the accounting information system can further play its efficient management role.

Through the above development history of traditional accounting information system, it can be seen that traditional AIS provides accounting information to managers and then provides services for their management decisions, although the MIS (management information system) stage can already provide business information to managers, but because business and financial information cannot be shared resulting in a lower degree of this information used by managers, so by organizing the traditional AIS functions as shown in Figure 5.

Industry financial integration AIS means an accounting information system that can realize business financial integration, which is an effective platform and tool for enterprises to realize business financial integration by using various modern computer technologies, advancing the financial work of enterprises to the business end, through which enterprises can not only obtain management information in terms of financial analysis, but also obtain management-related information directly from business data, and managers can use this business-side information for more in-depth analysis, realizing the integration of information flow and data flow.

The accounting information system of the combination of production and finance realizes the information sharing
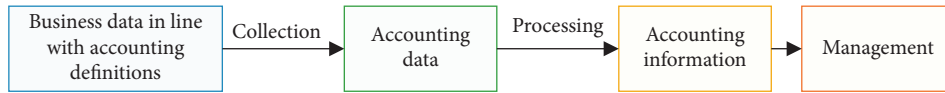
Figure 3: Mechanism of accounting information system.
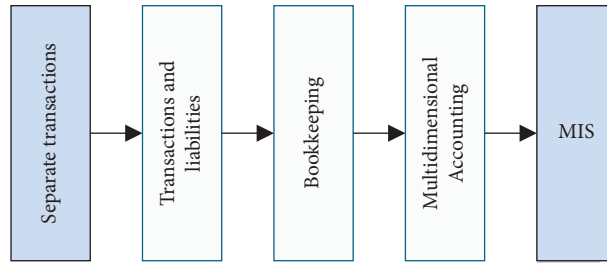
Figure 4: Evolution of traditional AIS.
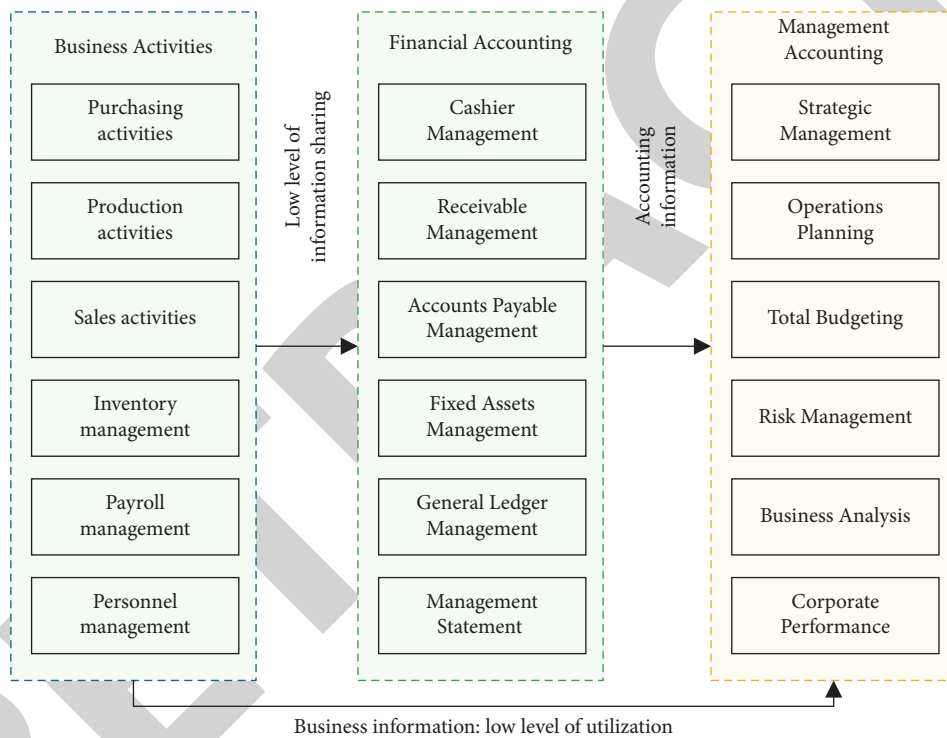
Figure 5: Traditional AIS function diagram.

of business and financial data, breaks through the limitation that traditional accounting information systems basically can only use accounting information to participate in management, improves the utilization of business information, and promotes a deeper combination of accounting and management; the combination of accounting and management makes accounting a powerful assistant of enterprise management. The functions of financial accounting and management accounting are therefore mutually reinforcing and inseparable, as shown in Figure 6.

3.2. Improvement Model. Based on the aforementioned problems of rigid accounting, rigid management, and rigid business processes in the application process, the design goal

of the flexible financial integration AIS is to make the financial integration AIS flexible, improve the self-adaptability and scalability of the system itself to changes in external requirements, and then shorten the system redevelopment cycle and reduce the cost of redevelopment, specifically including flexible input and data structure, flexible data flow, flexible business process, and flexible data output.

3.2.1. Flexible Input and Data Structure Design. Traditional industry and finance integration AIS for the development of data structure design is usually only specific database tables and fields, that is, the premise that the default later database table structure does not change, the data table
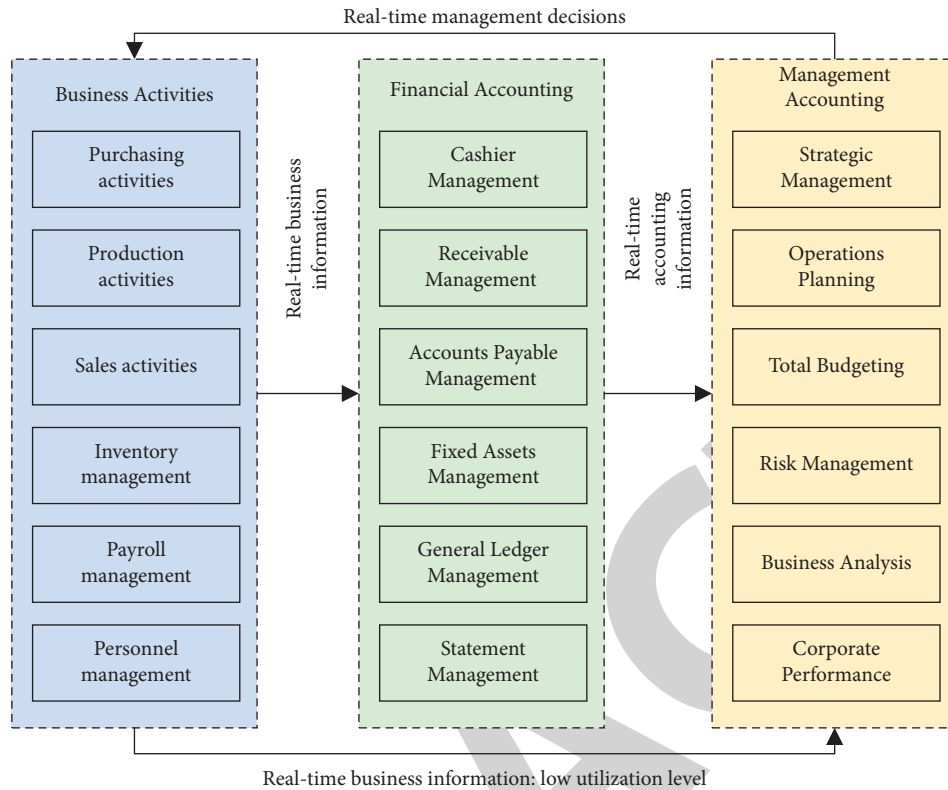
Figure 6: Functional diagram of AIS for business finance integration.

in the data items does not change. This rigid system does not take into account the possible adjustment of the data structure in the subsequent use of the enterprise during the initial design, and of course, there is no input space reserved for the user to configure the data structure at the front end, so the developed system lacks self-adaptability for the user to a certain extent in terms of input and data structure.

Two important concepts in the database related to the input and data structure design of the flexible industry financial integration AIS are triggers and stored procedures. The trigger mechanism ensures that the trigger action is executed only when the trigger event occurs and the trigger limits are met. Each table in the database can set a trigger, and the role is to establish the connection of multiple tables in the database to achieve the linkage of data in multiple tables. A stored procedure is a set of statements to complete a specific function, through the parameters set so that when the user performs similar operations on the database, there is no need to repeat the compilation, so the use of stored procedures can improve the efficiency of the database operation.

The design of the data structure in the flexible financial integration AIS is not only the specific database tables and fields, but also the "data dictionary," which stores not the general specific user data, but the structural data of various data items, and establishes the connection between the data dictionary and the entity database tables through triggers and stored procedures, so that when the structural data in the data dictionary changes, the corresponding entity table structure will also change accordingly.

The design of input in the flexible business financial integration AIS is to present the data dictionary stored in the database on the page to the user by setting up the data dictionary function card interface, reserving the input space for the user to configure the data structure. Using this function, the following two kinds of operations can be performed: first, you can create new original documents and enter the specific data items related to the content; second, you can modify the original documents in the data items (such as special enterprises in financial accounting or managerial decision-making needs may add some special data items on business documents, which you can add or modify in the original database forms) and thus meet the changing needs of enterprises for the data structure.

The "data dictionary" is a "warehouse" that can be used to store a variety of structural data. It should include the following two tables: one is the detail table (to store the content of the data items of each table of the database, including field names and field types), and the table structure as shown in Table 1.

The flexible implementation process of input and data structure is shown in Figure 7. The data update linkage between the business and finance fusion AIS and the corresponding entity tables in the database is done through triggers and stored procedures. When the user performs the operation of adding, deleting, or changing in the data dictionary function card of the AIS, the corresponding database is called using the database interface; the corresponding data changes are recorded in the detail table; the operation of adding, deleting, or changing then triggers the trigger

Table 1: Table of contents.

Field name	Meaning
id	Table number
T_name	Table name
T_type	Type
Creator	Creator

embedded in the detail table; the data modified by the user in the front-end page is recorded in the temporary table; the corresponding stored procedure is executed; and then, the corresponding entity table is modified. The modification of the entity table will be presented on the interface of the AIS in real-time, so that the user can realize the change in the data structure of the corresponding form in the database through the data dictionary function card on the AIS, which realizes the flexibility of the input and data structure.

3.2.2. Flexible Data Flow Design. Since the data structure in the traditional AIS is fixed, the flow of data items between them is also fixed. Although the flow of data items between documents, between documents and vouchers, and between documents/vouchers and reports is possible in the traditional rigid AIS, this flow is solidified and does not allow users to configure themselves, for example, some data grievances exist only in upstream documents and not in downstream documents, but managers need to add these data items that exist only in upstream documents to downstream for management purposes The administrator also needs to add these data items that exist only in the upstream documents to the downstream documents for management purposes. If the new data items do not exist in the upstream and downstream documents, it is difficult to configure the process of these extended data items in the system.

The design of the data flow in the flexible financial integration AIS focuses on the establishment of visualized document conversion rules between upstream and downstream documents, between various documents and vouchers, and between documents and reports, which can be configured by users. The specific design diagram is shown in Figure 8.

Document conversion rules: Document conversion rules are designed to make the data conversion between documents more convenient, and through the method of parameter configuration, the conversion rules are no longer rigid and unchangeable but can be flexibly deployed. With the rules to achieve data filtering, grouping, and merging, calculation and other configurations meet the business needs of the document conversion process. Document conversion rules are broadly divided into single-head conversion rules, entry conversion rules, auxiliary configuration, etc. The parameter configuration through the single-header conversion rules can establish the association of each data item between documents, and the parameter setting in the journal entry conversion rules can realize the reconfiguration of generated vouchers.
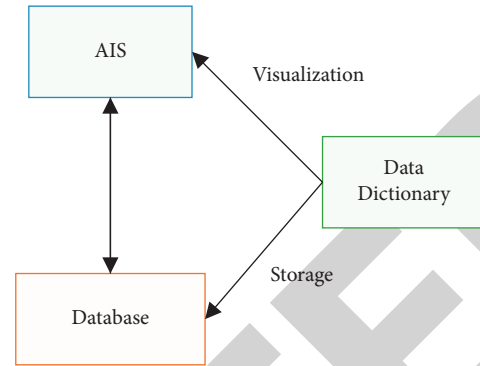
Figure 7: Design diagram of input and data structure flexibility.

3.2.3. Flexible Business Process Design. In the traditional rigid business finance system, due to the fixed setting of business processes, business users cannot adjust business processes according to their actual needs, and the integration of business and financial processes can only set up financial indicators according to business needs, and cannot optimize business processes according to the financial indicators of enterprises, and the setting of business processes can only realize the one-way business process of A-B-C one-way business process. With the large number of business needs of enterprises, the traditional rigid business process structure can no longer meet the needs of the complexity of enterprises today.

The core of business process design in flexible AIS is that users themselves can realize business process customization. Business process customization means that the system provides a common business process model in advance to support users to personalize the operation according to their needs, allowing users to realize the dynamic combination of processes or dynamic definitions without changing the source code, increasing the flexibility of business processes in the financial system. The flexible AIS provides users with the function of freely configuring business processes, and realizes the close connection between business process management and the AIS of financial integration.

The flexibility of business process customization is reflected in the following aspects, and the overall process of its operation is shown in Figure 9.

3.2.4. Flexible Data Output Design. The traditional financial integration system is relatively fixed in the final output report format and content, for example, the format of the four commonly used financial statement templates are relatively fixed, and the content is relatively fixed, so if the project name or data source inside the template report changes, the enterprise cannot change and adjust in time by itself, so the rigid financial integration AIS has caused the limitation of management analysis to a certain extent.

The design of flexible data output in the flexible industry financial integration AIS focuses on the user's ability to configure the content and format of information output, as mentioned above, for the final financial accounting reports and management accounting reports, the manager
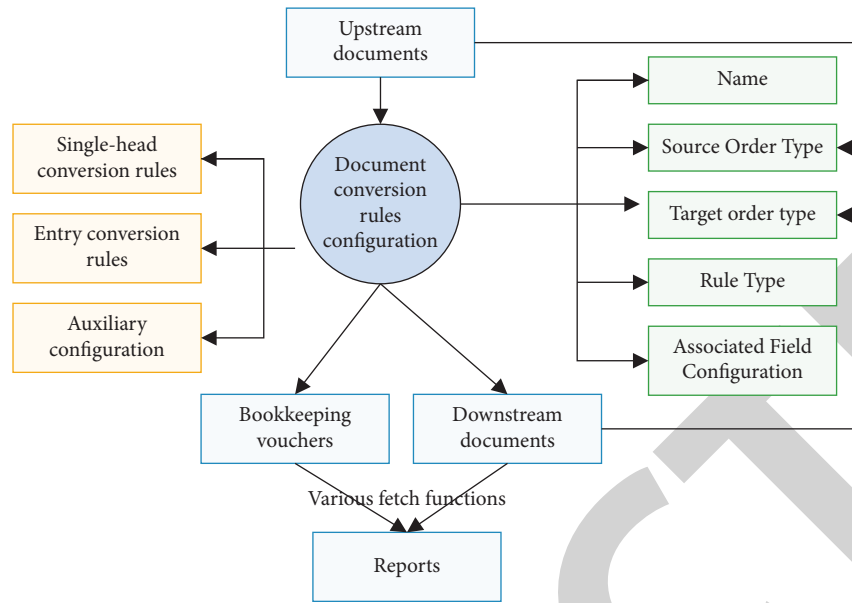
FIGURE 8: Data flow flexible design diagram.
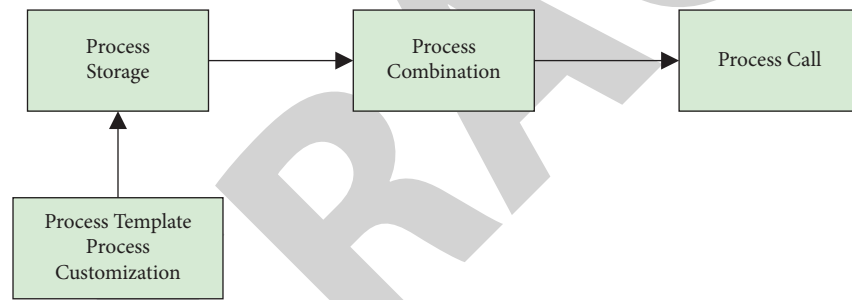
FIGURE 9: Business process flexibility design diagram.

can choose the output content and format at will, and if the items in the reports defined in the system template do not meet the actual needs, the user can customize the report format and content to meet the personalized needs of managers. Flexible AIS supports customizable report function, which allows users to design the report format, report items, sources, calculation, and processing methods by using the visualized pages provided and combining them with the actual situation of the unit and the department. The system will automatically generate the reports that the user wants according to his or her definition. Once the user's needs change, the user can modify the original report design or design a new report to meet his or her needs without modifying the accounting information system itself. That is, the core of the design of data output flexibility lies in the implementation of the custom report function, the specific design process of which is shown in Figure 10.

4. Case Study

A company is a large integrated modern enterprise group. With the gradual expansion of the group's scale, it became difficult to adapt the original financial and business model to the group's management needs, which to a certain extent hindered the group's development. To keep pace with the times, in the context of the Internet, it is imperative to make full use of new information technology tools for reform. We first show the degree of approval of different employees for the management upgrading of the financial accounting system in Figure 11.

Before the implementation of financial sharing, the finance department of a company was mainly responsible for daily accounting, expense reimbursement, current account management, fundraising and operation, investment management, budget management, tax reporting, statement preparation and analysis, and other work, mainly centralized financial management. With the development of a company, the number of subsidiaries, overseas branches, and strategic business units gradually increased, the group reformed and adopted the organizational form of group customer divisions, and established financial divisions within each division; from a centralized financial management mode to a decentralized financial management mode, each divisional financial division is responsible for its own local business corresponding to the expense
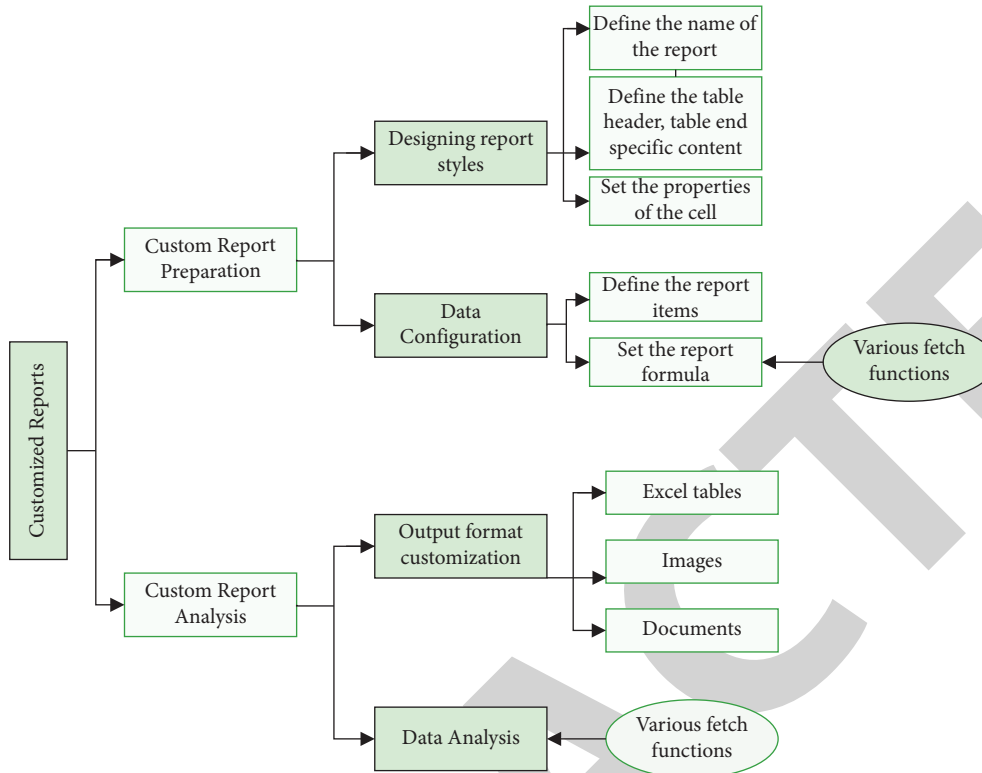
FIGURE 10: Design of custom reports.
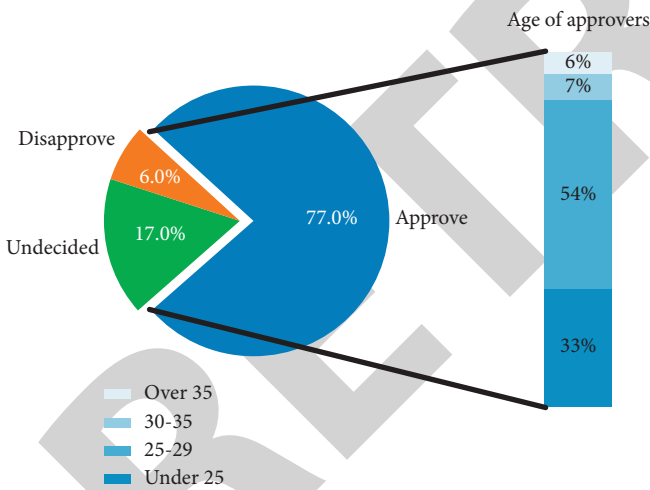
FIGURE 11: Different employees' opinions on the management upgrading of the financial accounting system.

reimbursement accounting and other work. Then, each business unit regularly sends business-related data to the accounting staff of the business unit, and the accounting department of each business unit submits the processed financial and business analysis data to the headquarters group for data aggregation and analysis.

4.1. Analysis of the Main Problems of a Company before the Integration of Industry and Finance

(1) *High Labor Cost and Low Value Creation.* A company's customer business units establish the same function as the finance department: repeatedly building a finance department is time-consuming and labor-intensive, and a large number of accounting staff increase the group's operating costs. The heavy accounting volume of each finance department takes up a lot of energy of accounting staff, making it difficult for them to withdraw business management and provide decision support for business strategy management.

(2) *Poor Information Communication.* First of all, a company arranges accounting personnel with the same functions in different group customer divisions, and the financial information is first aggregated and analyzed by the divisional accounting personnel and then submitted to the group headquarters, which may lead to the redundancy of personnel and departments, resulting in the untimely collection of financial information from the group headquarters, operational errors and problems such as information asymmetry between online and offline. Second, there is no good communication mechanism between business information and financial information, and the core data cannot be unified and centralized in the same system for business analysis and management. The dual-track system of business and finance makes it impossible to allocate and apply enterprise resources efficiently. In addition, the value application and decision analysis
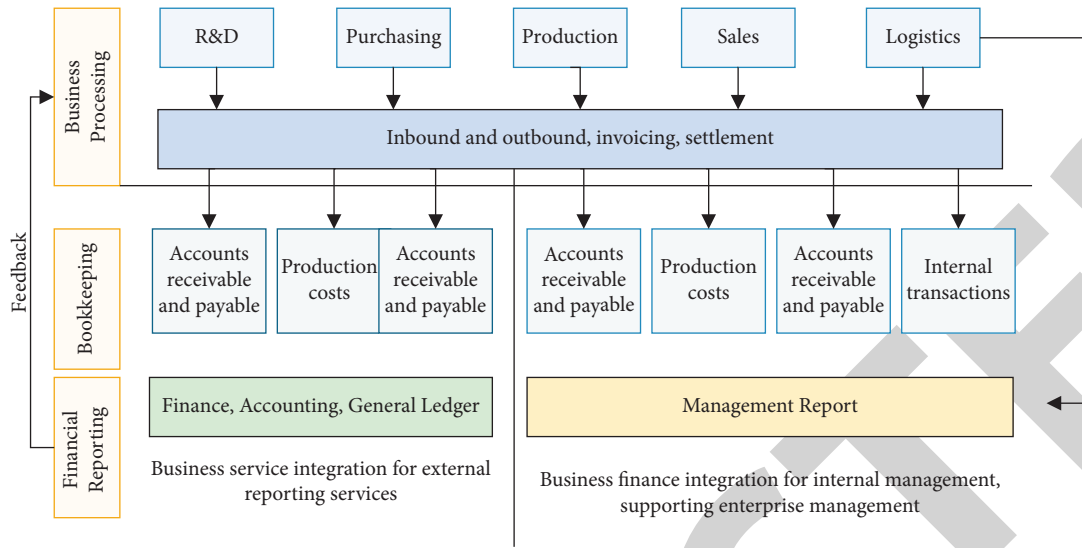
FIGURE 12: Variable conversion model of a company under the integration of industry and finance.

of financial management cannot provide support for business development quickly and timely, and the efficiency of business execution is low.

4.2. Implementation of a Company's Financial Integration in the Internet Era

4.2.1. Background and Significance of Implementation. With the continuous development of computer technology, approaching the "Internet" and reshaping the accounting process to break the "information silo" are undoubtedly crucial to realize the integration of business and finance of enterprises. In the background of the group's increasing business and continuous expansion, reshaping the correlation between business and finance, through the integration of business and finance, is conducive to breaking the awkward situation of information isolation of various departments, so that finance can provide timely and true feedback on business facts, and provide efficient support to the group's internal decision-making and control, to achieve "business pulling finance, finance supporting business." The key to the integration of business and finance lies in achieving the "two-wheel drive" of finance and business. The key to the integration of business and finance lies in how to reorganize the accounting process from the group business process reorganization. The following is an example of a company's implementation path, explaining how it uses the financial sharing platform to integrate business and finance and empower management.

4.2.2. Implementation Path. To realize the integration of business and finance for management empowerment, a company makes full use of the financial sharing platform. A company's financial sharing center is an integrated and unified accounting platform based on front-end business pull-through. All transactions, invoices, reconciliations, payments, and other processes in the front-end are
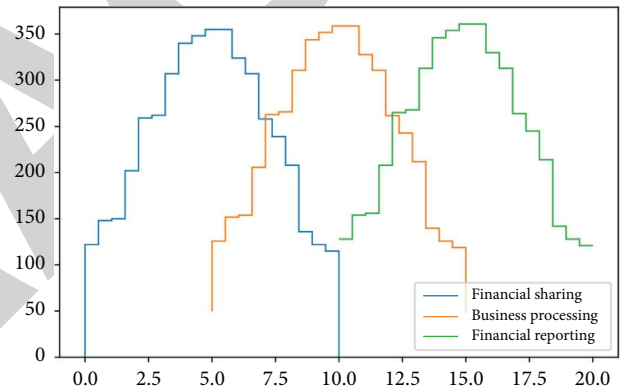
FIGURE 13: The distribution of different accounting operations.

collected as data collection points, and a large amount of data resources are collected and entered into the data platform in real-time to store the information, and the stored data are extracted, summarized, apportioned, offset and consolidated, and converted into caliber. The stored data are extracted, aggregated, apportioned, offset and consolidated, transformed, and then aggregated and displayed through the management dimension (see Figure 12).

We further analyzed the changes in different links of financial accounting operations in Figure 13.

Based on the report format and unified index system, the group establishes corresponding analysis models; creates a unified financial data and report platform; prepares financial statements; provides the group with standardized financial accounting, multi-dimensional cost and profitability analysis, and other services; and provides support for relevant information disclosure, group management, and decision-making (see Figure 14).

Based on the group's financial sharing unified data platform, the shared finance center has also built a multi-

FIGURE 14: The process of preparing a unified data report of a company.

FIGURE 15: The value of financial management with business management.

dimensional indicator analysis system, establishing multi-dimensional accountability indicators and analysis systems corresponding to main business income; profit before tax; operating net cash flow; major quality issues at the operation level, management level, and decision-making level, respectively; and using the group's big data platform for analysis and display. In Figure 15, we analyze the relationship between financial management and business management.

Based on the group's financial sharing unified data platform, the shared finance center has also built a multi-dimensional indicator analysis system, establishing multi-dimensional accountability indicators and analysis systems corresponding to main business income; profit before tax; operating net cash flow; major quality issues at the operation level, management level, and decision-making level, respectively; and using the group's big data platform for analysis and display.

After reshaping the financial process, a company's internal financial sharing center platform unified the entire process and buried information on key links, so that financial rules fully penetrate the whole process of related transactions, laying a solid data foundation for the group's later monthly reconciliation and data management analysis and improving the efficiency and timeliness of data provision. It also solves the problems of high labor cost and low enterprise value creation under the decentralized financial management model. The sharing center can also generate two sets of financial reports based on the corporate structure and management reports based on the management structure. After the integration of industry and finance, the operating budget execution report can be issued in real-time, allowing the group to monitor the specific implementation of the budget in real-time and providing strong support for group managers and decision-makers.

5. Conclusion

In conclusion, for enterprises, financial accounting management is crucial, and it is the basis of enterprise development, especially in the Internet era; enterprises need to strengthen the innovation of the financial accounting management mode to help meet the development needs of the times. But at present, it is difficult to adapt some enterprises' financial accounting management work to the development of the network era, and the management concept has not been updated in time. Enterprises must pay more attention to this, take reasonable decisions to optimize it, and further expand the field of financial accounting management by strengthening the construction of information technology and clarifying the outstanding problems, so that enterprises can obtain new development and improve the level of financial accounting management comprehensively.

Retraction

Retracted: Dynamic Evaluation of Intensive Land Use Based on Objective Empowerment by Entropy Method and Neural Network Algorithm

Computational Intelligence and Neuroscience

This article has been retracted by Hindawi following an investigation undertaken by the publisher [1]. This investigation has uncovered evidence of one or more of the following indicators of systematic manipulation of the publication process:

(1) Discrepancies in scope

(2) Discrepancies in the description of the research reported

(3) Discrepancies between the availability of data and the research described

(4) Inappropriate citations

(5) Incoherent, meaningless and/or irrelevant content included in the article

(6) Peer-review manipulation

The presence of these indicators undermines our confidence in the integrity of the article's content and we cannot, therefore, vouch for its reliability. Please note that this notice is intended solely to alert readers that the content of this article is unreliable. We have not investigated whether authors were aware of or involved in the systematic manipulation of the publication process.

Wiley and Hindawi regrets that the usual quality checks did not identify these issues before publication and have since put additional measures in place to safeguard research integrity.

We wish to credit our own Research Integrity and Research Publishing teams and anonymous and named external researchers and research integrity experts for contributing to this investigation.

The corresponding author, as the representative of all authors, has been given the opportunity to register their agreement or disagreement to this retraction. We have kept a record of any response received.

References

[1] T. Yang, H. Cheng, H. Zhao, and D. Cadasse, "Dynamic Evaluation of Intensive Land Use Based on Objective Empowerment by Entropy Method and Neural Network Algorithm," *Computational Intelligence and Neuroscience*, vol. 2022, Article ID 2429826, 7 pages, 2022.

Research Article

Dynamic Evaluation of Intensive Land Use Based on Objective Empowerment by Entropy Method and Neural Network Algorithm

Ting Yang,[1] Hanlie Cheng [ID],[2,3] Hailian Zhao,[4] and David Cadasse [ID][5]

[1]School of Public Administration, Chongqing Technology and Business University, Chongqing 400076, China
[2]School of Energy Resource, China University of Geosciences (Beijing), Beijing 434000, China
[3]COSL-EXPRO Testing Services (Tianjin) Co., Ltd., Tianjin 300457, China
[4]School of Soil and Water Conservation, Beijing Forestry University, Beijing 100083, China
[5]The King's School, BP1560, Bujumbura, Burundi

Correspondence should be addressed to David Cadasse; davidcadasse@ksu.edu.bi

In the past, the extreme value standardization of indicators, the traditional weighting method, and the multifactor comprehensive model of land intensive use inevitably linearly correlate the evaluation indicators with the evaluation objects, ignoring the direction differences of different indicators in different intervals. At the same time, these methods are also difficult to meet the change of evaluation index weight value with land use type, and cannot adapt to the actual situation of land use environment level and dynamic change. Considering the objectivity of nonlinear correlation moderate index and weight assignment, based on the standardization of quadratic function index and entropy assignment, this paper studies the intensive and dynamic use of land in development zones by different regions to improve the realistic fit of the evaluation model. The results show that the overall level of land intensive use in Chongqing center district and western Chongqing is better than that in northeast Chongqing and southeast Chongqing, roughly showing the state of "high in west and low in east."

1. Introduction

The more China promotes high-quality economic and social development and promotes ecological civilization construction, the more it needs to economize and make intensive use of every inch of nonrenewable land. Facing the dual pressure of protecting resources and ensuring development, the economical and intensive use of land has become an inevitable choice to change the way of land use, optimize resource allocation, expand new drivers of economic development, and make use of stock space [1–4]. At present, scholars and experts have carried out a lot of studies on land intensive use evaluation, internal coordination analysis, influencing factors research, evaluation index system construction, etc. [5–10]. Land intensive utilization evaluation method concentrates multifactor comprehensive evaluation method, the neural network algorithm, principal component analysis (PCA), the fuzzy hierarchy comprehensive evaluation method, etc. The neural network algorithm by selecting the evaluation index factor and factor of unit works is quantified by the appropriate model, calculation and merge, so as to realize the evaluation target; this is the most commonly used method. For example, standard deviation standardization method, ratio standardization method, range standardization method, etc, are common in calculation, while moderate index is often segmented, and positive index calculation method is adopted when the value is less than the ideal value, without fully considering the nonlinear relationship between evaluation index and evaluation result [11–17]. While positive correlation and negative correlation indicators in the evaluation of land intensive utilization is the most common, but the land use structure indicators such as plot ratio and building density, as well as appropriate population density, ratio and other indicators, as well as the commonly used dimensionless index method, cannot eliminate the difference in

characteristics, and are prone to overestimate some information loss caused by the level of intensity [18–22]. Based on the quadratic function indicator standardization evaluation index/evaluation results of both nonlinear relationship, it selects the index weight objective empowerment; confirm dynamic entropy weight-driven value analysis was used to explore the change of land intensive use in different time span; entropy index between different sizes directly reflects the degree of target state changes; the overall difference between limit and driving factors avoids the influence of human factors of subjective weighting methods such as Delphi method, analytic hierarchy process, and factor pair comparison method, improves the accuracy and effectiveness of calculation results, and improves the realistic goodness of fit of the evaluation model.

2. Research Methods and Data Sources

2.1. Research Methods

2.1.1. Standardization of Quadratic Function Indexes. The theoretical basis for the standardization of quadratic function indexes is the law of diminishing marginal utility. The land users in the study area are set as consumers, the standardized value of indicators is set as utility, and the actual value of indicators is set as consumption units. The process of intensive land users is the process of utility satisfaction of land users, and the behavior associated with appropriate indicators according to the law of diminishing marginal utility.

There are n quantitative evaluation indexes $X1, X2, \ldots, Xn$, and m samples constitute the index data matrix $P = \{Xij\} (i = 1, 2, \ldots, m; j = 1, 2, \ldots, n)$; Xij represents the value of the j item evaluation index of the ith sample. The current value of the j index is Xj. The ideal value of evaluation index Xj is X0. Weight is Wj; The standardized value is Yj, and the standardized formula of the quadratic function index is $Yj = aXj2 + bXj$.

When the actual value of the evaluation index Xj reaches the ideal state $X0$, it should be 1 after standardized treatment, and the evaluation value of the quadratic function index formed after standardization is between $[0, 1]$. The ideal value is $X0$. According to the function fixed point value $[X0, 1]$ and $[0, 0]$, parameters a and b in the model can be calculated:

$$b = \frac{2}{X_0}, a = \frac{1}{X_0}. \tag{1}$$

The improved calculation method of combination index standardization method is shown in formulas (1)–(3). A multifactor evaluation model is formed as formula (5), where J represents the land intensity score of the study area:

$$\text{positive indicators } Yj = \frac{(Xj - X\min)}{(X\max - Xmin)}, \tag{2}$$

$$\text{negative indicators } Yj = aXj2 + bXj, \tag{3}$$

$$\text{appropriate indicators } Yj = \frac{(X\max - Xj)}{(X\max - Xmin)}, \tag{4}$$

$$J = \sum_{j=1}^{n} (W_i \times y_j \times 100). \tag{5}$$

Take the derivative of J with respect to Yj in formula (4), the derivative of Yj with respect to Xj in formulas (1) and (3), $J' = 100 \times Wj$. Positive indicators: $Yj' = 1/(Xmax - Xmin)$. Negative indicators: $Yj' = -1/(Xmax - Xmin)$; it can be seen that the land intensity score J is linearly correlated with the standardized index Yj; appropriate indicators Yj in (5) is: $J' = 100 \times Wj (2aXj + b)$; it can be seen that the land intensity score J is linearly correlated with the standardized index Yj.

2.1.2. Entropy Value Method. In comprehensive evaluation, it is generally believed that the index weight value determined by entropy method is more objective and more reliable than the subjective weight method such as Delphi method and analytic hierarchy process. Entropy method is based on the information entropy theory. According to the difference of the information order degree contained in each evaluation index, the higher the order degree of a system is, the greater the information entropy is and the smaller its utility value is. Different entropy values between indicators are generally applicable for weight determination in time series evaluation. To calculate the index entropy e_j, the formula is as follows:

$$e_j = -\frac{1}{\ln m} \sum_{i-1}^{m} P_{ij} \times \ln P_{ij}. \tag{6}$$

Among them, P_{ij} is the contribution degree of a single indicator. The weight Wj is calculated by using the entropy value obtained, and the calculation formula is as follows:

$$W_j = \frac{gi}{\sum_{j-1}^{n} gi}. \tag{7}$$

Wj is the weight of the j index, and gi is the difference coefficient of the j index.

2.2. The Data Source. The data were mainly obtained from Chongqing Land use status change survey data, statistical yearbook from 2014 to 2018, land use and enterprise survey data of development zone, dynamic monitoring and supervision system data of land market, Urban and Rural Development Commission, natural Resources Bureau, etc.

3. The Study Area

As an important area of regional economic development, the development zone is the scientific and technological innovation base of industrial upgrading and regional development and also an important growth point of the sustainable development of urban economy. As of 2018, Chongqing has

eight national development zones and forty-one provincial-level development zones, including Xiyong Comprehensive Bonded Zone, Lianglu-Cuntan Free Trade Port Area, Chongqing Economic and Technological Development Zone, and Chongqing High-Tech industry development Zone. There are forty-nine development zones in total which have greatly promoted regional economic development. Based on the characteristic support development zone system of Chongqing center district, western Chongqing, northeast Chongqing, and southeast Chongqing as an example, this paper evaluated the dynamic situation of land intensive use from 2013 to 2017 by combining the quadratic function index standardization and entropy method weighting method. By the end of 2017, the Chongqing development zone covers an area of 665.97 square kilometers, with a land development rate of 71.23%, a total resident population of 2.0741 million, a total investment in industrial fixed assets of 1.149247 billion, and a total industrial tax revenue of 50.902 billion.

4. Result Analysis

4.1. Establishment of the Evaluation Index System. In this paper, a total of ten indicators $C1 - 1/C10 - 1)$ are selected as the evaluation indicators of the Industrial-led Development Zone, and seven indicators $C1 - 2/C10 - 2$ are selected as the evaluation indicators of the City-industry integration development zone, in which the idle rate of land $C10 - 1/C10 - 2$ is a negative indicator, and the building density $C5 - 1/C5 - 2$ and population density (C9-2) are appropriate indicators(Table 1). After the standardization of the evaluation index by the quadratic function, the ideal value of the evaluation index of building density in Chongqing center district at the end of 2017 is 56.83%, and the quadratic function value $Y = 2.149$. The ideal value of the evaluation index of population density is 383.66 people/hectare, and the quadratic function value $Y = 1.422$. The other evaluation indexes are all positive indicators.

4.2. Weight Analysis of Evaluation Indicators. The rationality of index weight directly affects the order of pros and cons of evaluation objects, thus greatly affecting the accuracy of comprehensive evaluation. The weight values of dynamic indicators of the industrial-led development zone are determined according to the entropy method, as shown in Table 2. The entropy weight of the city-industry integration development zone is WC1-2 = 0.122, WC2-2 = 0.124, WC4-2 = 0.121, WC5-2 = 0.125, WC8-2 = 0.143, WC9-2 = 0.121, and WC10-2 = 0.244.

4.3. Dynamic Comparative Analysis of Land Use Status. According to the analysis of the current situation values in different years, the land supply rate of development zones in Chongqing center district (A), western Chongqing (B), northeast Chongqing (C), and southeast Chongqing (D) was basically flat, which were all at Chongqing center district high level, respectively, 91.60%, 89.33%, 86.23% and 89.51%. The area with the best land supply is Chongqing center

district, and the area with the greatest supply potential is northeast Chongqing. The land construction rate, respectively, is 80.53%, 75.43%, 71.73%, and 67.40%. Chongqing center district has superior location conditions, and the soft and hard environmental conditions for industrial development are better. The land construction rate is the highest. Compared with the land supply rate of 84.26%, 89.71%, 87.52%, and 64.4% in 2013, and the land construction rate of 83.57%, 97.09%, 87.83%, and 82.72% in 2013, the land development rate in Chongqing center district, western Chongqing, and northeast Chongqing showed an overall trend of first decreasing and then increasing. The area in southeast Chongqing showed a trend of first rise and then decline, and the land construction rate showed a trend of saturation decline as a whole, as shown in Figure 1.

In terms of land use structure, intensity and benefit, the industrial land use rate in western Chongqing is higher than that in other three areas, and its dynamic change reaches the highest value of 76.39% in four years. Except for southeast Chongqing, the building density, comprehensive floor area ratio of industrial land, building coefficient of industrial land, and fixed asset input intensity of industrial land in the other three regions all showed an upward trend. The average tax revenue of industrial land in western Chongqing, northeast Chongqing, and southeast Chongqing was basically stable. By the end of 2017, there are 0.0.9% and 0.7% of idle land in Chongqing center district and southeast Chongqing, and the rate of idle land was relatively low. There is no idle land in western Chongqing and northeast Chongqing, and the land management performance is good. For newly built has not yet been put into production, the stable industrial land scale is larger; Chongqing center district has 0.09% idle land, leading to the both of industrial land tax with the year dropped substantially.

4.4. A Case Study on Comprehensive Evaluation of Land Use Intensity. According to the weight value of each evaluation index, the status value of the index ranked fifth was used as the ideal value of the corresponding index; after the standardization of indicators, the comprehensive score of land intensity was calculated. It can be divided into four grades: extensive utilization (<60), preliminary intensive utilization (60–70), basic intensive utilization (70–80), and highly intensive utilization (80–100).

On the whole, the intensity score of 49 development zones in Chongqing presents a state of "high in the west and low in the east." Chongqing center district is the political, economic, cultural, modern service center, and population agglomeration area of the whole city, and the development environment of high-tech industry is good. The second area is western Chongqing. As an important manufacturing base of the whole city, western Chongqing is an important area to gather new industries and population. The overall level of land intensive use in Chongqing center district and western Chongqing is better than that in northeast Chongqing and southeast Chongqing. 92% of the development zones of type I highly intensive utilization grade are distributed in Chongqing center district and western Chongqing. Only three development zones

Table 1: Evaluation index system of intensive utilization in the development zone.

The target layer A	Rule layer B	Index layer C	Index meaning
Land use status A1	Degree of land use B1	Land supply rate C1 – 1/C1 – 2	Refers to the ratio of the area of state-owned construction land already supplied to the area of land already supplied
		Land construction rate C2 – 1/C2 – 2	Refers to the ratio of built-up urban construction land area to state-owned construction land area
	Land use structure B2	Industrial land ratio C3-1	Refers to the percentage of industrial, mining and storage land area within the scope of built-up urban construction land and built-up urban construction land area
		Combined volume ratio C4 – 1/C5 – 2	Refers to the ratio of the total built-up area on the built-up urban construction land to the built-up urban construction land area
	Land use intensity B3	Building density C5 – 1/C5 – 2	Refers to the ratio of the total area of building basement within the completed urban construction land to the completed urban construction land area
		Comprehensive plot ratio of industrial land C6-1	Refers to the ratio of total built-up area of industrial land to industrial land area
		Building coefficient of industrial land C7-1	Refers to the percentage of built-up area of industrial land to industrial land
		Fixed asset input intensity of industrial land C8-1/Comprehensively equalize taxation C8-2	Refers to the ratio of accumulated fixed asset investment of industrial (logistics) enterprises within the scope of land used for urban construction to the area of land used for industrial, mining, and storage/refers to the ratio of total tax revenue of secondary and tertiary industries within the scope of land used for urban construction to the area of land used for urban construction
Land use efficiency A2	Industrial land input output benefit B4	Average tax on industrial land C9-1/The population density C9-2	Refers to the ratio of total tax revenue of industrial (logistics) enterprises within the scope of completed urban construction land to the area of industrial, mining and storage land/refers to the ratio of permanent resident population within the scope of evaluation to the area of completed urban construction land
Land management performance A3	Land use regulatory performance B5	Idle rate of land C10 – 1/C10 – 2	Refers to the ratio of idle land area to the development zone area

TABLE 2: Index weights of the time series.

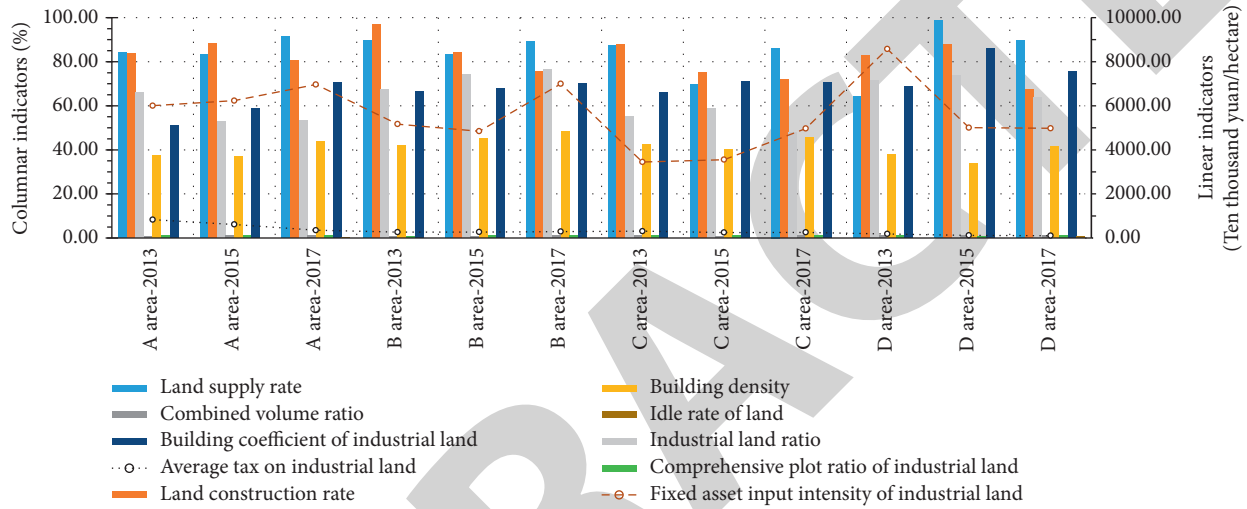| The target layer	Land use status							Land use efficiency		Land management performance
Index layer	C1	C2	C3	C4	C5	C6	C7	C8	C9	C10
2013				0.559				0.191		0.250
	0.053	0.119	0.055	0.118	0.102	0.060	0.052	0.071	0.120	0.250
2015				0.550				0.168		0.282
	0.073	0.061	0.083	0.106	0.082	0.063	0.081	0.070	0.099	0.282
2017				0.739				0.202		0.059
	0.066	0.078	0.095	0.142	0.076	0.088	0.194	0.139	0.063	0.059

FIGURE 1: Statistical chart of the current value of land intensive and economical use in the development zone.

in the whole city have the intensity score exceeding 90 points, including Chongqing Gangcheng Industrial Park in Chongqing center district 92.33 points, Chongqing Tongxing Industrial Park in Chongqing center district 90.70 points, and Chongqing Fuling Industrial Park in western Chongqing 92.38 points. There are 20 development zones of basic intensive utilization grade II, which are distributed in all four zones. Due to the limitation of terrain conditions in northeast Chongqing and southeast Chongqing, the land area of development zone is relatively small and the building coefficient of industrial land is relatively high, due to the large proportion of transportation land, public management land, and public service land in the development zone of northeast Chongqing; the realization rate of paid land use in the development zone is reduced to a certain extent, and the marketization degree of land supply is the lowest. The lowest score of intensity in northeast Chongqing is 50.83 in Chongqing Jiangjin Comprehensive Bonded Tax Zone and 56.19 in Chongqing Fengjie Industrial Park in western Chongqing, both of which belong to type IV extensive utilization grade. The development zones with the grade III of preliminary intensive utilization include Changshou Economic and Technological Development Zone with 67.04 points, Chongqing Chengkou Industrial Park with 61.40 points, and Chongqing Pengshui Industrial Park with 69.15 points.

Compared with the four regions in the time series, the Central District of Chongqing has the highest land intensity
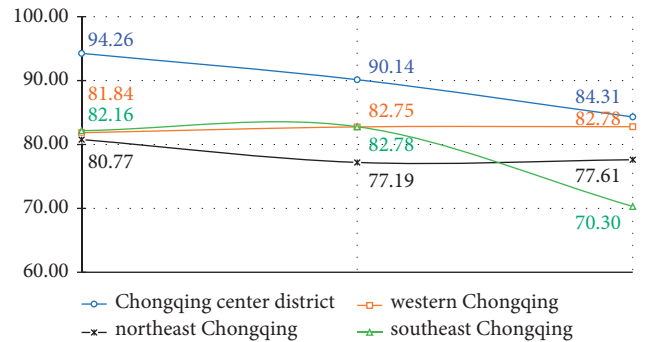

FIGURE 2: Dynamic change of land use intensity score from 2013 to 2017.

in the past four years, and the land intensity in the Central District of Chongqing has decreased year by year. However, at a high level, the degree of land intensity in the western part of Chongqing is increasing year by year. The central area of Chongqing and the western part of Chongqing both maintained above 80 points, and the northeast of Chongqing showed a trend of first decreasing and then slightly increasing, reflecting the basic intensive utilization level. Southeast Chongqing showed a trend of first slight increase and then strong decrease, as shown in Figure 2.

5. Conclusion

From the perspective of the change of the dynamic evaluation result data and the comprehensive function development of the development zone, in recent years, the Chongqing development zone are higher than the average level of the national development zones in the same year. The space for improving land use structure and land use intensity is gradually shrinking, and the overall level of intensity is relatively high. The development zone has been transformed from a single industrial park to an urban comprehensive functional zone, the land use structure has been further rationalized, and the supply of infrastructure facilities and public service land has increased. Compared with the changes over the years and the national level, the short board of land intensive use in Chongqing Development Zone lies in the low land use efficiency. Industrial land is below the national average national level development zone in the same year tax, and the comprehensive benefits of play is not enough.

The Chongqing development zone should be through the industry upgrading and transfer, improve the level and quality of land output per unit area, and reduce the consumption of social economic development on the land. The extensive road of development by relying on land expansion can no longer continue. The development mode of land use should be changed to further release the longitudinal and vertical space of internal land use. Tap the potential and invigorate the stock, and improve the postsupply supervision mechanism, to achieve the connotative intensive and sustainable development.

Data Availability

The figures and tables used to support the findings of this study are included in the article.

Conflicts of Interest

The authors declare that they have no conflicts of interest.

Acknowledgments

References

[1] G. Li, C. Fang, and B. Pang, "Quantitative measuring and influencing mechanism of urban and rural land intensive use in China," *Journal of Geographical Sciences*, vol. 24, no. 5, pp. 858–874, 2014.

[2] S. S. Y. Lau, R. Giridharan, and S. Ganesan, "Multiple and intensive land use: case studies in Hong Kong," *Habitat International*, vol. 29, no. 3, pp. 527–546, 2005.

[3] A. Kovács-Hostyánszki, A. Espíndola, A. J. Vanbergen, J. Settele, C. Kremen, and L. V. Dicks, "Ecological intensification to mitigate impacts of conventional intensive land use on pollinators and pollination," *Ecology Letters*, vol. 20, no. 5, pp. 673–689, 2017.

[4] R. Lal, *Soil surface management in the tropics for intensive land use and high and sustained production. Advances in Soil Science*, B. A Stewart, Ed., vol. 5, pp. 1–109, Springer, New York, NY, 1986.

[5] H. Yao, Z. L. He, M. J. Wilson, and C. D. Campbell, "Microbial biomass and community structure in a sequence of soils with increasing fertility and changing land use," *Microbial Ecology*, vol. 40, no. 3, pp. 223–237, 2000.

[6] H. Cheng, J. Wei, and Z. Cheng, "Study on Sedimentary Facies and Reservoir Characteristics of Paleogene sandstone in Yingmaili Block, Tarim basin," *Characterization of the Unconventional Continental Shale Oil Reservoirs*, vol. 2022, Article ID 1445395, pp. 1�14, 2022.

[7] J. Wei, H. Cheng, B. Fan, Z. Tan, L. Tao, and L. Ma, "Research and practice of" one opening-one closing" productivity testing technology for deep water high permeability gas wells in South China Sea," *Fresenius Environmental Bulletin*, vol. 29, no. 10, pp. 9438–9445, 2020.

[8] Z. K. Hou, H. L. Cheng, S. W. Sun, J. Chen, D. Q. Qi, and Z. B. Liu, "Crack propagation and hydraulic fracturing in different lithologies," *Applied Geophysics*, vol. 16, no. 2, pp. 243–251, 2019.

[9] J. Han, H. Cheng, Y. Shi, L. Wang, Y. Song, and W. Zhnag, "Connectivity analysis and application of fracture cave carbonate reservoir in Tazhong," *Science Technology and Engineering*, vol. 16, no. 5, pp. 147–152, 2016.

[10] R. Ortega-Álvarez and I. MacGregor-Fors, "Living in the big city: effects of urban land-use on bird community structure, diversity, and composition," *Landscape and Urban Planning*, vol. 90, no. 3-4, pp. 189–195, 2009.

[11] H. Luo, X. Li, S. Zheng, M. Li, and L. Song, "Study on synthesis evaluation of intensive land use and growth pattern transformation of towns," *Journal of Computers*, vol. 7, no. 8, pp. 1959–1966, 2012.

[12] T. H. Oliver, S. Gillings, J. W. Pearce-Higgins et al., "Large extents of intensive land use limit community reorganization during climate warming," *Global Change Biology*, vol. 23, no. 6, pp. 2272–2283, 2017.

[13] L. J. Sonter, D. J. Barrett, C. J. Moran, and B. S. Soares-Filho, "A land system science meta-analysis suggests we underestimate intensive land uses in land use change dynamics," *Journal of Land Use Science*, vol. 10, no. 2, pp. 191–204, 2015.

[14] X. Cen, C. Wu, X. Xing, M. Fang, Z. Garang, and Y. Wu, "Coupling intensive land use and landscape ecological security for urban sustainability: an integrated socioeconomic data and spatial metrics analysis in Hangzhou city," *Sustainability*, vol. 7, no. 2, pp. 1459–1482, 2015.

[15] L. Östlund, G. Hörnberg, T. H. DeLuca et al., "Intensive land use in the Swedish mountains between AD 800 and 1200 led to deforestation and ecosystem transformation with long-lasting effects," *Ambio*, vol. 44, no. 6, pp. 508–520, 2015.

[16] Y. Liu, J. Li, and Y. Yang, "Strategic adjustment of land use policy under the economic transformation," *Land Use Policy*, vol. 74, pp. 5–14, 2018.

[17] A. Bissett, A. E. Richardson, G. Baker, and P. H. Thrall, "Long-term land use effects on soil microbial community structure and function," *Applied Soil Ecology*, vol. 51, pp. 66–78, 2011.

[18] S. McIntyre and S. Lavorel, "A conceptual model of land use effects on the structure and function of herbaceous